

**PROCESS IMPROVEMENT AND MICROBIAL
CHARACTERISATION OF BIOLOGICAL NITROGEN
REMOVAL FOR TROPICAL WASTEWATER WITH LOW
CHEMICAL OXYGEN DEMAND/NITROGEN RATIO**

HOW SEOW WAH

**FACULTY OF ENGINEERING
UNIVERSITY OF MALAYA
KUALA LUMPUR**

2020

**PROCESS IMPROVEMENT AND MICROBIAL
CHARACTERISATION OF BIOLOGICAL NITROGEN
REMOVAL FOR TROPICAL WASTEWATER WITH
LOW CHEMICAL OXYGEN DEMAND/NITROGEN
RATIO**

HOW SEOW WAH

**THESIS SUBMITTED IN FULFILMENT OF THE
REQUIREMENTS FOR THE DEGREE OF DOCTOR OF
PHILOSOPHY**

**FACULTY OF ENGINEERING
UNIVERSITY OF MALAYA
KUALA LUMPUR**

2020

UNIVERSITY OF MALAYA
ORIGINAL LITERARY WORK DECLARATION

Name of Candidate: How Seow Wah

Matric No: KHA160032 (ISIS format); 17020471/2 (UMSIIS format)

Name of Degree: Doctor of Philosophy

Title of Project Paper/Research Report/Dissertation/Thesis (“this Work”):

Process Improvement and Microbial Characterisation of Biological Nitrogen Removal for Tropical Wastewater With Low Chemical Oxygen Demand/Nitrogen Ratio

Field of Study: Bioprocess Engineering

I do solemnly and sincerely declare that:

- (1) I am the sole author/writer of this Work;
- (2) This Work is original;
- (3) Any use of any work in which copyright exists was done by way of fair dealing and for permitted purposes and any excerpt or extract from, or reference to or reproduction of any copyright work has been disclosed expressly and sufficiently and the title of the Work and its authorship have been acknowledged in this Work;
- (4) I do not have any actual knowledge nor do I ought reasonably to know that the making of this work constitutes an infringement of any copyright work;
- (5) I hereby assign all and every rights in the copyright to this Work to the University of Malaya (“UM”), who henceforth shall be owner of the copyright in this Work and that any reproduction or use in any form or by any means whatsoever is prohibited without the written consent of UM having been first had and obtained;
- (6) I am fully aware that if in the course of making this Work I have infringed any copyright whether intentionally or otherwise, I may be subject to legal action or any other action as may be determined by UM.

Candidate’s Signature

Date:

Subscribed and solemnly declared before,

Witness’s Signature

Date:

Name:

Designation:

PROCESS IMPROVEMENT AND MICROBIAL CHARACTERISATION OF BIOLOGICAL NITROGEN REMOVAL FOR TROPICAL WASTEWATER WITH LOW CHEMICAL OXYGEN DEMAND/NITROGEN RATIO

ABSTRACT

Malaysia has one of the most established biological nitrogen removal in wastewater treatment plants (WWTPs) among the developing Southeast Asian countries. The current WWTPs' design and operating guidelines in Malaysia are mainly derived from other developed countries with more experiences in operating biological nitrogen removal. These design guidelines are good practices for WWTPs in the temperate climate region, but may not be optimal for the local wastewater characteristics and tropical climate in Malaysia. The local wastewater industry is keen to improve the design and operation of WWTPs to reduce the energy consumption and operating cost, which helps to foster a more cost-effective and sustainable industry. However, a complete understanding on the local wastewater conditions, such as the detailed characteristics and microbiology of tropical systems, are still lacking. This project aimed to develop an improved biological nitrogen removal in treating local wastewater. To achieve this aim, detailed wastewater characterisation were performed to formulate operating strategies for a low-cost biological nitrogen removal. The operating strategies were tested in lab-scale reactors. The microbial community were also investigated to understand the effects of these operating strategies on the microorganisms.

In the wastewater characterisation study, wastewater from six WWTPs in Kuala Lumpur was sampled to characterise their organic and nitrogen content. The results showed that soluble fraction of the tropical wastewater samples had low chemical oxygen demand-to-nitrogen ratio (COD/N). COD fractionation experiment further revealed that the readily-biodegradable COD (rbCOD) content was low, while slowly-biodegradable COD (sbCOD) from particulate settleable solids (PSS) in the wastewater

was the main source of biodegradable COD. The hydrolysis rate of PSS was accelerated in tropical temperatures ($30 \pm 2^\circ\text{C}$) to provide sbCOD for denitrification. Based on these wastewater characteristics, the low rbCOD content may be conducive for nitrification under low-dissolved-oxygen (low-DO) condition ($< 1 \text{ mg O}_2/\text{L}$) to reduce aeration energy. Also, sbCOD in the wastewater may be utilised to enhance the denitrification performance.

Batch experiments demonstrated active nitrification at low-DO concentration ($1 \text{ mg O}_2/\text{L}$). When low-DO nitrification ($0.9 \pm 0.1 \text{ mg O}_2/\text{L}$) was applied in a reactor, high ammonia removal efficiency ($93 \pm 6\%$) was achieved. Furthermore, utilising sbCOD in the post-anoxic stage of an oxic-anoxic (OA) reactor reduced the effluent nitrate concentration below the discharge limit in Malaysia. The recommended hydraulic retention time and sludge retention time (SRT) of the low-DO OA reactor developed in this study was 16 h and 20 d, respectively. Microbial analyses of the low-DO OA reactor showed that long SRT (20 d) promoted the growth of nitrifiers affiliated with *Nitrospira* to achieve a stable low-DO nitrification performance. Operating a low-DO OA process could reduce the WWTPs' energy consumption by 20% when compared with the existing process design.

A better understanding on the local wastewater conditions in this study, such as detailed characteristics and process microbiology, led to the development of a low-DO OA process. The low-DO OA process was an improved biological nitrogen removal in treating low COD/N tropical wastewater, which could help to encourage a more energy-efficient and cost-effective wastewater industry in Malaysia.

Keywords: hydrolysis, low-dissolved-oxygen, *Nitrospira*, post-anoxic, slowly-biodegradable COD

**PEMBAIKAN PROSES DAN PENCIRIAN MIKROORGANISMA UNTUK
PENYINGKIRAN NITROGEN SECARA BIOLOGI BAGI KUMBAHAN
TROIKA DENGAN NISBAH PERMINTAAN OKSIGEN KIMIA/NITROGEN
RENDAH**

ABSTRAK

Malaysia mempunyai salah satu sistem penyingkiran nitrogen secara biologi untuk loji rawatan kumbahan (WWTPs) yang termatang antara negara Asia Tenggara yang sedang membangun. Garis panduan untuk rekabentuk dan operasi WWTPs di Malaysia sebahagian besarnya diperolehi daripada negara-negara maju yang lebih berpengalaman dalam operasi penyingkiran nitrogen secara biologi. Garis panduan rekabentuk tersebut adalah amalan yang baik untuk WWTPs di kawasan iklim sederhana, tetapi mungkin tidak sesuai untuk ciri-ciri kumbahan tempatan dan iklim khatulistiwa di Malaysia. Industri kumbahan tempatan berminat untuk memperbaiki rekabentuk dan operasi WWTPs bagi mengurangkan penggunaan tenaga dan kos operasi, ia seterusnya akan memupuk sebuah industri yang lebih kos efektif dan mampan. Walau bagaimanapun, pengetahuan lengkap tentang ciri-ciri air kumbahan tempatan yang terperinci dan mikrobiologi dalam sistem tropika masih kekurangan. Projek ini bermatlamat untuk membangunkan penyingkiran nitrogen secara biologi yang lebih baik untuk merawat air kumbahan tempatan. Bagi mencapai matlamat tersebut, pencirian air kumbahan secara terperinci dijalankan untuk mencipta strategi-strategi operasi bagi penyingkiran nitrogen secara biologi yang berkos rendah. Strategi-strategi tersebut diuji dalam reaktor-reaktor berskala makmal. Komuniti mikroorganisma juga dikaji untuk memahami kesan-kesan strategi operasi terhadap struktur mikroorganisma.

Dalam kajian pencirian air kumbahan, sampel-sampel air kumbahan daripada enam WWTPs di Kuala Lumpur dikumpul bagi mencirikan kandungan bahan organik dan nitrogen. Keputusan analisis menunjukkan bahawa bahagian boleh larut kumbahan tropika yang disampel mempunyai nisbah permintaan oksigen kimia-ke-nitrogen

(COD/N) yang rendah. Eksperimen pemecahan COD juga menunjukkan bahawa kepekatan COD mudah dibiodegradasi (rbCOD) adalah rendah, manakala COD perlahan dibiodegradasi (sbCOD) daripada pepejal boleh mendap (PSS) dalam air kumbahan merupakan sumber COD boleh dibiodegradasi yang utama. Kadar hidrolisis PSS juga dipercepatkan pada suhu tropika ($30 \pm 2^\circ\text{C}$) untuk memekal sbCOD bagi proses pendenitritan. Berdasarkan ciri-ciri air kumbahan tersebut, kandungan rbCOD yang rendah mungkin kondusif untuk proses penitritan dalam keadaan oksigen larut rendah (low-DO) di bawah $1 \text{ mg O}_2/\text{L}$ bagi mengurangkan tenaga pengudaraan. Tambahan lagi, sbCOD dalam air kumbahan mungkin boleh diguna untuk meningkatkan prestasi proses pendenitritan.

Eksperimen kelompok berjaya menunjukkan penitritan yang aktif dalam keadaan low-DO ($1 \text{ mg O}_2/\text{L}$). Apabila strategi penitritan dalam keadaan low-DO ($0.9 \pm 0.1 \text{ mg O}_2/\text{L}$) digunapakai dalam sebuah reaktor, kecekapan penyingkiran ammonia yang tinggi ($93 \pm 6\%$) tercapai. Tambahan pula, penggunaan sbCOD dalam peringkat pasca-anoksik di sebuah reaktor oksik-anoksik (OA) menurunkan kepekatan nitrat dalam kumbahan terawat ke bawah had pembuangan di Malaysia. Masa pengekalan hidraulik dan masa pengekalan enapcemar (SRT) yang optimum adalah 16 jam dan 20 hari masing-masing untuk proses low-DO OA. Analisis mikroorganisma menunjukkan bahawa SRT yang panjang (20 hari) dalam reaktor low-DO OA merangsangkan penumbuhan bakteria penitritan berkait dengan *Nitrospira* untuk mencapai proses penitritan low-DO yang stabil. Proses low-DO OA mampu mengurangkan penggunaan tenaga sebanyak 20% berbanding dengan proses yang sedia ada.

Pemahaman ciri-ciri air kumbahan dan mikrobiologi proses rawatan kumbahan yang lebih lengkap dalam kajian ini telah meneraju pembangunan sebuah proses low-DO OA. Reaktor low-DO OA ini adalah penyingkiran nitrogen secara biologi yang diperbaiki

untuk merawat air kumbahan tropika yang mempunyai COD/N yang rendah, ianya boleh memupuk sebuah industri kumbahan di Malaysia yang lebih cekap dari segi penggunaan tenaga dan kos operasi.

Kata kunci: COD perlahan dibiodegradasi, DO rendah, hidrolisis, *Nitrospira*, pasca-anoksik

University of Malaya

ACKNOWLEDGEMENTS

First and foremost, I would like to thank my supervisors, Assoc. Prof. Ir. Dr. Adeline Chua Seak May and Assoc. Prof. Ir. Dr. Ngoh Gek Cheng, for their professional guidance throughout my PhD study. I wish to extend my gratitude to Prof. Thomas P. Curtis from Newcastle University, United Kingdom for offering his expertise and advice to improve my work.

Besides, I am thankful for the unwavering mental support from my family and friends, they helped me to get through the challenges that I faced in completing my PhD study. Their support gave me the strength to pursue my dream.

Let me also thank Ms. Lim Pek Boon, Mrs. Alijah Aris and all plant personnel from Indah Water Konsortium Sdn. Bhd. for coordinating sampling activities in the wastewater treatment plants.

Next, I would like to acknowledge the lab members in Bioprocess Laboratory for assisting in my PhD training and experiment work – Ms. Lim Shun Yue, Ms. Poh Phiak Kim, Mrs. Ainil Hawa, Dr. Tan Yee Tong and Mrs. Azira Idris. I am glad to have met the undergraduate research students who had lend me a hand in experiment setup as well – Mr. Go How Kean, Mrs. Najihah Roslee, Ms. Amira Armani, Ms. Sin Jia Huey and Ms. Sharon Wong Ying Ying.

I wish to express my appreciation to all the researchers abroad who had guided me in experiment works and manuscript preparation – Dr. Amy Bell, Dr. Mathew Brown, Dr. Matthew Wade, Dr. Tadashi Nittami and Dr. Tadashi Shoji.

Lastly, I am grateful for the PhD studentship financial assistance provided by University of Malaya Graduate Research Assistantship Scheme through Newton Advanced Fellowship (IF008-2016 / NA150341 / BH152910).

TABLE OF CONTENTS

Abstract	iii
Abstrak	v
Acknowledgements	viii
Table of Contents	ix
List of Figures	xvi
List of Tables.....	xxiii
List of Symbols and Abbreviations.....	xxvii
List of Appendices	xxxiv
CHAPTER 1: INTRODUCTION.....	1
1.1 Research Background	1
1.2 Problem Statement.....	2
1.3 Research Objectives.....	4
1.4 Structure of Thesis.....	5
CHAPTER 2: LITERATURE REVIEW.....	7
2.1 Wastewater Characteristics.....	7
2.1.1 Wastewater Parameters	7
2.1.1.1 Biochemical Oxygen Demand	7
2.1.1.2 Chemical Oxygen Demand Fractions	8
2.1.1.3 Total Organic Carbon and Dissolved Organic Carbon	10
2.1.1.4 Nitrogen Constituents.....	11
2.1.2 Tropical Wastewater Characteristics.....	12
2.1.3 Discharge Standards for Wastewater Treatment Plant's Effluent.....	14

2.2	The Nitrogen Cycle.....	14
2.3	Microbial Communities of Biological Nitrogen Removal	18
2.3.1	Ammonia-Oxidising Bacteria.....	18
2.3.2	Nitrite-Oxidising Bacteria	19
2.3.3	Complete Ammonia Oxidisers	20
2.3.4	Denitrifying Ordinary Heterotrophic Organisms	21
2.3.5	Detection Methods Based on Phylogenetic and Functional Gene Markers	23
2.3.5.1	16S Ribosomal Ribonucleic Acid Amplicon Sequencing.....	23
2.3.5.2	Quantitative Polymerase Chain Reaction.....	24
2.3.5.3	Fluorescence <i>in situ</i> Hybridisation and Quantitative Fluorescence <i>in situ</i> Hybridisation.....	26
2.4	Operating Conditions Influencing Biological Nitrogen Removal Performance....	27
2.4.1	Effect of Dissolved Oxygen on Nitrification	27
2.4.2	Effect of Biodegradable Chemical Oxygen Demand Fractions on Denitrification	29
2.4.2.1	Utilisation of Soluble Biodegradable Chemical Oxygen Demand	30
2.4.2.2	Mechanism of Utilisation of Particulate Biodegradable Chemical Oxygen Demand	30
2.4.2.3	Operating Strategies of Biological Nitrogen Removal in Treating Low Chemical Oxygen Demand-to-Nitrogen Wastewater	33
2.4.3	Effect of Hydraulic Retention Time and Organic Volumetric Loading Rate on Biological Nitrogen Removal	34

2.4.4	Effect of Sludge Retention Time and Food-to-Microbe Ratio on Biological Nitrogen Removal.....	35
2.5	Biological Nitrogen Removal Configurations for Wastewater Treatment.....	36
2.5.1	Pre-Anoxic Configurations.....	36
2.5.2	Post-Anoxic Configurations.....	41
2.5.3	Novel Configurations for Biological Nitrogen Removal.....	44
2.6	Summary of Chapter.....	46
CHAPTER 3: MATERIALS AND METHODS		47
3.1	Wastewater and Sludge Sampling.....	47
3.2	Fractionation of Chemical Oxygen Demand.....	48
3.2.1	Anoxic Yield Coefficient Determination Experiment.....	48
3.2.2	Nitrate Uptake Rate Experiment.....	49
3.2.3	Calculation of Readily-Biodegradable Chemical Oxygen Demand and Slowly-Biodegradable Chemical Oxygen Demand from Nitrate Uptake Rate Profiles.....	49
3.3	Estimation of Particulate Settleable Solids Hydrolysis Kinetic Coefficients at Tropical Temperature (30°C).....	50
3.3.1	Oxygen Uptake Rate Experiment.....	51
3.3.2	Calculation of Measured Oxygen Uptake Rate.....	52
3.3.3	Model Fitting of Activated Sludge Model 1 to Oxygen Uptake Rate Profiles.....	52
3.4	Batch Denitrification Activity Experiment Using Different Chemical Oxygen Demand Fractions as Carbon Source.....	54
3.5	Assessment of the Effect of Dissolved Oxygen on Sludge Nitrification Activity.....	55
3.5.1	Batch Nitrification Activity Experiment.....	55

3.5.2	Calculation of Specific Ammonia Uptake Rate and Model Fitting of Saturation Kinetic to Specific Ammonia Uptake Rate Profile.....	56
3.6	Lab-Scale Sequencing Batch Reactors Operation	56
3.6.1	Low-Dissolved-Oxygen Nitrification Sequencing Batch Reactor	57
3.6.1.1	Sequencing Batch Reactor Operation	57
3.6.1.2	Estimation of Energy Saving of Low-Dissolved-Oxygen Nitrification Process	58
3.6.2	Anoxic-Oxic Sequencing Batch Reactor.....	61
3.6.3	Low-Dissolved-Oxygen Oxidic-Anoxic Sequencing Batch Reactors	62
3.6.3.1	Parent Oxidic-Anoxic Sequencing Batch Reactor (OA-1).....	63
3.6.3.2	Parallel Oxidic-Anoxic Sequencing Batch Reactor (OA-2).....	64
3.7	Chemical Analyses of Wastewater Samples.....	65
3.7.1	Mixed Liquor Suspended Solids and Mixed Liquor Volatile Suspended Solids	65
3.7.2	Ammonium Ion, Nitrite Ion and Nitrate Ion	66
3.7.3	Dissolved Organic Carbon and Total Nitrogen.....	67
3.7.4	Chemical Oxygen Demand	67
3.8	Nitrifying and Denitrifying Microbial Community Analyses	67
3.8.1	Genomic Deoxyribonucleic Acid Extraction	67
3.8.2	Sequencing Library Template Preparation and Next-Generation Sequencing	68
3.8.2.1	Ion Torrent Workflow	68
3.8.2.2	Illumina MiSeq Workflow	69
3.8.3	Post-Sequencing Bioinformatics Analyses	69
3.8.3.1	Workflow for Ion Torrent Output Files.....	70
3.8.3.2	Workflow for Illumina MiSeq Output Files.....	70

3.8.4	Quantitative Polymerase Chain Reaction	71
3.8.5	Fluorescence <i>in situ</i> Hybridisation	75
CHAPTER 4: CHARACTERISATION OF TROPICAL WASTEWATER.....		77
4.1	Wastewater Temperature, pH, Suspended Solids, Chemical Oxygen Demand and Nitrogen Concentrations	77
4.2	Fractions of Wastewater Biodegradable Chemical Oxygen Demand	79
4.3	Particulate Settleable Solids Hydrolysis Kinetic Coefficients.....	84
4.4	Biodegradability of Particulate Settleable Solids in Batch Denitrification Activity Experiment.....	87
4.5	Summary of Chapter.....	91
CHAPTER 5: POTENTIAL AND FEASIBILITY OF LOW-DISSOLVED-OXYGEN NITRIFICATION FOR TROPICAL WASTEWATER TREATMENT		93
5.1	Effect of Dissolved Oxygen on Seed Sludge Nitrification Performance	93
5.2	Performance of Low-Dissolved-Oxygen Nitrification Sequencing Batch Reactor	95
5.2.1	Chemical Oxygen Demand and Ammoniacal Nitrogen Removal Efficiency	95
5.2.2	Rate of Nitrification.....	99
5.3	Proportional Abundance of Nitrifiers and Denitrifiers in Low-Dissolved-Oxygen Nitrification Sequencing Batch Reactor	100
5.4	Energy Savings of Low-Dissolved-Oxygen Nitrification Process	108
5.5	Summary of Chapter.....	109

CHAPTER 6: PROCESS IMPROVEMENT OF A CONVENTIONAL ANOXIC-OXIC PROCESS IN TREATING TROPICAL WASTEWATER 111

6.1 Nitrogen Removal Performance of Anoxic-Oxic Sequencing Batch Reactor..... 111

6.2 Nitrogen Removal Performance in OA-1 Parent Sequencing Batch Reactor 118

6.3 Effect of Sludge Retention Time and Hydraulic Retention Time on Low-Dissolved-Oxygen Oxidic-Anoxic Process 123

6.4 Changes in Populations of the Sludge Microbial Community 135

6.4.1 Microbial Community in the Anoxic-Oxic Sequencing Batch Reactor . 135

6.4.1.1 Nitrifying and Denitrifying Bacteria Population Using Quantitative Polymerase Chain Reaction Analysis..... 135

6.4.1.2 *Nitrospira* Community Analysis by 16S Ribosomal Ribonucleic Acid and β -Subunit Nitrite Oxidoreductase Gene Amplicon Sequencing 138

6.4.2 Microbial Community in OA-1 and OA-2 Sequencing Batch Reactors 144

6.4.2.1 Overview of Microbial Community by 16S Ribosomal Ribonucleic Acid Amplicon Sequencing 144

6.4.2.2 16S Ribosomal Ribonucleic Acid-Based Analysis of *Nitrospira* Community 148

6.4.2.3 Quantification of Ammonia-Oxidizing Bacteria and *Nitrospira* by Quantitative Polymerase Chain Reaction Analysis..... 151

6.5 Estimation of Operating Cost Reduction of Low-Dissolved-Oxygen Oxidic-Anoxic Process 157

6.6 Summary of Chapter 159

CHAPTER 7: CONCLUSIONS AND RECOMMENDATIONS 162

7.1 Conclusions 162

7.2	Novelties and Implications of Study	164
7.3	Recommendations for Future Works.....	165
	References	166
	List of Publications and Papers Presented	182
	Appendix A: Photos of Sequencing Batch Reactors' Setup	188
	Appendix B: Nitrate Uptake Rate Profiles of All Samples Taken From Wastewater Treatment Plants.....	189
	Appendix C: Raw Data for Batch Denitrification Activity Experiment	190
	Appendix D: Raw Data for Batch Nitrification Activity Experiment	192
	Appendix E: Raw Data for Low-Dissolved-Oxygen Nitrification Sequencing Batch Reactor Operation	195
	Appendix F: Raw Data for Anoxic-Oxic Sequencing Batch Reactor Operation.....	196
	Appendix G: Raw Data for OA-1 Sequencing Batch Reactor Operation.....	200
	Appendix H: Raw Data for OA-2 Sequencing Batch Reactor Operation.....	205

LIST OF FIGURES

Figure 2.1	Fractions of COD adapted from Henze, van Loosdrecht, Ekama, and Brdjanovic (2008) and Tchobanoglous et al. (2014).	9
Figure 2.2	Example of a time series plot of NO_3^- of NUR test adapted from Naidoo et al. (1998) and van Loosdrecht et al. (2016).	10
Figure 2.3	The nitrogen cycle adapted from Stein and Klotz (2016) depicting the microbial nitrogen transformations in five processes. 1 – Nitrogen fixation, 2 – assimilatory nitrite reduction to ammonia (ANRA) or dissimilatory nitrite reduction to ammonia (DNRA), 3 – nitrification, 4 – denitrification, 5 – anammox.	15
Figure 2.4	Nitrification pathway with the functional genes indicated below the arrows.	19
Figure 2.5	Denitrification pathway with the functional genes indicated below the arrows.	22
Figure 2.6	Plot of fluorescence intensity versus qPCR cycle to determine C_q values adapted from van Loosdrecht et al. (2016).	25
Figure 2.7	Models of transport and fate of organic substrate in wastewater adopted from (A) Activated Sludge Model 1 (ASM1) and (B) Activated Sludge Model 3 (ASM3).	31
Figure 2.8	Modified ASM1 with the product of cell decay decoupled from PSS in the wastewater.	32
Figure 2.9	The configuration of a MLE process.	37
Figure 2.10	The configuration of step-feed biological nitrogen removal.	40
Figure 2.11	The configuration of a Wuhrmann biomass decayer.	42

Figure 2.12	The configuration of a Bardenpho process.	43
Figure 3.1	An example $\text{NO}_x\text{-N}$ time profile indicating the y-intercepts a_{rbCOD} , a_{sbCOD} and a_{endo} adapted from Naidoo et al. (1998) and van Loosdrecht et al. (2016).	50
Figure 3.2	Setup of OUR experiment.	51
Figure 3.3	Setup of low-DO nitrification SBR.	58
Figure 3.4	Setup of AO and low-DO OA SBRs.	61
Figure 4.1	Determination of $Y_{OHO,ox}$ from the $\text{NO}_3\text{-N}$ and COD profiles.	80
Figure 4.2	Quantification of rbCOD and sbCOD from the $\text{NO}_x\text{-N}$ profile of NUR experiment.	80
Figure 4.3	COD fractions from wastewater fractionation experiments.	81
Figure 4.4	Fraction of rbCOD, sbCOD and bCOD relative to TCOD and (B) COD/TN ratios, the horizontal dash (– –) line corresponds to theoretical COD consumption per $\text{NO}_3\text{-N}$ reduced (4.2 g COD/g $\text{NO}_3\text{-N}$).	83
Figure 4.5	Measured and fitted OUR profiles from PSS hydrolysis kinetic parameter determination experiment. (A) WWTP 1, (B) WWTP 2, (C) WWTP 3, (D) WWTP 4, (E) WWTP 5 and (F) WWTP 6. r_H represents the PSS hydrolysis rate.	87
Figure 4.6	$\text{NO}_x\text{-N}$ and sCOD profiles for denitrification batch experiment using (A) filtered wastewater, (B) PSS in nutrient solution and (C) nutrient solution. sCOD data was not shown for set B and set C because the source of biodegradable organics for denitrification was not soluble.	89

Figure 5.1	The effect of DO on SAUR of the seed sludge from WWTP 1. The round markers denote the SAUR data determined from batch kinetic experiments while the solid line represents the saturation kinetic model fitted to the data.	94
Figure 5.2	Detailed profiles of (A) DO concentration, (B) pH, (C) NH ₄ -N, NO ₃ -N & NO ₂ -N concentrations and (D) sCOD concentrations on day 36 of SBR operation. DO concentration was below 0.5 mg/L throughout the reaction cycle, nitrification commenced only after sCOD had been depleted.	96
Figure 5.3	Overall sCOD profile of low-DO nitrification SBR.	96
Figure 5.4	Overall NH ₄ -N profile of low-DO nitrification SBR.	97
Figure 5.5	Overall NO ₃ -N profile of low-DO nitrification SBR.	98
Figure 5.6	Profiles of rates of accumulation for NH ₄ -N and NO ₃ -N throughout SBR operation.	100
Figure 5.7	Population dynamics of significant OTUs present in the low-DO nitrification SBR.	101
Figure 5.8	FISH images of fixed cell sample on day 43 showing total bacteria hybridised with probe EUBMIX (green) together with (A) & (B) betaproteobacterial AOB hybridised with probe Nso1225 (yellow) and (C) <i>Nitrospira</i> -related NOB hybridised with probe Ntspa662 (yellow). Scale bar in each image denotes 10 µm.	102
Figure 5.9	Neighbour-joining phylogenetic tree of the <i>Nitrospira sp.</i> 16S rRNA gene sequences showing the relationship (A) amongst all 223 OTUs belong to genus <i>Nitrospira</i> from this study, and (B) between the representative sequences of <i>Nitrospira sp.</i> (marked with *) obtained from the low-DO nitrification SBR and reference sequences in the GenBank database. All bootstrap values were shown in percentages of 1000 replicates. The heat map depicts the changes in percentage read abundance of Group A and Group B <i>Nitrospira</i> .	105

Figure 6.1	Detailed profiles of NH ₄ -N, NO ₃ -N and DOC in selected SBR cycles during (A) P1 on day 64; (B) P2 on day 113; (C) P3 on day 190 and (D) P4 on day 267.	112
Figure 6.2	Detailed profiles of pH and DO in selected SBR cycles during (A) P1 on day 64; (B) P2 on day 113; (C) P3 on day 190 and (D) P4 on day 267.	112
Figure 6.3	Overall MLSS and MLVSS profiles of AO SBR.	113
Figure 6.4	Overall sCOD profile of AO SBR.	113
Figure 6.5	Overall NH ₄ -N profile of AO SBR.	114
Figure 6.6	Overall NO ₃ -N profile of AO SBR.	114
Figure 6.7	Detailed profiles of NH ₄ -N, NO ₃ -N and DOC in OA-1 parent SBR during (A) P1 on day 63; (B) P2 on day 73 and (C) P3 on day 87.	119
Figure 6.8	Detailed profiles of pH and DO in OA-1 parent SBR during (A) P1 on day 63; (B) P2 on day 73 and (C) P3 on day 87.	120
Figure 6.9	Overall MLSS and MLVSS profiles of OA-1 parent SBR operation from P1 to P3.	120
Figure 6.10	Overall sCOD profile of OA-1 parent SBR operation from P1 to P3.	121
Figure 6.11	Overall NH ₄ -N profile of OA-1 parent SBR operation from P1 to P3.	121
Figure 6.12	Overall NO ₃ -N of OA-1 parent SBR operation from P1 to P3.	122
Figure 6.13	Detailed profiles of NH ₄ -N, NO ₃ -N and DOC of OA-1 during (A) P4 on day 43; (B) P5 on day 99 and (C) P6 on day 162.	126

Figure 6.14	Detailed profiles of NH ₄ -N, NO ₃ -N and DOC of OA-2 during (A) P4 on day 43; (B) P5 on day 99 and (C) P6 on day 162.	126
Figure 6.15	Detailed profiles of pH and DO of OA-1 during (A) P4 on day 43; (B) P5 on day 99 and (C) P6 on day 162.	127
Figure 6.16	Detailed profiles of pH and DO of OA-2 during (A) P4 on day 43; (B) P5 on day 99 and (C) P6 on day 162.	127
Figure 6.17	Overall MLSS and MLVSS profiles of (A) OA-1 and (B) OA-2 during optimisation operation P4 to P6.	128
Figure 6.18	Overall sCOD profile of (A) OA-1 and (B) OA-2 during optimisation operation P4 to P6.	129
Figure 6.19	Overall NH ₄ -N profile of (A) OA-1 and (B) OA-2 during optimisation operation P4 to P6.	130
Figure 6.20	Overall NO ₃ -N profile of (A) OA-1 and (B) OA-2 during optimisation operation P4 to P6.	131
Figure 6.21	(A) Relative abundance of betaproteobacterial AOB and <i>Nitrospira sp.</i> to the total bacteria population and (B) normalised abundance of <i>nirS</i> and <i>nosZ</i> to the bacterial 16S rRNA gene copy number throughout the four operating phases.	137
Figure 6.22	Vertical bar plot of the 25 most abundant genera in (A) the seed sludge (day 1) and (B) the low-DO AOA sludge (day 270) sorted based on their read abundance.	139
Figure 6.23	FISH images of low-DO AOA sludge on day 270 after hybridisation with FISH probes targeting bacteria (EUB338-MIX, green) and group-specific probes: (A) & (B) betaproteobacterial AOB (Nso1225, yellow) and (C) & (D) <i>Nitrospira</i> -related NOB (Ntspa662, yellow). The scale bar represents 10 µm.	140

Figure 6.24	Neighbour-joining tree based on the <i>Nitrospira</i> 16S rRNA sequences showing the phylogenetic relationships of the OTUs with the reference sequences in GenBank database, rooting with <i>Nitrosomonas</i> -related AOB. Bootstrap values are shown in percentages of 1000 replicates. The heat map depicts the percentage read abundance of the OTUs on day 1 and day 270 of the AO SBR operation.	141
Figure 6.25	Neighbour-joining tree based on the <i>nxrB</i> sequences showing the phylogenetic relationships of the OTUs with reference sequences in the GenBank database. Bootstrap values are shown in percentages of 1000 replicates. The heat map depict the read abundance of the OTUs on day 1 and day 270 of the SBR operation.	142
Figure 6.26	Percentage read abundance for the top 25 most abundant taxa in the seed sludge (SRT = 20 d, HRT = 24 h), OA-1 sludge (SRT = 20 d, HRT = 16 h) and OA-2 sludge (SRT = 10 d, HRT = 16 h) samples.	145
Figure 6.27	Neighbour-joining tree based on the <i>Nitrospira</i> 16S rRNA sequences showing the phylogenetic relationships of the OTUs with reference sequences in the GenBank database, rooting with <i>Nitrosomonas oligotropha</i> . Bootstrap values are shown in percentages of 1000 replicates. The heat map depicts the changes in percentage read abundance of each OTU in OA-1 and OA-2 from P1 to P6.	149
Figure 6.28	Relative abundance of betaproteobacterial AOB and <i>Nitrospira sp.</i> to the total bacteria population in (A) OA-1 from P1 to P3; (B) OA-1 from P4 to P6 and (C) OA-2 from P4 to P6.	153
Figure 6.29	Relative abundance of comammox and <i>Ca. Nitrospira nitrosa</i> to the total <i>Nitrospira</i> population in (A) OA-1 from P1 to P3; (B) OA-1 from P4 to P6 and (C) OA-2 from P4 to P6.	155
Figure A1	Photo of the setup for low-DO nitrification and OA-1 SBR.	188
Figure A2	Photo of the setup for AO and OA-2 SBR.	188

Figure B1 Representative NO_x-N uptake profiles from (A) WWTP 2, (B) 189
WWTP 3, (C) WWTP 4, (D) WWTP 5 and (E) WWTP 6.

University of Malaya

LIST OF TABLES

Table 2.1	Average composition of the wastewater in Malaysia, Singapore, Europe and United States (Cao et al., 2008; Henze, Harremoës, la Cour Jansen, & Arvin, 1997; Lee et al., 2010; Tchobanoglous et al., 2014)	13
Table 2.2	Discharge limits for NH ₄ -N and NO ₃ -N stipulated in Environmental Quality (Sewage) Regulation 2009 (Department of Environment, 2009)	14
Table 2.3	Process characteristics of pre-anoxic configurations (National Water Services Commission, 2009; Tchobanoglous et al., 2014)	38
Table 2.4	Advantages and disadvantages of the pre-anoxic configurations	40
Table 2.5	Process characteristics of post-anoxic configurations (Maryland Department of the Environment, 2016; Tchobanoglous et al., 2014; Wuhrmann, 1964)	42
Table 2.6	Advantages and disadvantages of the post-anoxic configurations	44
Table 3.1	Details of the six WWTPs in the Greater Kuala Lumpur region	48
Table 3.2	Process kinetics and stoichiometry for the modified ASM1 model fitting to OUR profiles (Gujer et al., 1999; Henze et al., 1987)	53
Table 3.3	Value of constants adopted for energy saving calculation (Tchobanoglous et al., 2014)	60
Table 3.4	Operating conditions of each phase for the lab-scale SBR	62
Table 3.5	Operating conditions of OA-1 in the 100-day start-up period	64

Table 3.6	Operating conditions of OA-1 and OA-2 SBRs in the 180-day optimisation study of the effect of HRT and SRT on the low-DO OA process performance	65
Table 3.7	Information of qPCR primers used in the study	72
Table 3.8	Number of gene copy per cell for the targeted genes in qPCR analysis	75
Table 3.9:	Information of FISH probe used in the study	76
Table 4.1	Mean wastewater temperature, pH, MLSS, COD and nitrogen data of each WWTP	78
Table 4.2	Mean wastewater rbCOD and sbCOD of each WWTP	81
Table 4.3	Kinetic parameter sensitivity ranking of modified ASM1 model	85
Table 5.1	Estimated energy required for aeration in conventional and low-DO nitrification process	109
Table 6.1	Comparison of operating conditions and effluent quality at steady-state during (A) OA-1 parent reactor operation, (B) OA-1 optimisation operation and (C) OA-2 optimisation operation	134
Table 6.2	Percentage read abundance of taxa related to hydrolysis of PSS in OA SBRs	146
Table 6.3	Estimation of energy cost reduction of low-DO OA process when compared with conventional AO process with equipment energy usage breakdown adapted from Ramli and Abdul Hamid (2017) and Sedlak (2018)	158
Table C1	pH, NO ₂ -N, NO ₃ -N and sCOD data for batch denitrification activity experiment using filtered wastewater	190

Table C2	Temperature, pH, NO ₂ -N and NO ₃ -N data for batch denitrification activity experiment using PSS in nutrient solution	190
Table C3	Temperature, pH, NO ₂ -N and NO ₃ -N data for batch denitrification activity experiment using blank nutrient solution	191
Table D1	Temperature, pH, NH ₄ -N, NO ₂ -N and NO ₃ -N data for batch nitrification activity experiment for DO = 0.35 ± 0.12 mg/L	192
Table D2	Temperature, pH, NH ₄ -N, NO ₂ -N and NO ₃ -N data for batch nitrification activity experiment for DO = 1.36 ± 0.17 mg/L	192
Table D3	Temperature, pH, NH ₄ -N, NO ₂ -N and NO ₃ -N data for batch nitrification activity experiment for DO = 2.32 ± 0.15 mg/L	193
Table D4	Temperature, pH, NH ₄ -N, NO ₂ -N and NO ₃ -N data for batch nitrification activity experiment for DO = 3.31 ± 0.17 mg/L	193
Table D5	Temperature, pH, NH ₄ -N, NO ₂ -N and NO ₃ -N data for batch nitrification activity experiment for DO = 5.26 ± 0.13 mg/L	194
Table D6	Temperature, pH, NH ₄ -N, NO ₂ -N and NO ₃ -N data for batch nitrification activity experiment for DO = 6.30 ± 0.12 mg/L	194
Table D7	Temperature, pH, NH ₄ -N, NO ₂ -N and NO ₃ -N data for batch nitrification activity experiment without air sparging for aeration (DO ≈ 0)	194
Table E1	MLSS, MLVSS, sCOD, NH ₄ -N, NO ₂ -N, NO ₃ -N and TN data for low-DO nitrification SBR operation	195
Table F1	MLSS, MLVSS, sCOD, NH ₄ -N, NO ₂ -N, NO ₃ -N and TN data for AO SBR operation during P1	196
Table F2	MLSS, MLVSS, sCOD, NH ₄ -N, NO ₂ -N, NO ₃ -N and TN data for AO SBR operation during P2	197

Table F3	MLSS, MLVSS, sCOD, NH ₄ -N, NO ₂ -N, NO ₃ -N and TN data for AO SBR operation during P3	198
Table F4	MLSS, MLVSS, sCOD, NH ₄ -N, NO ₂ -N, NO ₃ -N and TN data for AO SBR operation during P4	199
Table G1	MLSS, MLVSS, sCOD, NH ₄ -N, NO ₂ -N, NO ₃ -N and TN data for OA-1 SBR operation during P1	200
Table G2	MLSS, MLVSS, sCOD, NH ₄ -N, NO ₂ -N, NO ₃ -N and TN data for OA-1 SBR operation during P2	201
Table G3	MLSS, MLVSS, sCOD, NH ₄ -N, NO ₂ -N, NO ₃ -N and TN data for OA-1 SBR operation during P3	201
Table G4	MLSS, MLVSS, sCOD, NH ₄ -N, NO ₂ -N, NO ₃ -N and TN data for OA-1 SBR operation during P4	202
Table G5	MLSS, MLVSS, sCOD, NH ₄ -N, NO ₂ -N, NO ₃ -N and TN data for OA-1 SBR operation during P5	203
Table G6	MLSS, MLVSS, sCOD, NH ₄ -N, NO ₂ -N, NO ₃ -N and TN data for OA-1 SBR operation during P6	204
Table H1	MLSS, MLVSS, sCOD, NH ₄ -N, NO ₂ -N, NO ₃ -N and TN data for OA-2 SBR operation during P4	205
Table H2	MLSS, MLVSS, sCOD, NH ₄ -N, NO ₂ -N, NO ₃ -N and TN data for OA-2 SBR operation during P5	206
Table H3	MLSS, MLVSS, sCOD, NH ₄ -N, NO ₂ -N, NO ₃ -N and TN data for OA-2 SBR operation during P6	207

LIST OF SYMBOLS AND ABBREVIATIONS

Symbol / Abbreviation	Definition	Unit
A ₂ O	Anaerobic-anoxic-oxic	
<i>amo</i>	Ammonia monooxygenase gene	
<i>amoA</i>	α-subunit of ammonia monooxygenase gene	
<i>amoB</i>	β-subunit of ammonia monooxygenase gene	
Anammox	Anaerobic ammonia oxidation	
ANI	Average nucleotide identity	%
ANRA	Assimilatory nitrite reduction to ammonia	
AO	Anoxic-oxic	
AOA	Anoxic-oxic-anoxic	
AOB	Ammonia-oxidising bacteria	
ASM1	Activated Sludge Model 1	
ASM3	Activated Sludge Model 3	
AUR	Ammonia uptake rate	mg N/L·h
bCOD	Biodegradable chemical oxygen demand	mg/L
bCOD/TN	Biodegradable chemical oxygen demand-to-total nitrogen ratio	g COD/g N
<i>b_H</i>	Aerobic endogenous respiration of heterotrophic organisms	1/h
BLAST	Basic Local Alignment Search Tool	
BOD	Biochemical oxygen demand	
BOD ₅	5-day biochemical oxygen demand	
<i>C_{∞20}</i>	Saturated DO concentration at sea level and standard temperature (20°C) by diffused aeration	mg/L

Symbol / Abbreviation	Definition	Unit
C_{s20}^*	Saturated DO concentration at sea level and standard temperature (20°C)	mg/L
C_{st}^*	Saturated DO concentration at site temperature (30°C)	mg/L
CAS	Conventional activated sludge	
COD	Chemical oxygen demand	mg/L
COD/N	Chemical oxygen demand-to-nitrogen ratio	g COD/g N
Comammox	Complete ammonia oxidisers	
C_q	Threshold cycle	
DNA	Deoxyribonucleic acid	
DNRA	Dissimilatory nitrite reduction to ammonia	
DO	Dissolved oxygen	mg/L
DO_0	Dissolved oxygen concentration in previous tank	mg/L
DOC	Dissolved organic carbon	mg/L
DOHOs	Denitrifying ordinary heterotrophic organisms	
EA	Extended aeration	
F	Fouling factor for air diffuser	dimensionless
F/M	Food-to-microbe ratio	g BOD/g MLVSS·d
f_d	Fraction of cell mass as cell debris	dimensionless
FISH	Fluorescence <i>in situ</i> hybridisation	
f_p	Fraction of non-biodegradable decayed biomass	dimensionless
g	Gravitational acceleration constant	m/s ²
<i>hao</i>	Hydroxylamine oxidoreductase gene	
HRT	Hydraulic retention time	h

Symbol / Abbreviation	Definition	Unit
k_d	Endogenous decay coefficient for heterotrophs	1/d
k_{dn}	Endogenous decay coefficient for nitrifiers	1/d
k_H	Particulate settleable solids hydrolysis rate constant	1/h
K_O	Dissolved oxygen half-velocity constant for nitrification	mg/L
K_S	Saturation constant for readily-biodegradable chemical oxygen demand	mg/L
K_X	Particulate settleable solids hydrolysis saturation constant	g COD/g COD
Low-DO	Low-dissolved-oxygen	
L_{org}	Organic volumetric loading rate	kg BOD ₅ /m ³ ·d
M	Ideal gas molar volume	g/g·mol
MLE	Modified Ludzack-Ettinger	
MLR	Mixed liquor recycle	
MLSS	Mixed liquor suspended solids	mg/L
MLVSS	Mixed liquor volatile suspended solids	mg/L
MLSS/MLVSS	Ratio of mixed liquor volatile suspended solids to mixed liquor suspended solids	g MLVSS/g MLSS
MSIG	Malaysian Sewerage Industry Guidelines	
N ₂	Nitrogen gas	
N ₂ H ₄	Hydrazine	
N ₂ O	Nitrous oxide	
<i>nar / nap</i>	Nitrate reductase genes	
nbCOD	Non-biodegradable chemical oxygen demand	mg/L
NCBI	National Center for Biotechnology Information	

Symbol / Abbreviation	Definition	Unit
NGS	Next generation sequencing	
NH ₂ OH	Hydroxylamine	
NH ₃	Free ammonia	
NH ₄ ⁺	Ammonium	
NH ₄ -N	Ammoniacal nitrogen	mg/L
<i>nirS</i> / <i>nirK</i>	Nitrite reductase gene	
NO	Nitric oxide	
NO ₂ ⁻	Nitrite	
NO ₂ -N	Nitrite nitrogen	mg/L
NO ₃ ⁻	Nitrate	
NO ₃ -N	Nitrate nitrogen	mg/L
NOB	Nitrite-oxidising bacteria	
<i>nor</i>	Nitric oxide reductase gene	
<i>nosZ</i>	Nitrous oxide reductase gene	
NO _x -N	Sum of nitrite nitrogen and nitrate nitrogen	mg/L
NUR	Nitrate uptake rate	
<i>nxr</i>	Nitrite oxidoreductase gene	
<i>nxB</i>	β-subunit of nitrite oxidoreductase gene	
OA	Oxic-anoxic	
OTR	Oxygen transfer rate	kg O ₂ /d
OTR _{LIQUID}	Oxygen transfer rate to maintain bulk dissolved oxygen level in mixed liquor	kg O ₂ /d
OTR _{TOTAL}	Total oxygen transfer rate	kg O ₂ /d
OTU	Operational taxonomic unit	
OUR	Oxygen uptake rate	mg O ₂ /L·h

Symbol / Abbreviation	Definition	Unit
P_a	Standard barometric pressure	kPa
P_b	Barometric pressure at site elevation	kPa
PCR	Polymerase chain reaction	
PE	Population equivalent	
PSS	Particulate settleable solids	
$P_{X,bio}$	Rate of biomass wasted	kg VSS/d
Q	Influent flow rate	m ³ /d
QIIME	Quantitative Insights Into Microbial Ecology	
qPCR	Quantitative polymerase chain reaction	
Q_{RAS}	Recycle activated sludge flow rate	
Q_w	Waste sludge flow rate	
R	Ideal gas constant	kg·m ² /s ² ·kg·mol·K
RAS	Recycle activated sludge	
rbCOD	Readily-biodegradable chemical oxygen demand	mg/L
rbCOD/TN	Readily-biodegradable chemical oxygen demand-to-total nitrogen ratio	g COD/g N
r_H	Rate of particulate settleable solids hydrolysis	mg COD/L·h
r_{NH}	Rate of nitrification	
$r_{NH,max}$	Maximum nitrification rate	
rRNA	Ribosomal ribonucleic acid	
R_O	Oxygen transfer rate to maintain biological activities	kg O ₂ /d
S	Effluent biodegradable chemical oxygen demand	mg/L
SAUR	Specific ammonia uptake rate	mg N/g MLVSS·h

Symbol / Abbreviation	Definition	Unit
SAUR _{max}	Maximum specific ammonia uptake rate	mg N/g MLVSS·h
sbCOD	Slowly-biodegradable chemical oxygen demand	mg/L
SBR	Sequencing batch reactor	
sCOD	Soluble chemical oxygen demand	mg/L
sCOD/TN	Soluble chemical oxygen demand-to-total nitrogen ratio	g COD/g N
S_i	Influent biodegradable chemical oxygen demand	mg/L
S_{ij}	Sensitivity of model state variables towards change in parameter	dimensionless
SND	Simultaneous nitrification-denitrification	
S_o	Dissolved oxygen concentration in wastewater	mg/L
SOTR	Standard oxygen transfer rate	kg O ₂ /d
SRA	Sequence read archive	
SRT	Sludge retention time	d
S_s	Readily-biodegradable chemical oxygen demand concentration	mg/L
T	Wastewater temperature	°C
TCOD	Total chemical oxygen demand	mg/L
TCOD/TN	Total chemical oxygen demand-to-total nitrogen ratio	g COD/g N
TKN	Total Kjeldahl Nitrogen	mg/L
TN	Total nitrogen	mg/L
TOC	Total organic carbon	
<i>TrHB2</i>	2/2 haemoglobin type II gene	
V	Volume of reactor	L

Symbol / Abbreviation	Definition	Unit
WWTPs	Wastewater treatment plants	
X	Sludge concentration in the reaction tank	
X_e	Sludge concentration in the effluent	
X_H	Heterotrophic bacteria concentration	mg COD/L
X_I	Concentration of inert decayed products of heterotrophic bacteria	mg COD/L
X_R	Sludge concentration in the recycle activated sludge stream	
X_S	Slowly-biodegradable chemical oxygen demand concentration	mg/L
Y	Biomass yield from biodegradable chemical oxygen demand	g MLVSS/g BOD
Y_H	Heterotrophic growth yield	g COD/g COD
Y_n	Biomass yield from nitrogen	g MLVSS/g N
$Y_{OHO,ax}$	Anoxic yield coefficient	g COD/g COD
z_a	Sea level elevation	m
z_b	Site elevation	m
α	Mass transfer coefficient correction factor between wastewater and tap water	dimensionless
β	Saturation DO correction factor between wastewater and tap water	dimensionless
δ_j^{msqr}	Root mean square of j^{th} column in sensitivity analysis	dimensionless
μ_H	Maximum heterotrophic growth rate	1/h
$\sigma_{meas,i}$	Standard deviation of i^{th} measured data point	dimensionless
χ^2	Sum of squares of deviations	dimensionless

LIST OF APPENDICES

Appendix A	Photos of Sequencing Batch Reactors' Setup	190
Appendix B	Nitrate Uptake Rate Profiles of All Samples Taken From Wastewater Treatment Plants	191
Appendix C	Raw Data for Batch Denitrification Activity Experiment	192
Appendix D	Raw Data for Batch Nitrification Activity Experiment	194
Appendix E	Raw Data for Low-Dissolved-Oxygen Nitrification Sequencing Batch Reactor Operation	197
Appendix F	Raw Data for Anoxic-Oxic Sequencing Batch Reactor Operation	198
Appendix G	Raw Data for OA-1 Sequencing Batch Reactor Operation	202
Appendix H	Raw Data for OA-2 Sequencing Batch Reactor Operation	207

CHAPTER 1: INTRODUCTION

1.1 Research Background

Nitrogen pollution is a serious water pollution issue faced by developing countries worldwide. This pollution issue is increasingly threatening the water resources among the developing economies in the Southeast Asia region, such as Malaysia, Thailand and Indonesia. Human activities brought by the rapid development in these developing countries produce different sources of nitrogen pollution, including agricultural runoffs, discharge from livestock farms and inadequately-treated domestic wastewater. Inadequately-treated domestic wastewater is one of the largest point sources of nitrogen pollution. For instance in Malaysia, inadequately-treated wastewater contributed to 83% of the point-source nitrogen load into the environment (Department of Environment, 2017).

To reduce the nitrogen load from inadequately-treated wastewater, Malaysia introduced the effluent discharge limits of ammoniacal nitrogen ($\text{NH}_4\text{-N}$) and nitrate nitrogen ($\text{NO}_3\text{-N}$) for wastewater treatment plants (WWTPs) in the Environmental Quality (Sewage) Regulations 2009 (Department of Environment, 2009). The discharge limits for $\text{NH}_4\text{-N}$ and $\text{NO}_3\text{-N}$ were 5 mg/L and 10 mg/L, respectively, for WWTPs situated upstream of water intake points. The WWTPs situated downstream of water intake points must not discharge $\text{NH}_4\text{-N}$ and $\text{NO}_3\text{-N}$ above 20 mg/L and 50 mg/L, respectively. Consequently, the WWTPs in Malaysia integrated biological nitrogen removal into their process design and operation.

At present, decentralised WWTPs below 20000 population equivalent (PE) made up 98% of the WWTPs in Malaysia (Malaysian Water Association, 2017). The Malaysian Sewerage Industry Guidelines (MSIG) governs the design of these decentralised WWTPs (National Water Services Commission, 2009). The common process

configurations for WWTPs include conventional activated sludge (CAS) and extended aeration (EA). Following the new discharge limits for $\text{NH}_4\text{-N}$ and $\text{NO}_3\text{-N}$ in Environmental Quality (Sewage) Regulations 2009, MSIG mandated WWTPs to incorporate a pre-anoxic tank into their design. Thus, many WWTPs are operating in an anoxic-oxic (AO) configuration for biological nitrogen removal. The integration of biological nitrogen removal improved the WWTPs' design for the Malaysian wastewater industry, which has one of the most established nitrogen removal systems in the Southeast Asia region.

1.2 Problem Statement

The incorporation of a pre-anoxic tank in WWTPs laid a good foundation to attain biological nitrogen removal from the wastewater in Malaysia. However, the operating parameters of the WWTPs are largely adopted from other developed countries with more experiences in operating biological nitrogen removal. These operating parameters are good practices in treating wastewater in developed countries situated in the temperate climate region, but may not be optimal for local wastewater conditions and tropical climate in Malaysia. Some of these operating conditions require high energy consumption, which may lead to high operating cost. For example, the aeration tank should have a dissolved oxygen (DO) concentration above 2 mg $\text{O}_2\text{/L}$ to prevent nitrification process failure (National Water Services Commission, 2009; Tchobanoglous et al., 2014). A high-flow mixed liquor recycle (MLR) stream usually 4 to 6 times the flow rate of the influent is also required to enhance denitrification (National Water Services Commission, 2009; Tchobanoglous et al., 2014). In view of the high energy consumption and operating cost, the local wastewater industry in Malaysia aims to reduce the energy usage and operating cost to improve the sustainability of the WWTPs' operation. The move is in line with the United Nations World Water Assessment Programme (2017) emphasis on the use of low-cost

wastewater treatment systems for a more sustainable wastewater industry in the developing countries. Some examples of low-cost wastewater treatment systems developed in treating wastewater in the temperate region, such as Single reactor High Ammonia Removal Over Nitrite (SHARON) and anaerobic ammonia oxidation (anammox) process, reported potential operating cost reduction of 11% to 26% in WWTPs (M. K. Winkler & Straka, 2019). Therefore, the reduction of the energy usage and operating cost in local WWTPs may be achieved by improving the operating conditions to treat the wastewater in Malaysia.

A research gap to improve the wastewater treatment system in Malaysia is the lack of detailed wastewater characterisation data. Detailed wastewater characteristics are critical to formulate operating strategies for an efficient and low-cost wastewater treatment system. The wastewater characteristics data currently available focuses on general wastewater parameters such as chemical oxygen demand (COD), $\text{NH}_4\text{-N}$ and total nitrogen (TN). A previous study suggested that the tropical wastewater in Malaysia has a low COD content (Lee, Chua, Ong, & Ngoh, 2010). The low COD-to-N ratio (COD/N) of tropical wastewater in Malaysia (3.8 g COD/g N) was insufficient to achieve good denitrification performance, which requires a COD/N of 4 to 11 g COD/g N (Henze, Holm Kristensen, & Strube, 1994; Matějů, Čížinská, Krejčí, & Janoch, 1992). Nevertheless, the study by Lee et al. (2010) lacked detailed wastewater COD data from the particulate fraction. By performing a detailed wastewater COD characterisation, the operating conditions may be fine-tuned to effectively utilise COD from the particulate fraction for a more efficient and cost-effective biological nitrogen removal (Benneouala et al., 2017; Morgenroth, Kommedal, & Harremoes, 2002).

Another research gap is the knowledge on the microbial community in tropical biological nitrogen removal systems, which is currently not well understood. The

microbial assembly may be different in the tropical region, which may lead to a different growth kinetics suggested by the textbook. Understanding the microbiology of the tropical biological nitrogen removal system is critical to formulate operating strategies that promote the growth of functional microbes. The growth of microbes that require less stringent living conditions could also be exploited. An example of such microbes is nitrifiers that thrive in lower DO concentration ($< 1 \text{ mg O}_2/\text{L}$) in the aeration tank (Bellucci, Ofiteru, Graham, Head, & Curtis, 2011; G. Liu & Wang, 2013). Encouraging the growth of these microbes may reduce the energy usage and operating cost of WWTPs (Keene et al., 2017).

1.3 Research Objectives

The aim was to improve the process configuration to achieve an efficient and low-cost biological nitrogen removal system in treating the low COD/N tropical wastewater in Malaysia. The following five specific objectives are outlined to achieve the aforementioned project aim:-

1. To assess the detailed characteristics of low COD/N tropical wastewater in Malaysia.

The first step to develop an improved biological nitrogen removal system for tropical wastewater was detailed wastewater characterisation. The wastewater characteristics data is important to identify the treatability of the wastewater, such as the characteristics that are favourable to or can hinder the biological nitrogen removal.

2. To formulate the operating strategies of a low-cost biological nitrogen removal to treat low COD/N tropical wastewater.

The operating strategies to achieve an efficient and low-cost biological nitrogen removal in treating low COD/N tropical wastewater were hypothesised based on the

wastewater characterisation study. The feasibility of the proposed operating strategies was also studied.

3. To evaluate the long-term nitrogen removal performance of a low-cost biological nitrogen removal.

Lab-scale reactors were started up by applying the formulated operating strategies to monitor the long-term nitrogen removal performance. The operating conditions and reactor configurations were fine-tuned to attain high nitrogen removal efficiency.

4. To optimise the low-cost biological nitrogen removal operating conditions for maximum treatment capacity and efficiency.

The critical operating conditions, such as hydraulic retention time (HRT) and sludge retention time (SRT), of the low-cost biological nitrogen removal were optimised to maximise both the treatment efficiency and capacity.

5. To investigate the functional microbial community in the tropical biological nitrogen removal system.

The microbial community was investigated to gain a more complete understanding on the effects of the formulated operating strategies on microbial community.

1.4 Structure of Thesis

The thesis is presented in 8 chapters. The components of each chapter are outlined below:-

Chapter 1 describes the research background, problem statement and the objectives.

Chapter 2 presents literature review of the research project. The chapter details the relevant literature information from other research.

Chapter 3 presents the materials and methods used to conduct the studies in this project.

Chapter 4 discusses characteristics of low COD/N tropical wastewater in Malaysia and its implications on the design and operation of biological nitrogen removal.

Chapter 5 comprises results and discussion on the feasibility of applying low-dissolved-oxygen (low-DO) nitrification in treating tropical wastewater. Low-DO nitrification was an operating strategy proposed based on the wastewater characterisation study.

Chapter 6 presents findings on the long-term nitrogen removal performance and its microbial community of a lab-scale reactor applying the proposed operating strategies to achieve efficient and low-cost biological nitrogen removal.

Chapter 7 reports optimisation of HRT and SRT of the established low-cost biological nitrogen removal reactor. The effects of HRT and SRT on the microbial community were also presented.

Chapter 8 explains the conclusions and significance of the entire project, as well as the recommendations for future studies.

CHAPTER 2: LITERATURE REVIEW

2.1 Wastewater Characteristics

Wastewater contains different constituents that must be removed before discharging into the environment. Biological nitrogen removal is able to eliminate the biodegradable organics and nitrogen compounds in the wastewater. Characterising biodegradable organics and nitrogen compounds in the wastewater is important to evaluate the treatability of wastewater and the performance of biological nitrogen removal. This section reviews wastewater parameters to characterise biodegradable organics and nitrogen compounds in the wastewater and their typical compositions in the tropical wastewater.

2.1.1 Wastewater Parameters

The wastewater parameters commonly used to characterise the biodegradable organics are biochemical oxygen demand (BOD), COD, total organic carbon (TOC) and dissolved organic carbon (DOC). The concentrations of ammonium (NH_4^+), nitrite (NO_2^-), nitrate (NO_3^-) and TN are widely used to characterise nitrogen content of the wastewater.

2.1.1.1 Biochemical Oxygen Demand

BOD is a widely used wastewater characterisation parameter to determine the oxygen required to biologically stabilise the organic matter present in the wastewater (Tchobanoglous et al., 2014). The standard 5-day BOD (BOD_5) test involves incubating a diluted wastewater sample at 20°C for 5 d, the difference between the DO before and after the incubation gives the BOD_5 value of the wastewater (APHA/AWWA/WEF, 1998). The wastewater must be suitably diluted to ensure sufficient amount of nutrient and DO are available during the incubation period. A major disadvantage of BOD test is

the long measurement time (5 d or more), which limits its application in routine wastewater characterisation (Tchobanoglous et al., 2014).

2.1.1.2 Chemical Oxygen Demand Fractions

COD is the most common wastewater parameters measured routinely to determine biodegradable organics content in the wastewater. COD is a measure of the oxygen equivalent of the chemically-oxidised organic material in the wastewater using dichromate ions (Tchobanoglous et al., 2014). COD measurement is preferred over biochemical oxygen demand (BOD) measurement in routine wastewater characterisation due to the shorter measurement time for COD test (2.5 h) when compared with that of BOD test (5 d or more) (Tchobanoglous et al., 2014).

COD values of wastewater may include non-biodegradable compounds in the wastewater that reacted with the dichromate ion. Fractionation of COD into biodegradable COD (bCOD) and non-biodegradable COD (nbCOD) is important to characterise the amount of bCOD that can be removed in the biological nitrogen removal. For a wastewater sample, total COD (TCOD) is the sum of bCOD and nbCOD (Figure 2.1). The bCOD can be further classified into readily-biodegradable COD (rbCOD) and slowly-biodegradable COD (sbCOD). The rbCOD fraction consists of biodegradable soluble COD and biodegradable colloidal COD, which refer to the non-settleable organic matter with particle size smaller than 1.2 μm (Sophonsiri & Morgenroth, 2004). The sbCOD includes biodegradable particulate COD with particle size larger than 1.2 μm , these large particles are also known as particulate settleable solids (PSS) (Benneouala et al., 2017; Sophonsiri & Morgenroth, 2004). Soluble COD (sCOD) is another common parameter, which refers to the COD in wastewater after filtration through a 0.45- μm filter. sCOD is composed of biodegradable and non-biodegradable soluble COD.

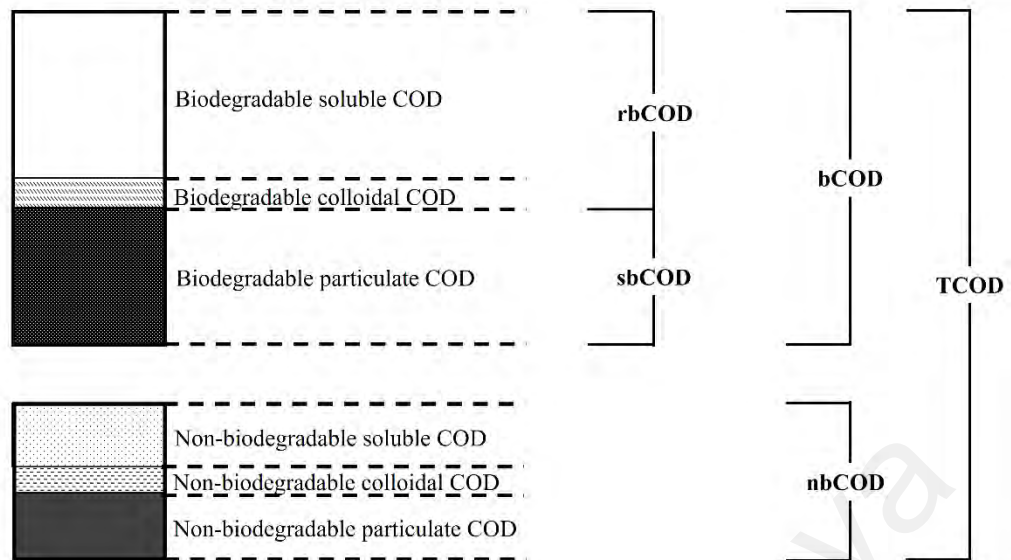


Figure 2.1: Fractions of COD adapted from Henze, van Loosdrecht, Ekama, and Brdjanovic (2008) and Tchobanoglous et al. (2014).

Domestic wastewater is typically biodegradable with bCOD content constituting 90% of the TCOD (Choi et al., 2017; Henze et al., 2008). Within the bCOD fraction, sbCOD can make up 26 – 70% of the total organic matter, while rbCOD may constitute only 6 – 25% of organic matter in the wastewater (Choi et al., 2017; Guellil, Thomas, Block, Bersillon, & Ginestet, 2001; Sophonsiri & Morgenroth, 2004). Thus, PSS providing the sbCOD may be an important source of biodegradable organics in the wastewater for biological nitrogen removal.

Nitrate uptake rate (NUR) experiment is a common method to quantify the concentrations of rbCOD and sbCOD in the wastewater samples (Naidoo, Urbain, & Buckley, 1998; van Loosdrecht, Nielsen, Lopez-Vazquez, & Brdjanovic, 2016). The principle of measurement is that biodegradation of rbCOD takes place before that for sbCOD for denitrification. The NUR during biodegradation of rbCOD occurs at a much higher rate than that for sbCOD, thus the biodegradation of rbCOD produces a line (green) with a higher slope than that during the biodegradation of sbCOD (yellow) in a time series plot of NO_3^- (Figure 2.2). The respective amount of NO_3^- consumed during

biodegradation of rbCOD and sbCOD, respectively, could be backtracked to calculate amount of rbCOD and sbCOD in the wastewater based on stoichiometry. The stoichiometric coefficient for COD consumed per $\text{NO}_3\text{-N}$ reduced reported by Muller, Wentzel, Loewenthal, and Ekama (2003) is $2.86/1 - Y_{\text{OHO},ax}$. Where $Y_{\text{OHO},ax}$ is the anoxic yield coefficient for heterotrophic bacteria.

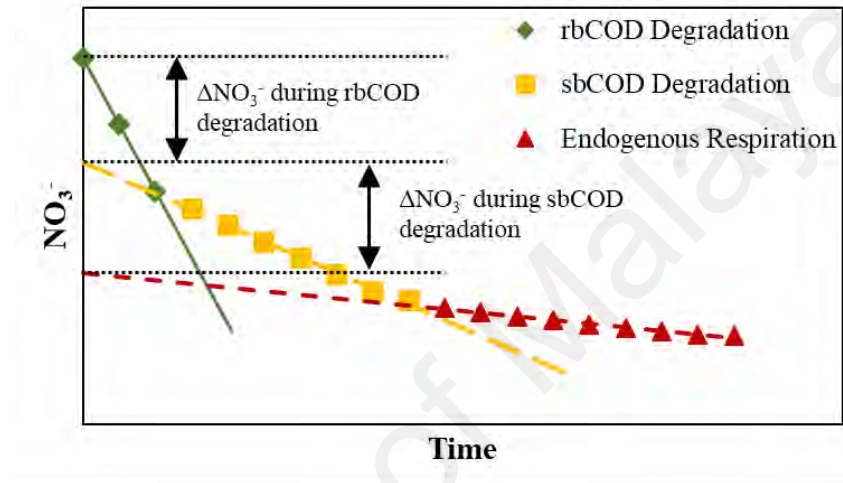


Figure 2.2: Example of a time series plot of NO_3^- of NUR test adapted from Naidoo et al. (1998) and van Loosdrecht et al. (2016).

2.1.1.3 Total Organic Carbon and Dissolved Organic Carbon

TOC is another common parameter to characterise organic matter in the wastewater, while DOC measures only the dissolved organic matter after filtration through a 0.45- μm filter (APHA/AWWA/WEF, 1998). TOC and DOC are measured by oxidative combustion of carbon in the wastewater into carbon dioxide gas, which is then quantified in a gas analyser (Tchobanoglous et al., 2014). TOC and DOC measurement is preferred over COD measurement during bulk sample analysis to reduce the amount of toxic chemicals, such as potassium dichromate and mercury sulphate used for COD measurement (Dubber & Gray, 2010). TOC exhibits a linear relationship with TCOD

for domestic wastewater, which is typically 0.3 times the TCOD value (Tchobanoglous et al., 2014).

2.1.1.4 Nitrogen Constituents

The individual nitrogen species in wastewater includes free ammonia (NH_3) or NH_4^+ , NO_2^- , NO_3^- and organic nitrogen compounds (Henze et al., 2008). The nitrogen content of the wastewater may also be measured aggregately as TN (Tchobanoglous et al., 2014).

Ammonia can exist as NH_4^+ and NH_3 in the wastewater. NH_3 is the unionized form of ammonia while NH_4^+ is the ionized form of ammonia. In an aqueous solution, the concentrations of NH_3 and NH_4^+ are dependent on the pH (Anthonisen, Loehr, Prakasam, & Srinath, 1976). The dominant form of ammonia for domestic wastewater around a neutral pH is NH_4^+ (Anthonisen et al., 1976). The presence of ammonia as NH_4^+ is more favourable than NH_3 as NH_3 is highly toxic (Camargo & Alonso, 2006; Kim, Lee, & Keller, 2006). NO_2^- is an unstable product from the oxidation of NH_4^+ , which can be further oxidised into NO_3^- . The accumulation of NO_2^- in wastewater treatment system is undesirable because high NO_2^- concentration can inhibit nitrification activity (Anthonisen et al., 1976). High NO_2^- accumulation is also a cause for nitrous oxide (N_2O) gas emission from the biological nitrogen removal, which is a highly potent greenhouse gas (Massara et al., 2017). NO_3^- has the highest oxidation state of all the nitrogenous compounds and is the terminal oxidation product of NH_4^+ .

Organic nitrogen in the wastewater originates from urea or proteinaceous compounds of plant and animal origin. Organic nitrogen made up 40% of nitrogen content in the raw wastewater as most of the organic nitrogen is decomposed into NH_4^+ along the sewer (Sattayatewa, Pagilla, Sharp, & Pitt, 2010; Water Environment Federation, 2005).

Organic nitrogen content in the wastewater is usually converted into NH_4^+ via ammonification before being removed by biological nitrogen removal pathway (Henze, Grady Jr, Gujer, V. R Marais, & Matsuo, 1987). The organic nitrogen fraction is characterised by Kjeldahl method, in which NH_4^+ in the wastewater is first boiled off, followed by a digestion step to convert the organic nitrogen into NH_4^+ (Tchobanoglous et al., 2014).

TN is a useful parameter to measure the aggregate nitrogen content in the wastewater. TN is defined as the sum of NH_3 , NH_4^+ , NO_2^- , NO_3^- and organic nitrogen present in a wastewater sample (Tchobanoglous et al., 2014). TN analysis is more convenient than measuring individual nitrogen species in the wastewater for routine wastewater characterisation. The principle of TN measurement is by oxidative combustion of nitrogen compounds in the wastewater sample to NO_x gas, which is subsequently quantified in a chemiluminescence gas analyser (Bekiari & Avramidis, 2013).

2.1.2 Tropical Wastewater Characteristics

Typical concentrations of organic and nitrogen content in the tropical wastewater are given in Table 2.1. Concentrations of the major constituents are compared with typical wastewater characteristics found in the textbook. Most of the parameters of major constituents in tropical wastewater are similar with the concentration range of typical wastewater characteristics in temperate climate. However, the concentration of sCOD in the tropical wastewater (105 – 123 mg/L) is lower than other literature values (Cao, Wah, Ang, & Raajeevan, 2008; Lee et al., 2010). Cao et al. (2008) suggests that high-temperature (30°C) wastewater in the tropical climate may have enhanced biodegradation of sCOD in the sewer system. A probable explanation for the similar

TCOD concentration is that PSS is not biodegraded in the sewer network, thus the sbCOD is largely preserved.

Table 2.1: Average composition of the wastewater in Malaysia, Singapore, Europe and United States (Cao et al., 2008; Henze, Harremoës, la Cour Jansen, & Arvin, 1997; Lee et al., 2010; Tchobanoglous et al., 2014)

Parameter	Average Value			
	Malaysia ¹	Singapore ²	Europe ³	United States ⁴
TCOD (mg/L)	381	468	370	508
sCOD (mg/L)	105	123	210	177
NH ₄ -N (mg/L)	20	33	30	20
TN (mg/L)	27	52	50	35
TCOD/TN (g COD/g N)	14	9	7	15
sCOD/TN (g COD/g N)	4	2	4	5

¹ Lee et al. (2010)

² Cao et al. (2008)

³ Henze et al. (1997)

⁴ Tchobanoglous et al. (2014)

COD/N is a useful parameter to assess the treatability of the wastewater by using biological nitrogen removal. Henze et al. (1994) recommended a wastewater COD/N of 6 to 11 g COD/g N for complete nitrogen removal. The average TCOD-to-TN ratio (TCOD/TN) and sCOD-to-TN ratio (sCOD/TN) for tropical wastewater in Table 2.1 are 9 – 14 g COD/g N and 2.4 – 3.9 g COD/g N, respectively. The TCOD/TN is above the recommended range, but the sCOD/TN is well below the range. The low sCOD/TN implies that rbCOD in the wastewater is not sufficient for biological nitrogen removal, sbCOD in the wastewater may be utilised to achieve good biological nitrogen removal performance.

2.1.3 Discharge Standards for Wastewater Treatment Plant's Effluent

A key objective of biological nitrogen removal is to remove nitrogenous compounds from the wastewater to a level below the local regulated limit. Many countries enact their regulations to limit the load of nitrogenous pollutants discharge from WWTPs. In Malaysia, the discharge limits for nitrogenous pollutants from WWTPs are stipulated in the Environmental Quality (Sewage) Regulation 2009 (Department of Environment, 2009). Table 2.2 shows the discharge limits of NH₄-N and NO₃-N for WWTPs in Malaysia. WWTPs that are within the water catchment areas must comply with Standard A, while those situated outside water catchment areas may comply with either Standard A or Standard B (Department of Environment, 2009).

Table 2.2: Discharge limits for NH₄-N and NO₃-N stipulated in Environmental Quality (Sewage) Regulation 2009 (Department of Environment, 2009)

Parameter	Discharge Limit (mg/L)	
	Standard A	Standard B
NH ₄ -N (enclosed water body)	5.0	5.0
NH ₄ -N (river)	10.0	20.0
NO ₃ -N (enclosed water body)	10.0	10.0
NO ₃ -N (river)	20.0	50.0

When the typical concentration of NH₄-N in tropical wastewater (Table 2.1) is compared with the discharge limit (Table 2.2), at least 10 mg/L of NH₄-N must be removed from the sewage. In addition, assuming all NH₄-N (20 – 33 mg/L) was nitrified, an equivalent concentration of NO₃-N will be produced. Treatment process to remove NO₃-N may be required for WWTPs.

2.2 The Nitrogen Cycle

The nitrogen cycle is a useful illustration to show the biochemical transformation of nitrogen compounds in the environment. The nitrogen cycle adapted from Stein and

Klotz (2016) is in general made up of four nitrogen transformation flows (Figure 2.3), namely ammonification, nitrification, denitrification and anaerobic ammonia oxidation (anammox).

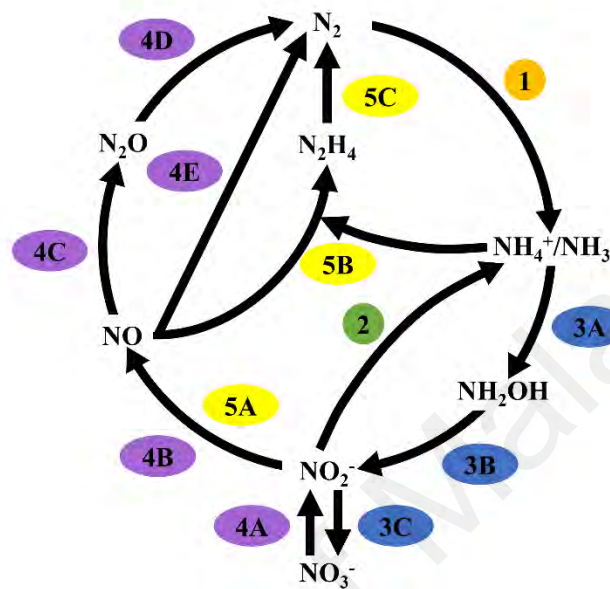
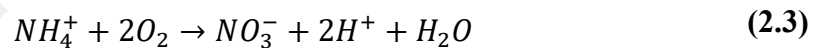
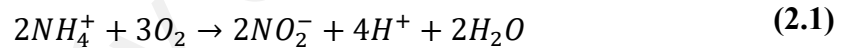


Figure 2.3: The nitrogen cycle adapted from Stein and Klotz (2016) depicting the microbial nitrogen transformations in five processes. 1 – Nitrogen fixation, 2 – assimilatory nitrite reduction to ammonia (ANRA) or dissimilatory nitrite reduction to ammonia (DNRA), 3 – nitrification, 4 – denitrification, 5 – anammox.

Ammonification refers to the processes that reduce organic and inorganic nitrogen compounds with higher oxidation states to NH_3 or NH_4^+ . Processes 1 and 2 (Figure 2.3) are the two possible pathways to achieve ammonification. Process 1 is the nitrogen fixation of atmospheric nitrogen gas (N_2) to ammonia. Process 2 refers to assimilatory nitrite reduction to ammonia (ANRA) or dissimilatory nitrite reduction to ammonia (DNRA), which reduces NO_2^- to ammonia in either an assimilatory or dissimilatory microbial activity (Stein & Klotz, 2016). ANRA is performed by bacteria, fungi, algae and plants to reduce NO_2^- into ammonia, the ammonia is subsequently assimilated for growth (Moreno-Vivián, Cabello, Martínez-Luque, Blasco, & Castillo, 1999). Ammonia

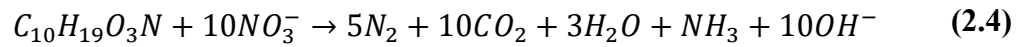
produced by DNRA are not assimilated into cells but released into the environment (van den Berg, van Dongen, Abbas, & van Loosdrecht, 2015).

Nitrification is the biological oxidation of NH_4^+ to NO_3^- , which is comprised of two steps. In the first step, NH_4^+ is oxidised into NO_2^- with the formation of an unstable intermediate hydroxylamine (NH_2OH). The processes 3A and 3B in Figure 2.3 collectively represent the first step, which is known as nitritation. In the second nitratation step, NO_2^- further oxidises into NO_3^- (process 3C, Figure 2.3). The stoichiometric equations representing nitritation, nitratation and nitrification reaction is shown in Equation 2.1, Equation 2.2 and Equation 2.3, respectively. The theoretical oxygen requirement for nitrification reaction is 4.57 g O_2 /g NH_4 -N (Tchobanoglous et al., 2014). pH of the wastewater decreases during nitrification due to the production of proton.



The third nitrogen transformation flow is denitrification, which is indicated by processes 4A to 4E (Figure 2.3). Denitrification is the biological reduction of NO_3^- to N_2 with the intermediates NO_2^- , nitric oxide (NO) and N_2O in an anoxic condition. The biological reduction of NO_3^- to N_2 requires sufficient biodegradable organics in the wastewater (Henze et al., 2008). Theoretically, 4.2 g COD is biodegraded per gram of NO_3 -N reduced (Matějů et al., 1992). The stoichiometric equation of denitrification pathway is represented by Equation 2.4, where $C_{10}H_{19}O_3N$ is a common chemical formula of biodegradable organics in wastewater (United States Environmental

Protection Agency, 1993). Denitrification process produces alkalinity, which increases the pH of wastewater.



The fourth nitrogen transformation flow is anammox, in which NH_4^+ is oxidised into N_2 using NO_2^- as the source of electron acceptor under anaerobic condition (Strous, Heijnen, Kuenen, & Jetten, 1998). The anammox pathway is composed of step 5A, 5B and 5C in Figure 2.3. 5A involves the reduction of NO_2^- into NO, the NO is then used as electron acceptor for the oxidation of NH_4^+ into hydrazine (N_2H_4) in step 5B. N_2H_4 is an intermediate product and is further oxidised into N_2 (Stein & Klotz, 2016). The pathway plays an important role in marine ecosystem and was applied in engineered systems (Kuenen, 2008). Anammox pathway is considered a more sustainable pathway for biological nitrogen removal when compared with the conventional nitrification-denitrification pathway. The reasons being anammox requires 60% less energy than aerobic nitrification pathway as the anammox reaction takes place in anaerobic condition (Ma et al., 2016). Anammox does not require organic carbon source as in the case for denitrification, which resulted in further cost savings (M. K. Winkler & Straka, 2019). Nevertheless, applying anammox pathway in domestic WWTPs is a challenge because domestic wastewater typically has low NH_4 -N concentration of between 30 – 100 mg/L (Cao, van Loosdrecht, & Daigger, 2017). Lackner et al. (2014) suggests that the enrichment of anammox bacteria requires high NH_4 -N concentration (500 – 1500 mg/L).

The conventional nitrification-denitrification pathway is widely employed in WWTPs to achieve biological nitrogen removal (M. K. Winkler & Straka, 2019). The major setback of the conventional nitrification-denitrification pathway is the stringent operating conditions. For instance, intensive aeration is required to deliver enough

oxygen for nitrification (Tchobanoglous et al., 2014; M. K. Winkler & Straka, 2019). In addition, treating domestic wastewater with low COD content may require dosing in external carbon source to boost the denitrification performance (Guerrero, Taya, Guisasola, & Baeza, 2012; Guo et al., 2016).

2.3 Microbial Communities of Biological Nitrogen Removal

In this section, the different groups of microorganisms and their functional gene inventory involve in the conventional nitrification-denitrification pathway were reviewed. The principles of the molecular techniques used to quantify these functional microorganisms was presented in this section.

2.3.1 Ammonia-Oxidising Bacteria

Ammonia-oxidising bacteria (AOB) performs nitrification step in the nitrification pathway (Seviour & Nielsen, 2010). Some important AOB in the wastewater treatment system belongs to the genera *Nitrosomonas* and *Nitrospira*, both of these genera belong to the class *Betaproteobacteria* (Seviour & Nielsen, 2010). *Nitrosomonas*-related AOB is an r-strategist as they preferably thrive in high-ammonia environment with a higher growth rate (Andrews & Harris, 1986). On the other hand, *Nitrospira*-related AOB is a k-strategist as they survive in low ammonia concentration with a lower growth rate (Andrews & Harris, 1986). In WWTPs, *Nitrosomonas sp.* is often the dominant AOB because of the availability of NH_4^+ in the domestic wastewater (Seviour & Nielsen, 2010).

The oxidation of NH_4^+ into NO_2^- is catalysed by two enzymes, namely ammonia monooxygenase (*amo*) and hydroxylamine oxidoreductase (*hao*) as shown in Figure 2.4 (Bergmann, Arciero, & Hooper, 1994; Hooper, Vannelli, Bergmann, & Arciero, 1997). *amo* converts NH_4^+ into NH_2OH , while *hao* further oxidises the NH_2OH into NO_2^- (Hooper et al., 1997). The genome of AOB contains the genes encoding for *amo* and

hao. The gene encoding for α -subunit of *amo* (*amoA*) is an important target gene to detect AOB in the activated sludge samples (Rotthauwe, Witzel, & Liesack, 1997).



Figure 2.4: Nitrification pathway with the functional genes indicated below the arrows.

2.3.2 Nitrite-Oxidising Bacteria

The second step of the nitrification pathway, nitratation, is performed by nitrite-oxidising bacteria (NOB), such as bacteria within the genera *Nitrospira* and *Nitrobacter* (Seviour & Nielsen, 2010). NOB has a more diverse phylogeny when compared with AOB. The genera *Nitrospira* and *Nitrobacter* belong to different phyla. The genus *Nitrospira* belongs to the phylum *Nitrospirae*, while the *Nitrobacter* is a genus under the phylum *Proteobacteria* (Ehrich, Behrens, Lebedeva, Ludwig, & Bock, 1995; Stackebrandt, Murray, & Trüper, 1988). *Nitrospira sp.* is classified as a k-strategist, while *Nitrobacter sp.* is an r-strategist. Since NO_2^- is usually an intermediate product of nitrification and is present in low concentration, the k-strategist *Nitrospira sp.* is commonly the dominant NOB in WWTPs (Mehrani, Sobotka, Kowal, Ciesielski, & Makinia, 2020; Seviour & Nielsen, 2010).

Nitratation is catalysed by the enzyme nitrite oxidoreductase (*nxr*; Figure 2.4), which oxidises NO_2^- into NO_3^- (Lucker et al., 2010). The genes encoding for the β -subunit of *nxr* (*nxrB*) is a common target gene to detect NOB in the environment (Perster et al., 2014; Vanparrys et al., 2007).

2.3.3 Complete Ammonia Oxidisers

Costa, Pérez, and Kreft (2006) speculated the existence of a single organism that is capable of oxidising NH_4^+ to NO_3^- because such organism would be able to generate more energy for their growth. Until recently, Daims et al. (2015) and van Kessel et al. (2015) discovered complete ammonia oxidisers (comammox) capable of oxidising NH_4^+ to NO_3^- . All the comammox known to date are affiliated with clade II of the genus *Nitrospira*, which includes *Nitrospira inopinata*, “*Candidatus Nitrospira nitrosa*” and “*Candidatus Nitrospira nitrificans*” (Daims et al., 2015; van Kessel et al., 2015). A kinetic analysis of an axenic culture of *Nitrospira inopinata* revealed that comammox are adapted to oligotrophic habitats (Kits et al., 2017). The metabolic characteristics of comammox are high affinity for NH_4^+ , low NH_4^+ uptake rate and higher growth yield when compared with AOB (Kits et al., 2017). Palomo et al. (2018) suggested that comammox may thrive in low-DO condition because its genome harbours a 2/2 hemoglobin type II (TrHb2) to scavenge oxygen. The significance of comammox in the WWTPs’ operation is still not well-understood. A global activated sludge microbial analysis found that *Nitrospira* is a core taxon in the WWTPs and is highly correlated with ammonia removal efficiency, thus corroborating an important role of *Nitrospira*-related comammox in WWTPs (L. Wu et al., 2019). Chao, Mao, Yu, and Zhang (2016) and Cotto et al. (2020) detected genes encoding for comammox *amoA* in full-scale activated sludge reactors using metagenomic analysis. Cotto et al. (2020) suggested that long SRT above 10 d is a primary selection factor for the growth of comammox in the reactors. Oppositely, a metagenomic analysis on six full-scale WWTPs in The Netherlands and China suggested that comammox did not play a significant role in wastewater treatment process (Gonzalez-Martinez, Rodriguez-Sanchez, van Loosdrecht, Gonzalez-Lopez, & Vahala, 2016).

Comammox harbours all the genes encoding for enzymes involved in the nitrification pathway, which include *amo*, *hao* and *nxr* as shown in Figure 2.4 (Palomo et al., 2018). The genes encoding for *amo* in comammox is phylogenetically distinct from the genes encoding for *amo* in AOB (Daims et al., 2015; van Kessel et al., 2015). Several studies designed detection assays targeting comammox *amoA* to detect their presence in the environment (Beach & Noguera, 2019; Fowler, Palomo, Dechesne, Mines, & Smets, 2018; Pjevac et al., 2017). Cotto et al. (2020) designed a method targeting the gene encoding for the β -subunit of *amo* (*amoB*) in comammox as assays targeting *amoA* may not be accurate. Distinguishing *Nitrospira*-related comammox from *Nitrospira*-related NOB is a challenge due to their close phylogenetic relationships (Koch, van Kessel, & Lucker, 2019). To date, both 16S rRNA-based and *nxB*-based methods are not recommended for distinguishing comammox from NOB (Cotto et al., 2020; Pjevac et al., 2017).

2.3.4 Denitrifying Ordinary Heterotrophic Organisms

Denitrification is performed by heterotrophic bacteria that could facultatively use nitrogen-bound oxygen, such as NO_2^- and NO_3^- , as an electron acceptor under anoxic condition (Tchobanoglous et al., 2014). Denitrifying ordinary heterotrophic organisms (DOHOs) are phylogenetically very diverse because many prokaryotes are able to use NO_3^- , NO_2^- , NO or N_2O as electron acceptor when the DO becomes the limiting substrate (Seviour & Nielsen, 2010). The common classes of DOHOs include *Alphaproteobacteria*, *Betaproteobacteria*, *Gammaproteobacteria* and *Actinobacteria*. Within the common classes, DOHOs related to the genera *Paracoccus*, *Azoarcus*, *Thauera* and *Comamonas* are among the most frequently detected in WWTPs (Seviour & Nielsen, 2010).

DOHOs possess five different genes that encode for all the denitrifying enzymes (Figure 2.5). The reduction of NO_3^- to NO_2^- is catalysed by two types of nitrate reductases (*nar* and *nap*). *nar* is membrane-bound, while *nap* is periplasmic-bound (Bell, Richardson, & Ferguson, 1990). The reduction of NO_2^- to NO is catalysed by nitrite reductase (*nirS* or *nirK*). Subsequently, the enzyme nitric oxide reductase (*nor*) catalyses the reduction of NO to N_2O . Finally, N_2O is reduced to N_2 by the expression of nitrous oxide reductase gene (*nosZ*). Though DOHOs possess the four genes that encode for all the denitrifying enzymes, environmental conditions such as a lack of biodegradable organics and high DO concentration may suppress the gene expression and cause incomplete denitrification (Mannina, Capodici, Cosenza, Di Trapani, & van Loosdrecht, 2017). Incomplete denitrification may cause the emission of potent greenhouse gases (NO and N_2O) from WWTPs (Massara et al., 2017).

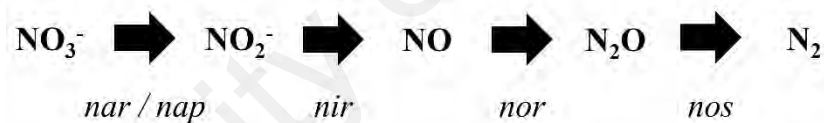


Figure 2.5: Denitrification pathway with the functional genes indicated below the arrows.

All the four genes that encode for the denitrifying enzymes (*nar/nap*, *nirS/nirK*, *nor* and *nosZ*) were used as functional gene markers to detect DOHOs in the environmental sludge samples (Bru, Sarr, & Philippot, 2007; Gabarro et al., 2013; Henry, Bru, Stres, Hallet, & Philippot, 2006). There were also attempts to use the same genes as to study the phylogenetic relationships of DOHOs but did not produce consistent phylogeny when compared with the 16S rRNA-based phylogeny (Braker, Fesefeldt, & Witzel, 1998; Heylen et al., 2006; Philippot, 2002). In addition, the denitrifying genes may transfer horizontally between phylogenetically-distant DOHOs, which renders the genes unsuitable for phylogenetic analysis (Philippot, 2002).

2.3.5 Detection Methods Based on Phylogenetic and Functional Gene Markers

The advent of molecular techniques targeting phylogenetic and functional gene markers of AOB, NOB, comammox and DOHOs provides a fast and reliable method to detect their presence in the environmental sludge samples (Seviour & Nielsen, 2010). 16S rRNA gene is widely used as a phylogenetic marker to identify the taxonomy of bacteria because the gene is present in all bacteria and is highly conserved (Seviour & Nielsen, 2010). On the other hand, functional genes allow researchers to target a specific group of bacteria performing a metabolic pathway, which is useful for the quantification of their population size (Daims, Nielsen, Nielsen, Schleifer, & Wagner, 2001; Rotthauwe et al., 1997). The following subsections highlight some of the most common molecular techniques used in wastewater research field.

2.3.5.1 16S Ribosomal Ribonucleic Acid Amplicon Sequencing

16S ribosomal ribonucleic acid (rRNA) amplicon sequencing is a common method to examine the microbial community in the environment samples. 16S rRNA amplicon refers to the amplification products of the 16S rRNA gene in polymerase chain reaction (PCR). The use of next-generation sequencing (NGS) platforms for 16S rRNA amplicon sequencing provides a high sequencing throughput within a short amount of time (Sanz & Köchling, 2019). Some examples of commercial NGS platforms include Ion Torrent, Illumina MiSeq and 454 Pyrosequencing. Ion Torrent platform reads the 16S rRNA amplicon sequences by detecting the amount of proton released caused by the incorporation of nucleotides during the synthesis a new strand of deoxyribonucleic acid (DNA) (Quail et al., 2012). Illumina MiSeq platform uses fluorescently-labelled nucleotides during DNA synthesis to identify the nucleotide base incorporated (Quail et al., 2012). 454 Pyrosequencing uses a similar sequencing-by-synthesis technique as in Illumina MiSeq, but the nucleotides were not fluorescently-labelled (Balzer, Malde, Lanzen, Sharma, & Jonassen, 2010). One specific type of nucleotide is added to the

sequencing wells at one time, the light signal emitted during hybridisation of nucleotide to the DNA strand is then recorded by a camera (Balzer et al., 2010).

The 16S rRNA amplicon sequences constructed from the NGS platforms are compared with the reference sequence database to assign taxonomy to the sequences. Downstream bioinformatics analysis uses statistical methods to examine the taxonomic structure and the diversity in the DNA samples (Caporaso et al., 2010). Constructing a phylogenetic tree based on the 16S rRNA amplicon sequences helps to visualise the evolutionary relationships of the microorganisms of interest (Hall, 2013). The application of 16S rRNA amplicon sequencing in wastewater research could be exemplified by L. Wu et al. (2019). The authors performed 16S rRNA amplicon sequencing for approximately 1200 activated sludge samples taken from 6 continents to study the global diversity of microbial community in wastewater treatment process. L. Wu et al. (2019) demonstrates the potential of high-throughput NGS platforms to gain a holistic insights into global microbial ecology that would not possible a few decades ago.

2.3.5.2 Quantitative Polymerase Chain Reaction

Quantitative PCR (qPCR) is a popular method to accurately quantify the population size of a specific group of microorganisms (Matsuda, Tsuji, Asahara, Kado, & Nomoto, 2007; van Loosdrecht et al., 2016). Short single-stranded oligonucleotides (15 – 30 bases) called qPCR primers determine the specificity of the assay. For instance, universal primers targeting bacterial 16S rRNA gene are used to quantify the total bacteria population size (He, Gall, & McMahon, 2007), while primers targeting functional gene markers are designed to quantify a specific bacteria group, such as AOB *amoA*, comammox *amoB* and DOHOs *nosZ* (Cotto et al., 2020; Henry et al., 2006; Rotthauwe et al., 1997). During qPCR, a specific region of the DNA is amplified

through repeated cycle of DNA denaturation, primer annealing and DNA strand elongation. A fluorescent dye SYBR Green I intercalates with the double-stranded DNA and emit fluorescent signal (Zipper, Brunner, Bernhagen, & Vitzthum, 2004). As the copy number of double-stranded DNA increases with each qPCR cycle, the intensity of the fluorescent signal also increases. Ultimately, the fluorescent signal emitted by the SYBR Green I dye becomes detectable at the threshold cycle (C_q ; Figure 2.6). A standard curve of the C_q values against the known copy number of target gene in standard solutions is subsequently plotted (Matsuda et al., 2007). By determining the C_q values of unknown samples, the C_q values can be compared with the standard curve and calculate the copy number of the target gene in the samples.

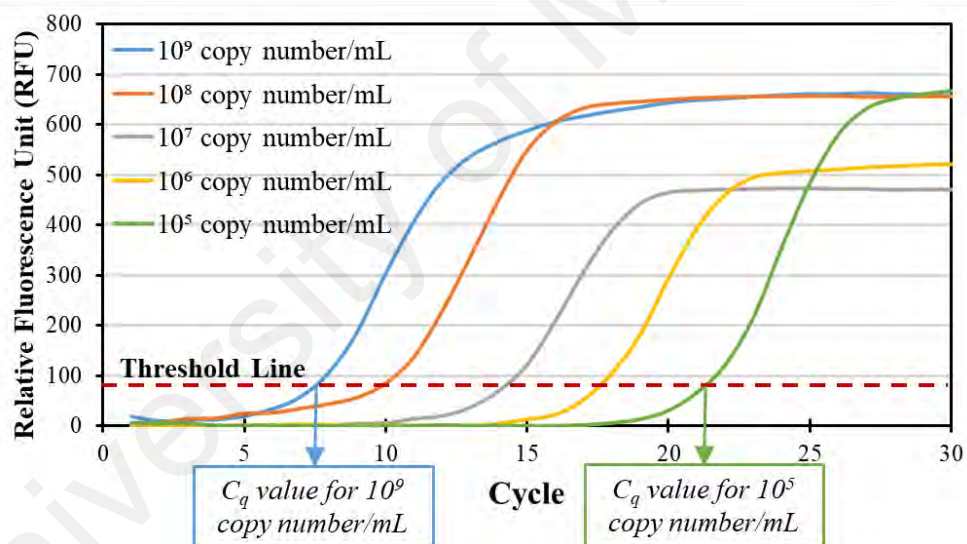


Figure 2.6: Plot of fluorescence intensity versus qPCR cycle to determine C_q values adapted from van Loosdrecht et al. (2016).

Beach and Noguera (2019) and Cotto et al. (2020) designed specific qPCR assays to target and quantify comammox bacteria down to species level by targeting the functional genes *amoA* and *amoB*. These research illustrated the high accuracy and specificity of qPCR assays that could not be achieved by 16S rRNA amplicon

sequencing. For this reason, quantification data from qPCR usually complements the overview of microbial assembly acquired from 16S rRNA amplicon sequencing.

2.3.5.3 Fluorescence *in situ* Hybridisation and Quantitative Fluorescence *in situ* Hybridisation

Fluorescence *in situ* hybridisation (FISH) allows *in situ* detection of bacteria cells in a sludge sample (Amann, Krumholz, & Stahl, 1990; Wagner, Rath, Koops, Flood, & Amann, 1996). FISH is a useful tool to target a specific group of bacteria and to visualise their cell morphology without cell isolation. FISH is an important molecular technique to complement the results acquired from 16S rRNA amplicon sequencing and qPCR (Baptista et al., 2014). Single-stranded oligonucleotide chains (17 – 34 bases) called FISH probes are designed to target the 16S rRNA of either the universal bacteria or a specific group of bacteria (Cui, Shu, & Li, 2016). The FISH probes targeting different groups of bacteria are labelled with different fluorescent dyes on its 5' end, such as FLUOS, Cy-5 and Cy-3 fluorophore (van Loosdrecht et al., 2016). The FISH probes' fluorophore can emit fluorescent signal when excited with light at a specific wavelength. Fixed cell samples may be co-hybridised with multiple FISH probes targeting universal bacteria and specific groups of bacteria. The hybridised cells on glass slide are observed under a fluorescence microscope. The cells hybridised with FISH probes would emit fluorescent light when excited with light at a specific wavelength.

Quantificative FISH (qFISH) is performed by estimating the area of the fluorescent signals emitted by cells hybridised with FISH probe. The ratio of the area of fluorescent signal from a group-specific FISH probe and that of a universal FISH probe gives an approximate proportional abundance of the specific microbes (Daims, Ramsing, Schleifer, & Wagner, 2001). For example, qFISH analysis of a sludge sample using a

specific probe targeting AOB (Nso1225) and a universal probe targeting most bacteria (EUBMIX) allows quantification of AOB in the sludge by dividing the area of fluorescent signals from Nso1225 and that from EUBMIX (Schmid et al., 2000).

2.4 Operating Conditions Influencing Biological Nitrogen Removal Performance

In the operation of a biological nitrogen removal, the DO concentration, the availability of bCOD in the wastewater, HRT and SRT are the critical operating conditions affecting the process performance and cost (Najafpour, 2015; Tchobanoglous et al., 2014). In this section, the effect of DO on nitrification and the effect of bCOD fractions on denitrification were reviewed. The effect of HRT, organic volumetric loading rate (L_{org}), SRT and food-to-microbe ratio (F/M) on the design of biological nitrogen removal was also discussed.

2.4.1 Effect of Dissolved Oxygen on Nitrification

DO is required for the oxidation of NH_3 to NO_2^- and NO_3^- . Hence, increasing DO concentration in nitrification process would accelerate the rate of nitrification. The increase in rate of nitrification follows a saturation kinetic model, in which the maximum rate of nitrification is reached at DO concentration between 3 and 4 mg O_2/L (Tchobanoglous et al., 2014). A common expression to express the rate of nitrification, r_{NH} , as a function of DO is represented by Equation 2.5,

$$r_{NH} = r_{NH,max} \left(\frac{S_O}{S_O + K_O} \right) \quad (2.5)$$

Where $r_{NH,max}$ is the maximum nitrification rate, S_O is the DO concentration in the wastewater and K_O is the DO half-velocity constant. High DO above 2 mg/L in the aerobic tank is often a strategy to prevent nitrification failure in WWTPs (Fitzgerald, Camejo, Oshlag, & Noguera, 2015). Aeration for nitrification may account for 70 –

80% of the total plant energy consumption in order to maintain high level of DO above 2 mg/L (Mulder et al., 2006; Ramli & Abdul Hamid, 2017). The energy-intensive aeration increased the carbon footprint of WWTPs. For example, wastewater industry in the United Kingdom releases approximately 5 million tonnes of carbon dioxide equivalent of greenhouse gases per year (Bellucci et al., 2011). Thus, overcoming the high DO requirement for nitrification is necessary to ensure a more sustainable WWTPs operation.

Operating nitrification process in a low-DO condition is a promising operating strategy to reduce the energy consumption used for aeration. Low-DO nitrification occurs in DO concentration below 1 mg/L, which is half of the DO concentration in a conventional nitrification process (2 mg O₂/L). Low-DO nitrification has been studied in both lab-scale and pilot-scale reactors (Arnaldos, Kunkel, Stark, & Pagilla, 2013; Bellucci et al., 2011; Fan et al., 2017; Keene et al., 2017). Bellucci et al. (2011) and Arnaldos et al. (2013) reported complete ammonia oxidation at low-DO concentrations but produced contradictory results. Bellucci et al. (2011) did not find any difference in the NH₄-N oxidation rate between their low-DO (0.5 mg/L) and high-DO (3 mg/L) reactors. On the other hand, Arnaldos et al. (2013) reported a NH₄-N oxidation rate in low-DO reactor (0.1 mg/L) half of that in their saturated DO reactor. In the pilot-scale study conducted by Fan et al. (2017), NH₄-N removal efficiency was close to 100% at both low (0.5 mg/L) and high DO (1 mg/L) conditions in a continuous anoxic-oxic process. Similarly, Keene et al. (2017) achieved 96% ammonia removal at 0.33 mg O₂/L in a pilot-scale anaerobic-anoxic-aerobic reactor. If the DO concentration in the nitrification tank was controlled at 0.33 mg/L, Keene et al. (2017) estimated a resultant 25% in energy saving when compared with high-DO operation (2.9 – 4.3 mg O₂/L).

Several studies suggested that low-DO condition shifted the nitrifying community (Fitzgerald et al., 2015; Keene et al., 2017; G. Liu & Wang, 2013; Mehrani et al., 2020). Fitzgerald et al. (2015) reported that AOB related to *Nitrosomonas oligotropha* were enriched under prolonged exposure to low-DO condition (0.3 mg O₂/L) for 100 days. Keene et al. (2017) had also showed that *Nitrosomonas* closely related to *N. oligotropha* was the most abundant AOB in their pilot-scale low-DO anaerobic-anoxic-aerobic reactor (0.33 mg O₂/L). The findings from Fitzgerald et al. (2015) and Keene et al. (2017) contradicted the previous understanding that *N. oligotropha* had a lower oxygen affinity than *Nitromonas europaeae* (Park & Noguera, 2007), thus further studies on low-DO nitrifying community is warranted. For the NOB community, G. Liu and Wang (2013) and Keene et al. (2017) suggested that low-DO condition (< 1 mg/L) exerted selection pressure on *Nitrospira*-related NOB due to their high substrate affinity. In addition, *Nitrospira*-related comammox may also thrive in low-DO condition, which may contribute to a stable nitrification performance (Daims et al., 2015; Palomo et al., 2018). Nonetheless, the metadata analysis performed by Mehrani et al. (2020) suggested that high *Nitrospira* population was expected under high-DO condition (> 3 mg O₂/L) and high influent NH₄-N (20 mg/L), which contradicted with several studies that reported high *Nitrospira* population under lower DO concentrations. Further genomic and transcriptomic approaches are required to validate the nitrifying role of *Nitrospira* in biological nitrogen removal systems.

2.4.2 Effect of Biodegradable Chemical Oxygen Demand Fractions on Denitrification

The sources of bCOD for denitrification process can be broadly classified into the soluble fraction (rbCOD) and particulate fraction (sbCOD) as discussed in Section 2.1.1.2. The following subsections highlight the effects of each of these bCOD fractions on denitrification performance.

2.4.2.1 Utilisation of Soluble Biodegradable Chemical Oxygen Demand

The denitrification performance can be hindered by low biodegradable organics in the low COD/N wastewater (X. Wang et al., 2015). Low COD/N wastewater is defined as wastewater with sCOD/TN lower than 3.5 g COD/g N (X. Wang et al., 2015). External carbon dosage may improve the efficiency of denitrification but the strategy significantly increases the operating cost. For instance, 2.7 g to 3.3 g of methanol is required to reduce 1 g of NO₃-N (Tchobanoglous et al., 2014). The procurement of chemicals and the advanced control mechanism for external carbon dosage system significantly increase the operating cost of WWTPs (Y. Shen, Yang, Wu, Zhang, & Zhang, 2019).

2.4.2.2 Mechanism of Utilisation of Particulate Biodegradable Chemical Oxygen Demand

To overcome the high cost for external carbon dosage system, there is a growing interest to utilise the sbCOD in PSS to enhance the denitrification performance. The PSS is usually removed via primary clarification before entering the secondary treatment train of WWTPs. The utilisation sbCOD by bacteria involves the adsorption of hydrolytic bacteria on the PSS, hydrolysis of PSS and metabolism (Morgenroth et al., 2002). The hydrolysis of PSS is the rate-determining step when utilising sbCOD for denitrification (Figure 2.7). The definitions of the symbols X_S , S_S , S_O , X_H and X_I used in Figure 2.7 are sbCOD concentration, rbCOD concentration, DO concentration, heterotrophic bacteria concentration and inert decayed product of X_H , respectively.

At 20°C, the denitrification rate when utilising sbCOD as the source of biodegradable organics was 7 times lower than the rate when utilising rbCOD (Ekama & Wentzel, 2008). Thus, providing sufficient anoxic HRT is a key process operating condition to utilise sbCOD for denitrification.

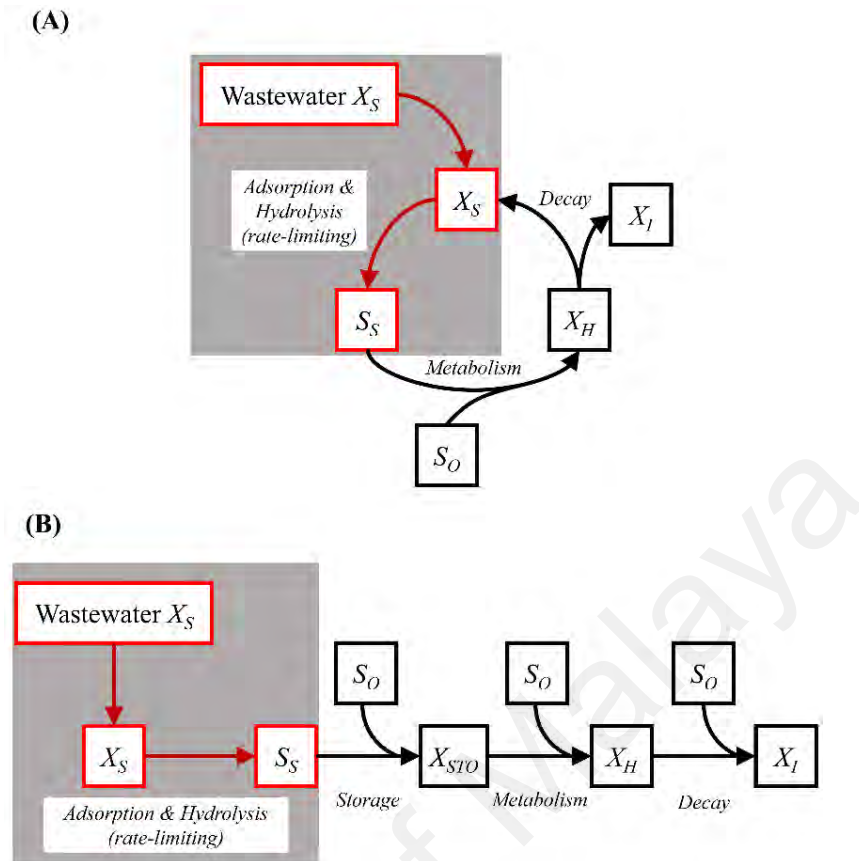


Figure 2.7: Models of transport and fate of organic substrate in wastewater adopted from (A) Activated Sludge Model 1 (ASM1) and (B) Activated Sludge Model 3 (ASM3).

Because sbCOD uptake is limited by the hydrolysis rate of PSS, studies were carried out to estimate the PSS hydrolysis kinetic coefficients (Benneouala et al., 2017; Morgenroth et al., 2002). Figure 2.7A and Figure 2.7B show the modelling approaches in the ASM1 and ASM3, respectively (Gujer, Henze, Mino, & van Loosdrecht, 1999; Henze et al., 1987). ASM1 adopts a death-regeneration concept for the endogenous decay of X_H into X_S and X_I , while the endogenous decay of X_H produces only X_I in ASM3 (Figure 2.7). The death-regeneration concept in ASM1 is difficult to model as the fraction of bacteria decaying into PSS is often unknown. Benneouala et al. (2017) and J. Wu, Yan, Zhou, and Xu (2014) reported a modified ASM1 for an easier modelling and estimation of PSS hydrolysis kinetic coefficients. The modified ASM1

uses the endogenous respiration concept in ASM3, thus avoiding the estimation of the fraction of bacteria decaying into PSS (Figure 2.8). However, the use of modified ASM1 is limited for batch experiments where the slow decay of X_H did not produce significant amount of X_S (Benneouala et al., 2017; J. Wu et al., 2014).

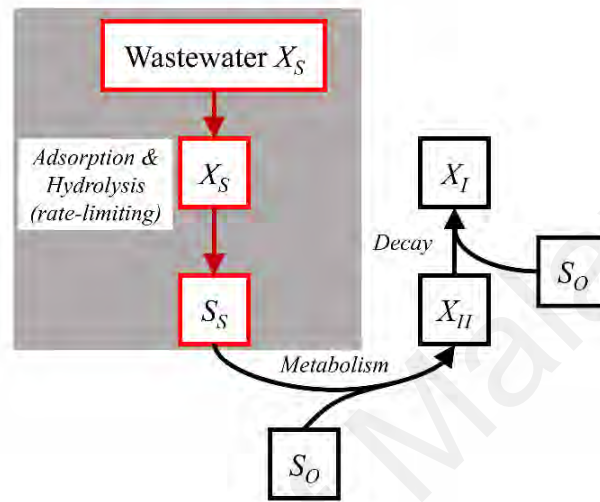


Figure 2.8: Modified ASM1 with the product of cell decay decoupled from PSS in the wastewater.

Fitting the modified ASM1 to the oxygen uptake rate (OUR) profile is a common method to estimate the PSS hydrolysis kinetic coefficients (Benneouala et al., 2017; Henze et al., 1987). By determining the OUR experimentally, the S_S uptake rate of bacteria and subsequently the rate of X_S hydrolysing into S_S could be backtracked. The rate of hydrolysis, r_H is expressed using saturation kinetics (Equation 2.6),

$$r_H = k_H \frac{X_S/X_H}{K_X + X_S/X_H} X_H \quad (2.6)$$

Where k_H is the hydrolysis rate constant and K_X is the hydrolysis saturation constant. The default values for k_H and K_X at 20°C are 0.09 1/h and 0.15 g COD/g COD, respectively (Henze et al., 1987). The Arrhenius relationship predicts that warm

wastewater in the tropical region (30°C) may double the PSS hydrolysis rate (Gujer et al., 1999).

2.4.2.3 Operating Strategies of Biological Nitrogen Removal in Treating Low Chemical Oxygen Demand-to-Nitrogen Wastewater

Using biological nitrogen removal in treating low COD/N wastewater (< 6 g COD/g N) is challenging because a COD/N range of 6 to 11 g COD/g N is required to ensure complete denitrification (Henze et al., 1994). Several research studies were conducted to develop operating strategies in treating low COD/N wastewater efficiently without using the costly external carbon dosage (Cao, Daigger, & van Loosdrecht, 2020; Gao et al., 2020; X. Wang et al., 2015; X. Wang, Wang, Zhao, Dai, & Peng, 2016; Zhao et al., 2018). X. Wang et al. (2015) reported enhanced TN removal efficiency from 65% to 77% by strengthening the intracellular carbon storage of denitrifying polyphosphate accumulating organisms in an anaerobic-aerobic reactor treating low COD/N wastewater (< 3.5 g COD/g N) in China. X. Wang et al. (2016) further enhanced the denitrification performance by utilising the intracellular carbon storage in the post-anoxic stage in an anaerobic-aerobic-anoxic reactor, which resulted in 92% TN removal from the low COD/N wastewater. A similar TN removal efficiency was also achieved in a continuous anaerobic-aerobic-anoxic reactor with suspended biofilm carrier in theoxic zone between 1 and 2 mg O₂/L (Zhao et al., 2018). Gao et al. (2020) fine-tuned the anaerobic-aerobic-anoxic reactor by recirculating the biomass from the sedimentation tank to the post-anoxic zone. The recirculating biomass stream increased the biomass concentrations to provide more intracellular carbon storage for post-anoxic denitrification, thereby increased the TN removal efficiency to 98%. In the case where intracellular carbon storage is not possible due to low phosphorus content in the wastewater, Cao et al. (2020) suggested that the use of fermented recycle activated sludge may supplement COD for denitrification process. The use of fermented sludge is

also recommended for wastewater with high inorganic solids as PSS in the wastewater contained lower bCOD (Cao et al., 2020).

Nonetheless, the use of intracellular carbon storage for post-anoxic denitrification mentioned above were developed for treating low COD/N wastewater with temperature of $22 \pm 1^\circ\text{C}$ in the temperate climate region (Gao et al., 2020; X. Wang et al., 2015; X. Wang et al., 2016; Zhao et al., 2018). The application of post-anoxic denitrification process may be efficient in treating tropical wastewater (30°C) because of the higher PSS hydrolysis rate as predicted by Arrhenius relationship. Further investigations are needed to determine the feasibility of a post-anoxic denitrification process in treating tropical wastewater with low COD/N.

2.4.3 Effect of Hydraulic Retention Time and Organic Volumetric Loading Rate on Biological Nitrogen Removal

HRT and SRT are the two critical design parameters for biological nitrogen removal. HRT indicates the average time the wastewater is retained in a reactor and in contact with the sludge for biological uptake of substrate (Najafpour, 2015). HRT is expressed as the ratio of the volume of reactor (V) and the influent flow rate (Q) as in Equation 2.7,

$$HRT = \frac{V}{Q} \quad (2.7)$$

The HRT of a system determines L_{org} and treatment capacity of a wastewater treatment system. L_{org} is defined as in Equation 2.8 (Tchobanoglous et al., 2014),

$$L_{org} = \frac{Q \cdot S_i}{V} = \frac{S_i}{HRT} \quad (2.8)$$

Where S_i is the influent bCOD. Shorter HRT implies higher L_{org} and treatment capacity, but the HRT must be sufficiently long to allow contact time between the wastewater and sludge for biological reactions to occur. Typical L_{org} should be between 0.3 and 0.6 kg BOD₅/m³·d for sufficient contact time for organic matter removal (National Water Services Commission, 2009). The typical HRTs were discussed in later sections on biological nitrogen removal configurations (Section 2.5).

2.4.4 Effect of Sludge Retention Time and Food-to-Microbe Ratio on Biological Nitrogen Removal

The SRT represents the average time the sludge is retained in a reactor (Tchobanoglous et al., 2014). The SRT is a ratio of the mass of sludge in the reaction tanks and the mass of sludge wasted daily. In an activated sludge process, the SRT is expressed as in Equation 2.9,

$$SRT = \frac{VX}{(Q - Q_w)X_e + Q_wX_R} \quad (2.9)$$

Where X is the sludge concentration in the reaction tanks, Q_w is the waste sludge flow rate, X_e is the sludge concentration in the effluent and X_R is the sludge concentration in the recycle activated sludge (RAS) stream. The range of SRT required for biological nitrogen removal varies widely between 3 – 18 d (Tchobanoglous et al., 2014). Short SRT value may wash out the slow-growing bacteria performing nitrification, which has a growth rate 6 to 7 times lower than the growth rate of bacteria performing bCOD oxidation (Tchobanoglous et al., 2014).

At constant HRT, SRT could affect biomass concentration and subsequently the F/M as shown in Equation 2.10 (Tchobanoglous et al., 2014),

$$F/M = \frac{Q \cdot S_i}{VX} = \frac{L_{org}}{X} \quad (2.10)$$

F/M typically ranges from 0.05 – 0.5 g BOD/g MLVSS·d for activated sludge systems (National Water Services Commission, 2009; Tchobanoglous et al., 2014).

2.5 Biological Nitrogen Removal Configurations for Wastewater Treatment

Based on the biochemistry and microbiology principles of biological nitrogen removal reviewed in the precedent sections, WWTPs may employ different process configurations to achieve biological nitrogen removal from the wastewater. The configurations using the conventional nitrification-denitrification pathway can be classified into two broad classes, namely pre-anoxic and post-anoxic configurations (Tchobanoglous et al., 2014). In this section, the common pre-anoxic and post-anoxic process configurations were reviewed. A few novel configurations for biological nitrogen removal were also discussed.

2.5.1 Pre-Anoxic Configurations

In pre-anoxic configurations, the wastewater first enters a pre-anoxic or anoxic tank for denitrification, where NO_3^- is reduced to N_2 gas. The wastewater then flows into anoxic tank for nitrification, where NH_4^+ is oxidised to NO_3^- . Most of the WWTPs are operating with pre-anoxic configurations (M. Winkler, Coats, & Brinkman, 2011). The common pre-anoxic configurations include Modified Ludzack-Ettinger (MLE) process, EA process with pre-anoxic tank and step-feed biological nitrogen removal (Barnard, 1974; Ludzack & Ettinger, 1962; National Water Services Commission, 2009; Tchobanoglous et al., 2014).

MLE process as shown in Figure 2.9 is one of the most common configurations used in WWTPs (Tchobanoglous et al., 2014). The process was developed by Ludzack and Ettinger (1962) by recycling the NO_3^- produced by nitrification in the oxic tank to an

upstream anoxic tank via the RAS line. By placing an anoxic tank upstream of the oxie tank, the bCOD can be removed by denitrification using NO_3^- as the electron acceptor. bCOD removal during denitrification is more economical than using aeration in the conventional activated sludge process. Moreover, the alkalinity produced during denitrification can act as a pH buffer against pH drop during the downstream nitrification. Barnard (1974) enhanced the NO_3^- recycle from the oxie tank to the anoxic tank using a high-flow MLR stream (Figure 2.9). The high-flow MLR stream is typically 4 to 6 times the flow rate of influent (National Water Services Commission, 2009; Tchobanoglous et al., 2014). Consequently, the pumping cost associated with the MLR stream significantly increases the energy consumption of the process. The design parameters for a MLE process are listed in Table 2.3. The effluent of MLE process typically contained unremoved TN in the form of $NO_3\text{-N}$ (Table 2.3), which may not comply with stringent discharge limits that mandate complete TN removal.

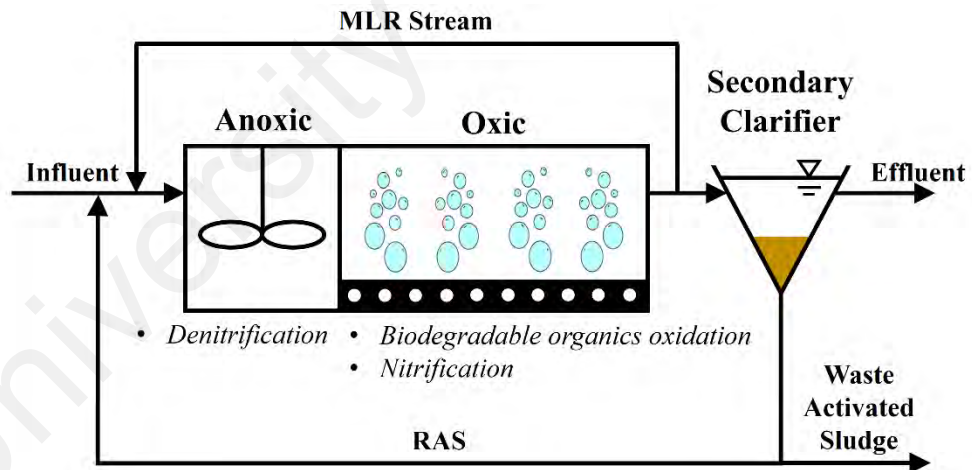


Figure 2.9: The configuration of a MLE process.

Table 2.3: Process characteristics of pre-anoxic configurations (National Water Services Commission, 2009; Tchobanoglous et al., 2014)

Characteristics	Process Configurations		
	MLE Process ^{1,2}	EA with Pre-Anoxic Tank ^{1,2}	Step-Feed Biological Nitrogen Removal ²
HRT, hr	12 – 16	18 – 24	3 – 5
SRT, d	5 – 10	> 20	3 – 15
Flow splitting ratio	-	-	3:7:6:4
DO concentration at oxic tank, mg/L	2.0	2.0	2.0
MLR flow rate	4 – 6 times influent flow rate	4 – 6 times influent flow rate	-
Mixed liquor suspended solids (MLSS), mg/L	1500 – 3000	2500 – 5000	1500 – 4000
F/M, g BOD/g MLVSS-d	0.25 – 0.50	0.05 – 1	0.2 – 0.4
Effluent TN, mg/L	6 – 10	6 – 10	< 5

¹ National Water Services Commission (2009)

² Tchobanoglous et al. (2014)

As of 2016, decentralised small-to-medium sized WWTPs (10000 – 30000 PE) made up 99% of the WWTPs in Malaysia (Malaysian Water Association, 2017). Most of these decentralised WWTPs were operating in EA configuration. After the introduction of the discharge limits for NH_4-N and NO_3-N in Environmental Quality (Sewage) Regulations 2009, these WWTPs operated in extended aeration (EA) configuration incorporated a pre-anoxic tank to achieve biological nitrogen removal. The EA process with pre-anoxic tank operates with an AO configuration similar to that of MLE process (Figure 2.9). A high-flow MLR stream 4 to 6 times the influent flow rate is required to recycle the unremoved NO_3^- from the oxic tank to the anoxic tank. A major advantage of EA process with pre-anoxic tank is the lower sludge production than that for MLE process (Tchobanoglous et al., 2014). The EA process with pre-anoxic tank uses long

HRT and SRT to create a low F/M, which starves the microbes in the system (Table 2.3). At extended aeration condition, the starved microbes undergo cell decay. The decayed products are then consumed by other living cells, which in turn lower the net sludge production. The long HRT and extended aeration condition in the oxic tank provide better process stability in handling shock organic and nitrogen loadings (Tchobanoglous et al., 2014). The oxic tank in EA process is typically larger than that for MLE process, which implies higher energy consumption for aeration. Ramli and Abdul Hamid (2017) reported that aeration, piping and pumping constituted 70% of the WWTPs' total operating cost. The main operating conditions recommended for EA plants with pre-anoxic tank are HRT 18 – 24 h, SRT > 20 d and DO in the oxic tank at 2 mg O₂/L (Table 2.3).

Another common pre-anoxic configuration is step-feed biological nitrogen removal (Figure 2.10). The influent is split into a few passes, typically 4 passes, and distributed into multiple AO stages arranged in series (Tchobanoglous et al., 2014). The flow distribution is uneven, with a typical splitting ratio of 3:7:6:4 (Table 2.3). By using the step-feeding approach, the high-flow MLR stream required in MLE and EA with pre-anoxic tank processes could be eliminated (Tchobanoglous et al., 2014). Effluent TN below 5 mg/L is attainable by using the step-feed biological nitrogen removal (Table 2.3). However, operating step-feed biological nitrogen removal requires advanced control systems for influent flow distribution and DO in each aeration tank (Tchobanoglous et al., 2014). The DO in the aeration tanks must be carefully controlled to prevent excess DO from entering the next AO stage, which can deteriorate the denitrification performance. Step-feed biological nitrogen removal is operated mostly in developed countries where expertise and resources are available. For example, Singapore Changi Water Reclamation Plant uses the advanced step-feed approach to

achieve good TN removal to below 5 mg/L (Cao et al., 2016). The advantages and disadvantages of the pre-anoxic configurations discussed is summarised in Table 2.4.

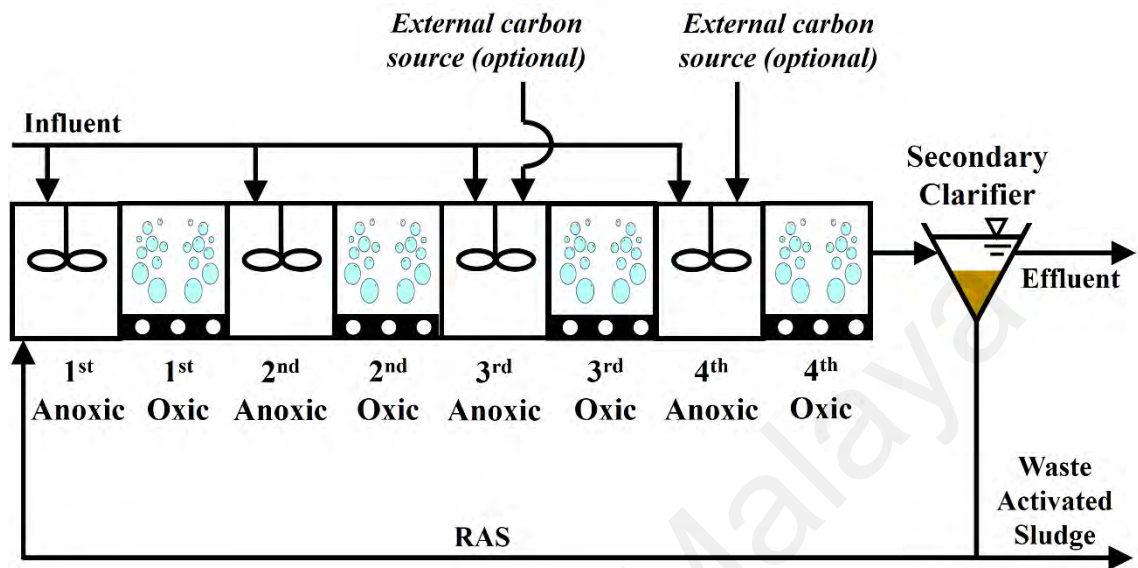


Figure 2.10: The configuration of step-feed biological nitrogen removal.

Table 2.4: Advantages and disadvantages of the pre-anoxic configurations

Process Configurations	Advantages	Disadvantages
MLE	<ul style="list-style-type: none"> • bCOD is removed by denitrification to save energy • Alkalinity produced during denitrification acts as pH buffer 	<ul style="list-style-type: none"> • High effluent TN • Requires a high-flow MLR stream
EA with pre-anoxic tank	<ul style="list-style-type: none"> • Lower sludge production • Able to handle shock organic and nitrogen loadings 	<ul style="list-style-type: none"> • High effluent TN • Requires a high-flow MLR stream • Extended aeration incurs additional energy consumption
Step-feed biological nitrogen removal	<ul style="list-style-type: none"> • Low effluent TN • Eliminate MLR stream 	<ul style="list-style-type: none"> • Requires advanced control systems for flow distribution and DO in oxic tanks

2.5.2 Post-Anoxic Configurations

In post-anoxic designs, the wastewater is first nitrified in an aerobic tank before entering a post-anoxic tank for denitrification. Some of the post-anoxic configurations used in activated sludge process include Wuhrmann biomass decayer and Bardenpho process (Barnard, 1974; Wuhrmann, 1964). Recent research studies recommended post-anoxic configurations to achieve stringent nitrogen discharge limit instead of using the more widely-used pre-anoxic configurations (Shi, Ma, Li, Zhang, & Peng, 2019; M. Winkler et al., 2011; Zhao et al., 2018).

The basic post-anoxic configuration is the Wuhrman biomass decayer (Wuhrmann, 1964), which follows an oxic-anoxic (OA) configuration (Figure 2.11). Wuhrmann biomass decayer does not require a high-flow MLR stream and may achieve low effluent TN below 3 mg/L (Table 2.5). The wastewater must contain sufficient alkalinity to buffer against pH drop during nitrification. Another main drawback of Wuhrman biomass decayer process is that most of the biodegradable organics is oxidised in the oxic tank. The remaining biodegradable organics may be insufficient to sustain efficient denitrification (Wuhrmann, 1964). Endogenous respiration of the biomass in the anoxic reactor may provide biodegradable organics for denitrification. Zhao et al. (2018) and Shi et al. (2019) recommended post-anoxic configurations in treating low COD/N wastewater (3.5 – 4.4 g COD/g N) and reported high TN removal (92 – 99%) in their post-anoxic reactors. However, the observed specific denitrification rate using endogenous source of biodegradable organics is 10 times lower than that using exogenous carbon sources (Murakami & Babcock, 1998; M. Winkler et al., 2011). The low specific denitrification rate may result in larger anoxic tank size. NH_4^+ is also released during endogenous respiration, thus increasing the TN concentration in the effluent. Alternatively, external carbon source can be added to the anoxic reactor to

boost denitrification, but at a higher operating cost. The characteristics of Wuhrmann biomass decayer is listed in Table 2.5.

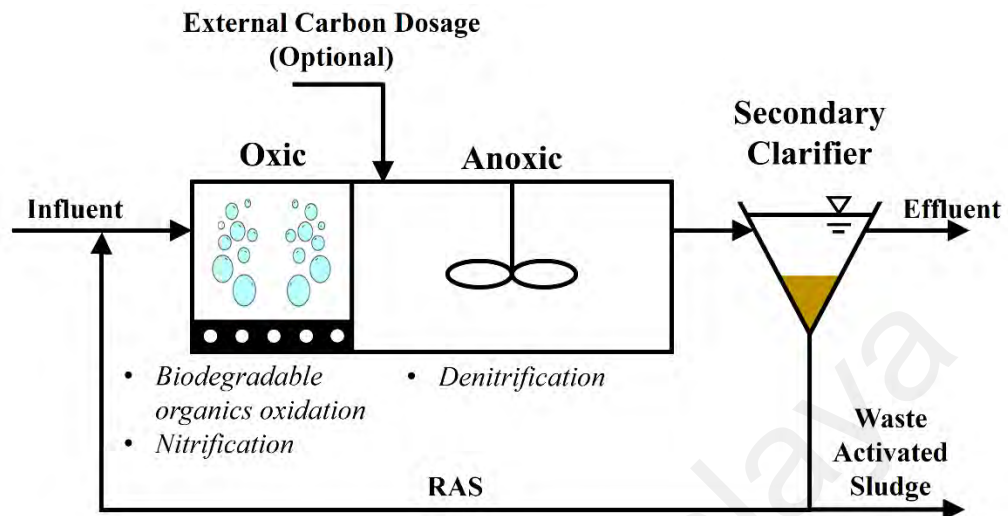


Figure 2.11: The configuration of a Wuhrmann biomass decayer.

Table 2.5: Process characteristics of post-anoxic configurations (Maryland Department of the Environment, 2016; Tchobanoglous et al., 2014; Wuhrmann, 1964)

Characteristics	Process Configurations	
	Wuhrmann Biomass Decayer ^{1,2}	Bardenpho ^{2,3}
HRT, hr	3 – 5	16 – 23 (1 st anoxic: 2 – 4, 1 st oxic: 8 – 12, 2 nd anoxic: 2 – 5, 2 nd oxic: 0.5 – 1)
SRT, d	-	16 – 18
DO concentration at oxic tank, mg/L	3 – 4	2 – 4
MLR flow rate	-	4 – 6 times influent flow rate
MLSS, mg/L	3000 – 4000	2000 – 6000
F/M, g BOD/g MLVSS·d	-	0.1 – 0.2
Effluent TN, mg/L	< 3	< 1

¹ Wuhrmann (1964)

² Tchobanoglous et al. (2014)

³ Maryland Department of the Environment (2016)

Bardenpho process combines pre-anoxic and post-anoxic configurations to enhance biological nitrogen removal (Barnard, 1974). The Bardenpho process consists of two AO stages in series, a MLR stream recycles the NO_3^- produced from the first stage to the first anoxic tank (Figure 2.12). The arrangement of two AO stages in series improves the effluent quality with lower TN concentration (< 1 mg/L). However, using multiple AO stages with MLR stream significantly increases the plant footprint and operating cost. DO in the first oxic tank must be carefully controlled between 2 to 4 mg O_2/L to prevent excess DO leaving the first AO stage from entering the post-anoxic tank (Table 2.5). External carbon sources is still needed in the post-anoxic tank as most of the bCOD has been oxidised in the first AO stage (Tchobanoglous et al., 2014). Table 2.6 lists the advantages and disadvantages of post-anoxic configurations for biological nitrogen removal.

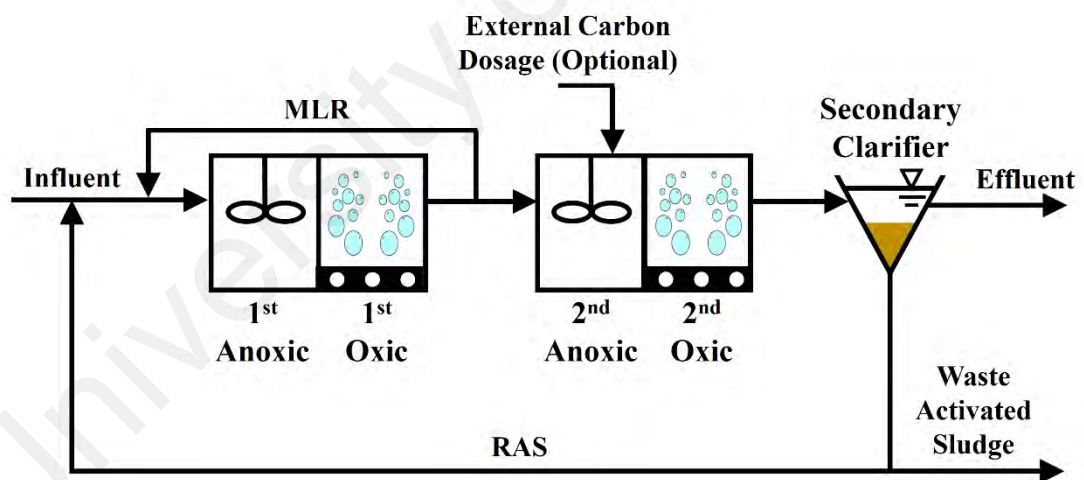


Figure 2.12: The configuration of a Bardenpho process.

Table 2.6: Advantages and disadvantages of the post-anoxic configurations

Process Configurations	Advantages	Disadvantages
Wuhrmann biomass decayer	<ul style="list-style-type: none">• Low effluent TN (< 3 mg/L)• Eliminates high-flow MLR stream	<ul style="list-style-type: none">• Require sufficient alkalinity in the wastewater for nitrification• Requires exogenous carbon source to boost denitrification
Bardenpho	<ul style="list-style-type: none">• Very low effluent TN (< 1 mg/L)	<ul style="list-style-type: none">• Large plant footprint• Requires a high-flow MLR stream• Requires external carbon source for post-anoxic tank

2.5.3 Novel Configurations for Biological Nitrogen Removal

Apart from the conventional configurations using nitrification-denitrification pathways, a few novel configurations exploiting nitritation and anammox pathways have been reported (Cao et al., 2017; Hellings, Schellen, Mulder, van Loosdrecht, & Heijnen, 1998; M. K. Winkler & Straka, 2019). Some of these novel configurations for biological nitrogen removal include nitritation-denitritation and partial nitritation-anammox process (M. K. Winkler & Straka, 2019).

Nitritation-denitritation configuration suppresses NOB activity and uses NO_2^- as the electron acceptor in denitritation (M. K. Winkler & Straka, 2019). The suppression of NOB activity may be achieved by SRT control and intermittent aeration. SRT control exploits the higher growth rate of AOB than that of NOB to washout NOB from the system. For instance, SRT of the nitritation-denitritation process should be between the minimum SRT of NOB (0.5 d at 30°C) and AOB (1 d at 30°C) to achieve stable nitritation (Hellings et al., 1998). Intermittent aeration strategy creates an oxygen-

limiting environment, which allows AOB to outcompete NOB due to AOB's higher oxygen affinity (Blackburne, Yuan, & Keller, 2008). However, Law et al. (2019) suggested that using oxygen competition to washout NOB may not be reliable as NOB with high oxygen affinity, such as *Nitrospira sp.*, may gradually dominate the nitrifying community. A major advantage of suppressing NOB activity in nitrification-denitrification process is the lower aeration cost, which reduced 25% of the aeration cost when compared with nitrification-denitrification pathway (M. K. Winkler & Straka, 2019). A downside to nitrification-denitrification process is that NO_2^- accumulation triggers the emission of N_2O , which is a highly potent greenhouse gas (Kampschreur, Temmink, Kleerebezem, Jetten, & van Loosdrecht, 2009).

Partial nitrification-anammox process is another documented novel configuration for biological nitrogen removal (Cao et al., 2017). In this process, part of the NH_4^+ in the wastewater is first oxidised into NO_2^- by partial nitrification, the NO_2^- is then used as an electron acceptor to oxidise the remaining NH_4^+ into N_2 via anammox pathway (Kuenen, 2008). Partial nitrification-anammox is attractive for the wastewater industry as it reduced the aeration energy up to 60% when compared with conventional nitrification-denitrification configurations (M. K. Winkler & Straka, 2019). Furthermore, partial nitrification-anammox does not require any carbon source. (M. K. Winkler & Straka, 2019) Widespread application of partial nitrification-anammox process in mainstream wastewater treatment systems is limited by low NH_4^+ concentration in domestic wastewater, which is not favourable for the growth of anammox bacteria (Cao et al., 2017).

Based on the review, novel configurations for biological nitrogen removal have severe limitations that hinder their application in WWTPs. Thus, these configurations are not the focus in this study.

2.6 Summary of Chapter

The important concepts on wastewater characteristics, biochemical transformations in biological nitrogen removal, microorganisms involve in the nitrification-denitrification pathways and biological nitrogen removal configurations designed for WWTPs were reviewed. The tropical wastewater characteristics, such as the COD and COD/N ratio, may influence the operating strategies to achieve efficient biological nitrogen removal from the wastewater. The current EA process with pre-anoxic tank adopted by many of the decentralised WWTPs in Malaysia is not optimised for the local wastewater condition in Malaysia. From the literature review, there are a few opportunities to improve the existing design, such as low-DO nitrification process and utilising sbCOD in post-anoxic denitrification. The improved design for biological nitrogen removal in treating the local wastewater may reduce the operating cost of WWTPs. In the following chapters, the methodology and findings from the development of a process improved for treating the tropical wastewater characteristics in Malaysia are presented.

CHAPTER 3: MATERIALS AND METHODS

3.1 Wastewater and Sludge Sampling

To obtain sludge and wastewater samples for batch experiments and reactor operations, grab samples of RAS and raw wastewater after preliminary treatment were collected from six WWTPs in the Greater Kuala Lumpur region from July 2017 to April 2019 (Table 3.1). These WWTPs' locations, configurations, HRT and SRT were listed in Table 3.1. WWTPs situated in different parts of the Greater Kuala Lumpur region were selected to characterise wastewater produced in a rapidly-developing area, which is a main point source for nitrogen pollution in Malaysia (Department of Environment, 2017). WWTP 1 and WWTP 2 are medium-sized plants (10000 – 30000 PE) operating in extended aeration with pre-anoxic tank to encourage biological nitrogen removal. WWTP 3 is a small decentralised plant (< 10000 PE) that uses a CAS system, while WWTP 4 is an aerated lagoon using mechanical aerators to artificially aerate the mixed liquor. Both WWTP 4 and 5 are not designed for biological nitrogen removal. WWTP 5 and WWTP 6 are two regional WWTPs (> 50,000 PE) that use A₂O reactor and SBR with anoxic selector designed for biological nitrogen removal. Kuala Lumpur has a tropical climate with daily temperature between 24°C and 34°C during the sampling period (National Centers for Environmental Information, 2019). This region has a separate sewer system. Activated sludge from the RAS stream and raw wastewater samples from WWTP 1 was collected weekly from July 2017 to October 2018 ($n = 66$). Two samples of activated sludge and raw wastewater from WWTP 2 to 6 were collected consecutively every two weeks from January 2019 to April 2019 ($n = 10$). The preliminary treatment in all the WWTPs includes bar screen and aerated grit chamber. The samples were stored at 4°C prior to use.

Table 3.1: Details of the six WWTPs in the Greater Kuala Lumpur region

Plant	Location	Plant Configuration	PE Range	HRT (hr)	SRT (d)
WWTP 1	Petaling Jaya	EA with pre-anoxic tank	10000 – 30000	18 – 24	> 20
WWTP 2	Puchong	EA with pre-anoxic tank	10000 – 30000	18 – 24	> 20
WWTP 3	Puchong	CAS	< 10000	6 – 16	5 – 10
WWTP 4	Puchong	Aerated lagoon	10000 – 30000	18 – 24	> 20
WWTP 5	Pantai Dalam	A ₂ O	> 50000	18 – 28	5 – 10
WWTP 6	Titivangsa	SBR with anoxic selector	> 50000	18 – 24	10 – 30

A₂O : Anaerobic-anoxic-oxic

SBR: Sequencing batch reactor

3.2 Fractionation of Chemical Oxygen Demand

The fractions of rbCOD and sbCOD in the wastewater were characterised using a method based on NUR (van Loosdrecht et al., 2016). The wastewater COD fractionation comprised of two separate batch experiments. The anoxic yield coefficient ($Y_{OHO,ax}$) was determined from the first experiment. The $Y_{OHO,ax}$ was then used for calculating the concentrations of rbCOD and sbCOD based on NUR profiles obtained from the second experiment.

3.2.1 Anoxic Yield Coefficient Determination Experiment

A 500-mL working volume beaker was used in $Y_{OHO,ax}$ determination experiment. The experiment was conducted by mixing the concentrated waste sludge from WWTP 1, potassium nitrate solution, allylthiourea solution and the wastewater from WWTP 1 that was filtered through a 0.45- μ m membrane filter (filtered wastewater) to form the reaction mixture. The initial composition of the reaction mixture was NO₃-N 100 mg/L, allylthiourea 20 mg/L and mixed liquor volatile suspended solids (MLVSS) 3000 mg/L. The experiment were carried out at room condition ($30 \pm 2^\circ\text{C}$). Mixed liquor samples

were collected every 15 min for COD and anion analyses (NO_3^-). The pH readings were recorded periodically from an 827 pH Lab with Primatrode (Metrohm, Switzerland).

3.2.2 Nitrate Uptake Rate Experiment

A 500-mL working volume beaker was used in the NUR experiments. The washed RAS from each WWTP, potassium nitrate solution, allylthiourea solution and raw wastewater from each WWTP were mixed to form the reaction mixture for each of the wastewater samples, respectively. The initial compositions of the reaction mixture was NO_3-N 100 mg/L, allylthiourea 20 mg/L and MLVSS 3000 mg/L. The batch experiments were carried out at room condition ($30 \pm 2^\circ C$). Mixed liquor samples were taken every 30 min for the first 2 h, followed by every 2 h until the end of the experiment for anion analysis (NO_2^- and NO_3^-). The pH readings were recorded periodically from an 827 pH Lab with Primatrode (Metrohm, Switzerland). Two sets of the wastewater fractionation experiments were conducted using wastewater from each WWTP listed in Table 3.1.

3.2.3 Calculation of Readily-Biodegradable Chemical Oxygen Demand and Slowly-Biodegradable Chemical Oxygen Demand from Nitrate Uptake Rate Profiles

The $Y_{OHO,ax}$ of the sludge was determined from the change of NO_3-N and COD from the $Y_{OHO,ax}$ determination batch test using filtered wastewater according to Equation 3.1 (Tchobanoglous et al., 2014),

$$Y_{OHO,ax} = 1 - \frac{2.86 \cdot \Delta NO_3 - N}{\Delta COD} \quad (3.1)$$

Once the $Y_{OHO,ax}$ is known, the rbCOD and sbCOD in each wastewater samples were calculated using Equation 3.2 and Equation 3.3, respectively (van Loosdrecht et al., 2016),

$$rbCOD = \frac{2.86}{1 - Y_{OHO,ax}} (a_{rbCOD} - a_{sbCOD}) \quad (3.2)$$

$$sbCOD = \frac{2.86}{1 - Y_{OHO,ax}} (a_{sbCOD} - a_{endo}) \quad (3.3)$$

Where a_{rbCOD} , a_{sbCOD} and a_{endo} are the y-intercepts of the rbCOD degradation, sbCOD degradation and the endogenous respiration lines on the NO_x-N time profile (Figure 3.1), respectively. NO_x-N is the sum of nitrite nitrogen (NO_2-N) and NO_3-N ($0.6 \cdot NO_2-N + NO_3-N$). The coefficient 2.86 g COD/g NO_3-N represents the oxygen equivalence term for NO_3-N . The rbCOD degradation, sbCOD degradation and endogenous respiration lines were fitted to the NO_x-N time profile by linear regression.

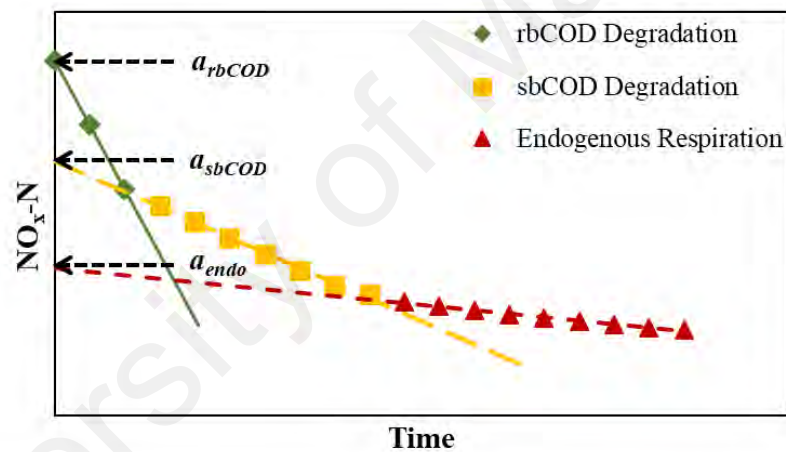


Figure 3.1: An example NO_x-N time profile indicating the y-intercepts a_{rbCOD} , a_{sbCOD} and a_{endo} adapted from Naidoo et al. (1998) and van Loosdrecht et al. (2016).

3.3 Estimation of Particulate Settleable Solids Hydrolysis Kinetic Coefficients at Tropical Temperature (30°C)

The PSS hydrolysis kinetic coefficients were estimated by fitting a modified ASM1 to the OUR profiles of different wastewater samples collected from WWTPs listed in Table 3.1. The estimated kinetic coefficients provided information on whether utilising sbCOD from PSS hydrolysis is a feasible operating strategy for biological nitrogen removal in treating the tropical wastewater samples.

3.3.1 Oxygen Uptake Rate Experiment

The PSS hydrolysis kinetic coefficients were determined using OUR experiment (van Loosdrecht et al., 2016). The OUR experiment setup consisted of two compartments, a 500-mL aerated vessel and a 100-mL airtight flask (Figure 3.2). The reaction mixture was circulated between the aerated vessel and the airtight flask. The reaction mixture in the aerated vessel was continuously aerated to maintain the DO concentration above 4 mg O₂/L. The circulation of mixed liquor between the aerated vessel and the airtight flask was cut off at a regular interval to measure the DO drop in the airtight flask for 10 min. The reaction mixture was prepared by mixing raw wastewater, allylthiourea solution and washed sludge from each WWTP in Table 3.1. The initial composition of the reaction mixture was 100 mg allylthiourea/L and 3000 mg MLVSS/L. The OUR experiment was conducted at room temperature (30 ± 2°C). Mixed liquor samples were taken regularly for cation analysis (NH₄⁺) to confirm negligible nitrification activity. Two sets of the OUR experiment were conducted for each WWTP.

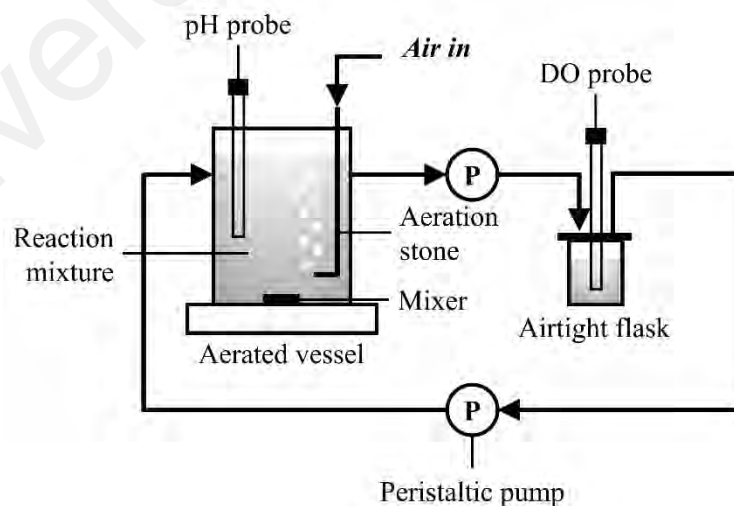


Figure 3.2: Setup of OUR experiment.

3.3.2 Calculation of Measured Oxygen Uptake Rate

The measured OUR was calculated based on the rate of DO drop in the airtight flask after the circulation between the aerated vessel and airtight flask was cut off according to Equation 3.4,

$$\text{Measured OUR} = -\frac{\Delta DO}{\Delta t} \quad (3.4)$$

Where ΔDO and Δt referred to the change in DO concentrations in the airtight flask and time interval when the DO drop was measured, respectively. A time series of measured OUR was obtained by plotting the measured OUR data points against the time when OUR was measured in the experiment.

3.3.3 Model Fitting of Activated Sludge Model 1 to Oxygen Uptake Rate Profiles

The hydrolysis kinetic constants were estimated by fitting a modified ASM1 to the OUR profiles (Henze et al., 1987). The decay of heterotrophic biomass was modelled using the endogenous respiration concept in ASM3 (Gujer et al., 1999). The combined model was adopted from Benneouala et al. (2017) and J. Wu et al. (2014) to model the hydrolysis of particulate matter in the wastewater. The activated sludge models were simulated using AQUASIM (Reichert, 1994). The process matrix, nomenclature and adopted values of the parameters are provided in Table 3.2. The initial concentrations of rbCOD and sbCOD of each wastewater sample were determined from the wastewater COD fractionation experiments. The kinetic parameters for aerobic growth and decay of heterotrophic biomass were fixed at temperature-corrected default values at 30°C as shown in Table 3.2 (Gujer et al., 1999; Henze et al., 1987).

Table 3.2: Process kinetics and stoichiometry for the modified ASM1 model fitting to OUR profiles (Gujer et al., 1999; Henze et al., 1987)

Processes	Components					Reaction Rate
	S_O	S_S	X_H	X_S	X_I	
Hydrolysis of X_S		1		-1		$k_H \frac{X_S/X_H}{K_X + X_S/X_H} X_H$
Aerobic growth of X_H	$1 - 1/Y_H$	$-1/Y_H$	1			$\mu_H \frac{S_S}{K_S + S_S} X_H$
Endogenous respiration of X_H	$f_p - 1$		-1		f_p	$b_H X_H$

Nomenclatures:-

b_H = Aerobic endogenous respiration of heterotrophic organisms (0.0125 1/h)

f_p = Fraction of non-biodegradable decayed biomass (0.08)

K_S = Saturation constant for rbCOD (20 mg/L)

Y_H = Heterotrophic growth yield (0.67 g COD/g COD)

μ_H = Maximum heterotrophic growth rate (0.49 1/h)

A sensitivity analysis of the kinetic parameters in the modified ASM1 model (k_H , K_X , μ_H , K_S and b_H) on the model state variables (S_O , S_S , X_H , X_S and X_I) using the methodology described by Brun, Kühni, Siegrist, Gujer, and Reichert (2002). The matrix entries for the sensitivity of the model state variables y_i towards 10% change in each kinetic parameter p_j were denoted as S_{ij} , which was calculated based on the mean temporal points of relative sensitivity function in AQUASIM using Equation 3.5,

$$S_{ij} = \frac{1}{N} \sum_{k=1}^N \left(\frac{p_j}{y_i} \frac{dy_i}{dp_j} \right)_k \quad (3.5)$$

The overall sensitivity of parameter p_j is denoted by the root mean square of the j^{th} column, δ_j^{msqr} according to Equation 3.6,

$$\delta_j^{msqr} = \sqrt{\frac{1}{n} \sum_{i=1}^n S_{ij}^2} \quad (3.6)$$

Where n is the total number of data points along the j^{th} column. A sensitivity ranking of the kinetic parameters was obtained by sorting the parameters in descending magnitude of δ_j^{msqr} .

The calibration of the hydrolysis kinetic parameters (k_H and K_X) was performed by minimising the sum of squares of deviations (χ^2) between the simulated and measured OUR. The simulated OUR and χ^2 were calculated using Equations 3.7 and 3.8,

$$\text{Simulated OUR} = - \left[\left(1 - \frac{1}{Y_H} \right) \mu_H \frac{S_S}{K_S + S_S} + (f_p - 1) b_H \right] X_H \quad (3.7)$$

$$\chi^2 = \sum_{i=1}^m \left(\frac{\text{Measured OUR}_i - \text{Simulated OUR}_i}{\sigma_{meas,i}} \right)^2 \quad (3.8)$$

Where $\sigma_{meas,i}$ is the standard deviation of i^{th} measured OUR data point, while m denotes the number of data points in the time series of measured OUR.

3.4 Batch Denitrification Activity Experiment Using Different Chemical Oxygen Demand Fractions as Carbon Source

To demonstrate the feasibility of using sbCOD as a carbon source for denitrification, three sets of batch denitrification activity experiment were carried out using filtered wastewater, PSS in nutrient solution and blank nutrient solution, respectively. The filtered wastewater and PSS in nutrient solution provided rbCOD and sbCOD, respectively, as the organic carbon source for denitrification. Raw wastewater from WWTP 1 was filtered through a 0.2- μm membrane filter. The filtrate was collected as the filtered wastewater, while the PSS retained on the membrane filter was suspended in a nutrient solution. The nutrient solution contained 1070 mg/L ammonium chloride, 1460 mg/L potassium dihydrogen phosphate, 660 mg/L magnesium sulphate heptahydrate, 20 mg/L allylthiourea and 3.33 mL/L of trace element solution adopted

from Ong, Chua, Lee, Ngoh, and Hashim (2012). A batch experiment was performed using a blank nutrient solution as control. The initial MLVSS and $\text{NO}_3\text{-N}$ concentrations of the reaction mixture for the three sets of experiment were 3000 mg/L and 100 mg/L, respectively. All batch experiments were conducted in room conditions ($30 \pm 2^\circ\text{C}$). Mixed liquor samples from the batch experiments were taken at a regular interval for COD and anion analyses (NO_2^- and NO_3^-). The DO readings were recorded using an InPro6850i DO probe (Mettler-Toledo, U.S.), while the pH readings were monitored using a 405-DPAS-SC-K851200 combination pH/temperature probe (Mettler-Toledo, U.S.).

3.5 Assessment of the Effect of Dissolved Oxygen on Sludge Nitrification Activity

The sludge nitrification activity test was used to study the feasibility of applying low-DO nitrification as an operating strategy for biological nitrogen removal in treating tropical wastewater. Batch nitrification activity experiment was conducted to determine the specific ammonia uptake rate (SAUR) at different DO concentrations. Saturation kinetic model was fitted to the SAUR profile to assess the effect of DO on the sludge nitrification activity.

3.5.1 Batch Nitrification Activity Experiment

The procedure of the batch experiment was adapted from van Loosdrecht et al. (2016). A 1-L beaker was used for the batch experiments. The concentrated sludge from WWTP 1, tap water, ammonium chloride solution and potassium carbonate solution were mixed to form the reaction mixture. The initial concentrations of $\text{NH}_4\text{-N}$ and alkalinity in the reaction mixture were 20 mg/L and 200 mg/L as calcium carbonate, respectively. The pH of the mixture was adjusted to between 7.5 and 8.0 at the beginning of each set of experiment using 1 M sodium hydroxide solution. The batch

experiments were performed at DO set points of 0 mg/L, 0.25 mg/L, 1.25 mg/L, 2.25 mg/L, 3.25 mg/L, 5.25 mg/L and 6.5 mg/L. Compressed air was sparged into the reaction mixture and a solenoid valve connected to a M300 Process 1-channel ½ DIN DO monitor was used to control the DO level in the reaction mixture. The batch experiment was performed under room conditions ($30 \pm 2^\circ\text{C}$). Mixed liquor samples were collected periodically for anion (NO_2^- and NO_3^-) and cation (NH_4^+) analyses.

3.5.2 Calculation of Specific Ammonia Uptake Rate and Model Fitting of Saturation Kinetic to Specific Ammonia Uptake Rate Profile

The value of ammonia uptake rate (AUR, in mg N/L·hr) of each DO set point was calculated from the slope of the time profile of $\text{NH}_4\text{-N}$ or $\text{NO}_x\text{-N}$ ($\text{NO}_2\text{-N} + \text{NO}_3\text{-N}$) obtained from each batch nitrification activity experiment. SAUR (in mg N/g MLVSS·hr) at each DO set point was calculated by dividing the AUR by the respective MLVSS concentration.

Saturation kinetic model was used to simulate the effect of DO on SAUR (Tchobanoglous et al., 2014), as shown in Equation 3.9,

$$SAUR = \frac{SAUR_{max} \cdot DO}{K_O + DO} \quad (3.9)$$

Where $SAUR_{max}$ is the maximum SAUR. $SAUR_{max}$ and K_O were determined by performing nonlinear regression in MATLAB (v7.3, The Math Works Inc., Natick, MA, USA) by minimising the squared error of the regression line.

3.6 Lab-Scale Sequencing Batch Reactors Operation

Three SBRs were operated (i) to evaluate the feasibility of using low-DO nitrification to treat tropical wastewater in a SBR, (ii) to investigate the long-term nitrogen removal performance in an AO SBR applying low-DO nitrification and

utilising sbCOD to enhance denitrification performance, and (iii) to optimise the operating conditions for an efficient and cost-effective low-DO OA SBR system. Wastewater samples from WWTP 1 was used as influent for all the lab-scale SBRs operation as most of the WWTPs (Table 3.1) had consistent wastewater characteristics. The photos showing the setup of the SBRs were provided in Appendix A.

3.6.1 Low-Dissolved-Oxygen Nitrification Sequencing Batch Reactor

3.6.1.1 Sequencing Batch Reactor Operation

The working volume of the SBR was 2 L (Figure 3.3). Seed sludge obtained from WWTP 1 was inoculated into the SBR to achieve an initial MLSS concentration of 2500 mg/L. Wastewater obtained from WWTP 1 was fed into the SBR as influent after settling. The SBR was operated in 6-h cycle, including 5 min filling phase; 300 min reaction phase; 50 min settling phase; 4 min decanting phase and 1 min idling phase. Overhead stirring mechanism was used for both mixing and aeration to maintain low-DO condition ($< 0.5 \text{ mg O}_2/\text{L}$) in the reactor. The impeller designed rotational speed was 300 rpm to ensure that DO concentration during the 300-min reaction phase was lower than 0.5 mg/L. The SBR was operated with a HRT of 15 h and a SRT of 20 d, which corresponded to an effluent withdrawal rate of 0.8 L/cycle and sludge wastage rate of 50 mL/cycle. The HRT was shortened to 10 h (effluent withdrawal rate = 1.2 L/cycle) after 21 d of reactor operation due to excessive accumulation of $\text{NO}_3\text{-N}$ in the reactor. The DO concentration, temperature and pH were monitored online using InPro6850i DO probe coupled with M300 Process 1-channel 1/2 DIN DO monitor (Mettler-Toledo, U.S.) and Ceragel CPS71D digital pH sensor (Endress + Hauser, Germany). Mixed liquor samples were taken from the reactor hourly during the reaction phase in two sampling campaigns per week for chemical analyses (MLSS, MLVSS, NH_4^+ , NO_2^- , NO_3^- , DOC, TN and COD).

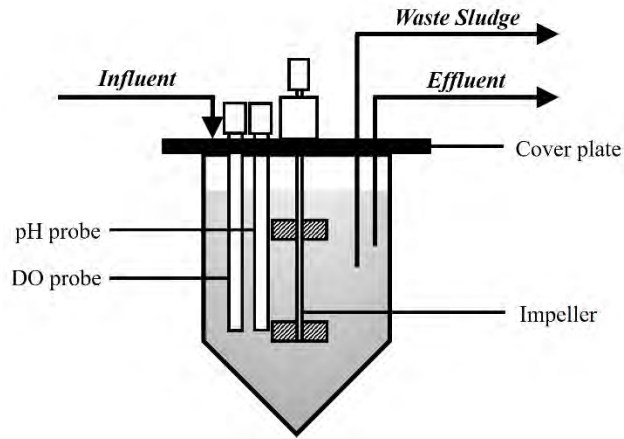


Figure 3.3: Setup of low-DO nitrification SBR.

3.6.1.2 Estimation of Energy Saving of Low-Dissolved-Oxygen Nitrification Process

The amount of energy reduction to operate a low-DO nitrification process (0.5 mg/L) relative to conventional nitrification process (2 mg/L) was estimated based on oxygen transfer rate (OTR) to maintain the biological activities, R_O and the bulk DO level in the mixed liquor, OTR_{LIQUID} (Keene et al., 2017; Tchobanoglous et al., 2014). The R_O was calculated using Equation 3.10 and Equation 3.11,

$$R_O = Q(S_i - S) - 1.42P_{X,bio} + 4.33Q(TKN) \quad (3.10)$$

$$P_{X,bio} = \frac{QY(S_i - S)}{1 + (k_d)SRT} + \frac{f_d k_d QY(S_i - S)SRT}{1 + (k_d)SRT} + \frac{QY_n(TKN)}{1 + (k_{dn})SRT} \quad (3.11)$$

Where S_i is the influent bCOD, S is the effluent bCOD, $P_{X,bio}$ is the biomass wasted, TKN is the total Kjeldahl nitrogen of influent, Y is the biomass yield from bCOD, k_d is the endogenous decay coefficient for heterotrophs, f_d is the fraction of cell mass as cell debris, Y_n is the biomass yield from nitrogen and k_{dn} is the endogenous decay coefficient for nitrifiers.

The OTR_{LIQUID} at a DO concentration was calculated using Equation 3.12,

$$OTR_{LIQUID} = [(Q - Q_{RAS})DO] + (Q(DO - DO_0)) \quad (3.12)$$

Where Q_{RAS} is the RAS flow rate and DO_0 is the DO concentration in previous tank.

The total OTR for a DO concentration, OTR_{TOTAL} was the sum of R_O and OTR_{LIQUID} (Equation 3.13),

$$OTR_{TOTAL} = OTR_{LIQUID} + R_O \quad (3.13)$$

The OTR_{TOTAL} was converted to the standard oxygen transfer rate, $SOTR$ using Equation 3.14 and Equation 3.15,

$$SOTR = \left(\frac{OTR_{TOTAL}}{\alpha F} \right) \left\{ \frac{C_{\infty 20}^*}{\left[\beta \frac{C_{st}^*}{C_{s20}^*} \left(\frac{P_b}{P_a} \right) C_{\infty 20}^* - DO \right]} \right\} [(1.024)^{20-T}] \quad (3.14)$$

$$\frac{P_b}{P_a} = \exp \left[- \frac{gM(z_b - z_a)}{RT} \right] \quad (3.15)$$

Where α is the mass transfer coefficient correction factor between wastewater and tap water, F is the fouling factor for air diffuser, $C_{\infty 20}^*$ is the saturated DO concentration at sea level and standard temperature (20°C) by diffused aeration, β is the saturation DO correction factor between wastewater and tap water, C_{st}^* is the saturated DO concentration at site temperature (30°C), C_{s20}^* is the saturated DO concentration at sea level and standard temperature (20°C), P_b is the barometric pressure at site elevation, P_a is the standard barometric pressure, T is the wastewater temperature, g is the gravitational acceleration constant, M is the ideal gas molar volume, z_b is the site

elevation, z_a is the sea level elevation and R is the ideal gas constant. $C_{s20}^* = C_{\infty20}^*$ for surface aeration.

The energy required for the surface aeration at a DO concentration was calculated using Equation 3.16,

$$\text{Energy required} = \frac{SOTR}{1.3} \quad (3.16)$$

Where 1.3 is the oxygen transfer capability coefficient (in kg O₂/kW·hr) for high-speed surface aerator at standard conditions (20°C, 1 atm) (Tchobanoglous et al., 2014). The values of each constant adopted in the calculation are listed in Table 3.3, while the operational parameters were adopted from the plant data from WWTP 1.

Table 3.3: Value of constants adopted for energy saving calculation
(Tchobanoglous et al., 2014)

Constant	Adopted Value
α	0.9
β	0.95
C_{s20}^*	9.092 mg/L
$C_{\infty20}^*$	9.092 mg/L
C_{st}^*	7.559 mg/L
F	1
f_d	0.15
g	9.81 m/s ²
k_d	0.18 1/d
k_{dn}	0.23 1/d
M	28.97 g/g·mol
P_a	101.325 kPa
R	8314 kg·m ² /s ² ·kg·mol·K
T	30°C
Y	0.45 g MLVSS/g BOD
Y_n	0.15 g MLVSS/g N

3.6.2 Anoxic-Oxic Sequencing Batch Reactor

The AO SBR has a working volume of 2 L, with an initial MLSS concentration of 2500 mg/L (Figure 3.4). The wastewater sampled weekly from WWTP 1 was fed into the reactor as influent. The SBR was operated consecutively for 270 d in four different operating phases (Table 3.4). In Phase 1 (P1), the SBR was operated in a conventional AO configuration with a DO concentration of 1.7 ± 0.2 mg/L in the oxic phase. The DO concentration in the oxic phase was subsequently reduced to 0.9 ± 0.1 mg/L during Phase 2 (P2) to assess the long-term effect of DO reduction on the AO process. In P1 and P2, settled wastewater was used as the reactor feed. From Phase 3 (P3) onwards, raw wastewater without subjecting to settling was used as the reactor feed. The process was modified into a low-DO anoxic-oxic-anoxic (AOA) configuration in Phase 4 (P4) with the incorporation of a post-anoxic denitrification stage to encourage NO_3^- removal.

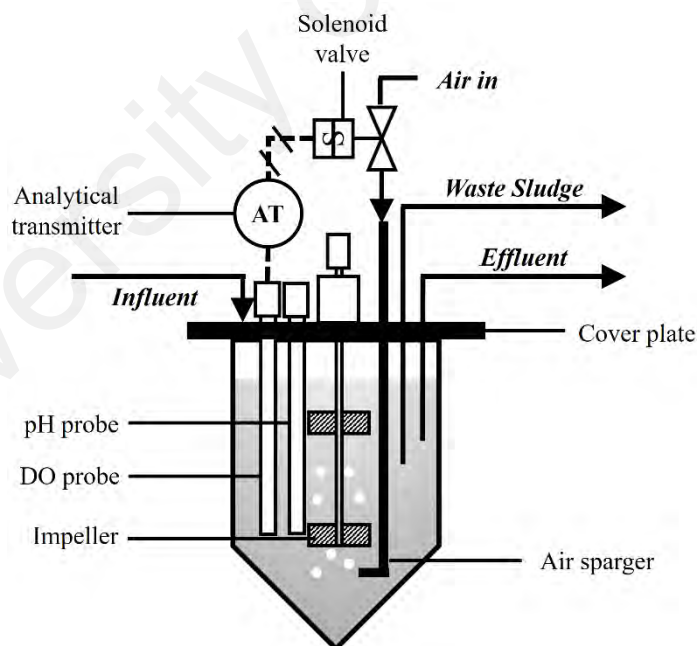


Figure 3.4: Setup of AO and low-DO OA SBRs.

Table 3.4: Operating conditions of each phase for the lab-scale SBR

Operating Period	P1	P2	P3	P4
Duration	Day 1 – 70	Day 71 – 115	Day 116 – 190	Day 191 – 270
Process	Conventional AO	Low-DO-AO	Low-DO-AO	Low-DO- AOA
DO Concentration in Oxic Phase (mg/L)	1.7 ± 0.2	0.9 ± 0.1	0.9 ± 0.1	0.9 ± 0.1
Reactor Feed	Settled wastewater	Settled wastewater	Raw wastewater	Raw wastewater

The 12-h SBR cycle consisted of 5 min filling phase, 180 min anoxic phase, 480 min oxic phase, 50 min settling phase, 4 min decanting phase and 1 min idling phase. In P4, the oxic phase was shortened to 240 min and an equal time period of a post-anoxic phase was configured after the oxic phase. The HRT was fixed at 24 h by withdrawing the effluent at a rate of 1 L/cycle during the decanting phase. The sludge withdrawal rate was set at 50 mL/cycle to achieve a SRT of 20 d. The operating temperature of the SBR was at room temperature ($30 \pm 2^\circ\text{C}$). The DO concentration, the pH and the temperature were monitored on-line using an InPro6850 DO probe (Mettler-Toledo, U.S.) and a 405-DPAS-SC-K851200 combination pH/temperature probe (Mettler-Toledo, U.S.). The DO concentration was controlled using a built-in solenoid valve of Winpact FS-06 Series fermenter (Major Science, U.S.). Mixed liquor samples were collected at a regular interval to show the evolution of nitrogen species (NH_4^+ , NO_2^- , NO_3^- and TN) and DOC concentrations in the reactor.

3.6.3 Low-Dissolved-Oxygen Oxic-Anoxic Sequencing Batch Reactors

Two 2-L working volume SBRs operating in low-DO OA configuration. The setup of the low-DO OA SBRs were similar to Figure 3.4. A first parent SBR (OA-1) was started up, followed by simultaneous operation of OA-1 and another parallel SBR (OA-2) to optimise the HRT and SRT of the low-DO OA process.

3.6.3.1 Parent Oxidic-Anoxic Sequencing Batch Reactor (OA-1)

Seed sludge from WWTP 1 was inoculated into OA-1 to achieve an initial MLSS concentration of 2500 mg/L. Raw wastewater from WWTP 1 was fed into OA-1 as influent. OA-1 was operated in a 12-h cycle, including 5 min filling phase; 660 min reaction phase; 50 min settling phase; 4 min decanting phase and 1 min idling phase. The reaction phase consisted of an oxic phase and a consecutive anoxic phase. The oxic-to-anoxic duration ratio and the DO concentration in the oxic phase were fine-tuned during the OA-1 operation. The operating conditions of OA-1 are summarised in Table 3.5. In P1, OA-1 was operated with 3 h oxic phase and 8 h anoxic phase (oxic:anoxic ratio of 3:8). The oxic:anoxic ratio was adjusted to 4:7 in P2 to enhance the ammonia removal. In P3, the DO concentration in the oxic phase was fine-tuned to 0.4 ± 0.2 mg/L to reduce sbCOD consumption in the oxic phase. The HRT and SRT of OA-1 was 16 h and 20 d, respectively. The HRT of OA-1 was controlled by decanting 1.2 L of clarified effluent per cycle, while 50 mL of mixed liquor was wasted each cycle at the end of reaction phase to fix the SRT at 20 d. The reactor was operated in room conditions ($30 \pm 2^\circ\text{C}$). The DO concentration, temperature and pH of OA-1 were monitored on-line using an InPro6850i DO probe coupled with a M300 Process 1-channel $\frac{1}{2}$ DIN DO monitor (Mettler-Toledo, U.S.) and a Ceragel CPS71D digital pH sensor (Endress + Hauser, Germany). The DO concentration in OA-1 was controlled using a solenoid valve connected to the M300 Process 1-channel $\frac{1}{2}$ DIN DO monitor. Two sampling campaigns were carried out per week to monitor the DOC and nitrogen (NH_4^+ , NO_2^- , NO_3^- and TN) removal performances.

Table 3.5: Operating conditions of OA-1 in the 100-day start-up period

Operating Period	P1	P2	P3
Duration	Day 1 – 70	Day 71 – 85	Day 86 – 100
Oxic:Anoxic Ratio	3:8	4:7	4:7
DO Concentration in Oxic Phase (mg/L)	0.8 ± 0.2	0.8 ± 0.2	0.4 ± 0.2

3.6.3.2 Parallel Oxic-Anoxic Sequencing Batch Reactor (OA-2)

To optimise the HRT and SRT of the low-DO OA process, a parallel OA-2 SBR was started up. Waste sludge from OA-1 was inoculated into OA-2 to reach an initial MLSS concentration of 2500 mg/L. OA-2 has the same source of influent (WWTP 1) as the parent reactor OA-1. OA-1 and OA-2 were operated at the same operating conditions as in P3 (Table 3.5) for three weeks to ensure that both OA-1 and OA-2 reached the same treatment performance before commencing the optimisation study (P4 to P6 in Table 3.6). During P4, OA-1 and OA-2 were operated at SRTs of 20 d and 10 d, respectively, to study the effect of SRT on the OA reactors' nitrogen removal performance. To manipulate the SRT to 10 d, the mixed liquor wastage rate was increased to 100 mL per cycle in OA-2. The HRT of both OA-1 and OA-2 were reduced to 12 h in P5 to investigate the effect of increased wastewater loading on the treatment efficiency of OA reactor system. The HRT of the SBRs were manipulated by reducing the cycle time from 12 h to 8 h. The optimum HRT and SRT were obtained based on the reactor data in P4 and P5, OA-1 and OA-2 were then operated at the optimum operating conditions in P6 for validation. Both reactors were operated under room temperatures ($30 \pm 2^\circ\text{C}$). The DO concentration, pH and temperature in OA-2 were monitored on-line using an InPro6850 DO probe (Mettler-Toledo, U.S.) and a 405-DPAS-SC-K851200 combination pH/temperature probe (Mettler-Toledo, U.S.). The DO concentration was controlled using a built-in solenoid valve of Winpact FS-06 Series fermenter (Major

Science, U.S.). Two sampling campaigns were carried out per week for OA-1 and OA-2 to monitor their carbon and nitrogen removal performances.

Table 3.6: Operating conditions of OA-1 and OA-2 SBRs in the 180-day optimisation study of the effect of HRT and SRT on the low-DO OA process performance

Operating Period		P4	P5	P6
Duration		Day 1 – 70	Day 71 – 110	Day 111 – 180
OA-1	HRT (h)	16	12	16
	SRT (d)	20	20	20
OA-2	HRT (h)	16	12	16
	SRT (d)	10	10	20

3.7 Chemical Analyses of Wastewater Samples

Chemical analyses were performed to measure the MLSS, MLVSS, NH_4^+ , NO_2^- , NO_3^- , DOC, TN and COD concentrations in the wastewater samples collected from the WWTPs for wastewater characterisation. The same analyses were carried out for mixed liquor samples collected from the SBRs to monitor the carbon and nitrogen removal performances.

3.7.1 Mixed Liquor Suspended Solids and Mixed Liquor Volatile Suspended Solids

The MLSS and MLVSS measurement methods were adopted from APHA/AWWA/WEF (1998). 1.2- μ m glass microfiber discs were used to filter the suspended solids from the wastewater samples. The glass microfiber discs were pre-treated at 550°C for 15 min and weighed before analysis. Wastewater was filtered through the pre-treated and weighed glass microfiber discs, the solids retained on the glass microfiber discs was dried at 105°C for 1 h in a Jouan EU115 oven (Thermo Fisher Scientific, U.S.) to a constant weight. MLSS was calculated using Equation 3.17,

$$MLSS = \frac{(A - B) \times 1000}{\text{sample volume, } L} \quad (3.17)$$

Where A is the weight of glass microfiber disc with solid residue after drying at 105°C for 1 h, and B is the weight of pre-treated glass microfiber disc.

The dried solids on glass microfiber disc was ignited at 550°C for 15 min to volatilise the organic matter in a KL 15/11 muffled furnace (ThermConcept, Germany) and weighed. The MLVSS was determined using Equation 3.18,

$$MLVSS = \frac{(A - C) \times 1000}{\text{sample volume, } L} \quad (3.18)$$

Where C is the weight of glass microfiber disc with solid residue after ignition at 550°C for 15 min.

3.7.2 Ammonium Ion, Nitrite Ion and Nitrate Ion

The concentrations of cation (NH_4^+) and anion (NO_2^- and NO_3^-) species in the wastewater samples were analysed using an 861 Advanced Compact Ion Chromatography (Metrohm, Switzerland) after filtration through a $0.2\text{-}\mu\text{m}$ regenerated cellulose syringe filter. The column used for cation analysis was Metrosep C 4 – 150/4.0 (Metrohm, Switzerland) with an eluent solution consisted of 1.7 mM nitric acid and 0.7 mM dipicolinic acid. For anion analysis, a Metrosep A Supp 5- 150/4.0 column (Metrohm, Switzerland) was used. The reagents for anion analysis include deionised water, 0.01 M sulphuric acid solution as a regeneration solution, and an eluent solution containing 3.2 mM sodium carbonate and 1 mM sodium bicarbonate. The concentration of each ion was obtained by comparing the area of the respective conductivity peak with that of standard solutions.

3.7.3 Dissolved Organic Carbon and Total Nitrogen

All wastewater samples were filtered through a 0.45- μm acetate cellulose syringe filter immediately after sampling prior to DOC and TN analyses using a TOC-V CSN total organic carbon analyser coupled with a TNM-1 nitrogen measuring unit (Shimadzu, Japan). The DOC and TN concentrations in the filtered samples were measured using oxidative combustion-infrared analysis and oxidative combustion-chemiluminescence principle, respectively. The measurement methods comply with the standard methods (APHA/AWWA/WEF, 1998).

3.7.4 Chemical Oxygen Demand

The sCOD of the wastewater samples were measured using a high range COD test vial (Hach, U.S.) after filtration through a 0.45- μm cellulose acetate syringe filter. The TCOD of the raw wastewater was measured using the high range COD test vial (Hach, U.S.) without filtration. All test vials were digested at 150°C for 2 h in a DRB COD digester (Hach, U.S.). The digested samples were analysed in a DR/890 colorimeter (Hach, U.S.) to obtain the COD readings.

3.8 Nitrifying and Denitrifying Microbial Community Analyses

Sludge samples were collected regularly from the SBRs for microbial community analyses. The genomic DNA from the sludge was extracted for sequencing and qPCR analyses, while the fixed sludge samples were analysed using FISH.

3.8.1 Genomic Deoxyribonucleic Acid Extraction

The genomic DNA from the sludge samples were extracted using NucleoSpin Soil DNA Extraction Kit (Macherey-Nagel, Germany) according to the manufacturer's instructions. The NucleoSpin Soil DNA Extraction Kit uses a spin column-based DNA extraction method. The DNA was eluted and stored at -20°C in 5 mM Tris(hydroxymethyl)aminomethane hydrochloride, pH 8.5 buffer solution until use.

3.8.2 Sequencing Library Template Preparation and Next-Generation Sequencing

The genomic DNA extracted from the sludge samples was used to prepare the 16S rRNA gene and *nxB* library template. The gene library templates were subsequently sequenced on NGS platforms for high-throughput sequencing. Ion Torrent sequencing platform was applied for the 16S rRNA gene library templates obtained from low-DO nitrification SBR's and low-DO OA SBRs' samples. Illumina MiSeq sequencing platform was used for the 16S rRNA gene and *nxB* library templates prepared from the AO SBR's samples.

3.8.2.1 Ion Torrent Workflow

To prepare the 16S rRNA amplicon sequencing library template from the DNA samples, the DNA samples were amplified using a FastStart High Fidelity PCR System (Roche Diagnostics Ltd., UK). The V4 and V5 regions of the 16S rRNA genes were amplified using a pair of barcoded universal primers F515/R926 (F515: 5'- GTG CCA GCM GCC GCG GTA A -3'; R926: 5'- CCG TCA ATT CCT TTR AGT TT -3') targeting both the domains *Bacteria* and *Archaea* (Quince, Lanzen, Davenport, & Turnbaugh, 2011). Each DNA template was amplified in a 50 μ L PCR reaction mixture, which consisted of 1.0 μ L of each primer set (10 μ M), 6.5 μ L of High Fidelity PCR Master (Sigma-Aldrich, UK), 40.5 μ L molecular grade water (Sigma-Aldrich, UK) and 1.0 μ L of DNA extract. The PCR amplification was performed in a Techne TC-5000 thermocycler (Bibby Scientific, UK) with initial denaturation at 95°C for 2 min, followed by 30 cycles of denaturation at 95°C for 30 s, annealing at 55°C for 30 s and elongation at 72°C for 45 s. The final elongation of the PCR amplification was carried out at 72°C for 7 min.

PCR amplified product was subsequently purified using an AGENCOURT AMPure XP beads PCR purification kit (Beckman Coulter, Ireland). The purified PCR samples were quantified using a Qubit™ dsDNA HS Assay Kit with a Qubit® 2.0 Fluorometer (Invitrogen, U.S.). Prior to amplicon sequencing, all of the purified PCR samples were diluted to 500 pM each and for equi-molar pooling. The PCR product size selection of the pooled samples was performed using a Pippin Prep System (Sage Science, U.S.) as recommended for Ion Torrent workflow. Clonal amplifications of the PCR products were performed on Ion Sphere™ Particles (ISP) and ISPs were enriched using Ion OneTouch 2 (Thermo Fisher Scientific, U.S.) prior to amplicon sequencing on Ion Torrent Personal Genome Machine (PGM™) (Thermo Fisher Scientific, U.S.).

3.8.2.2 Illumina MiSeq Workflow

The Illumina MiSeq library template preparation and sequencing were carried out by Nova Lifetech Pte. Ltd. (Singapore). Both the 16S rRNA and *nxB* fragments in the DNA extract sampled on day 1 and day 270 were amplified using the barcoded primers for sequencing library preparation. The barcoded primer pair 341F/805R (341F: 5'-CCT ACG GGN GGC WGC AG-3'; 805R: 5'-GAC TAC GVG GGT ATC TAA TCC-3') was used to amplify the 16S rRNA gene fragments in both the domain *Bacteria* and *Archaea* (Herlemann et al., 2011). The *nxB* of all *Nitrospira* lineages were amplified using the primers *nxB*169f/*nxB*638r (*nxB*169f: 5'-TAC ATG TGG TGG AAC A-3'; *nxB*638r: 5'-CGG TTC TGG TCR ATC A-3') with sample-specific barcodes (Pester et al., 2014). The 16S rRNA and *nxB* amplicons were sequenced using a high-throughput Illumina MiSeq sequencing platform (Illumina, U.S.).

3.8.3 Post-Sequencing Bioinformatics Analyses

The output files generated from the NGS was analysed using Quantitative Insights Into Microbial Ecology (QIIME) v1.8.0 (Caporaso et al., 2010). Different

bioinformatics workflows were recommended for the output files generated from Ion Torrent and Illumina MiSeq platforms.

3.8.3.1 Workflow for Ion Torrent Output Files

The barcoded sequences were first demultiplexed and trimmed with the minimum average quality score of 20 and minimum sequence length of 100. An open reference operational taxonomic unit (OTU) picking of the sequence data was then performed by clustering the sequences with a minimum 97% similarity into OTUs using uclust method. A minimum sequence similarity of 97% is widely accepted to represent taxonomic relatedness down to species level (Schloss & Handelsman, 2005). The representative sequence of the OTUs were aligned against the latest GreenGenes database using PyNAST algorithm. Aligned representative sequences of the OTUs were filtered to eliminate recurring alignment gap. The chimeric sequences in the aligned representative sequences were identified and filtered using ChimeraSlayer method. The filtered and aligned sequences were then used for core diversity analyses in QIIME to generate taxa plots. In addition, the same 16S rRNA fragment sequences were aligned with reference sequences found in National Center for Biotechnology Information (NCBI) GenBank database to construct a phylogenetic tree with neighbour-joining method using MEGA7 (Kumar, Stecher, & Tamura, 2016).

Our 16S rRNA amplicon nucleotide sequences from the low-DO nitrification SBR's samples were deposited into NCBI's Sequence Read Archive (SRA) under the accession numbers SRX3284361:SRX3284366. The SRA accession numbers for the low-DO OA SBRs' samples are SRX7115993:SRX7116016.

3.8.3.2 Workflow for Illumina MiSeq Output Files

The adaptor sequences were trimmed from the sequencing output files using PhiX Sequencing Control V3. The low quality reads were then filtered with the threshold

quality score of Q20. BBMerge was used to merge the filtered paired-end reads (Bushnell, Rood, & Singer, 2017), the joint reads shorter than 150 bp and longer than 600 bp were removed. The reads were aligned with the Greengenes reference alignment (gg_13_8) with the identified chimeric sequences filtered. After the quality assessment, *de novo* clustering was performed by grouping the reads with 97% identity into OTUs using UPARSE (Edgar, 2013). Taxonomies of the clustered OTUs were assigned based on the Greengenes database (gg_13_8). Core diversity analyses in QIIME was used to generate taxa plots from the OTUs. Phylogenetic relationship of the OTUs was analysed using MEGA7 (Kumar et al., 2016). The OTUs and the reference genes downloaded from the GenBank database were aligned using MUSCLE algorithm and phylogenetic trees were constructed using neighbour-joining method. The 16S rRNA and *nxB* amplicon sequence SRA accession numbers are SRR8237468 and SRR8210165, respectively.

3.8.4 Quantitative Polymerase Chain Reaction

The amplification reactions for all qPCR assays was carried out using a CFX96 Real-Time PCR Detection System (BioRad, U.S.) in triplicate. The qPCR reaction mixture (20 μ L) contained 10 μ L iQTM SYBR[®] Green Supermix (BioRad, U.S.), 1 μ L of the DNA template (50 ng), 2 μ L of forward and reverse primers (3 μ M). The qPCR protocol for all the primer pairs consisted of an initial denaturation at 95°C for 3 min, subsequently followed by 40 cycles of denaturation at 94°C for 30 s, annealing for 45 s at 48°C to 64°C and extension at 72°C for 30 s. The list of primers and their respective annealing temperatures are listed in Table 3.7.

Table 3.7: Information of qPCR primers used in the study

Primer Name	Sequence (5' – 3')	Target Gene	Annealing Temperature (°C)	Reference
<i>Primers for domain Bacteria</i>				
341f 534r	CCT ACG GGA GGC AGC AG ATT ACC GCG GCT GCT GG	Bacterial 16S rRNA genes	60	He et al. (2007)
<i>Primers for nitrifiers</i>				
amoA-1F amoA-2R	GGG GTT TCT ACT GGT GGT CCC CTC KGS AAA GCC TTC TTC	AOB <i>amoA</i>	55	Rotthauwe et al. (1997)
NSR1113f NSR1264r	CCT GCT TTC AGT TGC TAC CG GTT TGC AGC GCT TTG TAC CG	<i>Nitrospira</i> 16S rRNA genes	60	Dionisi et al. (2002)
Ntsp-amoA 162F Ntsp-amoA 359R	GGA TTT CTG GNT SGA TTG GA WAG TTN GAC CAC CAS TAC CA	Total comammox <i>Nitrospira amoA</i>	48	Fowler et al. (2018)
Nitrosa amoA-469F Nitrosa amoA-812R	GCG ATT CTG TTT TAT CCC AGC AAC CCG TGT GCT AAC GTG GCG	<i>Ca. Nitrospira</i> <i>nitrosa amoA</i>	64	
Inopinata amoA-410F Inopinata amoA-815R	TCA CCT TGT TGC TAA CTA GAA ACT GG TCC GCG TGA GCC AAT GT	<i>Nitrospira</i> <i>inopinata amoA</i>	64	Beach and Noguera (2019)
Nitrificans amoA-463F Nitrificans amoA-836R	ATG TTC GCG GCA CTG TT CCA GAA AGT TTA GCT TTG TCG CCT	<i>Ca. Nitrospira</i> <i>nitrificans amoA</i>	64	

Table 3.7: Information of qPCR primers used in the study, continued

Primer Name	Sequence (5' – 3')	Target Gene	Annealing Temperature (°C)	Reference
<i>Primers for denitrifiers</i>				
nirSCd3aF	AAC GYS AAG GAR ACS GG	<i>nirS</i>	60	Throbäck, Enwall, Jarvis, and Hallin (2004)
nirSR3cd	GAS TTC GGR TGS GTC TTS AYG AA			
nosZ2F	CGC RAC GGC AAS AAG GTS MSS GT	<i>nosZ</i>	60	Henry et al. (2006)
nosZ2R	CAK RTG CAK SGC RTG GCA GAA			

Copy number of the target DNA in the samples were quantified using standard curves for each qPCR assay in Table 3.7. To construct the standard curves, PCR product obtained from the amplification reactions of each target genes in Table 3.7 was purified using a NucleoSpin Extract II kit (Macherey-Nagel, Germany). The purity and DNA concentration of the purified PCR product were quantified using a NanoDrop ND-2000 spectrophotometer (Thermo Fisher Scientific, U.S.). The measured DNA concentration was used to calculate copy number of the target DNA as described by Whelan, Russell, and Whelan (2003). The qPCR standards were prepared by ten-fold serial dilution of the purified PCR products, which ranged from 10^3 copy number/ μL to 10^9 copy number/ μL for each qPCR assay. The standard curves were then constructed by plotting C_q as a function of the logarithm of target DNA's copy number.

All target DNA's copy number per μL were normalised with the number of gene copy in a cell to convert the DNA's copy number into cell number per μL (Baptista et al., 2014). The numbers of gene copy in a cell of the targeted genes are listed in Table 3.8. Once the cell number were obtained, the percentage relative abundance of targeted bacteria groups (betaproteobacterial AOB, *Nitrospira sp.* and denitrifiers) to the total bacteria population was determined using Equation 3.19,

$$\text{Relative Abundance} = \frac{\text{Cell number of targeted bacteria}}{\text{Cell number of total bacteria}} \times 100\% \quad (3.19)$$

For the *Nitrospira* community analysis, the percentage relative abundance of each comammox group (total comammox, *Ca. Nitrospira nitrosa*, *Nitrospira inopinata* and *Ca. Nitrospira nitrificans*) to the total *Nitrospira* population was calculated using Equation 3.20,

$$\text{Relative Abundance} = \frac{\text{Cell number of comammox group}}{\text{Cell number of total Nitrospira}} \times 100\% \quad (3.20)$$

Table 3.8: Number of gene copy per cell for the targeted genes in qPCR analysis

Target Gene	Number of Gene Copy per Cell	Reference
AOB <i>amoA</i>	2	McTavish, Fuchs, and Hooper (1993)
<i>nirS</i>	1	Kandeler, Deiglmayr,
<i>nosZ</i>	1	Tscherko, Bru, and Philippot (2006)
Total bacterial 16S rRNA gene	4.2	Vetrovsky and Baldrian (2013)
<i>Nitrospira</i> 16S rRNA gene	1	Stoddard, Smith, Hein, Roller, and Schmidt (2015)
Comammox <i>Nitrospira</i> clade A <i>amoA</i>	1.3	
<i>Ca. Nitrospira nitrosa amoA</i>	2	Palomo et al.
<i>Nitrospira inopinata amoA</i>	1	(2018)
<i>Ca. Nitrospira nitrificans amoA</i>	1	

3.8.5 Fluorescence *in situ* Hybridisation

Sludge samples were fixed using a 4% paraformaldehyde solution as described by Amann et al. (1990). The protocol for FISH was adopted from Amann, Ludwig, and Schleifer (1995). The fixed samples were hybridised with EUB338-MIX to target microorganisms within the domain *Bacteria*, and with the group-specific probes (Table 3.9). The 5'-end of the probe EUB338 MIX was attached with 6-FAM fluorophore, while all other probes have Cy-3 fluorophore attached to the 5'-end of the probes. The probes were procured from Integrated DNA Technologies Pte. Ltd. (Singapore) and Sigma-Aldrich (Suffolk, United Kingdom). The hybridised slides were viewed under DM2500 fluorescence microscope (Leica Microsystems, Germany), images were captured using DFC310 FX cooled charged-coupled device digital colour camera (Leica Microsystems, Germany).

Table 3.9: Information of FISH probe used in the study

Probe Name	Sequence (5' – 3')	Specificity	Formamide Concentration (%)	Reference
<i>Probes for domain Bacteria</i>				
EUB338^a	GCT GCC TCC CGT AGG AGT	Most bacteria	35	Amann et al. (1990)
EUB338-II^a	GCA GCC ACC CGT AGG TGT	<i>Plantomycetales</i>	35	Daims et al. (1999)
EUB338-III^a	GCT GCC ACC CGT AGG TGT	<i>Verrucomicrobiales</i>	35	Daims et al. (1999)
<i>Probes for nitrifiers</i>				
Nso1225	CGC CAT TGT ATT ACG TGT GA	Betaproteobacterial AOB	35	Mobarry et al. (1996)
NIT3	CCT GTG CTC CAG GCT CCG	Genus <i>Nitrobacter</i> (NOB)	40	Wagner et al. (1996)
Ntspa662	GGA ATT CCG CGC TCC TCT	Genus <i>Nitrospira</i> (NOB)	35	Daims, Nielsen, et al. (2001)
Ntspa476	CTG CAG GTA CCG TCC GAA	<i>Ca. Nitrospira nitrosa</i> and <i>Ca. Nitrospira nitrificans</i>	20	van Kessel et al. (2015)

^a Equi-molar mix of EUB338, EUB338-II and EUB338-III was used as EUB338-MIX

CHAPTER 4: CHARACTERISATION OF TROPICAL WASTEWATER

4.1 Wastewater Temperature, pH, Suspended Solids, Chemical Oxygen Demand and Nitrogen Concentrations

The first objective to develop an improved biological nitrogen removal configuration for tropical wastewater in Malaysia is to characterise the wastewater in detail. To characterise tropical wastewater in Malaysia, wastewater samples were sampled from six WWTPs (Section 3.1) and subjected to wastewater chemical analyses (Section 3.7).

The tropical wastewater characteristics, including temperature, pH, MLSS, MLVSS, $\text{NH}_4\text{-N}$, TN, sCOD and TCOD were listed in Table 4.1, based on three replicates for WWTP 1, and two replicates each for WWTPs 2, 3, 4, 5 and 6. The tropical wastewater samples in this study has a temperature between 28°C and 33°C (Table 4.1). The pH of the wastewater samples was at near-neutral condition (6.5 – 7.5) as shown in Table 4.1. The wastewater MLSS ranged from 70 mg/L to 297 mg/L, while the MLVSS ranged from 57 mg/L to 263 mg/L. The $\text{NH}_4\text{-N}$ and TN concentrations of the tropical wastewater in this study (Table 4.1) were characteristics of a moderate-strength wastewater (20 – 30 mg/L for $\text{NH}_4\text{-N}$, 35 – 50 mg/L for TN) (Henze et al., 1997; Tchobanoglous et al., 2014). The $\text{NO}_2\text{-N}$ and $\text{NO}_3\text{-N}$ in the wastewater samples were < 0.5 mg/L at all times. Besides, Table 4.1 shows that the tropical wastewater samples have low sCOD concentrations. The sCOD of the wastewater ranged from 55 to 170 mg/L, while the TCOD ranged from 160 to 640 mg/L. The sCOD in the wastewater is significantly lower than the concentrations (180 – 210 mg/L) found in temperate climate regions (Henze et al., 1997; Tchobanoglous et al., 2014). Cao et al. (2008) reported a similar range of sCOD values (123 mg/L) for wastewater in Singapore. The tropical temperature (24 – 34°C) experienced in Malaysia and Singapore may have enhanced the biodegradation of sCOD in the sewer network (Cao et al., 2008). The sCOD/TN of the tropical wastewater was between 3 to 6 g COD/g N (Table 4.1), which was lower than

the recommended ratio of between 6 and 11 for complete denitrification (Henze et al., 1994). The TCOD/TN was significantly higher than the recommended ratio for complete denitrification. Moreover, the MLVSS-to-MLSS ratio (MLVSS/MLSS) ranged between 0.7 and 0.9, which was higher than the typical MLVSS/MLSS between 0.7 and 0.75 (Henze et al., 1997). Cao et al. (2020) suggested that a high wastewater MLVSS/MLSS indicated large fraction of biodegradable PSS in the wastewater. Based on the COD, MLSS and MLVSS data, a significant fraction of the biodegradable organics may be present in the PSS as sbCOD to supplement biodegradable organics for denitrification in low soluble COD/N tropical wastewater. NUR experiments were then performed to quantify the rbCOD and sbCOD to support the hypothesis.

Table 4.1: Mean wastewater temperature, pH, MLSS, COD and nitrogen data of each WWTP

WWTP	1	2	3	4	5	6
Temperature (°C)	29 ± 1	29 ± 1	31 ± 1	31 ± 2	29 ± 1	31 ± 2
pH	7.2 ± 0.2	7.1 ± 0.4	6.8 ± 0.9	6.8 ± 0.2	7.1 ± 0.3	7.2 ± 0.4
MLSS (mg/L)	297 ± 169	70 ± 14	84 ± 28	145 ± 109	138 ± 12	251 ± 106
MLVSS (mg/L)	263 ± 133	113 ± 72	64 ± 42	57 ± 1	127 ± 1	217 ± 86
NH ₄ -N (mg/L)	21 ± 4	23 ± 1	23 ± 5	19 ± 4	18 ± 1	29 ± 2
TN (mg/L)	26 ± 4	30 ± 1	32 ± 2	24 ± 5	23 ± 1	33 ± 2
sCOD (mg/L)	85 ± 39	171 ± 2	105 ± 1	104 ± 20	81 ± 5	89 ± 4
TCOD (mg/L)	492 ± 133	373 ± 82	215 ± 81	188 ± 16	270 ± 55	413 ± 97
sCOD/TN (g COD/g N)	3.2 ± 1.0	5.7 ± 0.3	3.2 ± 0.2	4.4 ± 0.1	3.6 ± 0.1	2.7 ± 0.1
TCOD/TN (g COD/g N)	20 ± 9	13 ± 3	7 ± 2	8 ± 1	12 ± 2	13 ± 4
MLVSS/MLSS	0.9 ± 0.1	0.8 ± 0.1	0.7 ± 0.3	0.8 ± 0.2	0.9 ± 0.1	0.9 ± 0.1

4.2 Fractions of Wastewater Biodegradable Chemical Oxygen Demand

To further determine the different fractions of bCOD, such as rbCOD and sbCOD, in the tropical wastewater samples, wastewater fractionation experiments (Section 3.2) was performed using two wastewater samples from each WWTP. The wastewater fractionation consisted of $Y_{OHO,ax}$ determination experiment (Section 3.2.1) and NUR experiment (Section 3.2.2).

A COD and $\text{NO}_3\text{-N}$ profile was obtained from the $Y_{OHO,ax}$ determination experiment (Figure 4.1). The COD and $\text{NO}_3\text{-N}$ were depleted as expected in the $Y_{OHO,ax}$ batch test. The $Y_{OHO,ax}$ of the sludge was 0.4 g COD/g COD as determined using Equation 3.1. The $Y_{OHO,ax}$ of tropical sludge was similar to the $Y_{OHO,ax}$ values (0.42 – 0.53 g COD/g COD) in the literature (Muller et al., 2003; van Loosdrecht et al., 2016). Once the $Y_{OHO,ax}$ was determined, the rbCOD and sbCOD concentrations in the wastewater were determined based on NUR experiment. A $\text{NO}_x\text{-N}$ uptake rate profile was obtained from the NUR experiment of each wastewater sample, an example of $\text{NO}_x\text{-N}$ profile from WWTP 1 is shown in Figure 4.2. The remaining $\text{NO}_x\text{-N}$ profiles are provided in Appendix B. The change in $\text{NO}_x\text{-N}$ during rbCOD and sbCOD degradation was used to quantify rbCOD and sbCOD in the wastewater using Equation 3.2 and Equation 3.3, respectively. The period when rbCOD degradation and sbCOD degradation occurred were indicated in green diamonds and yellow squares, respectively (Figure 4.2).

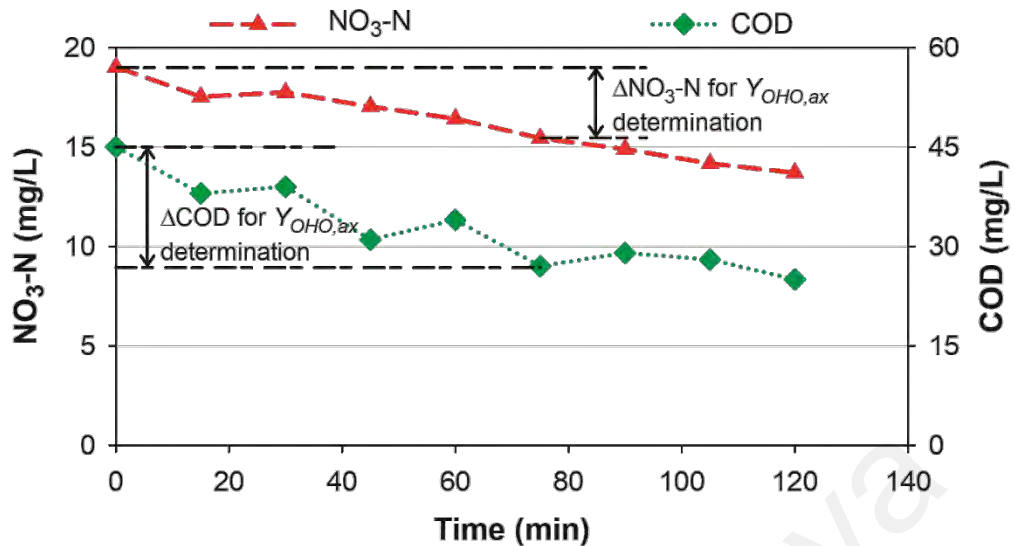


Figure 4.1: Determination of $Y_{OHO,ax}$ from the NO_3-N and COD profiles.

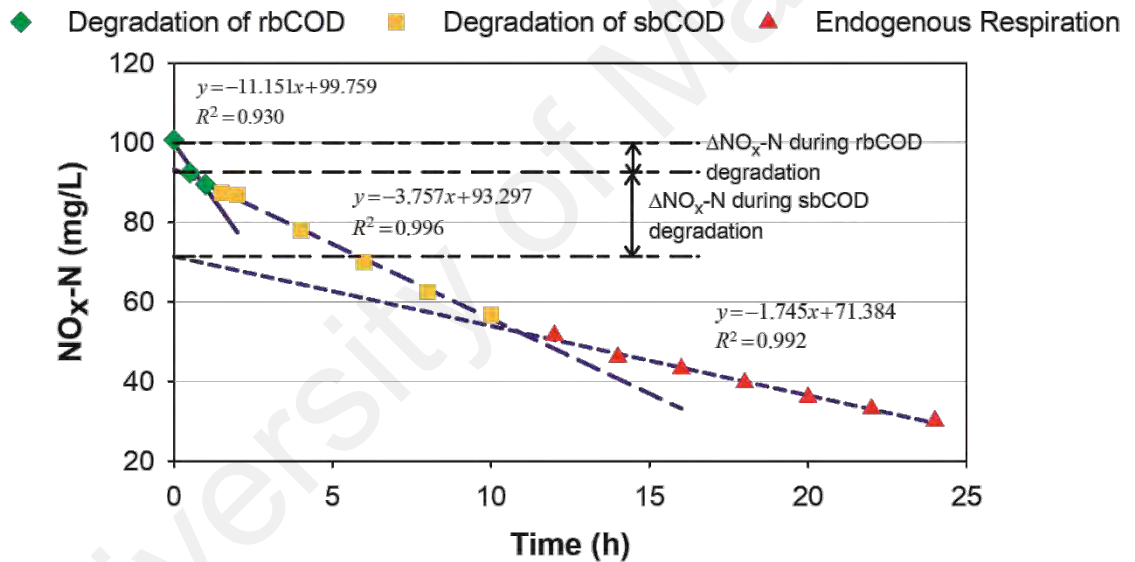


Figure 4.2: Quantification of rbCOD and sbCOD from the NO_x-N profile of NUR experiment.

The rbCOD and sbCOD concentrations in the wastewater sample from each WWTP are listed in Table 4.2, based on three replicates for WWTP 1 and two replicates each for WWTPs 2, 3, 4, 5 and 6. The rbCOD made up 3 – 40% of the TCOD, while the sbCOD constituted 15 – 60% of the TCOD (Figure 4.3). The fraction of biodegradable COD (bCOD = rbCOD + sbCOD) relative to TCOD was 30 – 90%. WWTP 2 had a lower bCOD content than the rest of the WWTPs as WWTP 2 was situated close to an

industrial estate. The influent MLSS of WWTP 2 and WWTP 3 were also lower (70 – 84 mg/L) when compared with the rest of the WWTPs (138 – 297 mg/L), which contributed to the lower bCOD content. WWTP 4 operating in CAS configuration may have a lower sbCOD from the NUR experiments as the sludge was not acclimated for biological nitrogen removal and the WWTP has a shorter SRT (5 – 10 d) than the other WWTPs (> 20 d). Thus, the tropical wastewater samples had low soluble biodegradable organics (rbCOD) and most of the biodegradable organics was present in PSS (sbCOD).

Table 4.2: Mean wastewater rbCOD and sbCOD of each WWTP

WWTP	1	2	3	4	5	6
rbCOD (mg/L)	53 ± 33	34 ± 8	18 ± 8	69 ± 32	50 ± 9	39 ± 23
sbCOD (mg/L)	250 ± 66	78 ± 44	78 ± 16	83 ± 15	143 ± 23	159 ± 23

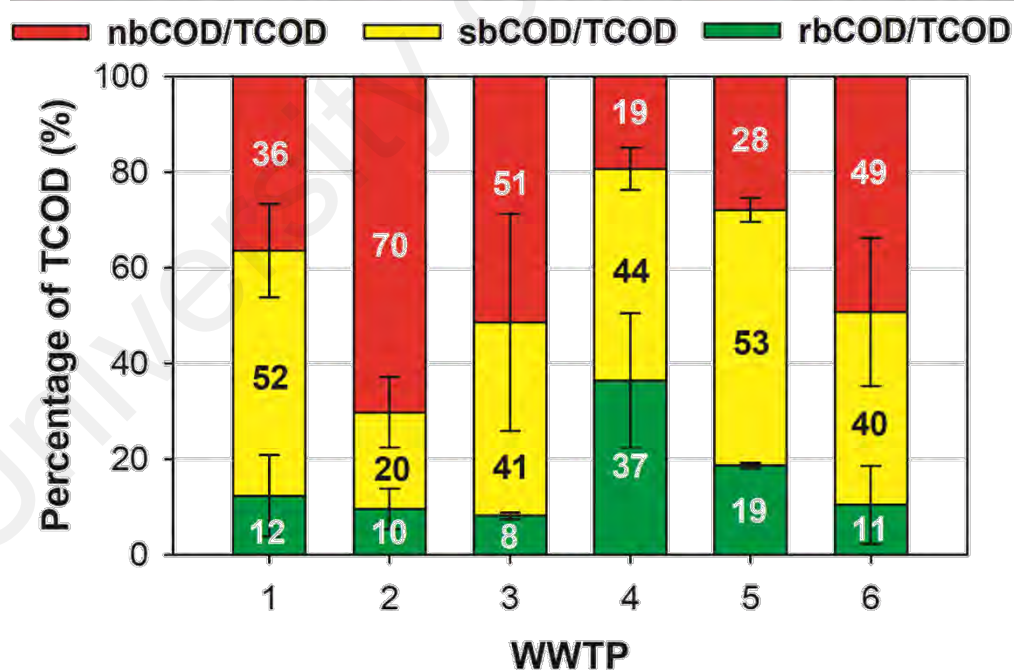


Figure 4.3: COD fractions from wastewater fractionation experiments.

Interestingly, the warm wastewater temperature approximately at 30°C did not significantly degrade the sbCOD in the sewer network as observed for rbCOD. Drewnowski and Makinia (2013) and Benneouala et al. (2017) suggested that the biodegradation of sbCOD process occurred in three steps. Firstly, the bacteria have to colonise the surface of PSS, then extracellular enzyme is secreted for hydrolysis, and finally the product of hydrolysis is consumed by bacteria. Benneouala et al. (2017) also found that the hydrolysis of PSS sampled upstream of the sewer network exhibited a lag phase where bacteria colonisation on PSS occurred, whereas the lag phase was not observed in PSS sampled downstream of the sewer network. The Greater Kuala Lumpur region has a high density of WWTPs of 2021 plants in an area of 2793 km², which may result in a short sewer HRT (Malaysian Water Association, 2017). The short HRT in the sewer may have prevented most of the sbCOD from biodegradation. However, other areas with warm temperature and long sewer HRT may observe significant biodegradation and change in the compositions of biodegradable organics (W. Li, Zheng, Ma, & Liu, 2019; Yun, Yun, Lee, & Yoo, 2013).

From the results of NUR experiment, rbCOD made up a minor portion of the bCOD while sbCOD was the largest fraction of bCOD in the tropical wastewater. Low rbCOD concentration in the wastewater may be conducive for active low-DO nitrification by reducing the oxygen competition between heterotrophs and nitrifiers. Satoh, Okabe, Norimatsu, and Watanabe (2000) reported a decrease in the AOB population relative to heterotrophs when biodegradable organics was introduced, suggesting that heterotrophs may outcompete AOB for oxygen. Hanaki, Wantawin, and Ohgaki (1990) also suggests that addition of bCOD would hamper nitrification performance by encouraging heterotrophs' growth. In low-DO nitrification, the lower DO concentration (< 1 mg O₂/L) relative to the conventional nitrification (2 mg O₂/L) may reduce the aeration demand and energy usage of WWTPs by 25% (Keene et al., 2017).

In addition, the ratio of rbCOD-to-TN (rbCOD/TN) ranged from 0.5 – 3.5 g COD/g N, which was much lower than the theoretical COD required for denitrification (Figure 4.4). Thus, the soluble biodegradable organics in the wastewater was insufficient for denitrification. By considering both rbCOD and sbCOD in the tropical wastewater, the bCOD-to-TN ratio (bCOD/TN; 3.0 – 15.0 g COD/g N) was significantly higher than rbCOD/TN. If sbCOD could be utilised for denitrification, the denitrification performance of the WWTPs would be enhanced.

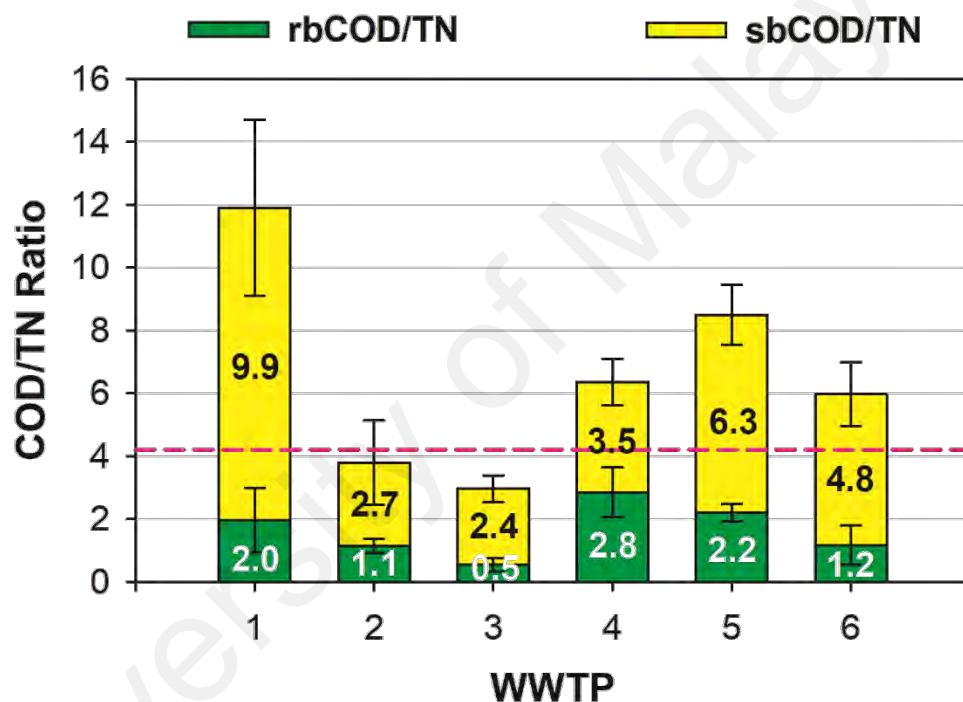


Figure 4.4: Fraction of rbCOD, sbCOD and bCOD relative to TCOD and (B) COD/TN ratios, the horizontal dash (– –) line corresponds to theoretical COD consumption per NO₃-N reduced (4.2 g COD/g NO₃-N).

From the wastewater fractionation data, the tropical wastewater in this study has low rbCOD content. The low rbCOD concentration is conducive for low-DO nitrification but insufficient to achieve complete denitrification. sbCOD may improve the denitrification performance if PSS could be hydrolysed at a high rate. The warm wastewater temperature in the tropical region ($30 \pm 2^\circ\text{C}$) may enhance the PSS

hydrolysis rate as PSS hydrolysis is an enzymatic reaction that occurs faster at higher temperature (Morgenroth et al., 2002). Cao et al. (2020) also suggested that WWTPs in the warm climate regions could utilise sbCOD in PSS to significantly improve the denitrification performance due to the higher PSS hydrolysis rate. In the following section, the PSS hydrolysis rate constants were determined at tropical temperatures.

4.3 Particulate Settleable Solids Hydrolysis Kinetic Coefficients

The PSS hydrolysis kinetic coefficients at tropical temperatures were determined using OUR experiments (Section 3.3.1 and Section 3.3.2). A modified ASM1 was then fitted to the OUR profiles to estimate the values of k_H and K_X (Section 3.3.3).

Based on the sensitivity analysis described in Section 3.3.3, a sensitivity ranking of all the kinetic parameters was listed in Table 4.3. The sensitivity ranking revealed that the kinetic parameters for hydrolysis process (k_H and K_X) were among the top three most sensitive parameters in the modified ASM1 model. The results from the sensitivity analysis were consistent with the literature that hydrolysis kinetic constants are most critical to the modelling output (Insel, Orhon, & Vanrolleghem, 2003; Ristow & Hansford, 2001). To determine the PSS hydrolysis kinetics at tropical temperature, k_H and K_X in the modified ASM1 model were sensitive for calibration by fitting the simulated OUR to the measured OUR profiles. For the purpose of calibration, the values of μ_H , K_S and b_H can be fixed at temperature-corrected default values as demonstrated by J. Wu et al. (2014) and Benneouala et al. (2017).

Table 4.3: Kinetic parameter sensitivity ranking of modified ASM1 model

Rank	Parameter	δ_j^{msqr}
1	K_X	9.367
2	μ_H	8.722
3	k_H	4.966
4	K_S	1.993
5	b_H	0.426

The OUR profiles were shown in Figure 4.5. The modified ASM1 fitted the OUR data well, the p -values were above the level of significance of 0.05 in the χ^2 Test (Figure 4.5). The first point of each OUR profile was excluded in the χ^2 Test due to systematic error during the measurement of the first OUR value. In the PSS hydrolysis reaction rate equation (Table 3.2), k_H represents the maximum PSS hydrolysis rate. The value of k_H was 0.24 1/h, which was 2 times higher than the literature values (0.10 – 0.15 1/h) from similar ASM1 simulation of PSS hydrolysis at 20°C (Drewnowski & Makinia, 2013; Henze et al., 1987; J. Wu et al., 2014). K_X is the affinity constant of hydrolytic bacteria for PSS, which should be independent of temperature. The K_X value estimated from the AQUASIM simulation (0.28 g COD/g COD) was approximately twice the default value (0.15 g COD/g COD) in ASM1 (Henze et al., 1987). The higher k_H value here implied that PSS hydrolysis rate is accelerated in warm wastewater temperature. The k_H value was also 1.3 times higher than the temperature-corrected k_H value (0.19 1/h), which implied that Arrhenius temperature correction may no longer be valid for PSS hydrolysis at 30°C. Long SRT operation of the WWTPs above 20 d may have promoted higher population of hydrolytic bacteria (S. Li, Wu, & Liu, 2019), which may result in a higher k_H than the value predicted by Arrhenius relationship. The hydrolysis kinetic parameters have to be determined experimentally to model the PSS hydrolysis rate in ASM1 accurately at tropical temperatures. On the other hand, the K_X value (the affinity of the bacteria for PSS) is an intrinsic parameter that should be

independent of temperature. The K_X value obtained here (0.28 g COD/g COD) was 2 times higher than the default value (0.15 g COD/g COD at 20°C) (Henze et al., 1987). The higher K_X value in this study implied that bacteria in the sludge had a lower affinity for PSS than that predicted by ASM1. The higher k_H and K_X values of the sludge may indicate the presence of r-strategist organisms in the hydrolysis process. r-strategist organisms proliferate in environment where substrate is not limiting because of their high maximum growth rate but low substrate affinity. Oppositely, k-strategist organisms tend to grow in substrate-limiting condition as they have higher substrate affinity but lower maximum growth rate than r-strategists (Arnaldos et al., 2015). Arnaldos et al. (2015) suggested that exposing bacteria community under high substrate concentration for a prolonged period may favour the proliferation of r-strategist organisms. Overall, the higher PSS hydrolysis rate suggested that sbCOD abundant in the wastewater could be a propitious source of biodegradable organics for biological denitrification in the tropical wastewater treatment process.

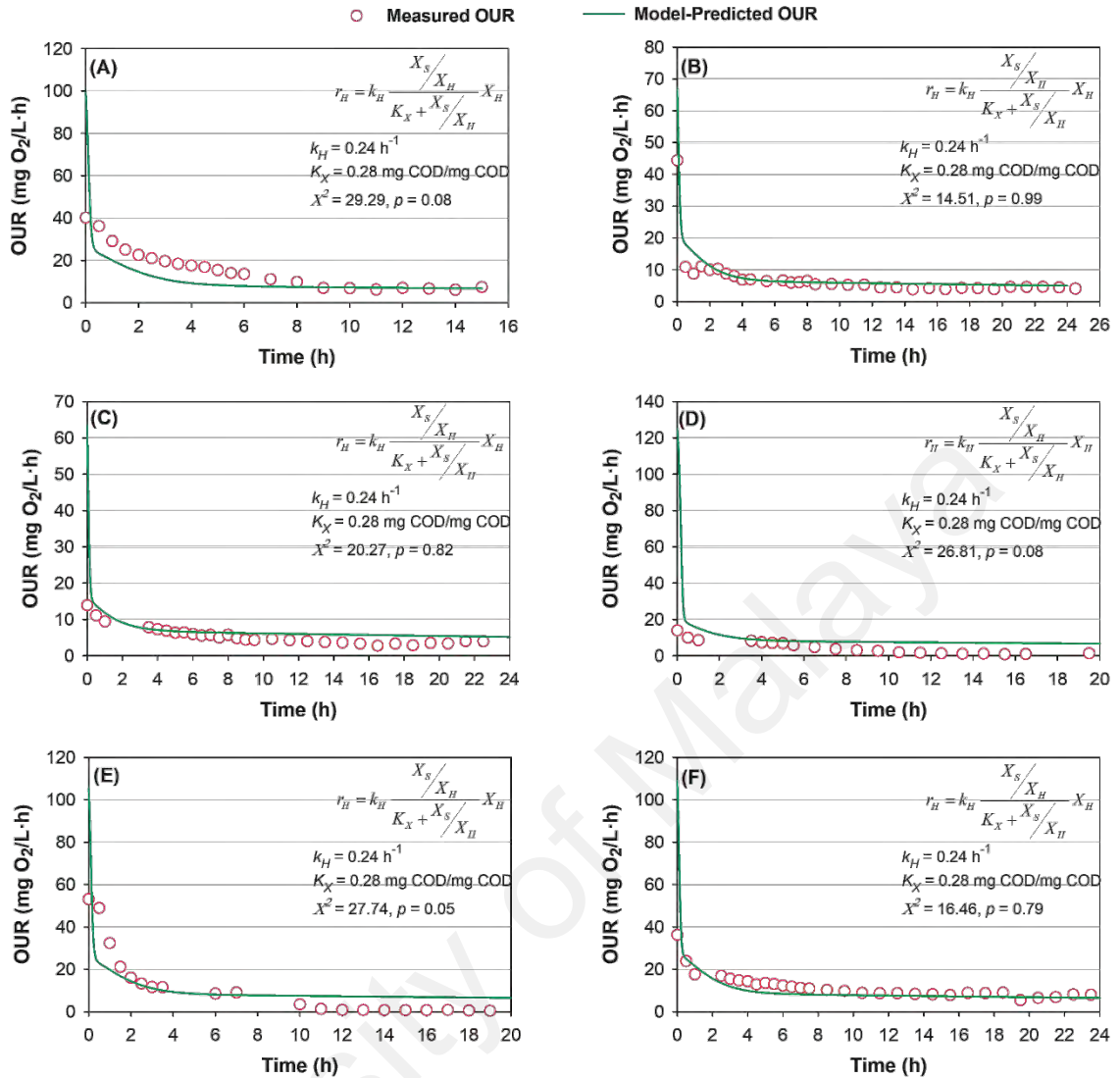


Figure 4.5: Measured and fitted OUR profiles from PSS hydrolysis kinetic parameter determination experiment. (A) WWTP 1, (B) WWTP 2, (C) WWTP 3, (D) WWTP 4, (E) WWTP 5 and (F) WWTP 6. r_H represents the PSS hydrolysis rate.

4.4 Biodegradability of Particulate Settleable Solids in Batch Denitrification Activity Experiment

The denitrification batch activity experiments were subsequently performed to demonstrate that PSS could be utilised for denitrification according to Section 3.4. The $\text{NO}_x\text{-N}$ profiles for the denitrification batch experiments using filtered wastewater (set A), PSS in nutrient solution (set B) and blank nutrient solution (set C) are provided in

Figure 4.6. The raw data used for plotting Figure 4.6 were given in Appendix C. The initial COD concentration of set A and set B were similar (60 mg/L). However, only 5 mg $\text{NO}_x\text{-N/L}$ was denitrified in set A using rbCOD in the filtered wastewater for denitrification (Figure 4.6A), while sbCOD from the PSS in set B successfully reduced 15 mg $\text{NO}_x\text{-N/L}$ (Figure 4.6B). Negligible denitrification performance was observed in set C (Figure 4.6C), which was a negative control to confirm that the nutrient solution did not contain any biodegradable organics for denitrification. The results implied that PSS in the wastewater had a higher biodegradability than sCOD in the filtered wastewater for denitrification. The result is consistent with some studies that suggested that sbCOD from PSS in the wastewater could be a major source of bCOD for denitrification (Choi et al., 2017; Sophonsiri & Morgenroth, 2004). Particle size distribution and chemical composition analyses of wastewater by Sophonsiri and Morgenroth (2004) suggested that 23 – 49% of the PSS in wastewater could be biodegradable. Choi et al. (2017) also reported that around 96% of the PSS in the wastewater could be degraded biologically, while only 25% of the sCOD in the wastewater is biodegradable. Thus, using sbCOD for denitrification in the tropical wastewater treatment is, in principle, an effective method to enhance NO_3^- removal from the tropical wastewater.

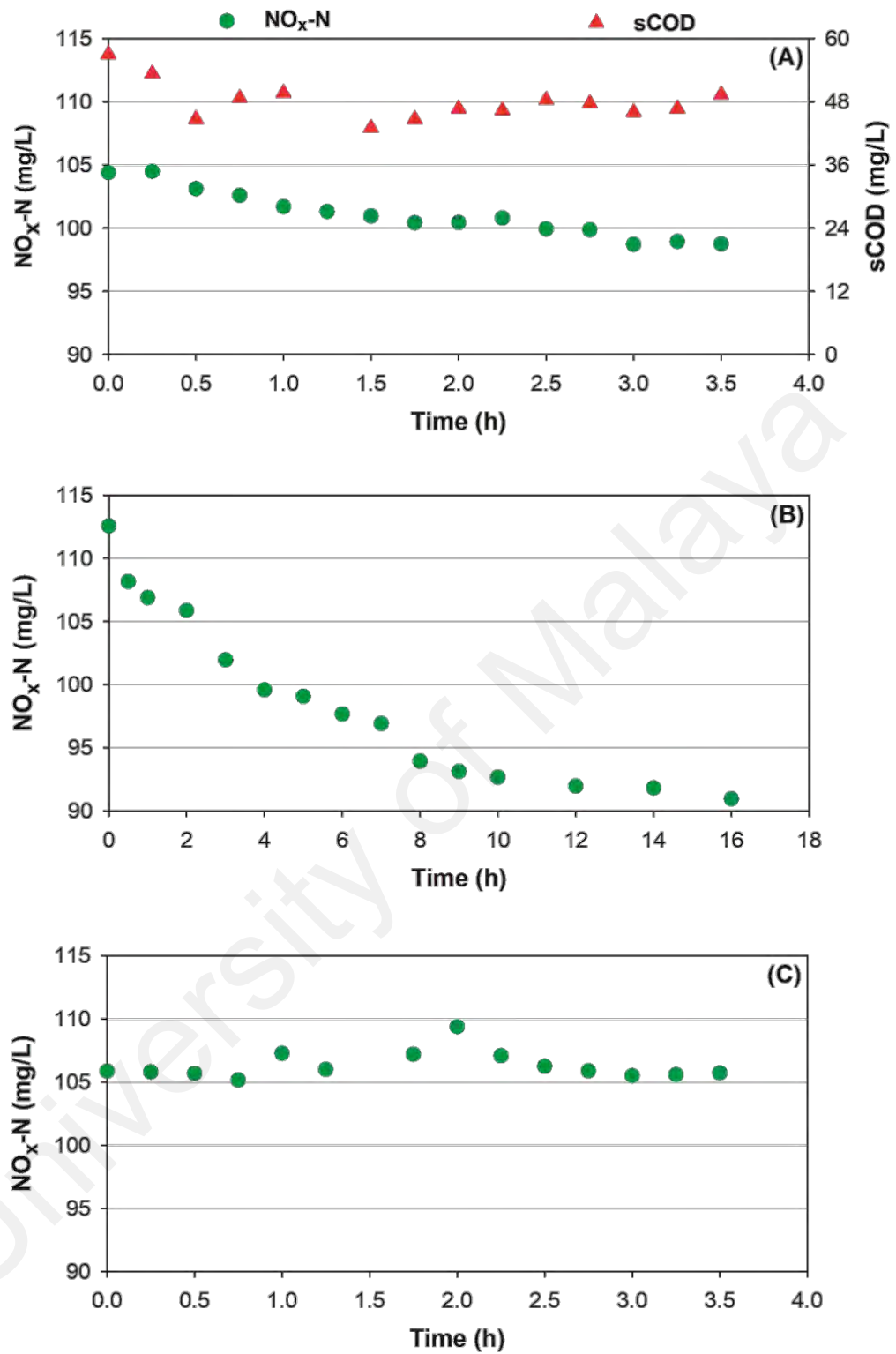


Figure 4.6: $\text{NO}_x\text{-N}$ and sCOD profiles for denitrification batch experiment using (A) filtered wastewater, (B) PSS in nutrient solution and (C) nutrient solution. sCOD data was not shown for set B and set C because the source of biodegradable organics for denitrification was not soluble.

By utilising sbCOD in PSS to enhance the denitrification performance, WWTPs may omit the primary clarifier in the design to reduce the capital cost (Cao et al., 2020). Using sbCOD as a source of biodegradable organics for denitrification may also reduce the operating cost of the process when compared with the conventional external carbon dosage. The traditional external carbon dosage system requires additional procurement cost on organic compounds, such as glycerol, methanol and ethanol (Z. Shen & Wang, 2011). Complex carbon dosage control system must also be installed to ensure optimal carbon dosing rate, which prevents carbon breakthrough and high NO_x^- in the effluent (Q. Wang, Chen, & Chen, 2017). Using sbCOD as the source of biodegradable organics in the denitrification step will eliminate these additional operating cost for external carbon dosage system.

On the other hand, using sbCOD for denitrification requires longer anoxic HRT to allow adequate time for the hydrolysis of PSS in the wastewater, which is the rate-limiting step (Drewnowski & Makinia, 2013; Tas et al., 2009). PSS hydrolysis rate under anoxic condition was also known to be 2.5 times lower than the rate at aerobic condition (Henze et al., 1987). The $\text{NO}_x\text{-N}$ uptake profile in Figure 4.2 shows that the specific denitrification rate during sbCOD degradation ($0.9 \text{ mg N/g MLVSS}\cdot\text{hr}$) was 2 times lower than that during rbCOD degradation ($1.8 \text{ mg N/g MLVSS}\cdot\text{hr}$). Similar magnitude of reduction in specific denitrification rate was observed in other $\text{NO}_x\text{-N}$ uptake profiles (Figure A1 in Appendix). For WWTPs operating in AO configuration, a potential solution to accommodate the longer anoxic HRT is to modify part of the aerobic tank into an anoxic tank. MSIG recommended an aerobic HRT of 12 – 16 h for the EA plants with pre-anoxic tank in Malaysia (National Water Services Commission, 2009). The long aerobic HRT provides excess aerobic HRT and resulted in merely the aerobic heterotrophic consumption of sbCOD. The latter part of the aerobic tank may be

modified into an anoxic tank to promote degradation and utilisation of sbCOD for denitrification.

4.5 Summary of Chapter

The first study fulfilled the first objective on assessing detailed wastewater characteristics of tropical wastewater in Malaysia. Part of the second objective on formulating operating strategies to achieve a low-cost biological nitrogen removal in treating tropical wastewater in Malaysia was also addressed.

Firstly, from the results of NUR experiment, rbCOD made up a minor portion of the bCOD while sbCOD was the largest fraction of bCOD in the tropical wastewater. The low rbCOD content of the wastewater may be a favourable condition to operate a low-DO nitrification process.

Secondly, the PSS hydrolysis rate at tropical temperature was approximately 2 times higher than the default value at 20°C, suggesting that sbCOD may be utilised by heterotrophic bacteria as a source of biodegradable organics in the denitrification process. Batch denitrification activity experiment using sbCOD as the sole carbon source further verified that sbCOD from PSS in wastewater was more biodegradable than sCOD. The results implied that WWTPs operating with biological nitrogen removal in Malaysia may utilise sbCOD in the wastewater to enhance denitrification performance.

Based on the results obtained, most the WWTPs in Malaysia currently operating in an EA process incorporated with a pre-anoxic tank (AO configuration) could adopt low-DO nitrification ($< 1 \text{ mg O}_2/\text{L}$) to significantly reduce the aeration energy. In addition, the high wastewater sbCOD content and warm climate in Malaysia may provide the advantage for WWTPs to utilise sbCOD for denitrification, which could eliminate the

need to purchase external carbon sources when treating low COD/N tropical wastewater in Malaysia. These proposed operating strategies could imply significant energy and cost savings, thus improving the sustainability of WWTPs.

University of Malaya

CHAPTER 5: POTENTIAL AND FEASIBILITY OF LOW-DISSOLVED-OXYGEN NITRIFICATION FOR TROPICAL WASTEWATER TREATMENT

5.1 Effect of Dissolved Oxygen on Seed Sludge Nitrification Performance

From the wastewater characterisation study, the tropical wastewater in this study contained low concentration of rbCOD. Hanaki et al. (1990) and Satoh et al. (2000) suggested that wastewater low in biodegradable organics may be favourable for low-DO nitrification. The effect of DO on the nitrification performance was investigated using sludge sampled from WWTP 1 according to methods in Section 3.5.

The relationship between SAUR and DO was described by saturation kinetics (Figure 5.1). The raw data of $\text{NH}_4\text{-N}$, $\text{NO}_2\text{-N}$ and $\text{NO}_3\text{-N}$ for the batch nitrification activity experiment used for calculating SAUR and plotting Figure 5.1 were provided in Appendix D. From the nonlinear regression, the value of K_O of the sludge was 0.22 mg/L. The values of K_O for nitrifiers reported in the literatures range from 0.10 to 1.0 mg/L (Keene et al., 2017; Manser, Gujer, & Siegrist, 2005). Hence, the seed sludge in this work may have a relatively high affinity for oxygen. Low-DO condition did not significantly reduce the SAUR, the rate being 70% of the maximum at 0.5 mg $\text{O}_2\text{/L}$.

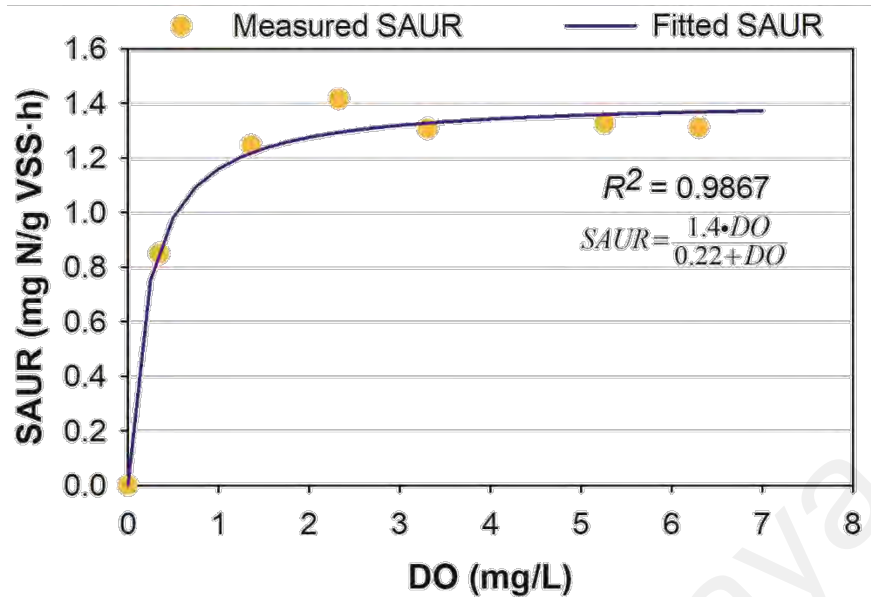


Figure 5.1: The effect of DO on SAUR of the seed sludge from WWTP 1. The round markers denote the SAUR data determined from batch kinetic experiments while the solid line represents the saturation kinetic model fitted to the data.

The maximum SAUR was 1.4 mg N/g MLVSS·hr (Figure 5.1). The maximum SAUR value was in the lower range of literatures' values, which range between 1 and 3 mg N/g MLVSS·hr (Arnaldos et al., 2013; Q. Yang et al., 2016).

The curve fitting using saturation kinetics suggested that nitrifiers in the seed sludge had high oxygen affinity, which matched with the survival strategies of k-strategists, such as *Nitrosospira sp.* and *Nitrospira sp.* (Seviour & Nielsen, 2010). *Nitrospira sp.* was reported to be abundant in full-scale WWTPs and in low-DO reactors (G. Liu & Wang, 2013; Q. Yang et al., 2016). In the full-scale WWTPs, pockets of low-DO zones were found in the macro-environment of the aerobic tank (Daigger & Littleton, 2014). The non-uniform DO distribution in the macro-environment may be favourable for the growth of k-strategist nitrifiers.

The results from the batch nitrification activity test at different DO levels showed that the sludge has high oxygen affinity with maximum SAUR at around 1 mg O₂/L.

Thus, the sludge may be suitable to operate a nitrification process at low-DO condition ($< 1 \text{ mg O}_2/\text{L}$) in treating the tropical wastewater.

5.2 Performance of Low-Dissolved-Oxygen Nitrification Sequencing Batch Reactor

The batch experiment data in section 5.1 indicated that operating a nitrification reactor at low-DO condition is, in principle, feasible. However, the conditions were artificial, which consisted a synthetic medium with only NH_4^+ and alkalinity as feed. Therefore, the effect of low-DO condition on nitrification was investigated in a nitrification SBR fed with real wastewater. The following sections discuss the low-DO nitrification SBR performance and rate of nitrification. The raw data of MLSS, MLVSS, sCOD, $\text{NH}_4\text{-N}$, $\text{NO}_2\text{-N}$, $\text{NO}_3\text{-N}$ and TN of the low-DO nitrification SBR were given in Appendix E.

5.2.1 Chemical Oxygen Demand and Ammoniacal Nitrogen Removal Efficiency

The SBR was operated for 43 d at DO concentration below 0.5 mg/L (Figure 5.2A). The initial MLSS and MLVSS concentrations were 2400 mg/L and 1800 mg/L respectively. Both MLSS and MLVSS concentrations reduced in the first 15 d of SBR operation, after which both concentrations were maintained at $1500 \pm 200 \text{ mg/L}$ and $1300 \pm 160 \text{ mg/L}$ respectively. The sCOD removal and nitrification were both stable after 15 d of SBR operation (Figure 5.3). The SBR typically removed sCOD and $\text{NH}_4\text{-N}$ adequately. The effluent sCOD was $18 \pm 5 \text{ mg/L}$ (Figure 5.3) and the residual organic matter might represent small fraction of non-biodegradable COD (Figure 5.2D). Effluent $\text{NH}_4\text{-N}$ was often less than 2 mg/L (Figure 5.4). The one peak of effluent $\text{NH}_4\text{-N}$ on day 39 was associated with the failure of the impeller.

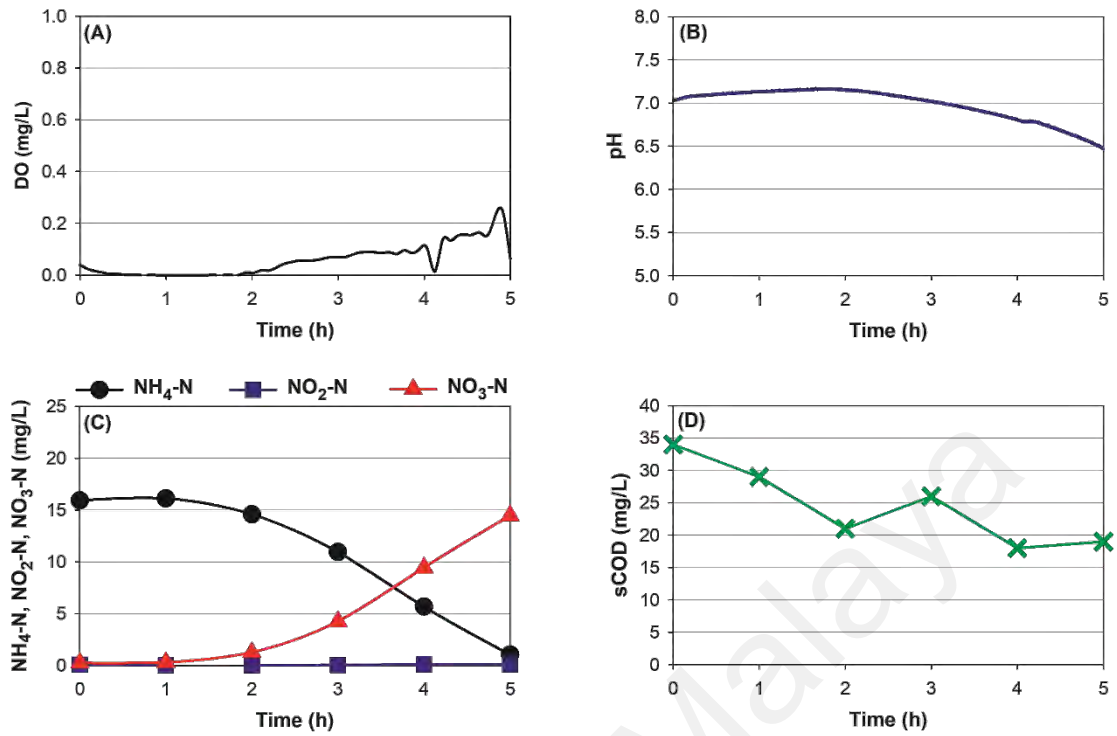


Figure 5.2: Detailed profiles of (A) DO concentration, (B) pH, (C) NH₄-N, NO₃-N & NO₂-N concentrations and (D) sCOD concentrations on day 36 of SBR operation. DO concentration was below 0.5 mg/L throughout the reaction cycle, nitrification commenced only after sCOD had been depleted.

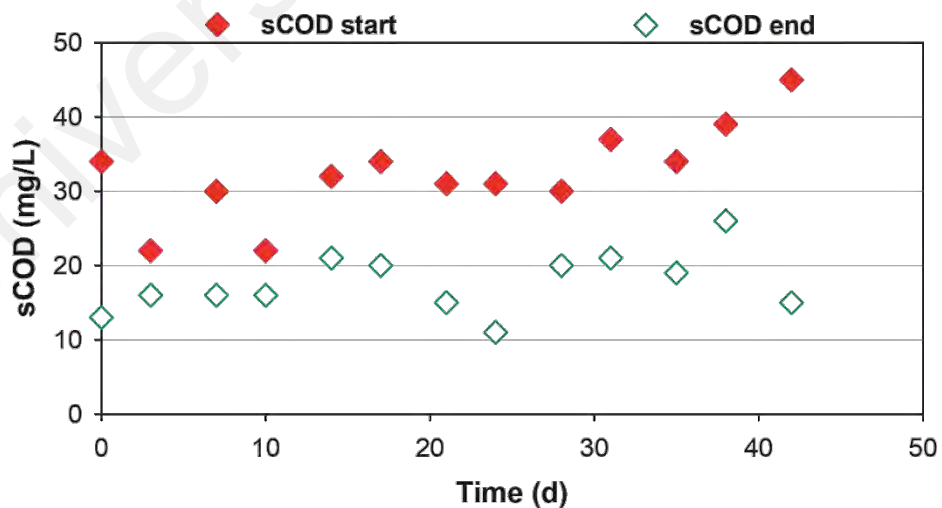


Figure 5.3: Overall sCOD profile of low-DO nitrification SBR.

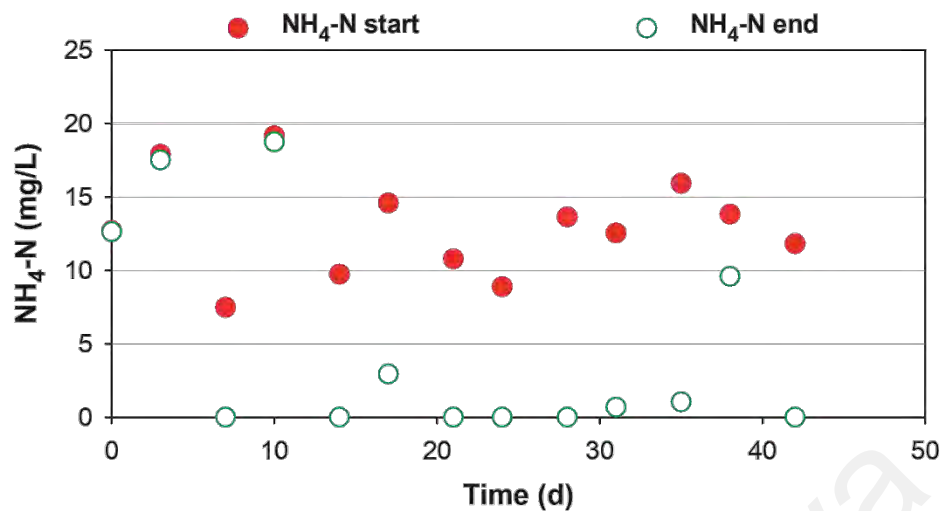


Figure 5.4: Overall NH₄-N profile of low-DO nitrification SBR.

The adaptation period in this study (15 d) was much shorter than 25 and 140 d reported by Fitzgerald et al. (2015) and Arnaldos et al. (2013) respectively. The rapid appearance of active nitrification could be caused by either the more rapid growth of nitrifiers at warmer temperature or the high proportion of suitably adapted organisms in the seed sludge. Ofițeru and Curtis (2009) developed a simple model to simulate the adaptation of AOB to low-DO condition. Their simulation suggested that the adaptation is more sensitive to the initial AOB concentrations than the nitrifiers' maximum growth rate. Presumably the seed sludge used in low-DO nitrification studies by Arnaldos et al. (2013) and Fitzgerald et al. (2015) were from conventional aerobic sludge and so a longer acclimation period was required for the adaptation of aerobic sludge in low-DO condition.

Despite the low DO concentrations, all the NH_4^+ was converted into NO_3^- (Figure 5.5). Accumulation of NO_2^- was not detected in a typical SBR cycle (Figure 5.2C). Low DO level is conventionally associated with the accumulation of NO_2^- in the nitrification process. However, more recent studies showed that low-DO nitrification could exert selection pressure on certain lineages of NOB that possess high oxygen affinity, thus making NOB a better competitor of oxygen than AOB (Daebel, Manser, & Gujer, 2007;

Law et al., 2019; G. Liu & Wang, 2013). Consequently, NO_2^- consumption by NOB is always higher than its production by AOB. Furthermore, high NH_3 concentration is a significant factor of NO_2^- accumulation (Kampschreur et al., 2009). NH_3 concentration approximately 9 mg N/L is sufficient to inhibit oxidation of NO_2^- to NO_3^- . NH_3 concentration in the wastewater of this study was less than 0.5 mg/L based on acid dissociation of NH_4^+ . Hence, both increased oxygen affinity of NOB and negligible NH_3 concentration might have contributed to complete oxidation of NH_4^+ to NO_3^- .

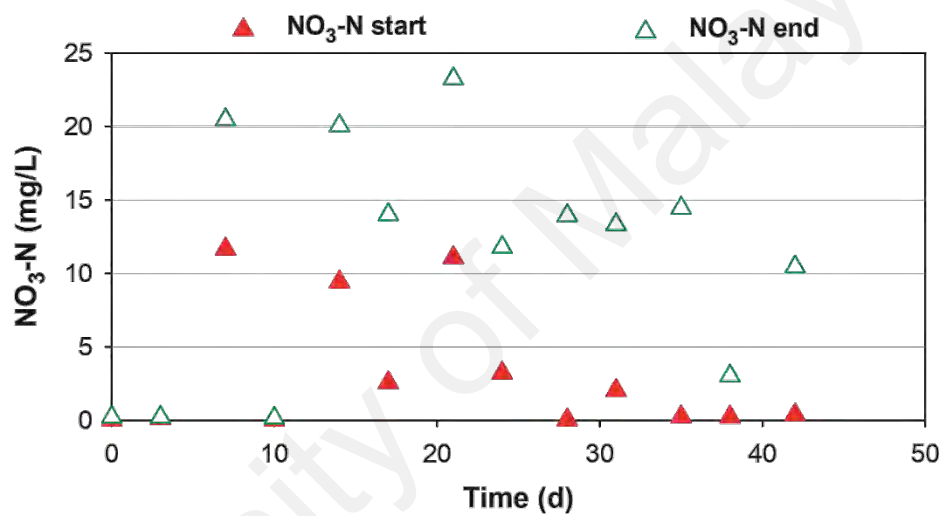


Figure 5.5: Overall NO_3 -N profile of low-DO nitrification SBR.

Surprisingly, Figure 5.5 shows that the NO_3 -N at the beginning of the cycle was negligible between day 29 and day 43, which suggests a loss in NO_3 -N in the SBR. Assuming denitrification did not occur, the NO_3 -N from the previous SBR cycle would be carried over to the next cycle. The NO_3 -N at the end of a SBR cycle was around 15 mg/L (Figure 5.5). At the volume exchange ratio of 0.6 for the low-DO nitrification SBR, the theoretical NO_3 -N at the start of an SBR cycle is $15 \times (1 - 0.6) = 0.6$ mg/L if denitrification did not occur. Denitrification clearly did not occur during the reaction phase because the increase in NO_3 -N is equivalent to the NH_4 -N reduction (Figure 5.4 and Figure 5.5). Thus, denitrification may have occurred during the settling phase.

Significant denitrification in clarification step has been reported by previous studies (Mikola et al., 2014; Siegrist et al., 1995). The condition in the settling phase is favourable for denitrification because of the anoxic environment, the decay of biomass was found to provide the COD required for denitrification (Siegrist et al., 1995).

5.2.2 Rate of Nitrification

The specific rate of accumulation of $\text{NH}_4\text{-N}$ and $\text{NO}_3\text{-N}$ were 1.8 ± 0.4 mg N/g MLVSS·hr though low DO concentration was maintained (Figure 5.6). The rate of $\text{NH}_4\text{-N}$ uptake at steady-state low-DO nitrification SBR operation (above 15 d; Figure 5.6) appeared to be 1.3 times higher than that of the seed sludge (Figure 5.1). A modest increase in rate of nitrification was expected as the sludge adapts to low-DO condition. When compared with literature, Q. Yang et al. (2016) reported 3 mg N/g MLVSS·hr of $\text{NH}_4\text{-N}$ uptake at DO concentration between 1 and 2 mg/L. Low-DO nitrification study conducted by Arnaldos et al. (2013) also reported nitrification rate close to 4 mg N/g MLSS·hr at DO concentration of 0.1 mg/L. Thus, the rate of nitrification in this work was still relatively low. One of the reasons could be the high nitrifier abundance in other studies (Arnaldos et al., 2013; Q. Yang et al., 2016). For example, Arnaldos et al. (2013) found that nitrifiers constituted nearly half of the total bacteria in their reactor. Also, Q. Yang et al. (2016) reported nitrifiers' abundance in the order of 10^{10} copies/g MLVSS, which was significantly higher than the typical abundance (10^6 to 10^8 copies/mL) published elsewhere (Bellucci et al., 2011; Fitzgerald et al., 2015).

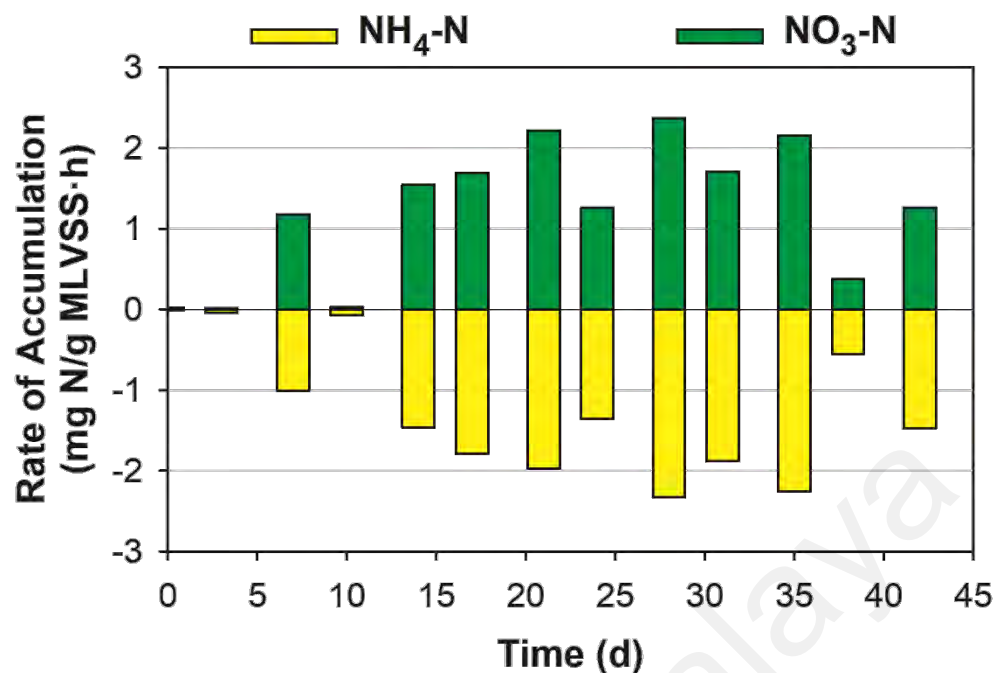


Figure 5.6: Profiles of rates of accumulation for NH₄-N and NO₃-N throughout SBR operation.

The low-DO nitrification SBR performance data clearly demonstrated that good nitrification performance could be attained under low-DO condition (0.5 mg O₂/L). The high nitrification efficiency could be attributed to the low COD content of tropical wastewater. Apart from the low COD/N characteristic of tropical wastewater in this study, the nitrifying community in the low-DO nitrification SBR may also play an important role in achieving good nitrification performance. In the next section, the microbial community of the low-DO nitrification SBR was investigated.

5.3 Proportional Abundance of Nitrifiers and Denitrifiers in Low-Dissolved-Oxygen Nitrification Sequencing Batch Reactor

To elucidate the nitrifying community in the low-DO nitrification SBR, 16S rRNA amplicon sequencing was performed on the sludge using the IonTorrent workflow. FISH analysis was also used to validate the presence of the nitrifiers in the low-DO sludge.

16S rRNA amplicon sequencing data identified more than 746 known taxonomies but only 20 taxonomies were present in more than 1% throughout the SBR operation. The top three most abundant organisms in the sludge were Family *Saprospiraceae* ($13 \pm 2\%$), Order *Sphingobacteriales* ($5 \pm 1\%$) and Order *envOPS12* ($3 \pm 0.5\%$). Figure 5.7 shows the four most abundant taxonomies that associate with nitrification and denitrification. The information was extracted from the taxa plots generated by core diversity analysis in QIIME.

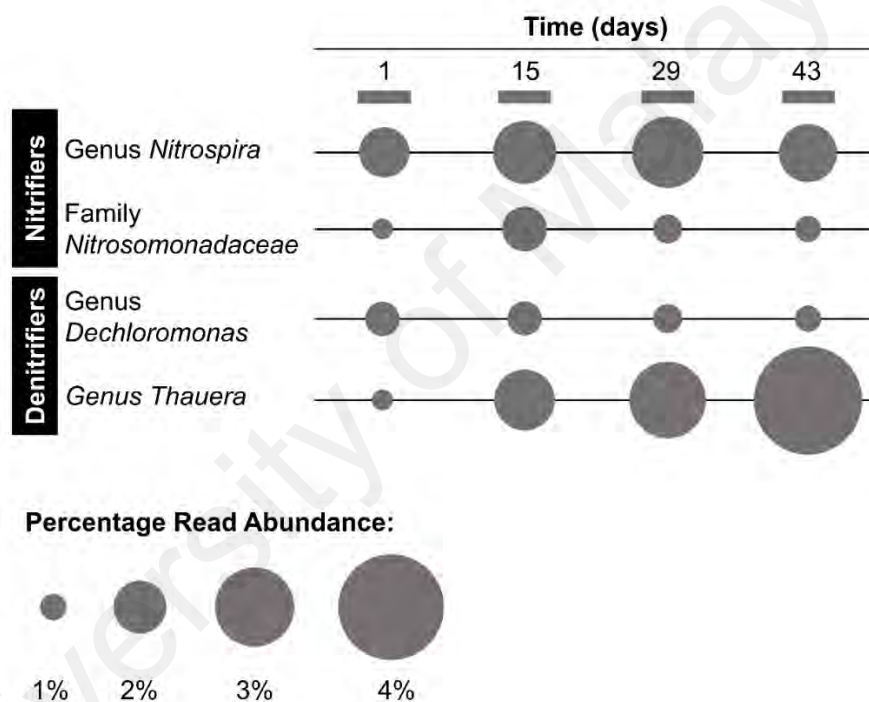


Figure 5.7: Population dynamics of significant OTUs present in the low-DO nitrification SBR.

The microbes related to the Family *Nitrosomonadaceae* and Genus *Nitrospira* were found to be the most abundant AOB and NOB, respectively. *Nitrobacter*-related NOB were not detected by 16S rRNA amplicon sequencing. FISH analysis supported the presence of *Nitrosomonadaceae*-related AOB and *Nitrospira*-related NOB detected by 16S rRNA amplicon sequencing (Figure 5.8).

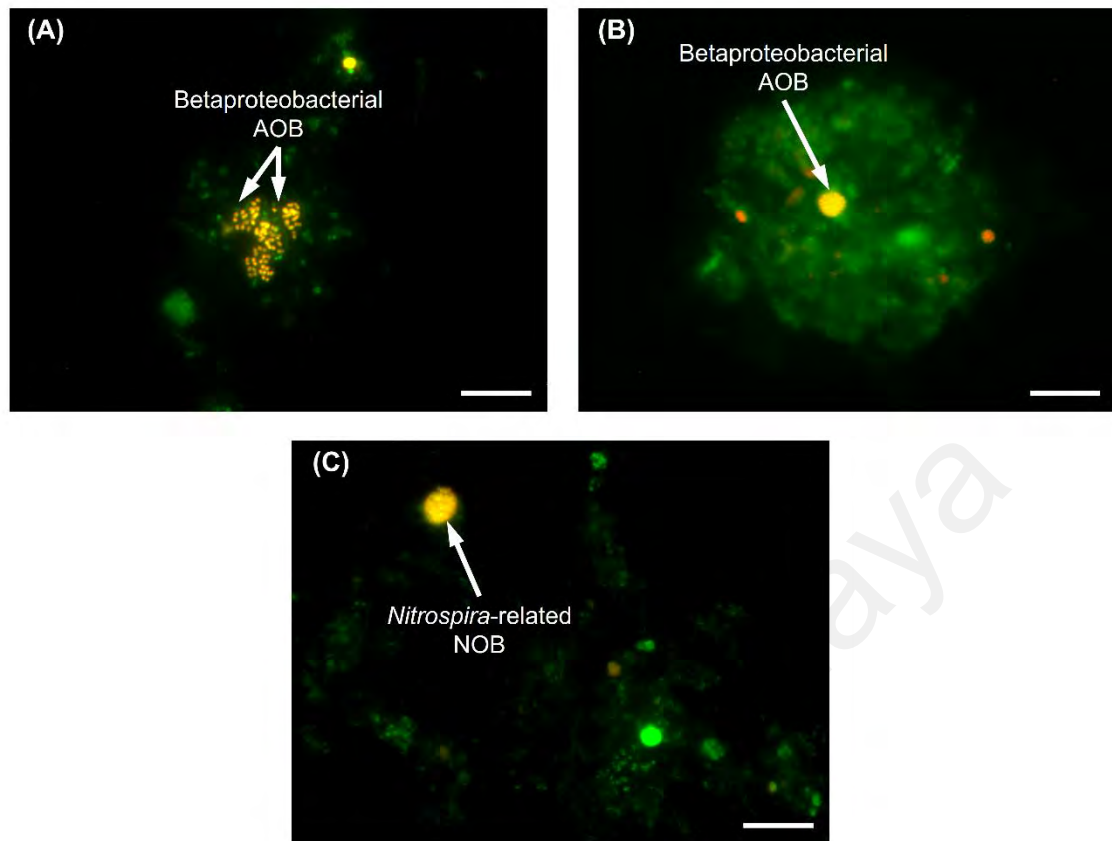


Figure 5.8: FISH images of fixed cell sample on day 43 showing total bacteria hybridised with probe EUBMIX (green) together with (A) & (B) betaproteobacterial AOB hybridised with probe Nso1225 (yellow) and (C) *Nitrospira*-related NOB hybridised with probe Ntspa662 (yellow). Scale bar in each image denotes 10 µm.

Genus *Nitrospira* and Family *Nitrosomonadaceae* each represent 1% to 3% of total sequence read abundance. The Family *Nitrosomonadaceae* was known to be able to oxidise NH_4^+ autotrophically to NO_2^- . Members of the Genus *Nitrospira* were known to be chemolithoautotrophic aerobic NOB. *Nitrospira*-related NOB has been described as k-strategist organisms that survive in low substrate concentrations. Strains related to *Nitrospira sp.* have been observed in other nitrification studies (Law et al., 2019; Q. Yang et al., 2016). For instance, Q. Yang et al. (2016) observed the coexistence of large population of *Nitrospira sp.* with AOB in an aerobic tank with reduced DO (1 – 2 mg

O₂/L) of a water reclamation plant in Singapore. Law et al. (2019) also reported a high population of *Nitrospira sp.* in a partial nitrification reactor when operated at low DO condition (0.5 – 1.5 mg O₂/L).

To further examine the diversity and phylogeny of the unidentified *Nitrospira sp.*, a phylogenetic tree was constructed for all the 224 OTUs within the *Nitrospira* genus obtained from 6 samples on day 1, 8, 15, 22, 29 and 43 (Figure 5.9A). Most of the OTUs are clustered into two equally divided groups, termed Group A and Group B here. The average nucleotide identity (ANI) within each group is $98 \pm 2\%$ based on *p*-distance matrix, which suggested OTUs in each clade could be related down to species level (sequence similarity > 97%). Thus, a representative sequence from each group was generated based on the highest frequency of nucleotide base at each position. The representative sequences were aligned with other known *Nitrospira* 16S rRNA-coding sequences to construct a phylogenetic tree (Figure 5.9B). The numbers in parentheses of Figure 5.9B indicate the frequencies of OTUs exhibiting the same 16S rRNA gene sequences. The defined sublineages of the genus *Nitrospira* (Daims, Nielsen, et al., 2001) were also indicated by roman numerals adjacent to the square brackets. The shaded branches indicate the closest phylogenetic relationship between the present study sequence and the available reference sequence. Figure 5.9B shows that Group A (52% of the total *Nitrospira* OTUs) of the *Nitrospira sp.* detected in this study was closely related to *Nitrospira defluvii*, while Group B (47% of the total *Nitrospira* OTUs) was closely related to one of the comammox strains, *Ca. Nitrospira nitrosa* (van Kessel et al., 2015). The heat map in Figure 5.9B shows that Group A and Group B *Nitrospira* co-existed with each other throughout the 43-day low-DO nitrification SBR operation. The percentage read abundance of both groups fluctuated narrowly between 0.9% and 1.5%, which suggested that neither Group A nor Group B outcompeted each other. The co-existence of comammox with canonical NOB was reported in a full-scale WWTP

operating with a deep oxidation ditch ($DO < 0.1 \text{ mg/L}$) in Taiwan based on the metatranscriptomics data of *amoA* and *nxr* (Y. Yang et al., 2020). Fujitani et al. (2020) also found that comammox *Nitrospira* (*Ca. Nitrospira nitrosa*) could thrive together with *Nitrospira defluvii* when the influent $\text{NH}_4\text{-N}$ concentration was kept between 40 – 50 mg/L in continuous feeding fixed bed reactor for comammox enrichment. The results from Y. Yang et al. (2020) and Fujitani et al. (2020) suggested that *Nitrospira defluvii* and comammox may perform nitrification simultaneously. Thus, the nitrifying roles of *Nitrospira defluvii* and comammox were further discussed.

University of Malaya

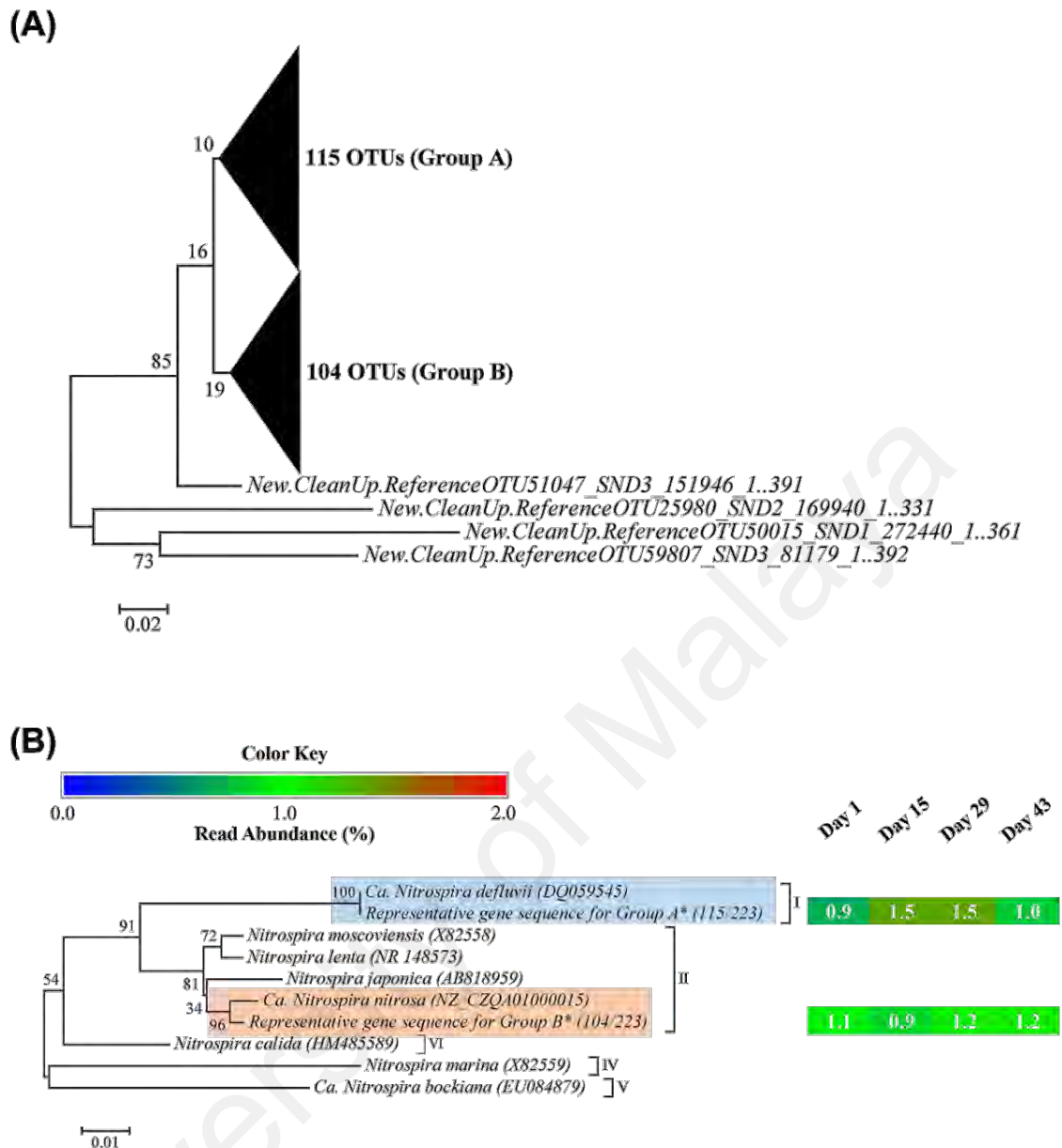


Figure 5.9: Neighbour-joining phylogenetic tree of the *Nitrospira sp.* 16S rRNA gene sequences showing the relationship (A) amongst all 223 OTUs belong to genus *Nitrospira* from this study, and (B) between the representative sequences of *Nitrospira sp.* (marked with *) obtained from the low-DO nitrification SBR and reference sequences in the GenBank database. All bootstrap values were shown in percentages of 1000 replicates. The heat map depicts the changes in percentage read abundance of Group A and Group B *Nitrospira*.

Nitrospira defluvii was classified into the sublineage I of *Nitrospira sp.* based on 16S rRNA phylogeny and it is an important NOB in wastewater treatment (Daims, Nielsen, et al., 2001; Lucker et al., 2010). Lucker et al. (2010) found that the key enzyme *nxr* in *Nitrospira defluvii* differs significantly with other *Nitrospira sp.* but share the closest homolog with an anammox bacteria (“*Candidatus* Kuenenia stuttgartiensis). *Nitrospira defluvii* also lacked a protection mechanism against oxidative stress commonly present in *Nitrospira* (Lucker et al., 2010). A study by Park and Noguera (2008) revealed that 6 out of 7 OTUs obtained from a low-DO reactor (0.12 – 0.24 mg/L) were affiliated by *Nitrospira defluvii* while only 5 out of 10 clones obtained from a high-DO reactor (8.7 mg/L) were related to *Nitrospira defluvii*. The authors concluded that *Nitrospira defluvii* favour low-DO conditions and cannot adapt to transition to high DO concentrations (Park & Noguera, 2008). Thus, *Nitrospira defluvii* may be an important NOB in low-DO nitrifying systems (Mehrani et al., 2020).

van Kessel et al. (2015) identified some strains of the genus *Nitrospira* as comammox bacteria, so called because of their ability to completely oxidise NH_4^+ to NO_3^- . The Basic Local Alignment Search Tool (BLAST) alignment of the representative 16S rRNA gene sequence of Group B in this work and *Ca. Nitrospira nitrosa* showed 99% sequence identity. Therefore, the presence of comammox-related *Nitrospira sp.* supported the earlier finding on complete oxidation of NH_4^+ to NO_3^- in the low-DO nitrification SBR. The other two strains of comammox bacteria, *Nitrospira inopinata* and *Ca. Nitrospira nitrificans* were phylogenetically distant from the members of the *Nitrospira sp.* detected in this study (Daims et al., 2015; van Kessel et al., 2015). Thus, these two comammox strains were not included in Figure 5.9B.

The role of comammox bacteria in wastewater treatment system is still uncertain (Chao et al., 2016; Gonzalez-Martinez et al., 2016; van Kessel et al., 2015).

Phylogenetic analyses conducted by van Kessel et al. (2015) suggested that *Ca. Nitrospira nitrosa* was present in engineered systems, including wastewater treatment plant and drinking water distribution system. Conversely, both Chao et al. (2016) and Gonzalez-Martinez et al. (2016) inferred that comammox-like bacteria probably do not play an important role because of their low abundance (< 0.1%) in wastewater treatment plants. Chao et al. (2016) hypothesised that the operating conditions in wastewater treatment plants are not favourable for the growth of comammox bacteria as they are known to proliferate in low-substrate (< 10 mg NH_4^+ /L, < 22 mg NO_2^- /L) and hypoxic conditions (< 0.1 mg O_2 /L) (van Kessel et al., 2015). In this study, the low-substrate and the low-DO environment in the nitrification SBR could promote the growth of comammox-related bacteria. The comammox-related *Nitrospira sp.* was also detected in the seed sludge of the low-DO nitrification SBR, suggesting their potential role in nitrification in the tropical WWTPs. Nonetheless, Y. Yang et al. (2020) suggested that the functional roles of comammox and canonical nitrifiers in different wastewater treatment system habitats cannot be deduced directly from their abundance data. More transcriptomic studies are needed to elucidate the effects of environmental conditions on the nitrifying gene expressions in different nitrifiers, thereby allowing researchers to quantify the contributions of comammox and canonical nitrifiers in nitrification process.

The 16S rRNA amplicon sequencing data also indicated the potential presence of DOHOs related to the Genera *Dechloromonas* and *Thauera*. The genera *Dechloromonas* and *Thauera* were present with average abundances of 1.3% and 2.8% respectively (Figure 5.7). Interestingly, the Genus *Thauera* was present in less than 1% in the inoculum but gradually enriched to beyond 4%. However, 16S rRNA amplicon sequencing data alone was not sufficient to deduce the presence of DOHOs in the low-DO nitrification SBR. In the subsequent long-term SBR operations (Chapter 6), more

accurate quantification method based on qPCR for the denitrifying genes were applied to prove the presence of DOHOs in the process.

The microbial community analyses for low-DO nitrification SBR showed that nitrifiers related to *Nitrospira* dominated the nitrifying community. Among the *Nitrospira* OTUs detected, half of the OTUs were affiliated with *Nitrospira defluvii* and another half were more closely related to *Ca. Nitrospira nitrosa*. The high nitrification efficiency in the low-DO nitrification SBR could be attributed to the presence of these k-strategist *Nitrospira*. The presence of OTUs related denitrifiers also highlight potential denitrification activity under anoxic condition.

5.4 Energy Savings of Low-Dissolved-Oxygen Nitrification Process

This study showed that low-DO nitrification is a suitable operating strategy to treat the tropical wastewater low in rbCOD. Applying low-DO nitrification may reduce the aeration demand and the energy usage in the WWTPs. The amount of energy reduction to operate a low-DO nitrification process (0.5 mg/L) relative to conventional nitrification process (2 mg/L) could be estimated based on OTR to maintain biological activities and bulk DO level in the tropical wastewater (30°C). The calculation assumed surface aerator was used to provide aeration. The estimated energy reduction is 23% of the energy required to operate the process at 2 mg O₂/L (Table 5.1). Keene et al. (2017) estimated a similar magnitude of energy reduction (25%) when operating a biological nutrient removal process at 0.33 mg O₂/L relative to higher DO concentrations (0.9 – 4.3 mg/L). The reduction in aeration energy requirement offers an attractive strategy to improve the energy efficiency of WWTPs as aeration units accounted for 70% of the energy usage (Ramli & Abdul Hamid, 2017).

Table 5.1: Estimated energy required for aeration in conventional and low-DO nitrification process

Parameters	Estimated Value		Remarks
	Conventional (2 mg/L)	Low DO (0.5 mg/L)	
OTR_{LIQUID} (kg O ₂ /d)	12	3	OTR to maintain bulk DO concentration
OTR_{TOTAL} (kg O ₂ /d)	650	640	Total OTR required
SOTR (kg O ₂ /d)	1010	780	Total OTR required at standard condition (20°C, 1 atm)
Energy required (kWh/d)	780	600	

5.5 Summary of Chapter

The low-DO nitrification study in this chapter addressed objective 2 to demonstrate the feasibility of applying low-DO nitrification as a proposed operating strategy of an improved process for biological nitrogen removal in treating low COD/N tropical wastewater. Besides, 16S rRNA amplicon sequencing was also used to investigate the microbial community to achieve objective 5.

The batch nitrification activity experiment under different DO concentrations showed that nitrification at DO below 1 mg O₂/L was attainable. Subsequently, a low-DO nitrification SBR was operated and confirmed that high nitrification efficiency could be achieved at low-DO condition (0.5 mg O₂/L). Microbial community analyses revealed that k-strategist *Nitrospira* with high oxygen affinity dominated the nitrifying community. *Nitrospira* closely affiliated with comammox (*Ca. Nitrospira nitrosa*) may also contribute to the good nitrification performance in low-DO nitrification SBR. An energy saving analysis based on OTR suggested that using low-DO nitrification (0.5 mg O₂/L) could lead to 23% aeration energy reduction when compared with conventional nitrification process operated at 2 mg O₂/L.

In the following chapter, low-DO nitrification was applied as one of the operating strategies in a long-term biological nitrogen removal reactor for an improved process in treating low COD/N tropical wastewater.

University of Malaya

CHAPTER 6: PROCESS IMPROVEMENT OF A CONVENTIONAL ANOXIC-OXIC PROCESS IN TREATING TROPICAL WASTEWATER

6.1 Nitrogen Removal Performance of Anoxic-Oxic Sequencing Batch Reactor

In the previous chapters, low-DO nitrification and utilisation of sbCOD for denitrification were identified as the two operating strategies to achieve an efficient and low-cost biological nitrogen removal in treating low COD/N tropical wastewater. In this chapter, the long-term performance of applying low-DO nitrification and utilising sbCOD in treating low COD/N tropical wastewater were investigated in a biological nitrogen removal reactor. A biological nitrogen removal SBR operating in AO configuration was started up for the study. AO configuration was selected because most of the WWTPs in Malaysia is operating in this configuration. Applying low-DO nitrification and utilising sbCOD for denitrification may help the WWTPs operating in AO process to improve the sustainability.

The steady-state detailed profiles of $\text{NH}_4\text{-N}$, $\text{NO}_3\text{-N}$ and DOC concentrations for each of the four operating phases are shown in Figure 6.1, and the detailed pH and DO profiles for each operating phase are shown in Figure 6.2. The long-term variations of MLSS & MLVSS, sCOD, $\text{NH}_4\text{-N}$ and $\text{NO}_3\text{-N}$ concentrations are provided in Figure 6.3, Figure 6.4, Figure 6.5 and Figure 6.6, respectively. The raw data of AO SBR, including MLSS, MLVSS, sCOD, $\text{NH}_4\text{-N}$, $\text{NO}_2\text{-N}$, $\text{NO}_3\text{-N}$ and TN, were provided in Appendix F.

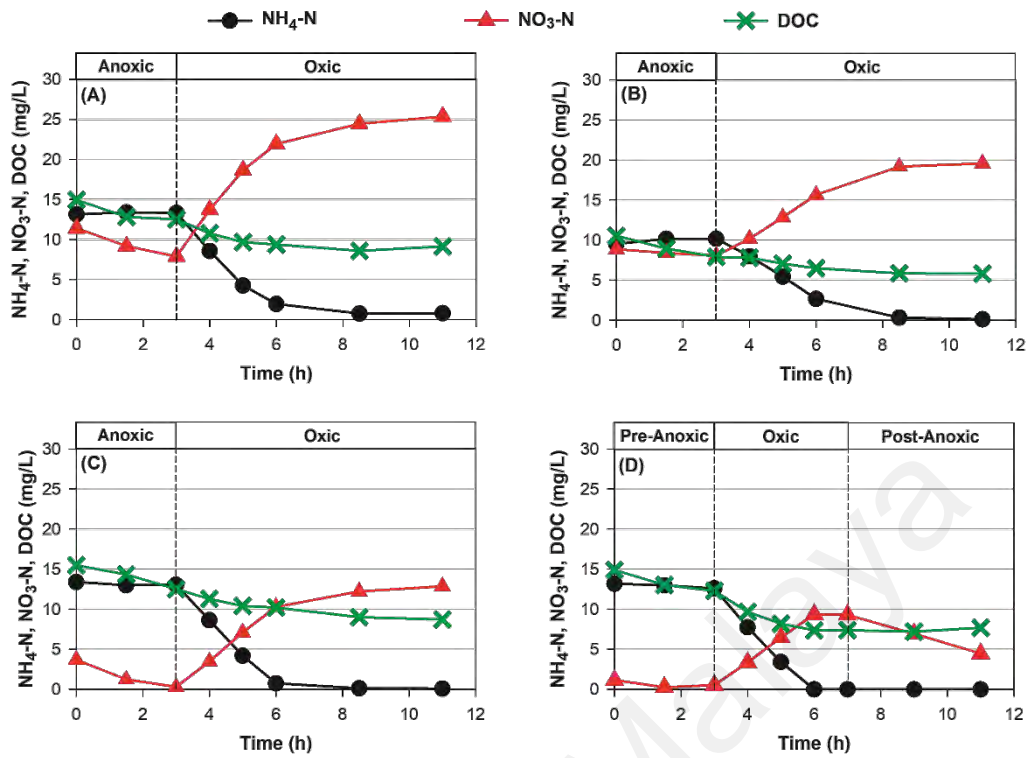


Figure 6.1: Detailed profiles of $\text{NH}_4\text{-N}$, $\text{NO}_3\text{-N}$ and DOC in selected SBR cycles during (A) P1 on day 64; (B) P2 on day 113; (C) P3 on day 190 and (D) P4 on day

267.

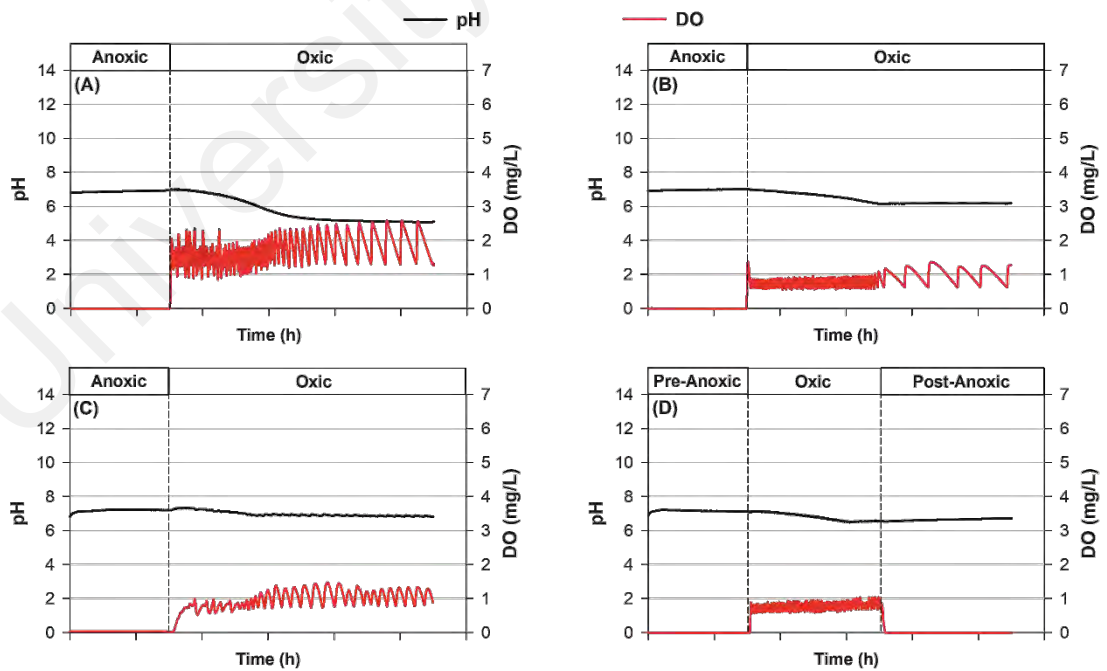


Figure 6.2: Detailed profiles of pH and DO in selected SBR cycles during (A) P1 on day 64; (B) P2 on day 113; (C) P3 on day 190 and (D) P4 on day 267.

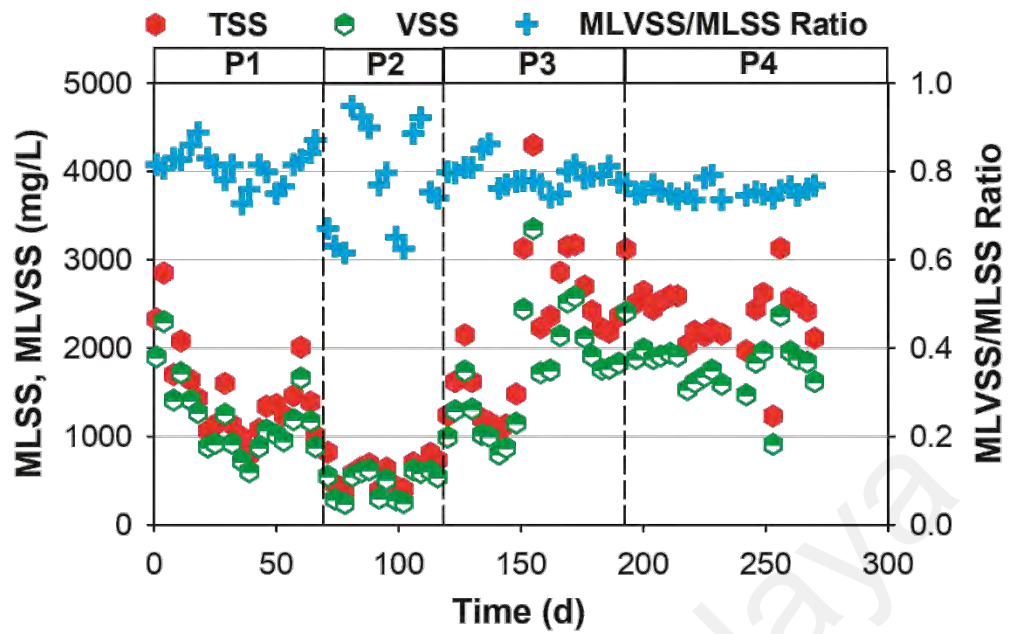


Figure 6.3: Overall MLSS and MLVSS profiles of AO SBR.

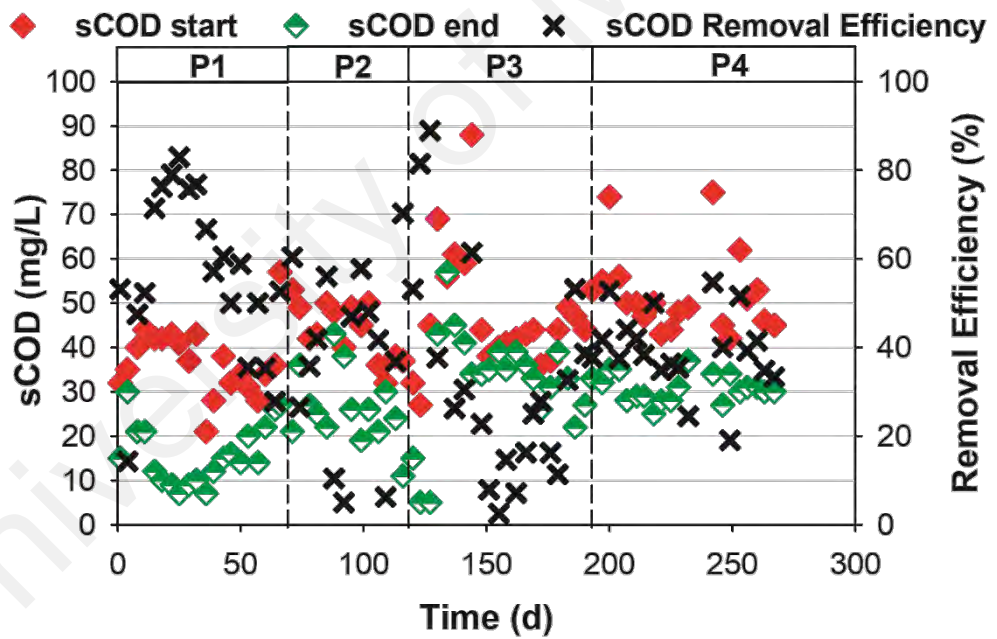


Figure 6.4: Overall sCOD profile of AO SBR.

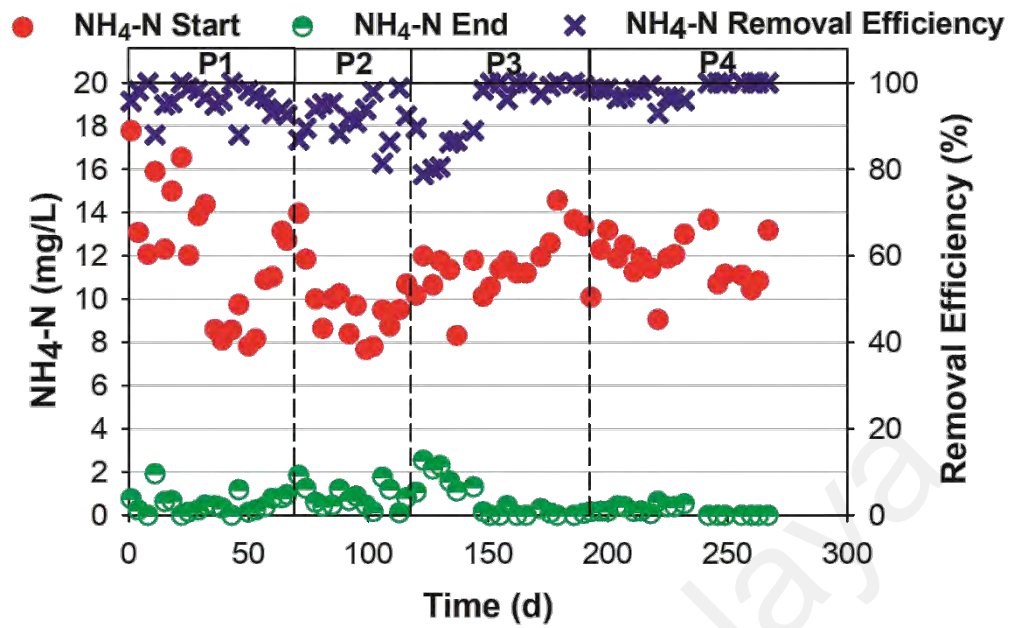


Figure 6.5: Overall NH₄-N profile of AO SBR.

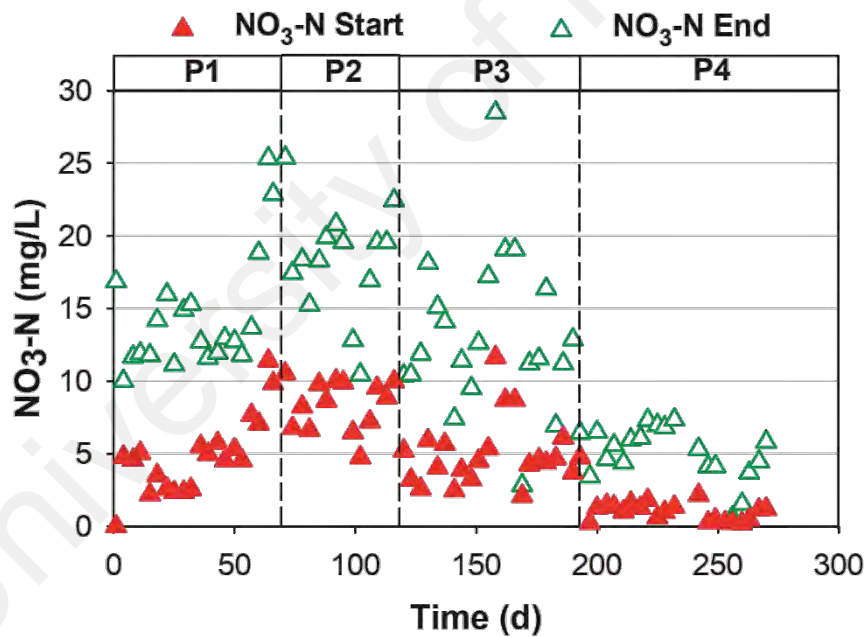


Figure 6.6: Overall NO₃-N profile of AO SBR.

During the initial phase (P1), the SBR was operated in a conventional AO configuration with a high-DO oxic phase (1.7 ± 0.2 mg/L; Figure 6.2A). Figure 6.1 shows that the effluent contained low concentrations of NH₄-N (0.6 ± 0.5 mg/L). The nitrification efficiency was $95 \pm 4\%$ throughout P1 with an average specific nitrification

rate of 4.3 ± 1.4 mg N/g MLVSS·hr. The effective $\text{NH}_4\text{-N}$ removal was expected as a DO concentration of around 2 mg/L is recommended to ensure complete nitrification in the WWTPs (Tchobanoglous et al., 2014).

In the second phase (P2), the operation of the SBR was switched to an AO configuration with a low-DO oxic phase (0.9 ± 0.1 mg/L; Figure 6.2B) to investigate the feasibility of incorporating low-DO nitrification and stability of nitrification performance at low-DO condition in a tropical biological nitrogen removal system. The MLSS and MLVSS concentrations decreased to 600 ± 150 mg/L and 470 ± 160 mg/L, respectively (Figure 6.3). The MLSS and the MLVSS concentrations in P2 were 2.5 times lower than that during P1. The drop in the MLSS and the MLVSS concentrations could be due to the lower biomass yield under low-DO concentration, which mimicked a pseudo-anoxic condition. Muller et al. (2003) found that the anoxic biomass yield was 30 – 40% lower than that under aerobic condition, which was similar to the reduction of the MLSS and the MLVSS concentrations during P2. The $\text{NH}_4\text{-N}$ removal efficiency and the specific nitrification rate were consistent, which were $93 \pm 6\%$ and 3.8 ± 0.5 mg N/g MLVSS·hr, respectively. The nitrification performance in P2 was comparable to that during P1 (Figure 6.1A and Figure 6.1B). Thus, complete and stable nitrification efficiency could be achieved in low-DO condition at the same HRT as the conventional nitrification process (> 2 mg $\text{O}_2\text{/L}$), which confirmed that low-DO nitrification could be adopted by tropical WWTPs to reduce their energy consumption. As a typical characteristic of an AO process, the effluent $\text{NO}_3\text{-N}$ was high (18 ± 4 mg/L). The presence of $\text{NO}_3\text{-N}$ at the start of SBR reaction phase was caused by NO_3^- carryover from the previous cycle. The $\text{NO}_2\text{-N}$ concentration was always less than 1 mg/L and was insignificant when compared with the $\text{NO}_3\text{-N}$ concentration (Figure 6.1B). Furthermore, the lack of biodegradable organics in the settled wastewater also

contributed to the poor denitrification performance in the anoxic phase, which led to excessive NO_3^- accumulation.

To enhance the denitrification performance in the anoxic phase, raw wastewater was used as the reactor influent during P3. The previous wastewater characterisation studies (Chapter 4) demonstrated that the sbCOD in PSS made up 15 – 60% of TCOD in the raw wastewater and the PSS was hydrolysed at a high rate to provide sbCOD for denitrification. Figure 6.1C clearly shows an improved denitrification performance during the anoxic phase of P3 when compared with P1 and P2, which led to a lower NO_3 -N accumulation and carryover. For instance, the initial NO_3 -N in the SBR cycle was lower in P3 (4 mg/L) when compared with P1 and P2 (10 mg/L). Using raw wastewater as the influent during P3 caused a temporary decline in the nitrification efficiency to $84 \pm 4\%$ until day 172 (Figure 6.5). The reason for the lower nitrification efficiency could be due to the increased competition for oxygen between the heterotrophs and the nitrifiers (Satoh et al., 2000). Nevertheless, the nitrification efficiency in the SBR was restored to $92 \pm 8\%$ after day 172, presumably due to the selection of nitrifiers possessing a higher affinity for oxygen. Fitzgerald et al. (2015) and Keene et al. (2017) suggested that nitrifiers with higher oxygen affinity will be selected when oxygen becomes a limiting substrate in the environment. To further reduce the effluent NO_3 -N, a post-anoxic phase was incorporated in the final period (P4).

The SBR was subsequently changed from a low-DO AO to a low-DO AOA configuration in P4. The NH_4 -N removal efficiency remained high ($98 \pm 2\%$) as in the previous operating phases (Figure 6.2C). The post-anoxic phase removed approximately 60% of the NO_3 -N produced during nitrification (Figure 6.1D), which reduced the effluent NO_3 -N to 5.7 ± 1.3 mg/L (Figure 6.6). The effluent NO_3 -N in P4 was lower

than the effluent discharge standard A (10 mg/L) stipulated by Malaysia's Environmental Quality (Sewage) Regulations 2009 (Department of Environment, 2009). Most of the denitrification activity in the low-DO AOA process was attributed to the post-anoxic phase, similar observations were reported in several studies on post-anoxic denitrification processes (Shi et al., 2019; X. Wang et al., 2016; Zhao et al., 2018). The constant DOC concentration during the post-anoxic phase implied that sbCOD in the wastewater was utilised by the denitrifiers (Figure 6.1D). Apart from the exogenous carbon sources (rbCOD and sbCOD), the long SRT of the SBR (20 d) may have promoted endogenous respiration to complement the source of biodegradable organics for denitrification. Interestingly, the NO_3^- production was less than the ammonia consumption during the oxic phase in P4 (Figure 6.1D). Only 9 mg $\text{NO}_3\text{-N/L}$ was produced while 13 mg $\text{NH}_4\text{-N/L}$ was removed, suggesting the occurrence of simultaneous nitrification-denitrification (SND). Both the low DO concentration in the oxic phase (0.9 ± 0.1 mg/L; Figure 6.2D) and the concomitant oxidation of DOC during nitrification (Figure 6.1D) may have contributed to SND (Daigger & Littleton, 2014; Keene et al., 2017).

The improvement in the denitrification performance in P3 and P4 when compared with P1 and P2 showed that the raw wastewater contained sufficient biodegradable organics in the form of rbCOD and sbCOD to encourage denitrification activity. Conversely, denitrification efficiency using solely rbCOD in the settled wastewater was low in P1 and P2. The incorporation of a post-anoxic phase demonstrated that the high PSS hydrolysis rate in the warm wastewater (30°C) provided sufficient biodegradable organics to achieve low effluent $\text{NO}_3\text{-N}$. Thus, by maintaining a constant HRT (24 h), modifying an AO process into an AOA configuration could enhance the nitrogen removal from wastewater, thus obviating the need for external carbon sources. Negligible denitrification activity were observed in the pre-anoxic phase (Figure 6.1D),

which suggested that the AOA configuration may be further simplified into an OA configuration in the subsequent section.

6.2 Nitrogen Removal Performance in OA-1 Parent Sequencing Batch Reactor

From the previous study on the long-term nitrogen removal performance of an AO SBR applying low-DO nitrification and utilising sbCOD for denitrification, the AO process was modified into a low-DO AOA process. The low-DO AOA process attained good nitrogen removal performance, but the reactor operating conditions have to be further optimised. In this section, the low-DO AOA process was simplified into a low-DO OA process due to the negligible denitrification activity in the pre-anoxic phase. A parent SBR operating in low-DO OA configuration, named OA-1, was set up to establish a low-DO OA process to treat the low COD/N tropical wastewater.

The representative detailed profiles of the parent SBR (OA-1) showing the evolution of $\text{NH}_4\text{-N}$, $\text{NO}_3\text{-N}$ and DOC in a SBR cycle in P1, P2 and P3, respectively, are given in Figure 6.7. The detailed pH and DO profiles of OA-1 in P1, P2 and P3 are provided in Figure 6.8. Figure 6.9, Figure 6.10, Figure 6.11 and Figure 6.12 show the long-term reactor data on MLSS & MLVSS, sCOD, $\text{NH}_4\text{-N}$ and $\text{NO}_3\text{-N}$, respectively. The raw data of the OA-1 SBR during P1 to P3 (MLSS, MLVSS, sCOD, $\text{NH}_4\text{-N}$, $\text{NO}_2\text{-N}$ and $\text{NO}_3\text{-N}$) were given in Appendix G. In P1, OA-1 was operated in 3 h oxic phase and 8 h anoxic phase. The oxic:anoxic ratio of 3:8 resulted in an oxic HRT of 4 h. The oxic HRT was selected based on the previous low-DO AOA study, which suggested that an oxic HRT of 4 to 6 h was sufficient to achieve complete nitrification. The steady-state MLSS and MLVSS after $2 \times \text{SRT}$ (40 d) during P1 were 2470 ± 360 mg/L and 1860 ± 290 mg/L, respectively (Figure 6.9). The NH_4^+ removal in OA-1 was incomplete (Figure 6.7A). The average effluent $\text{NH}_4\text{-N}$ was 2.0 ± 1.8 mg/L (Figure 6.11). The $\text{NH}_4\text{-N}$ removal efficiency was fluctuating throughout P1 (70 – 100%). OA-1 achieved

complete NO_3^- removal in the anoxic phase (Figure 6.7A). The effluent NO_3^- -N was 0.4 ± 0.2 mg/L (Figure 6.12). The active NO_3^- removal efficiency with a constant DOC concentration in OA-1 (Figure 6.7A) showed that sbCOD from the raw wastewater was utilised for denitrification in a post-anoxic denitrification. Post-anoxic denitrification process enabled higher nitrogen removal efficiency when compared with the conventional pre-anoxic denitrification process. Some post-anoxic denitrification processes in the literature reported consistent TN removal around 92% to 94% (G. Wang, Xu, Zhou, Wang, & Yang, 2017; Zhao et al., 2018). In comparison, the TN removal of OA-1 in P1 was fluctuating between 70 – 100%, further fine-tuning of DO and length of oxic phase was performed in P2 and P3 to improve the nitrogen removal efficiency.

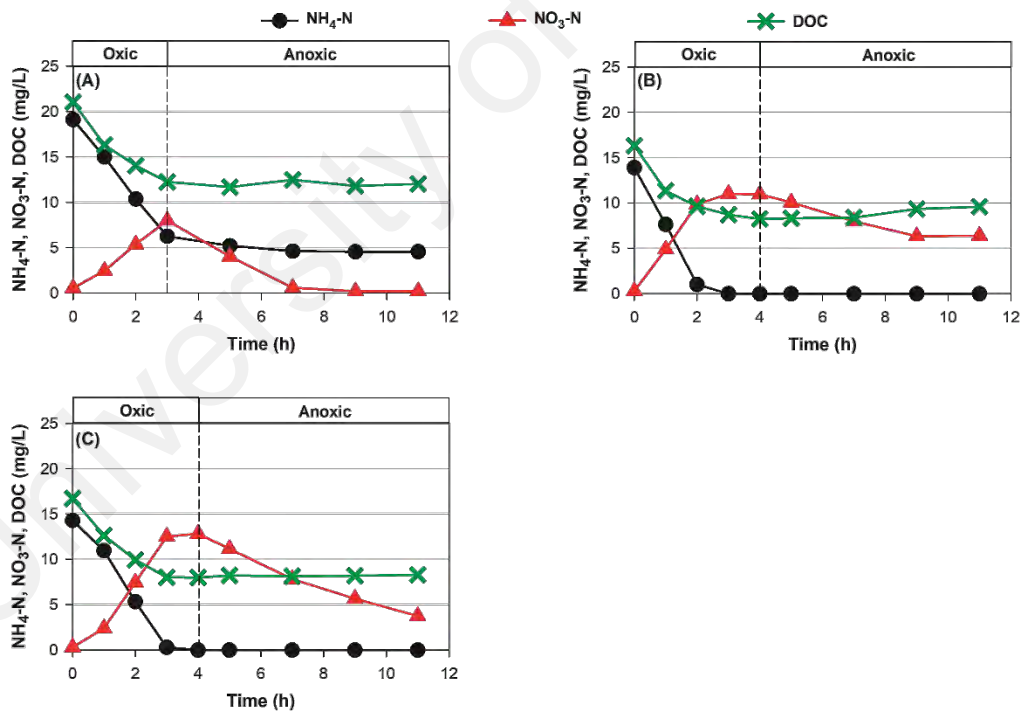


Figure 6.7: Detailed profiles of NH_4 -N, NO_3 -N and DOC in OA-1 parent SBR during (A) P1 on day 63; (B) P2 on day 73 and (C) P3 on day 87.

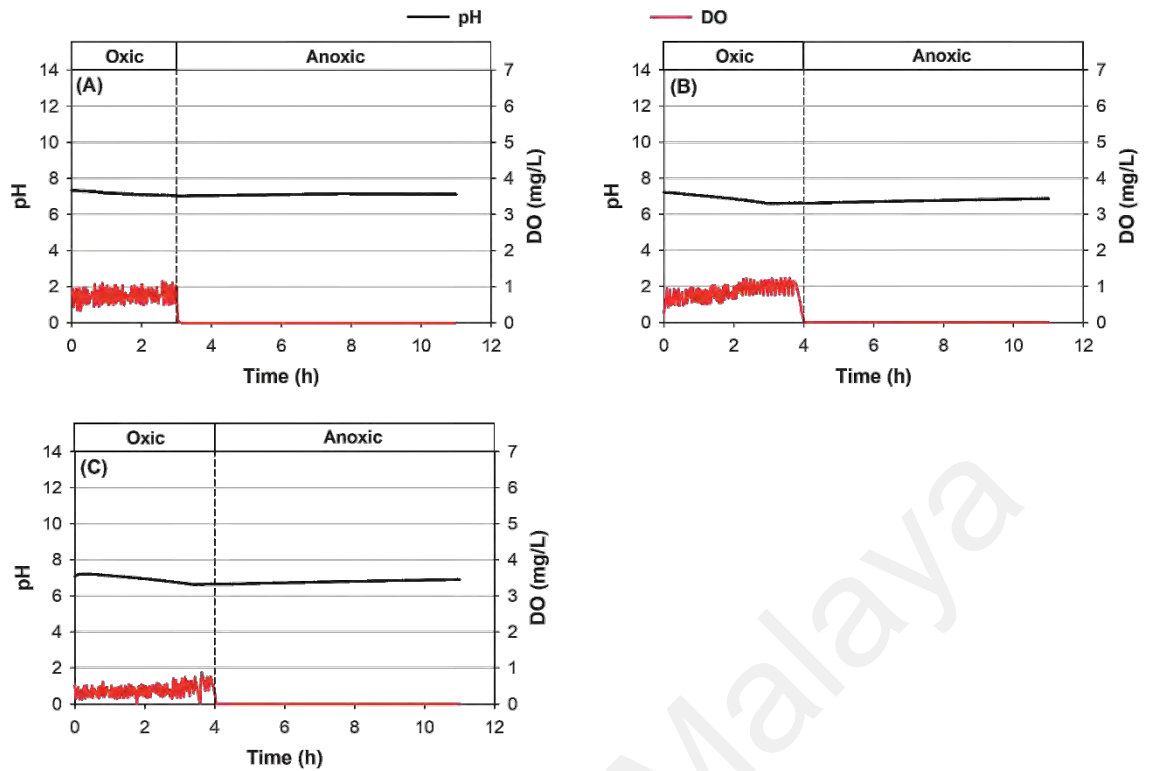


Figure 6.8: Detailed profiles of pH and DO in OA-1 parent SBR during (A) P1 on day 63; (B) P2 on day 73 and (C) P3 on day 87.

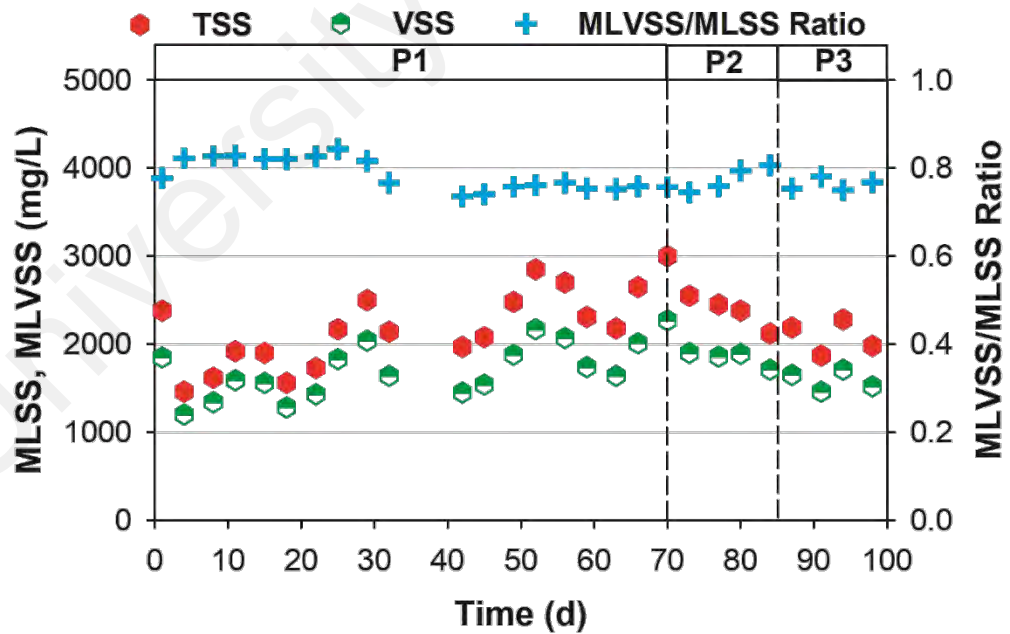


Figure 6.9: Overall MLSS and MLVSS profiles of OA-1 parent SBR operation from P1 to P3.

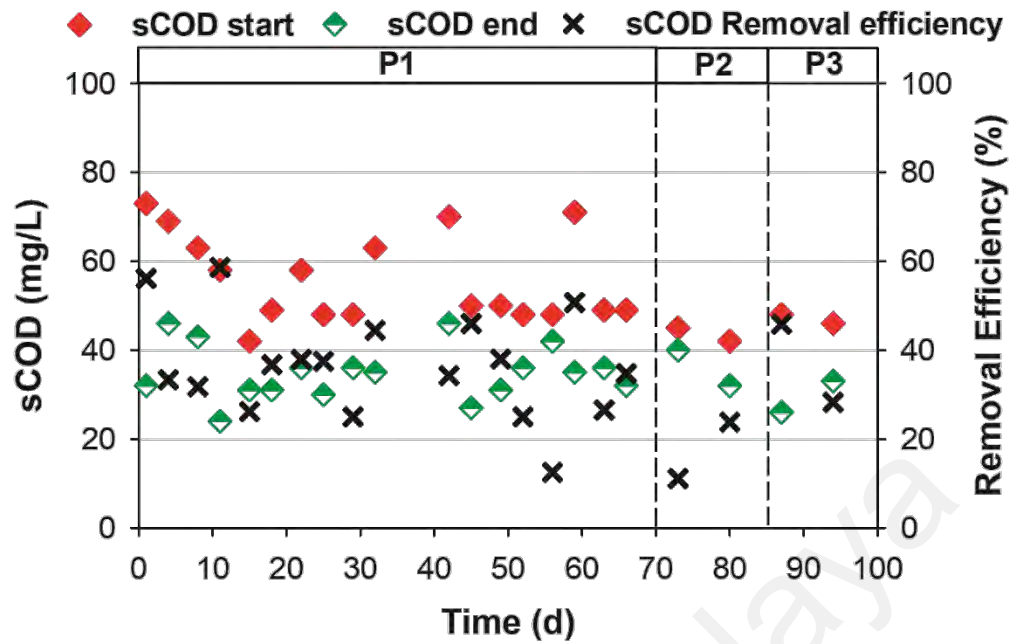


Figure 6.10: Overall sCOD profile of OA-1 parent SBR operation from P1 to P3.

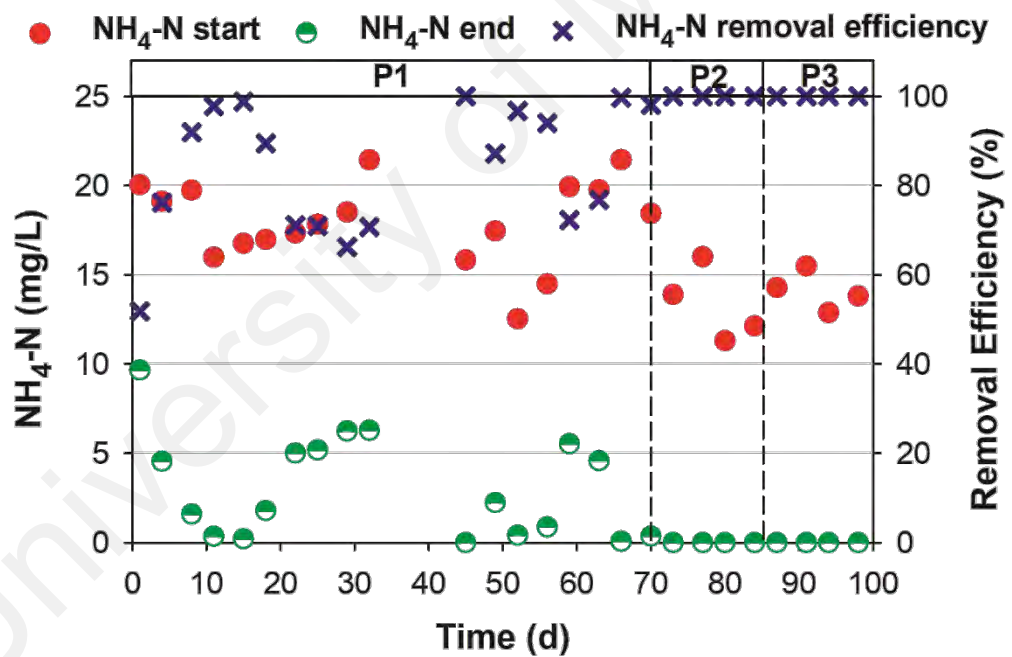


Figure 6.11: Overall NH₄-N profile of OA-1 parent SBR operation from P1 to P3.

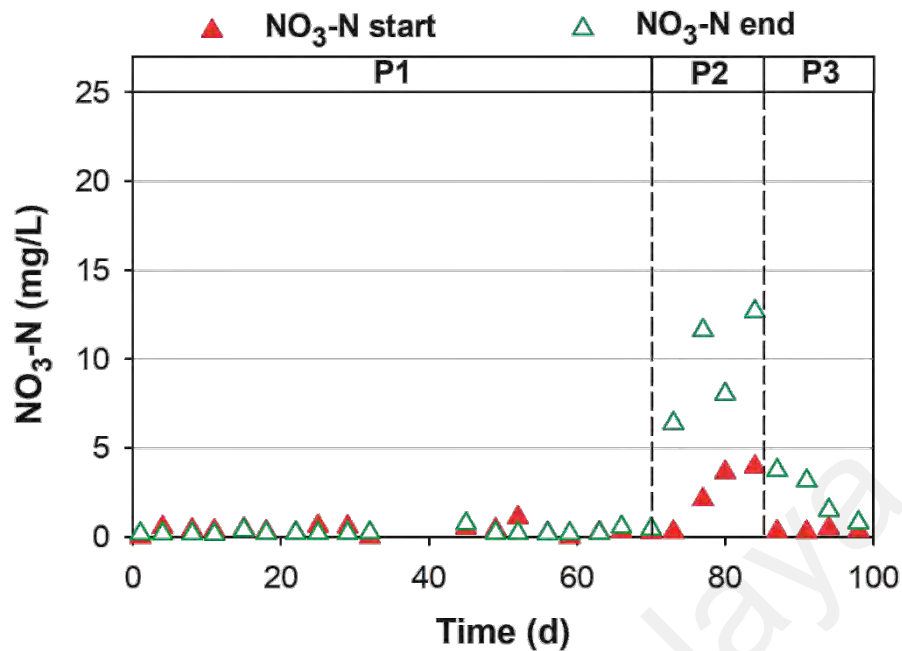


Figure 6.12: Overall NO₃-N of OA-1 parent SBR operation from P1 to P3.

To improve the NH_4^+ removal efficiency, the oxic phase was lengthened from 3 h in P1 to 4 h in P2. The MLSS and MLVSS concentrations were similar to that in P1 at 2380 ± 180 mg/L and 1840 ± 90 mg/L (Figure 6.9). All NH_4^+ in the wastewater was removed with a nitrification efficiency close to 100% in P2 (Figure 6.7B). However, the denitrification performance deteriorated, with an average effluent NO₃-N of 9.7 ± 3.0 mg/L (Figure 6.12). The effluent NO₃-N exceeded the Standard A (10 mg NO₃-N/L) of the Malaysian Environmental Quality (Sewage) Regulations 2009 (Department of Environment, 2009). The increased length of the oxic phase (4 h) in P2 may have encouraged the consumption of sbCOD by heterotrophs in the oxic phase. Thus, the denitrifying bacteria did not have sufficient biodegradable organics to carry out denitrification in the anoxic phase (Figure 6.7B). The remaining DOC in the wastewater (9.6 mg/L) represented the non-biodegradable fraction of DOC, which cannot be utilised for biological denitrification activity.

The DO concentration in the oxic phase was then reduced from 0.8 ± 0.2 mg/L in P2 to 0.4 ± 0.2 mg/L in P3 (Figure 6.8C). The reduction in DO increased the oxygen

competition between heterotrophs and nitrifiers in OA-1, which may reduce the consumption of biodegradable organics by heterotrophs in the oxic phase (Hanaki et al., 1990; Satoh et al., 2000). The MLSS and MLVSS concentrations in P3 were 2080 ± 190 mg/L and 1590 ± 115 mg/L, respectively (Figure 6.9). The nitrification performance was not affected by the DO reduction in P3. The NH_4^+ removal efficiency in P3 was close to 100% as in P2 (Figure 6.7C). The specific nitrification rate was constant in P1, P2 and P3. Based on the representative profiles in Figure 6.7, the biomass specific nitrification rate for P1, P2 and P3 were 2.7 mg N/g MLVSS·hr, 3.4 mg N/g MLVSS·hr and 2.7 mg N/g MLVSS·hr, respectively. By reducing the DO in the oxic phase, the effluent NO_3-N in P3 decreased to 2.3 ± 1.4 mg/L (Figure 6.12). The effluent NO_3-N was successfully reduced to meet the discharge limit (10 mg/L) set out in the Environmental Quality (Sewage) Regulations 2009 (Department of Environment, 2009). The enhanced denitrification activity in P3 when compared with P2 (Figure 6.7B and Figure 6.7C) implied that DO reduction decreased the sbCOD uptake by heterotrophs in the oxic phase and preserved most of the sbCOD for denitrification in the anoxic phase.

A low-DO OA process was established to treat low COD/N tropical wastewater by utilising sbCOD in the raw wastewater as a source of biodegradable organics in the post-anoxic denitrification stage. The key operating strategy of an efficient low-DO OA process was to minimise the sbCOD consumption by the heterotrophic bacteria in the oxic phase. In the following section, the operating conditions of the low-DO OA process was further optimised to ensure maximum treatment efficiency and capacity.

6.3 Effect of Sludge Retention Time and Hydraulic Retention Time on Low-Dissolved-Oxygen Oxidic-Anoxic Process

HRT and SRT were selected for the optimisation study because these critical design parameters significantly affect the treatment efficiency and capacity. The effects of

HRT and SRT on the low-DO OA process performance were studied in P4, P5 and P6 by operating two parallel reactors, OA-1 and OA-2 (Table 3.6). The representative profiles of $\text{NH}_4\text{-N}$, $\text{NO}_3\text{-N}$ and DOC in OA-1 and OA-2 for each operating phase are shown in Figure 6.13 and Figure 6.14, respectively, while the pH and DO profiles of OA-1 and OA-2 are provided in Figure 6.15 and Figure 6.16, respectively. The long-term variations of MLSS & MLVSS, sCOD, $\text{NH}_4\text{-N}$ and $\text{NO}_3\text{-N}$ of both OA SBRs (OA-1 & OA-2) are shown in Figure 6.17, Figure 6.18, Figure 6.19 and Figure 6.20, respectively. The raw data of OA-1 during optimisation operation from P4 to P6 were given in Appendix G, while the raw data of OA-2 for the same operating periods (P4 – P6) were provided in Appendix H. In P4, OA-1 and OA-2 were operated at a SRT of 20 d and 10 d, respectively (Table 3.6). OA-2 was operated at SRT of 10 d to investigate the feasibility of operating the low-DO OA process at a typical SRT for CAS system. Both OA-1 and OA-2 had the same HRT of 16 h. The MLSS in OA-1 and OA-2 were 1920 ± 240 mg/L (Figure 6.17A) and 1640 ± 270 mg/L (Figure 6.17B), respectively. The MLVSS in OA-1 and OA-2 were 1440 ± 240 mg/L (Figure 6.17A) and 1210 ± 190 mg/L (Figure 6.17B), respectively. OA-2 had a lower MLSS and MLVSS when compared with OA-1 because of the shorter SRT (10 d) than OA-1 (20 d). OA-1 achieved complete NH_4^+ removal (Figure 6.13A) but the NH_4^+ removal efficiency in OA-2 was only 60% (Figure 6.14A). The average effluent $\text{NH}_4\text{-N}$ of OA-1 and OA-2 in P4 were 0.3 ± 0.1 mg/L (Figure 6.19A) and 2.5 ± 2.0 mg/L (Figure 6.19B), respectively. Both OA-1 and OA-2 attained effluent $\text{NO}_3\text{-N}$ below 0.3 mg/L (Figure 6.13A and Figure 6.14A), which complies with the Environmental Quality (Sewage) Regulations 2009 (Department of Environment, 2009). The lower SRT in OA-2 (10 d) deteriorated the nitrification performance. Figure 6.13A and Figure 6.14A show that the specific rate of nitrification in OA-2 (1.4 mg N/g MLVSS·hr) was 1.7 times lower than that in OA-1 (2.4 mg N/g MLVSS·hr). The lower specific nitrification rate in OA-2 was caused by

the shorter aerobic SRT (3 d) when compared with the aerobic SRT in OA-1 (7 d). The aerobic SRT in OA-2 was too short for the growth of slow-growing nitrifiers, which commonly has a minimum SRT of 5 d (B. Li & Wu, 2014; X. Liu, Kim, & Nakhla, 2018). X. Liu et al. (2018) also suggested that a longer SRT is required for a stable nitrification process at low-DO condition (0.8 mg O₂/L) to account for the lower growth rate of nitrifiers at low-DO condition. Based on the results in P4, a longer SRT (20 d) was more conducive for low-DO OA reactor system to achieve complete NH_4^+ removal.

University of Malaya

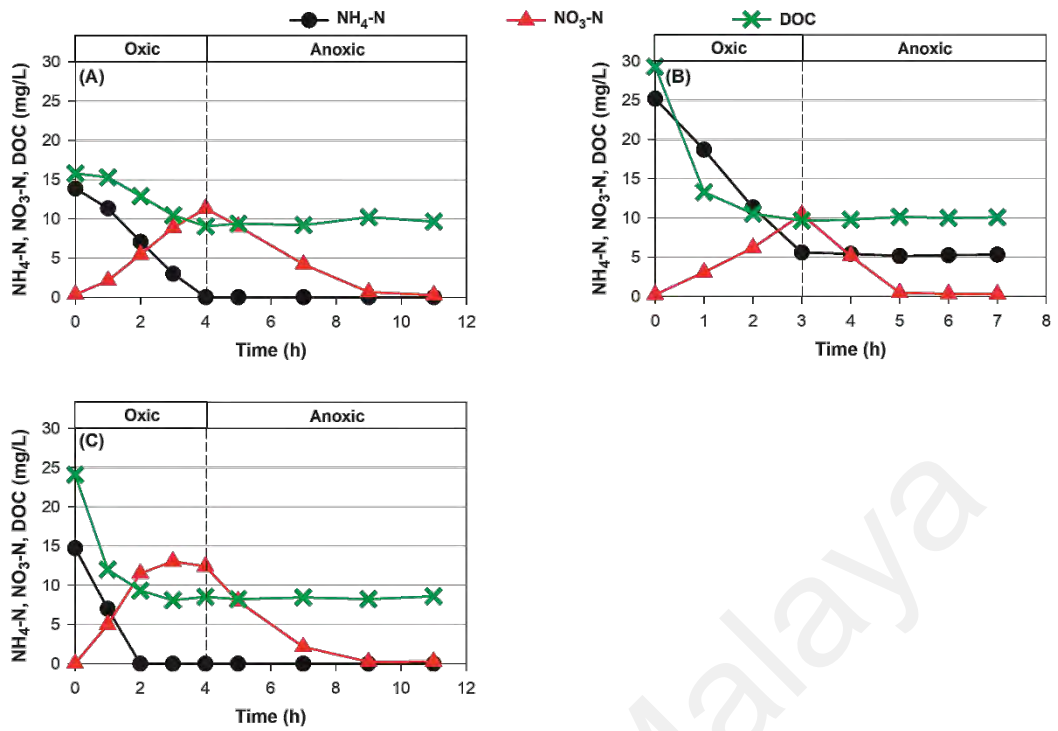


Figure 6.13: Detailed profiles of $\text{NH}_4\text{-N}$, $\text{NO}_3\text{-N}$ and DOC of OA-1 during (A) P4 on day 43; (B) P5 on day 99 and (C) P6 on day 162.

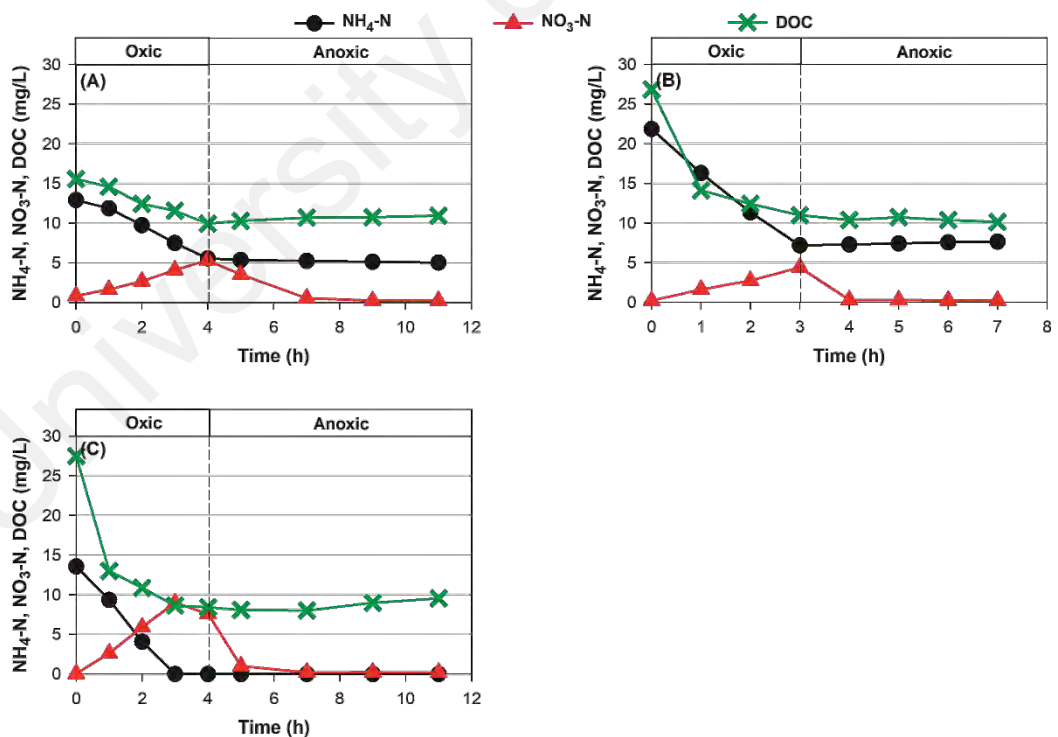


Figure 6.14: Detailed profiles of $\text{NH}_4\text{-N}$, $\text{NO}_3\text{-N}$ and DOC of OA-2 during (A) P4 on day 43; (B) P5 on day 99 and (C) P6 on day 162.

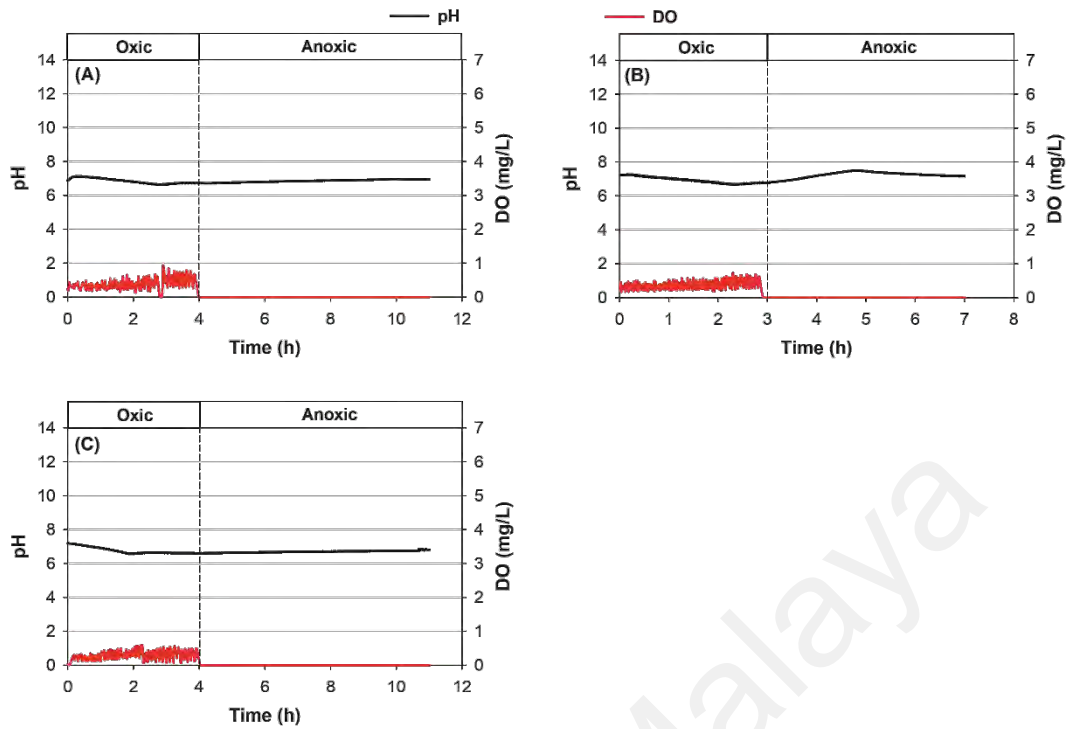


Figure 6.15: Detailed profiles of pH and DO of OA-1 during (A) P4 on day 43; (B) P5 on day 99 and (C) P6 on day 162.

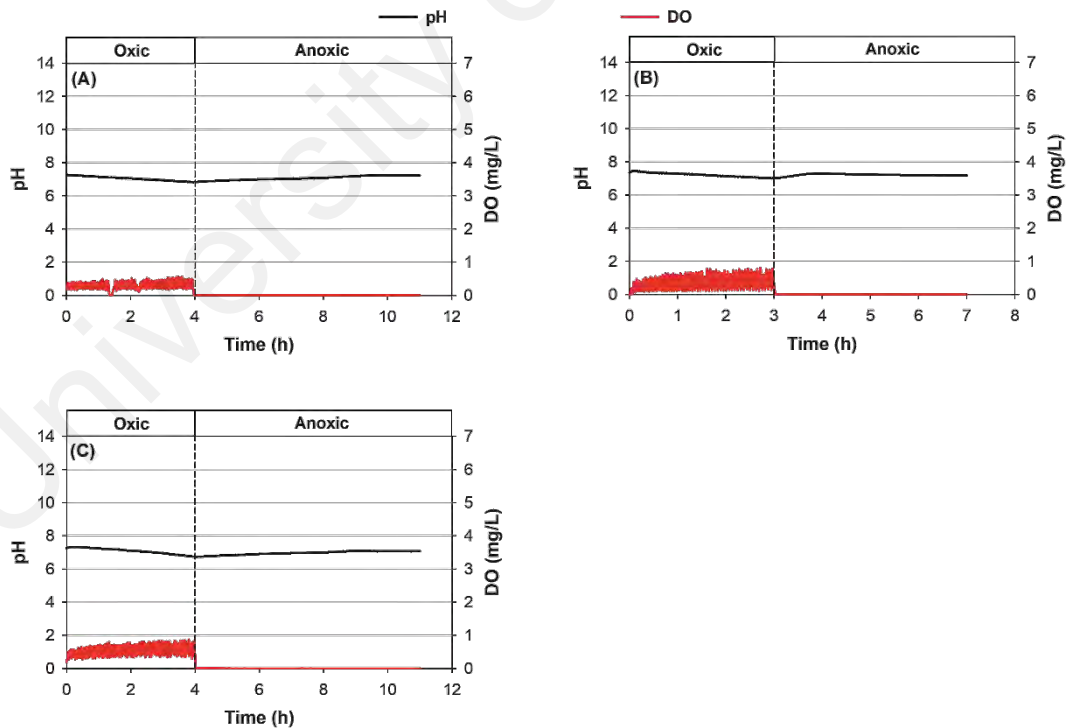


Figure 6.16: Detailed profiles of pH and DO of OA-2 during (A) P4 on day 43; (B) P5 on day 99 and (C) P6 on day 162.

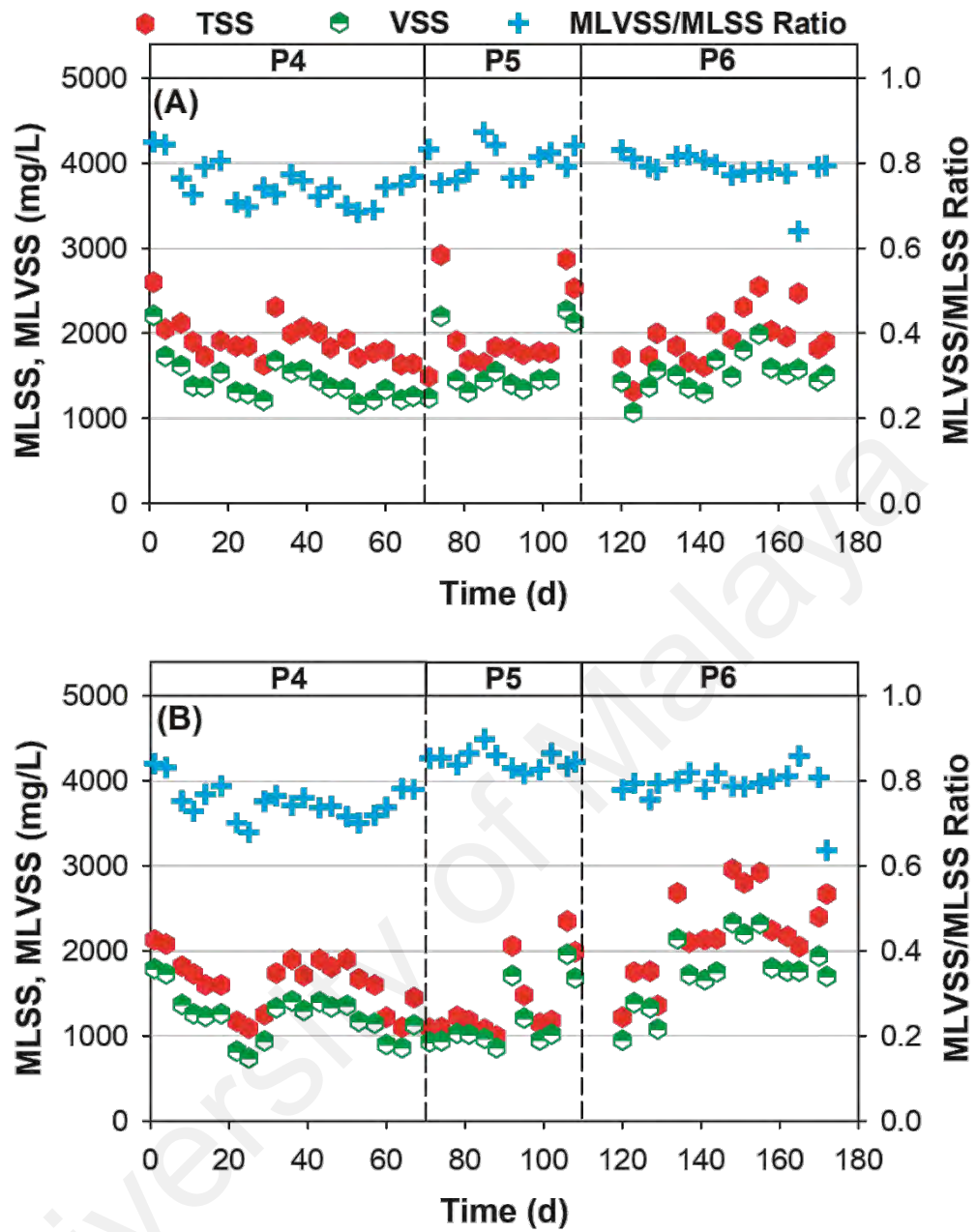


Figure 6.17: Overall MLSS and MLVSS profiles of (A) OA-1 and (B) OA-2 during optimisation operation P4 to P6.

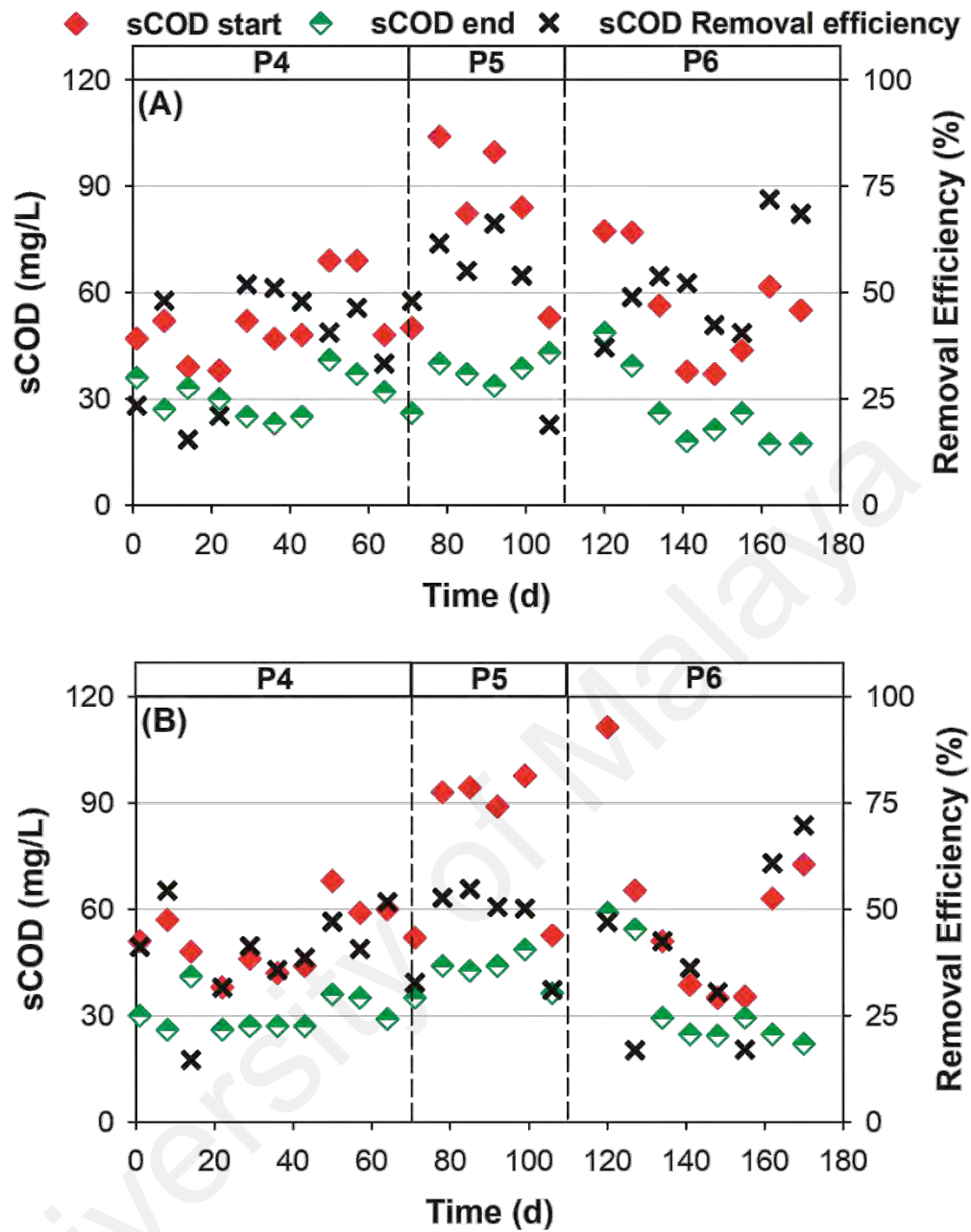


Figure 6.18: Overall sCOD profile of (A) OA-1 and (B) OA-2 during optimisation operation P4 to P6.

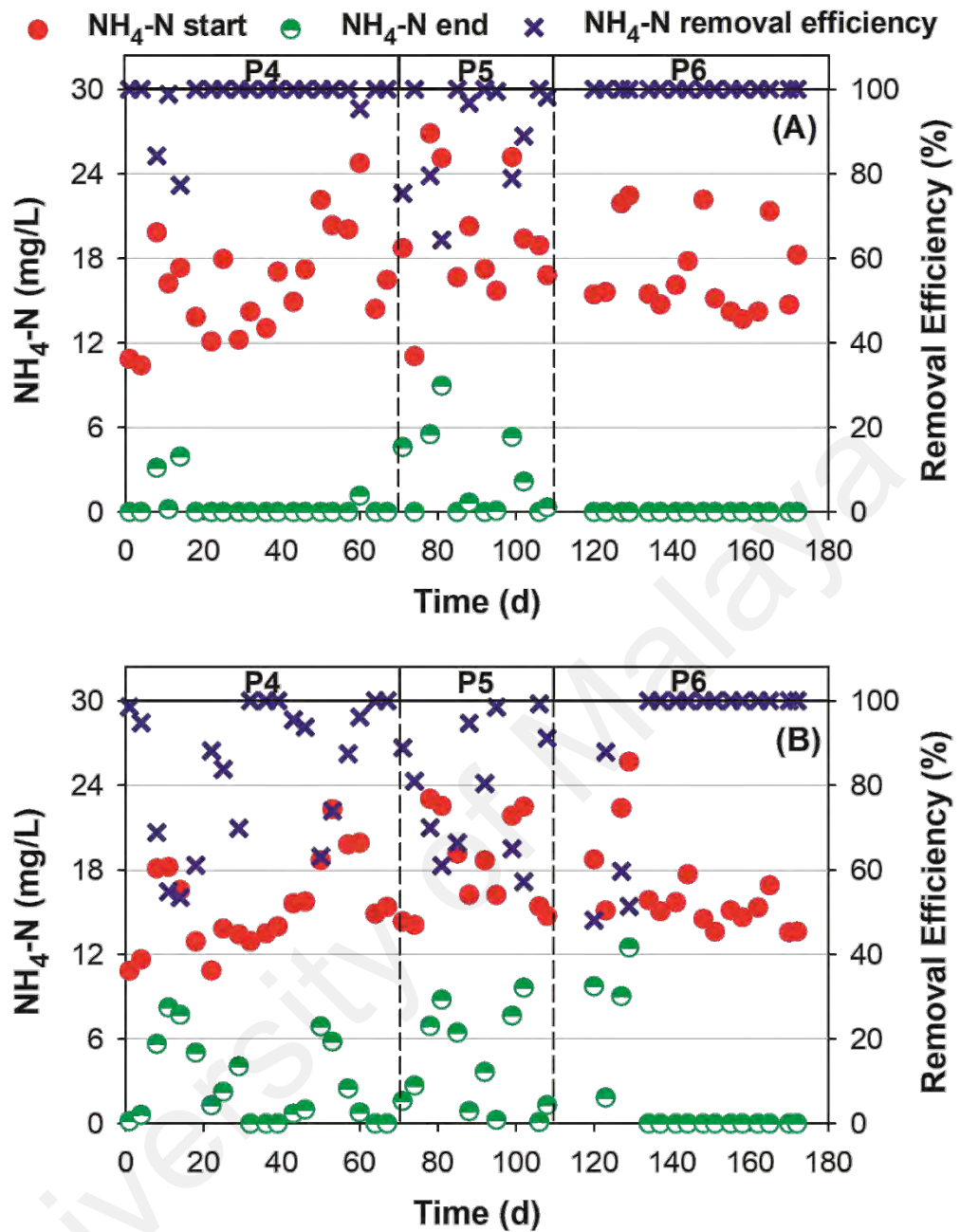


Figure 6.19: Overall $\text{NH}_4\text{-N}$ profile of (A) OA-1 and (B) OA-2 during optimisation operation P4 to P6.

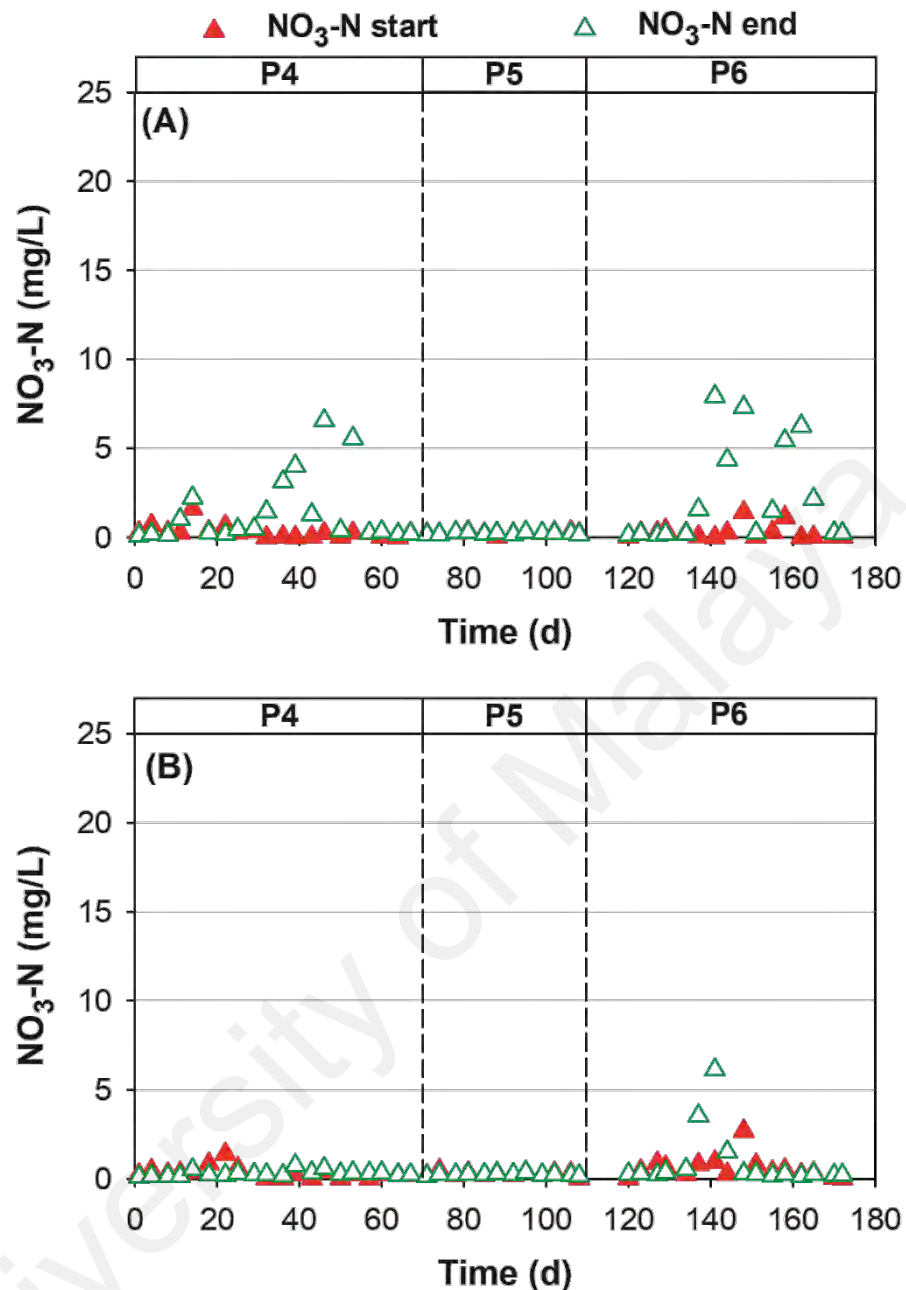


Figure 6.20: Overall NO₃-N profile of (A) OA-1 and (B) OA-2 during optimisation operation P4 to P6.

To investigate the effect of HRT on the low-DO OA process, the HRT in both OA-1 and OA-2 was reduced to 12 h in P5 (Table 3.6). The MLSS and MLVSS in OA-1 were 2000 ± 490 mg/L and 1600 ± 370 mg/L, respectively, which was constant relative to MLSS and MLVSS in OA-1 during P4 (Figure 6.17A). The MLSS (1410 ± 460 mg/L) and MLVSS (1190 ± 370 mg/L) in OA-2 were also constant when compared with the MLSS and MLVSS in OA-2 during P4 (Figure 6.17B). After the HRT was shortened in

P5, the nitrification efficiency in both OA-1 and OA-2 reduced (Figure 6.13B and Figure 6.14B). The nitrification efficiency in OA-1 and OA-2 were 79% (Figure 6.13B) and 65% (Figure 6.14B), respectively. The effluent $\text{NH}_4\text{-N}$ of OA-1 was 3.0 ± 2.3 mg/L in P5 (Figure 6.19A), which was 10 times higher than the effluent $\text{NH}_4\text{-N}$ of OA-1 in P4 (0.3 ± 0.1 mg/L; Figure 6.19A). The effluent $\text{NH}_4\text{-N}$ of OA-2 during P5 (4.2 ± 3.5 mg/L; Figure 6.19B) was also higher than that in P4 (2.5 ± 2.0 mg/L; Figure 6.19B). Both OA-1 and OA-2 achieved high NO_3^- removal efficiency. The denitrification efficiency in the anoxic phase of OA-1 and OA-2 were 97% and 95%, respectively (Figure 6.13B and Figure 6.14B). The reduced NH_4^+ removal efficiency suggested that the length of oxic phase in P5 (3 h) was too short to supply DO for complete nitrification in the low-DO OA process. At the low-DO condition (0.4 ± 0.2 mg O_2 /L; Figure 6.15B and Figure 6.16B), the specific nitrification rates were 4.2 mg N/g MLVSS·hr and 3.0 mg N/g MLVSS·hr in OA-1 and OA-2, respectively (Figure 6.13B and Figure 6.14B). The required length of oxic phase to remove all the $\text{NH}_4\text{-N}$ in the wastewater was 3.3 – 6.2 h. Thus, HRT of 16 h was needed for complete nitrification in the low-DO OA SBR.

The results in P4 and P5 suggested that a long SRT (20 d) and a HRT of 16 h were the recommended operating parameters to achieve an efficient nitrogen removal performance in the low-DO OA process. These operating conditions were verified in P6 by running both OA-1 and OA-2 at the recommended HRT and SRT (Table 3.6). The MLSS and MLVSS of OA-1 were 1940 ± 320 mg/L and 1510 ± 210 mg/L, respectively (Figure 6.17A). The MLSS and MLVSS of OA-2 showed an increase in P6 to 2460 ± 340 mg/L and 1930 ± 240 mg/L, respectively (Figure 6.17B). The longer SRT in OA-2 during P6 (20 d) when compared with P4 and P5 (10 d) increased the MLSS and MLVSS due to reduced sludge wastage. Both OA-1 and OA-2 achieved complete nitrification. $\text{NH}_4\text{-N}$ was not detected in the effluent of both OA-1 and OA-2 during P6

(Figure 6.13C and Figure 6.14C). Besides, OA-1 and OA-2 attained good denitrification performance during P6. The effluent $\text{NO}_3\text{-N}$ in OA-1 and OA-2 were below 0.3 mg/L (Figure 6.13C and Figure 6.14C). This study showed that nitrification performance was more sensitive towards the operating conditions (HRT and SRT), when compared with the consistent denitrification performance at different HRT and SRT. The slow-growing nitrifiers contributed to the poor nitrification performance at shorter SRT. The shorter HRT and SRT may wash out the nitrifiers, which grow slower than the denitrifying heterotrophic bacteria (B. Li & Wu, 2014). Reducing the HRT in P4 shortened the length of oxic phase in P4, which reduced the capability of the low-DO OA process to remove NH_4^+ in the influent. For example, a study by H. Li, Zhang, Yang, and Kamagata (2013) highlighted the reduction in HRT of a CAS system from 20 h to 15 h could reduce the nitrification efficiency from 99% to 85%.

Table 6.1 summarises the operating conditions and steady-state effluent quality from the operation of parent SBR (OA-1) and parallel SBR (OA-2). From the OA-1 parent reactor operation, the reduction of DO concentration to 0.4 ± 0.2 mg O_2/L and lengthening of oxic phase to 4 hours produced better effluent quality with low $\text{NO}_3\text{-N}$ (2.3 ± 1.4 mg/L) and $\text{NH}_4\text{-N}$ (not detected). During P4, longer SRT (20 d) in OA-1 produced a lower effluent $\text{NH}_4\text{-N}$ (0.3 ± 0.1 mg/L) than that in OA-2 (2.5 ± 1.9 mg/L), the shorter SRT (10 d) in OA-2 was not conducive for nitrifiers' growth (B. Li & Wu, 2014; X. Liu et al., 2018). The reduction of HRT to 12 h in both OA-1 and OA-2 during P5 increased the effluent $\text{NH}_4\text{-N}$ due to insufficient oxic HRT for nitrification. The operation of OA-1 and OA-2 at HRT and SRT of 16 h and 20 d improved the effluent $\text{NH}_4\text{-N}$ and $\text{NO}_3\text{-N}$ consistent with that during P3 (Table 6.1). To further relate the reactor performance with the functional microbial community of the biological nitrogen removal in treating low COD/N tropical wastewater, the next section discusses the microbial analyses of the sludge sampled from the lab-scale AO and OA SBRs.

Table 6.1: Comparison of operating conditions and effluent quality at steady-state during (A) OA-1 parent reactor operation, (B) OA-1 optimisation operation and (C) OA-2 optimisation operation

(A) OA-1 Parent Reactor Operation			
Operating Period	P1	P2	P3
Duration	Day 1 – 70	Day 71 – 85	Day 86 – 100
Oxic:Anoxic Ratio	3:8	4:7	4:7
DO Concentration in Oxic Phase (mg/L)	0.8 ± 0.2	0.8 ± 0.2	0.4 ± 0.2
Effluent NH₄-N (mg/L)	2.0 ± 1.8	n.d.	n.d.
Effluent NO₃-N (mg/L)	0.4 ± 0.2	9.7 ± 3.0	2.3 ± 1.4
(B) OA-1 Optimisation Operation			
Operating Period	P4	P5	P6
Duration	Day 1 – 70	Day 71 – 110	Day 111 – 180
HRT (h)	16	12	16
SRT (d)	20	20	20
Effluent NH₄-N (mg/L)	0.3 ± 0.1	3.0 ± 2.3	n.d.
Effluent NO₃-N (mg/L)	1.9 ± 1.4	0.2 ± 0.1	2.9 ± 2.4
(C) OA-2 Optimisation Operation			
Operating Period	P4	P5	P6
Duration	Day 1 – 70	Day 71 – 110	Day 111 – 180
HRT (h)	16	12	16
SRT (d)	10	10	10
Effluent NH₄-N (mg/L)	2.5 ± 1.9	4.2 ± 3.5	n.d.
Effluent NO₃-N (mg/L)	0.3 ± 0.2	0.2 ± 0.1	1.6 ± 0.9

6.4 Changes in Populations of the Sludge Microbial Community

The molecular analyses described in Section 3.8 were applied to the sludge and DNA samples from AO and OA SBRs, which elucidated the effects of the changes in operating conditions on the microbial community.

6.4.1 Microbial Community in the Anoxic-Oxic Sequencing Batch Reactor

The changes in the sludge microbial community in response to applying low-DO nitrification and utilising sbCOD to enhance denitrification performance in the AO SBR were first discussed in this section. Molecular methods, including qPCR, 16S rRNA amplicon sequencing (Illumina MiSeq workflow) and FISH were used to investigate the changes in functional microbial community in the AO SBR.

6.4.1.1 Nitrifying and Denitrifying Bacteria Population Using Quantitative Polymerase Chain Reaction Analysis

The abundances of betaproteobacterial AOB and *Nitrospira sp.* relative to the total bacteria population were quantified by qPCR using the primer pairs amoA1F/2R and NSR1113F/1264R (Table 3.7). The average relative abundances for AOB and *Nitrospira sp.* were $0.03 \pm 0.02\%$ and $2.7 \pm 1.2 \%$, respectively (Figure 6.21A). The population of AOB and *Nitrospira sp.* in the SBR were similar to that of the seed sludge. This could be explained by the similar operating conditions (AO configuration, SRT and HRT) between the lab-scale AO SBR and WWTP 1. The population of *Nitrospira sp.* was 2 orders of magnitude higher than that of AOB (Figure 6.21A). Large populations of *Nitrospira sp.* relative to that of AOB have been reported in the tropical region, where the wastewater can be at 30°C (Q. Yang et al., 2016). Q. Yang et al. (2016) found that the *Nitrospira*-related NOB population outnumbered the AOB population in their activated sludge samples, with NOB/AOB abundance ratio of approximately 5. The large *Nitrospira* population in the tropical sludge is different from

the conventional understanding of the activated sludge nitrifying community in the temperate climate region. M. K. Winkler, Bassin, Kleerebezem, Sorokin, and van Loosdrecht (2012) proposed that the theoretical NOB/AOB abundance ratio should be 0.5. Activated sludge microbial community assessment studies by Saunders, Albertsen, Vollertsen, and Nielsen (2016) and Keene et al. (2017) in the temperate climate region (20°C – 25°C) also reported *Nitrospira*-related NOB population approximately half of that for AOB. The warm wastewater in this study (30°C) may have encouraged the growth of *Nitrospira* population as the optimal temperature range for its growth is between 28 – 32°C (Mehrani et al., 2020; Zhou, Li, Xu, & Yu, 2018). Apart from the wastewater temperature, the low-DO condition in the reactor (0.9 ± 0.1 mg/L) may have contributed to the unusually high proportional abundance of *Nitrospira sp.* in the sludge. Long-term WWTPs population dynamics in Cao et al. (2018) suggested that a DO reduction from 1.7 mg O₂/L to 1.0 mg O₂/L caused a significant increase in the *Nitrospira* population.

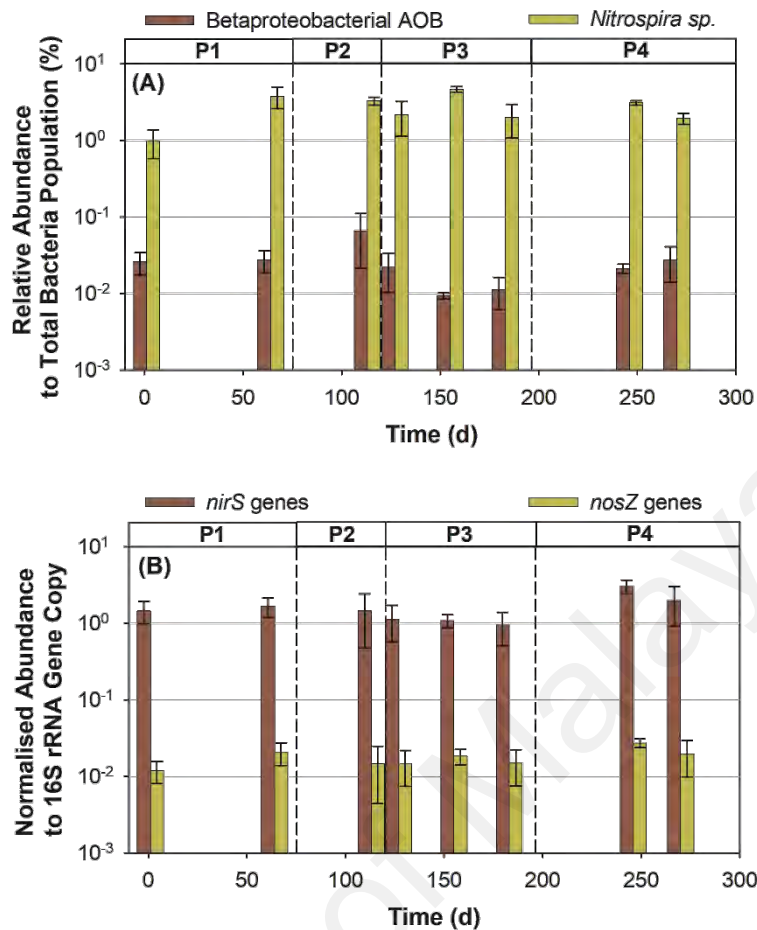


Figure 6.21: (A) Relative abundance of betaproteobacterial AOB and *Nitrospira sp.* to the total bacteria population and (B) normalised abundance of *nirS* and *nosZ* to the bacterial 16S rRNA gene copy number throughout the four operating phases.

The denitrification potential of the sludge was consistent throughout the reactor operation. The qPCR data showed that the normalised abundance of *nirS* and *nosZ* in the SBR remained constant (Figure 6.21B). The relative abundance of *nirS* were consistently 2 orders of magnitude higher than *nosZ*. Gabarro et al. (2013) found that *nirS* was the most abundant denitrifying genes for biological nitrogen removal, which may be up to three *nirS* copies for every ten 16S rRNA copies. On the other hand, the *nosZ* to 16S rRNA ratio in the sludge was about 3:100, which was the typical range reported for environmental samples (Gabarro et al., 2013).

The qPCR analysis on AO SBR revealed that the nitrifying community in the SBR was dominated by *Nitrospira sp.*. The *Nitrospira* population was much larger than expected as theory suggested that NOB population should be half of that for AOB (M. K. Winkler et al., 2012). Moreover, the denitrifying gene copy number was consistent through the reactor operation. The following section discusses the *Nitrospira* community in AO SBR more in-depth.

6.4.1.2 *Nitrospira* Community Analysis by 16S Ribosomal Ribonucleic Acid and β -Subunit Nitrite Oxidoreductase Gene Amplicon Sequencing

The disproportionately high abundance of *Nitrospira sp.* in the sludge prompted a 16S rRNA amplicon sequencing and bioinformatics analyses to validate the population size of *Nitrospira sp.* in the sludge. The combined number of sequence reads from the two samples on day 1 and day 270 was 133469, which were distributed across 9015 OTUs. The OTUs were further classified into 566 genera. The top 25 most abundant genera on day 1 and day 270 are plotted in Figure 6.22. The Genus *Nitrospira* was the second most abundant genera in both samples, which made up 4.8% and 5.7% of the total reads on day 1 and day 270, respectively. The only two taxa related to nitrifying organisms were *Nitrospira* and uncultured *Nitrosomonadaceae* (Figure 6.22). The read abundance of *Nitrospira* was 10 times higher than that for uncultured *Nitrosomonadaceae*. Furthermore, the FISH images of low-DO AOA sludge on day 270 showed that the positive signals for AOB (Figure 6.23A and Figure 6.23B) are markedly less than that for *Nitrospira sp.* (Figure 6.23C and Figure 6.23D). The outcome of the molecular methods used in the current study (qPCR, 16S rRNA amplicon sequencing and FISH) confirmed that the *Nitrospira* population was larger than that for AOB.

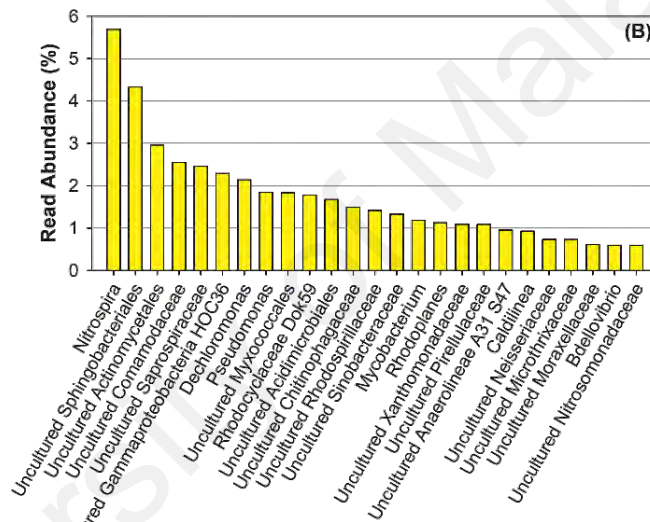
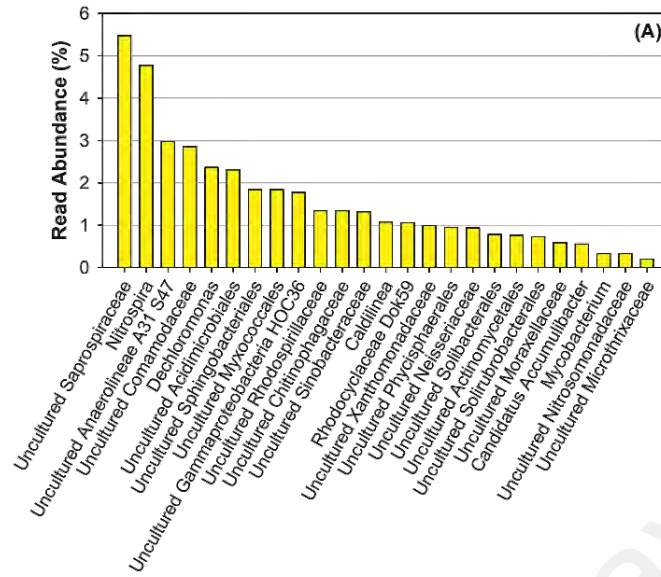


Figure 6.22: Vertical bar plot of the 25 most abundant genera in (A) the seed sludge (day 1) and (B) the low-DO AOA sludge (day 270) sorted based on their read abundance.

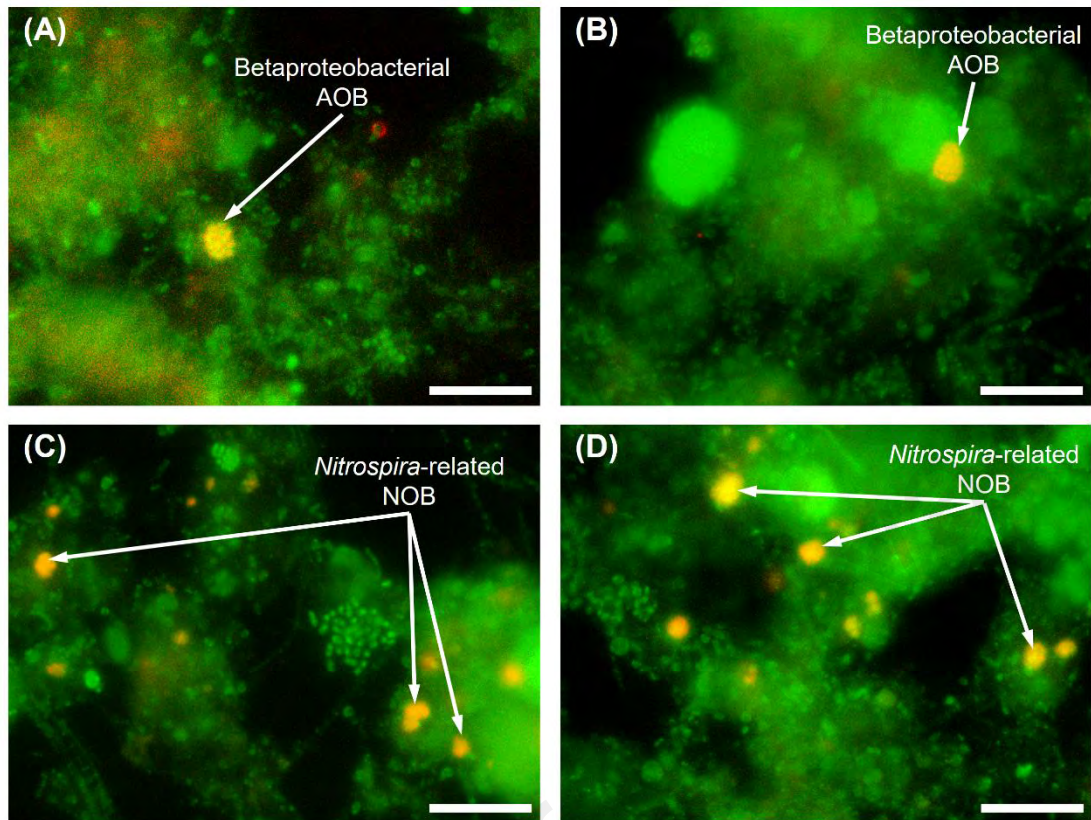


Figure 6.23: FISH images of low-DO AOA sludge on day 270 after hybridisation with FISH probes targeting bacteria (EUB338-MIX, green) and group-specific probes: (A) & (B) betaproteobacterial AOB (Nso1225, yellow) and (C) & (D) *Nitrospira*-related NOB (Ntspa662, yellow). The scale bar represents 10 μ m.

16S rRNA-based phylogenetic trees (Figure 6.24) were constructed to investigate the diversity of the *Nitrospira* community. The phylogenetic tree was pruned to show only the OTUs with percentage read abundance above 0.1% in either day 1 or day 270 sample. The phylogenetic tree constructed from the 16S rRNA amplicons (Figure 6.24) was congruent to that constructed from the *nxrB* amplicons (Figure 6.25), which suggests that most of the *Nitrospira*-related OTUs were clustered into two groups, namely Group A and Group B. OTUs in Group A are related to *Nitrospira defluvii* with an ANI of $94 \pm 3\%$, while those in Group B are more closely affiliated with comammox (*Ca. Nitrospira nitrosa* and *Ca. Nitrospira nitrificans*) with an ANI of $96 \pm 2\%$. A similar *Nitrospira* community was detected in the low-DO nitrification SBR (< 0.5 mg

O₂/L). These results suggested that low-DO condition favoured the proliferation of both *Nitrospira defluvii* and comammox.

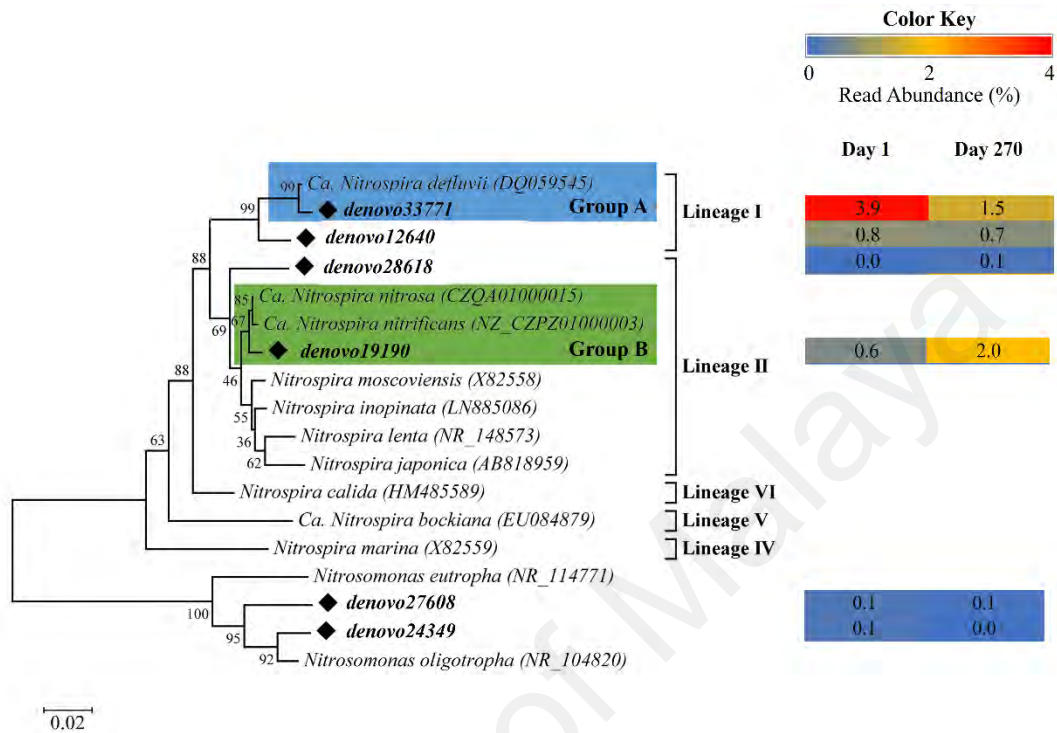


Figure 6.24: Neighbour-joining tree based on the *Nitrospira* 16S rRNA sequences showing the phylogenetic relationships of the OTUs with the reference sequences in GenBank database, rooting with *Nitrosomonas*-related AOB. Bootstrap values are shown in percentages of 1000 replicates. The heat map depicts the percentage read abundance of the OTUs on day 1 and day 270 of the AO SBR operation.

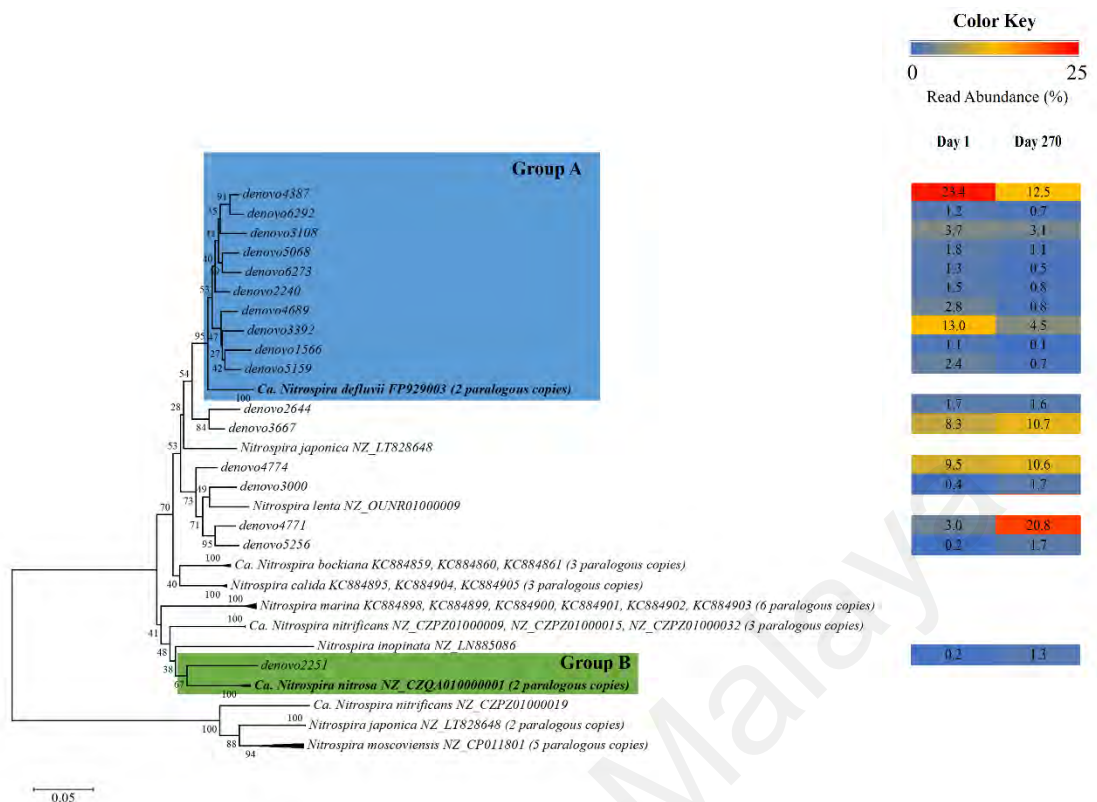


Figure 6.25: Neighbour-joining tree based on the *nxB* sequences showing the phylogenetic relationships of the OTUs with reference sequences in the GenBank database. Bootstrap values are shown in percentages of 1000 replicates. The heat map depicts the read abundance of the OTUs on day 1 and day 270 of the SBR operation.

The heat maps in Figure 6.24 and Figure 6.25 depict the percentage read abundance of *Nitrospira*-related OTUs in the seed sludge (day 1) and the low-DO AOA sludge (day 270). Overall, the read abundance of Group B affiliated with comammox *Nitrospira* seemed to increase in the low-DO AOA sludge (Day 270; 2.0%) when compared with the seed sludge (Day 1; 0.6%). Conversely, the read abundance of Group A related to *Nitrospira defluvii* reduced to 1.5% on Day 270 when compared with 3.9% on Day 1. The OTUs in Group B constituted half of the total *Nitrospira* OTUs in the low-DO AOA sludge. The characteristics of low COD/N tropical wastewater and long SRT operation of the low-DO AOA process may have caused the increased Group B

OTUs when compared with the seed sludge. Kits et al. (2017) reported that comammox *Nitrospira* activity peaks at 37°C and thrives in an oligotrophic environment. In view of the warm wastewater temperature (30°C) and the low-strength wastewater characteristics ($\text{NH}_4\text{-N} = 22 \pm 3 \text{ mg/L}$), comammox *Nitrospira* may play a significant nitrifying role in the tropical wastewater treatment systems. Cotto et al. (2020) also suggested that long SRT operation above 10 d may select comammox, which allowed Group B related to comammox *Nitrospira* to outcompete Group A affiliated with *Nitrospira defluvii* for a stable nitrification performance in the low-DO AOA process. Moreover, comammox *Nitrospira* were often detected in low-DO condition (Daims et al., 2015). Palomo et al. (2018) suggested that comammox *Nitrospira* has a high affinity for oxygen because its genome harbours a 2/2 haemoglobin type II (TrHb2) to scavenge oxygen. Thus, the low-DO condition ($0.9 \pm 0.1 \text{ mg O}_2\text{/L}$) in the SBR could also be a selection factor for comammox *Nitrospira*.

The phylogenetic tree based on *nxB* also revealed that OTUs closely related to *Nitrospira lenta* had a higher read abundance of 1.7 – 20.8% in the low-DO AOA sludge when compared to 0.2 – 9.5% in the seed sludge (Figure 6.25). Based on a physiology and genomic analysis of *Nitrospira lenta*, *Nitrospira lenta* had a high NO_2^- affinity and survived better than *Nitrospira defluvii* (Lineage I) under extremely low $\text{NO}_2\text{-N}$ concentrations less than 0.1 mg/L (Maixner et al., 2006; Sakoula, Nowka, Spieck, Daims, & Lucker, 2018). The low $\text{NO}_2\text{-N}$ in the AO SBR may help *Nitrospira lenta* to increase in abundance for NO_2^- oxidation, which may also lead to a reduced read abundance of *Nitrospira defluvii* consistent with the NO_2^- oxidation physiology study performed by Maixner et al. (2006).

A phylogenetic analysis of the *Nitrospira* community by 16S rRNA and *nxB* amplicon sequencing revealed two groups of *Nitrospira* that were also present in the

low-DO nitrification SBR (Section 5.3). The first group is a NOB that thrives in low-DO condition (*Nitrospira defluvii*), while the second group was closely related to a comammox species (*Ca. Nitrospira nitrosa*). Thus, *Nitrospira* could be an important nitrifier contributing to low-DO nitrification in tropical biological nitrogen removal.

6.4.2 Microbial Community in OA-1 and OA-2 Sequencing Batch Reactors

To understand the population changes in the nitrifying community during the establishment and optimisation of low-DO OA process, the sludge sampled from OA-1 and OA-2 were subjected to 16S rRNA amplicon sequencing and qPCR analyses and discussed in the following sections.

6.4.2.1 Overview of Microbial Community by 16S Ribosomal Ribonucleic Acid Amplicon Sequencing

The 16S rRNA gene fragments of three DNA samples were extracted and sequenced from the seed sludge (SRT = 20 d, HRT = 24 h), sludge from OA-1 (SRT = 20 d, HRT = 16 h) and OA-2 (SRT = 10 d, HRT = 16 h) during P4, respectively (Figure 6.26). The top 25 most abundant taxa in the three samples were compared to investigate the microbial community shift in the OA reactors operating with different SRTs. The number of reads from the 16S rRNA amplicon sequencing was 297508, the sequences from the three samples were distributed across 1355 taxa. The five most abundant taxa and their respective read abundance in the seed sludge were Family *Saprospiraceae* (12%), Family *Chitinophagaceae* (4.8%), Genus *Nitrospira* (4.5%), Family *Sinobacteraceae* (4.2%) and Order *Sphingobacteriales* (4.2%). Saunders et al. (2016) also detected the similar core taxa in 13 Danish WWTPs. The seed sludge shared the similar microbial community structure with the sludge from OA-1 and OA-2. Similar abundant taxa was obtained for seed sludge, OA-1 sludge and OA-2 sludge (Figure 6.26).

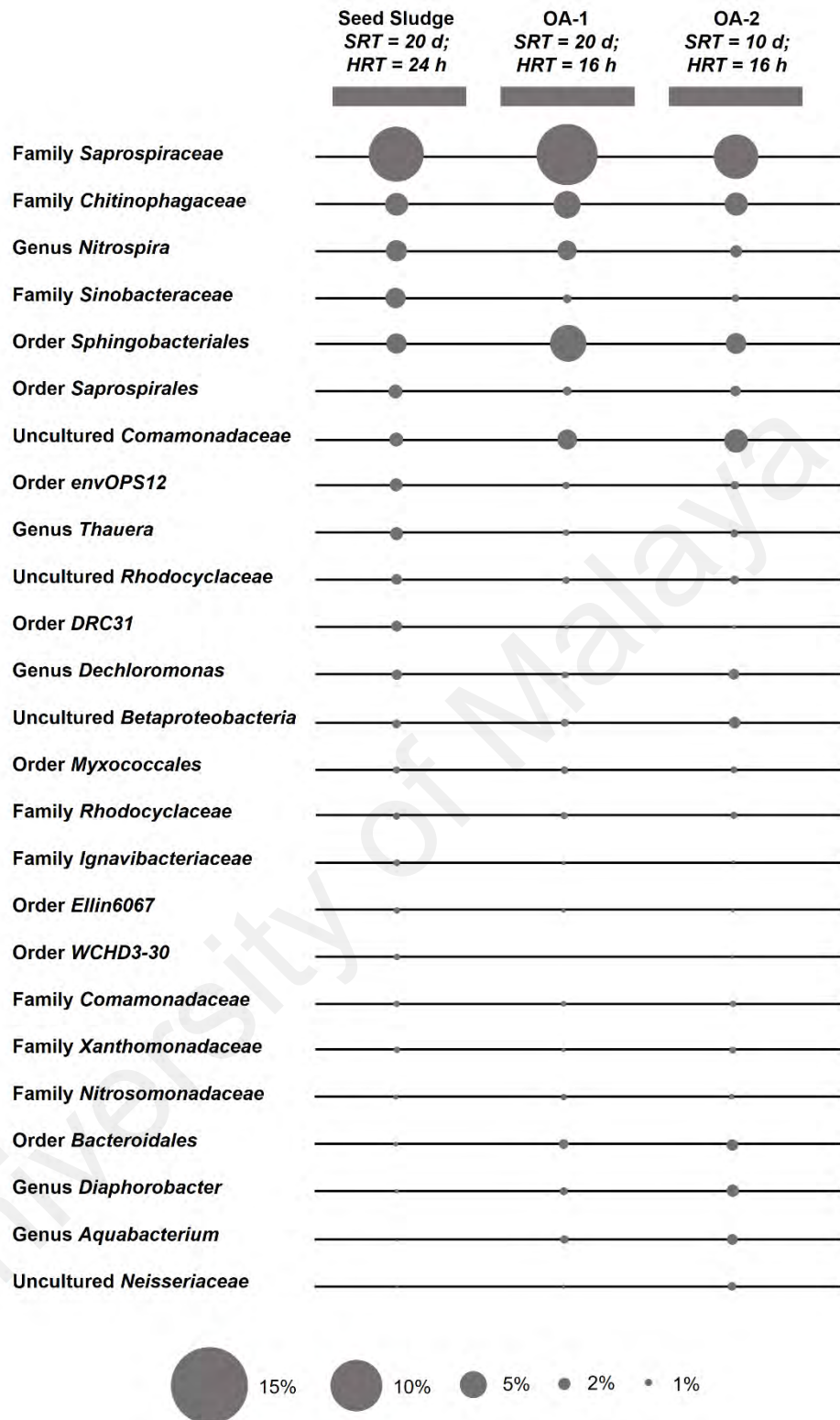


Figure 6.26: Percentage read abundance for the top 25 most abundant taxa in the seed sludge (SRT = 20 d, HRT = 24 h), OA-1 sludge (SRT = 20 d, HRT = 16 h) and OA-2 sludge (SRT = 10 d, HRT = 16 h) samples.

Several taxa among the top 25 most abundant taxa in the OA SBRs (Figure 6.16) were related to hydrolysis of PSS in the wastewater. These taxa are summarised in Table 6.2. The taxa related to hydrolysis were more abundant in the seed sludge and OA-1 (SRT = 20 d) when compared with OA-2 (SRT = 10 d) as shown in Table 6.2. The higher population of hydrolytic bacteria at longer SRT operation was presumably caused by the proliferation of slow-growing hydrolytic bacteria under longer SRT systems (S. Li et al., 2019). For instance, Family *Saprospiraceae*, Order *Sphingobacteriales* and Order *Saprospirales* were involved in protein and complex carbon molecule hydrolysis (McIlroy & Nielsen, 2014; Xia, Kong, Thomsen, & Halkjaer Nielsen, 2008), their read abundances in seed sludge and OA-1 (SRT = 20 d) were 2 to 3 times higher than those in OA-2 (SRT = 10 d). Family *Chitinophagaceae* was also 1.2 to 1.4 times higher in the seed sludge and OA-1 when compared with OA-2, the Family *Chitinophagaceae* was reported to be capable of degrading chitin (Rosenberg, 2014). S. Li et al. (2019) showed that higher abundance of hydrolytic bacteria under longer SRT systems (40 d) when compared with shorter SRT operation (< 20 d) significantly increased the hydrolysis rate constant (k_H) by 4 times. Thus, the higher read abundance of taxa related to hydrolytic bacteria under longer SRT operation (20 d) agreed with the higher k_H (0.24 1/h) when compared with the temperature-corrected literature values (0.10 – 0.15 1/h) as discussed in Section 4.3.

Table 6.2: Percentage read abundance of taxa related to hydrolysis of PSS in OA SBRs

Taxa	Read Abundance (%)		
	Seed Sludge SRT = 20 d HRT = 24 h	OA-1 SRT = 20 d HRT = 16 h	OA-2 SRT = 10 d HRT = 16 h
Family <i>Saprospiraceae</i>	12.1	11.8	4.1
Family <i>Chitinophagaceae</i>	4.8	5.7	4.0
Order <i>Sphingobacteriales</i>	4.2	5.1	2.0
Order <i>Saprospirales</i>	2.8	3.7	2.3

Two taxa related to nitrifying bacteria were detected among the top 25 most abundant taxa, which were Genus *Nitrospira* and Family *Nitrosomonadaceae*. The Genus *Nitrospira* dominated the nitrifying community in both OA-1 (4.0%) and OA-2 (2.4%), which was a similar observation when compared with the high *Nitrospira* population in the low-DO AOA sludge (Chapter 6). The read abundance of the Family *Nitrosomonadaceae* in both OA-1 and OA-2 were 1.1% and 1.0%, respectively. Several studies identified *Nitrospira* as the dominant nitrifying bacteria for biological nitrogen removal (Cao et al., 2018; L. Wu et al., 2019). Cao et al. (2018) found that operating a low-DO nitrification process (1.0 mg O₂/L) significantly increased the *Nitrospira* population by 200 times when compared with a high-DO process (1.7 mg O₂/L). L. Wu et al. (2019) identified *Nitrospira* as the core taxon related to nitrification from about 1200 activated sludge samples collected from six continents. The high abundance of *Nitrospira* globally indicated that *Nitrospira* may play an important role in NO₂⁻ oxidation and complete ammonia oxidation (Daims, Lucker, & Wagner, 2016; van Kessel et al., 2015; L. Wu et al., 2019).

The large population of *Nitrospira* warranted a more detailed analysis on its community to further infer their role in the low-DO OA process. The next section uses 16S rRNA-based method to investigate changes in *Nitrospira* community in the low-DO OA SBRs.

6.4.2.2 16S Ribosomal Ribonucleic Acid-Based Analysis of *Nitrospira* Community

A 16S rRNA gene-based phylogenetic tree was constructed to examine the community structure of *Nitrospira* in the low-DO OA process (Figure 6.27). The phylogenetic tree is pruned to show only the OTUs with percentage read abundance above 0.1% in any one sample. Most of the *Nitrospira*-related OTUs were classified into two groups, namely Group A and Group B (Figure 6.27). OTUs belonged to Group A were closely related to *Nitrospira defluvii*, which is a NOB thriving in low-DO condition (Lucker et al., 2010). The OTUs in Group B were more closely affiliated with comammox (Daims et al., 2015; van Kessel et al., 2015). A similar *Nitrospira* community was found in the low-DO nitrification and low-DO AOA SBRs operating at the similar SRT (20 d). The *Nitrospira*-related OTUs in Group A and Group B coexisted and had a similar percentage read abundances with each other in the seed sludge (Figure 6.27). The *Nitrospira* OTUs in Group A showed a 2.0 – 2.5 times increase in read abundance between day 84 and day 98 during OA-1 parent SBR operation when the DO was reduced from 0.8 ± 0.2 mg O₂/L to 0.4 ± 0.2 mg O₂/L (Figure 7.2B and Figure 7.2C). The enrichment of Group A *Nitrospira* indicated that *Nitrospira defluvii* may play a significant role in achieving stable low-DO nitrification process in the OA reactor system. Oppositely, comammox decreased in read abundance during OA-1 parent SBR operation and remained undetected from P1 to P6 (Figure 6.27). A probable reason for the lower comammox abundance in the low-DO OA SBRs than that in low-DO AOA SBR is that the OA SBRs were operated with a shorter HRT (12 – 16 h) when compared with a HRT of 24 h in the low-DO AOA SBR. The shorter HRT in the OA reactor increased the NH₄⁺ loading. The higher substrate loading inhibited the growth of comammox, which preferably proliferate in oligotrophic environment (Kits et al., 2017).

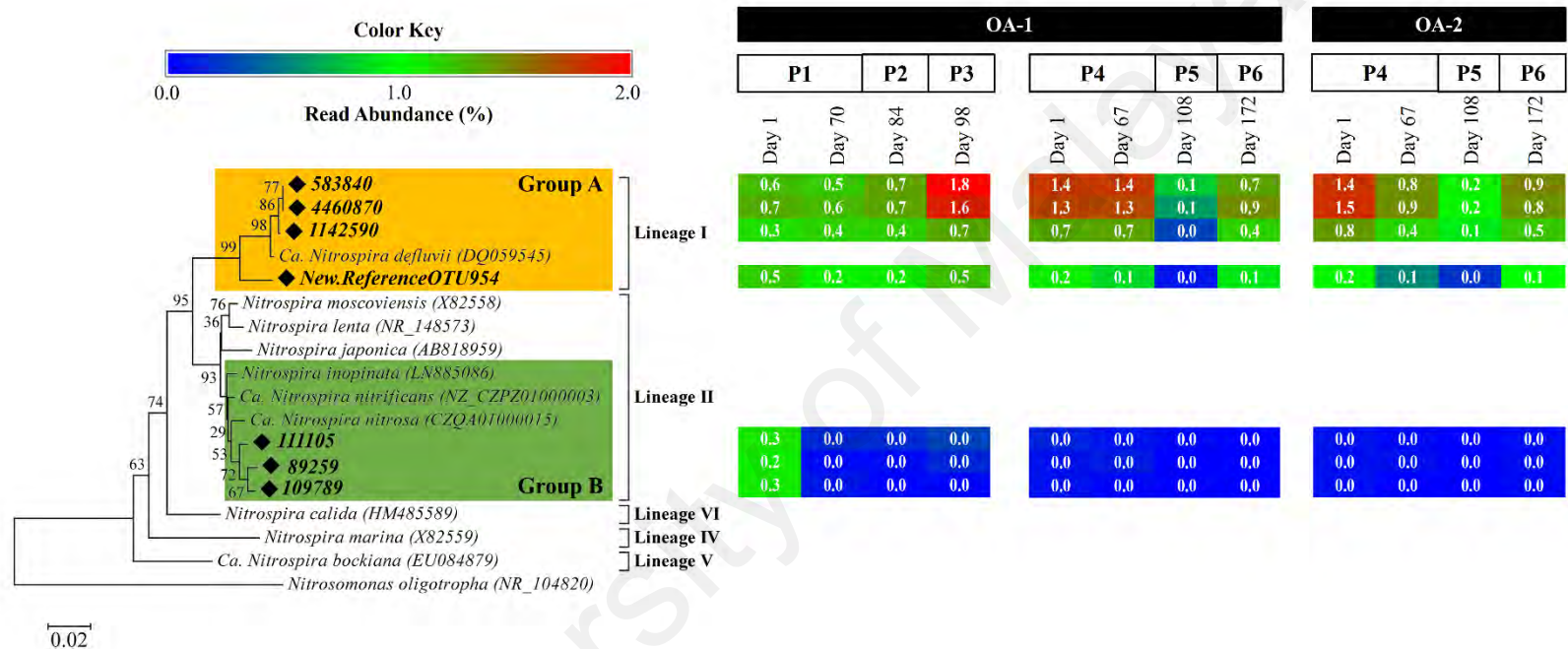


Figure 6.27: Neighbour-joining tree based on the *Nitrospira* 16S rRNA sequences showing the phylogenetic relationships of the OTUs with reference sequences in the GenBank database, rooting with *Nitrosomonas oligotropha*. Bootstrap values are shown in percentages of 1000 replicates. The heat map depicts the changes in percentage read abundance of each OTU in OA-1 and OA-2 from P1 to P6.

The shorter SRT in OA-2 optimisation (10 d) caused a reduction in read abundance for Group A *Nitrospira* between day 1 and day 67 (Figure 6.27). The read abundance for Group A *Nitrospira* in OA-1 remained unchanged from day 1 to day 67 during the optimisation study because the SRT was maintained at 20 d (Figure 6.27). Vuono et al. (2015) had similar observations whereby at SRT below 12 d, washout of k-strategist *Nitrospira* occurred in a sequencing batch membrane bioreactor, which led to a loss of nitrification activity. The read abundance of *Nitrospira*-related OTUs decreased significantly on day 108 during the OA-1 and OA-2 optimisation study as the HRT reduced from 16 h to 12 h. The decreased *Nitrospira* population was linked to the deteriorated nitrogen removal performance during P5 (Figure 6.13B and Figure 6.14B). Operating OA-1 and OA-2 at the recommended HRT (16 h) and SRT (20 d) partially recovered the population of Group A *Nitrospira* on day 172 during the optimisation study (Figure 6.27). The increase in *Nitrospira* population corresponded with the restoration of nitrification activity in both OA-1 and OA-2 during P6 (Figure 6.13C and Figure 6.14C). A similar systemic perturbation study on the reduction of SRT from 30 d to 12 d was performed on a sequencing batch membrane bioreactor in Colorado, United States, which led to a decrease in TN removal efficiency from $94 \pm 3\%$ to $83 \pm 6\%$ (Vuono et al., 2015). Subsequent increase of SRT back to 30 d successfully recovered the TN removal efficiency to $92 \pm 3\%$ after operating the reactor for $2 \times$ SRT (54 d), but the nitrifying population abundance in the reactor was only 57% of that in pre-disturbance state (Vuono et al., 2015). Similar to the recovery of *Nitrospira* in the OA-1 and OA-2 SBRs in this study, Vuono et al. (2015) reported only the increase in read abundance for *Nitrospira defluvii* in the Lineage I *Nitrospira*. The recovery of *Nitrospira defluvii* was consistent with other studies that suggested Lineage I *Nitrospira* had a higher tolerance towards changes in environmental conditions, such as DO and NO_2^- concentrations (Mehrani et al., 2020; Nowka, Off, Daims, & Spieck, 2015). The

lower nitrifying population abundance and diversity may indicate functional redundancy of nitrifiers in the pre-disturbance community and the nitrifying community could recover to the pre-disturbance state if the reactor was operated for a longer period (Vuono et al., 2015).

Though 16S rRNA-based phylogeny is widely accepted to study the phylogenetic relationships between different species of microbes, Koch et al. (2019) suggested that 16S rRNA-based phylogeny alone is not recommended to differentiate OTUs of *Nitrospira* down to species level. 16S rRNA-based methods should be used together with functional genes-based methods for confirmation. Thus, the next section used qPCR assays targeting the functional genes (*amoA*) to validate the presence of Group A (NOB) and Group B (comammox) *Nitrospira* in the low-DO OA SBRs. The presence of AOB related to the Family *Nitrosomonadaceae* in the sludge was also verified by qPCR assay targeting *amoA* of betaproteobacterial AOB to elucidate the potential roles of nitrifiers in the low-DO OA process.

6.4.2.3 Quantification of Ammonia-Oxidizing Bacteria and *Nitrospira* by Quantitative Polymerase Chain Reaction Analysis

The percentage relative abundances of betaproteobacterial AOB and *Nitrospira sp.* to the total bacteria population in the OA SBRs are shown in Figure 6.28. The percentage relative abundances of betaproteobacterial AOB to the total bacteria population in the OA SBRs was consistent. For instance, the percentage relative abundance of betaproteobacterial AOB during OA-1 parent reactor operation (P1 – P3) varied between 0.004% and 0.01%, the abundances in OA-1 and OA-2 during optimisation study were also consistently between 0.005% – 0.02% and 0.003% – 0.01%. For the *Nitrospira* population, the changes in the percentage read abundance obtained from qPCR (Figure 6.28) agreed with the read abundances from the 16S rRNA amplicon

sequencing data (Figure 6.27). During P1 to P3, the percentage relative abundance of *Nitrospira* to the total bacteria population increased from 0.3% to 1.2% (Figure 6.28A), which corresponded with the 2.0 – 2.5 increase in read abundance of *Nitrospira* (Figure 6.27). At the end of P4 (day 67) in Figure 6.28B and Figure 6.28C, the percentage relative abundance of *Nitrospira* to the total bacteria population in OA-2 ($0.5 \pm 0.2 \%$) was half of that in OA-1 ($1.0 \pm 0.1\%$). This finding was consistent with the lower read abundance of *Nitrospira* in OA-2 than that in OA-1 (Figure 6.27) because of the shorter SRT operation in OA-2 (10 days). Subsequently in P5, the relative abundances of *Nitrospira* to the total bacteria population in both OA-1 and OA-2 showed a drop to $0.3 \pm 0.02\%$ and $0.1 \pm 0.03\%$, respectively, due to the reduction of HRT in both SBRs to 12 hours. In P6, the *Nitrospira* relative abundances restored in OA-1 and OA-2 (Figure 6.28B and Figure 6.28C), which also agreed with the higher read abundances of *Nitrospira* from the 16S rRNA sequencing data (Figure 6.27). Overall, the qPCR data showed that the *Nitrospira* population in the OA SBRs were higher than betaproteobacterial AOB, which was consistent with the 16S rRNA sequencing data. The higher *Nitrospira* population was also in line with the microbial community analysis for low-DO nitrification SBR and AO SBR, most likely caused by the low-DO condition and long SRT operation as discussed in Section 5.3 and Section 6.4.1. Further qPCR analysis on the *Nitrospira* community was conducted to validate the presence of the *Nitrospira* closely affiliated with comammox in the OA SBRs.

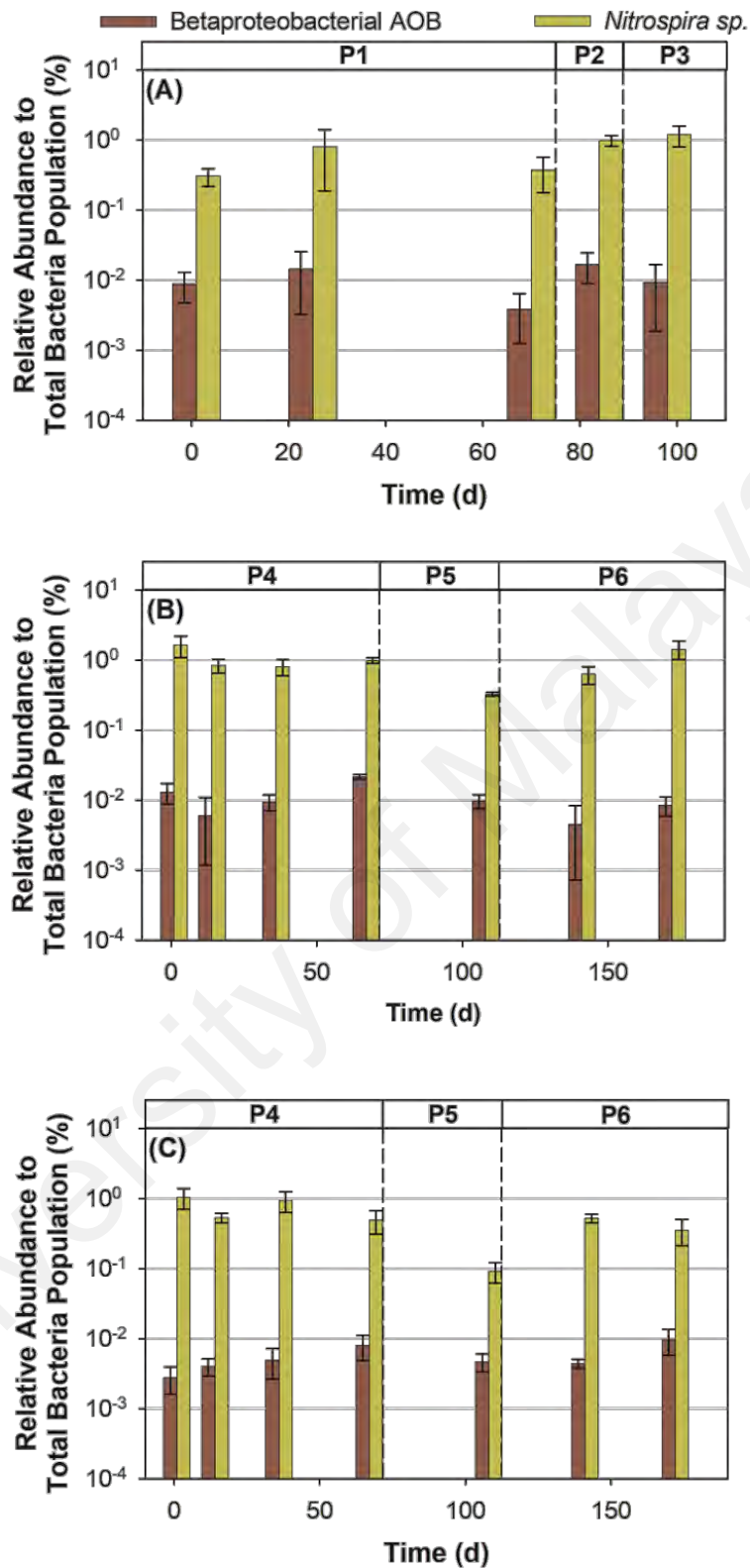


Figure 6.28: Relative abundance of betaproteobacterial AOB and *Nitrospira sp.* to the total bacteria population in (A) OA-1 from P1 to P3; (B) OA-1 from P4 to P6 and (C) OA-2 from P4 to P6.

To confirm the population sizes of Group A (NOB) and Group B (comammox) *Nitrospira* in the low-DO OA SBR, qPCR was applied to quantify the relative abundance of comammox to the total *Nitrospira* population using primers targeting comammox *amoA* (Figure 6.29). Comammox made up 69% of the *Nitrospira* community in the seed sludge (Figure 6.28A). Thus, both 16S rRNA amplicon sequencing (Figure 6.27) and qPCR data (Figure 6.29) showed that comammox *Nitrospira* coexisted with *Nitrospira*-related NOB in the seed sludge. Only one known comammox species (*Ca. Nitrospira nitrosa*) was detected in the seed sludge, which constituted 3% of the total *Nitrospira* community. The primer pairs targeting the other two species of comammox (Inopinata amoA-410F/815R for *Nitrospira inopinata* and Nitrificans amoA-463F/836R for *Ca. Nitrospira nitrificans*) were applied to the samples (Table 3.7) but no fluorescent signals were obtained from the qPCR analysis. Beach and Noguera (2019) found the same comammox species (*Ca. Nitrospira nitrosa*) in low-DO nitrification bioreactors (0.2 – 0.7 mg O₂/L) operated at long SRTs (80 d). Cotto et al. (2020) and Roots et al. (2019) had also identified that long SRT (> 10 d) was a main selection factor for the growth of *Nitrospira*-related comammox in full-scale conventional nitrification-denitrification bioreactors. The comammox population reduced in the OA-1 parent SBR operation (Figure 6.29A). The comammox population then fluctuated between 8 – 12% in OA-1 parent SBR (Figure 6.29A), 10 – 23% in OA-1 during optimisation study (Figure 6.29B) and 4 – 12% in OA-2 during optimisation study (Figure 6.29C). No known comammox species was detected in the steady-state low-DO OA process (Figure 6.29). The low relative abundance of *Ca. Nitrospira nitrosa* to the comammox population indicated that novel comammox species may be present in the sludge.

█ *Nitrospira* NOB
 █ Comammox
 Ca. Nitrospira nitrosa

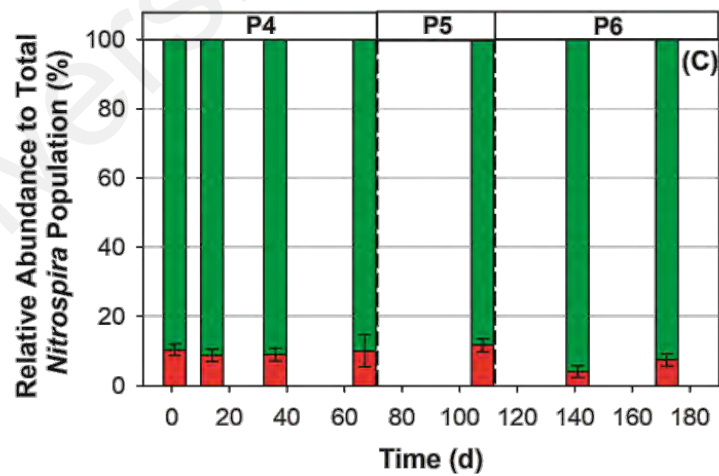
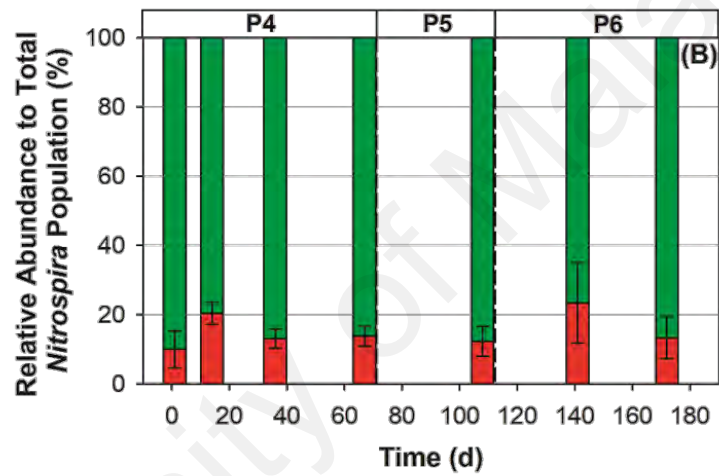
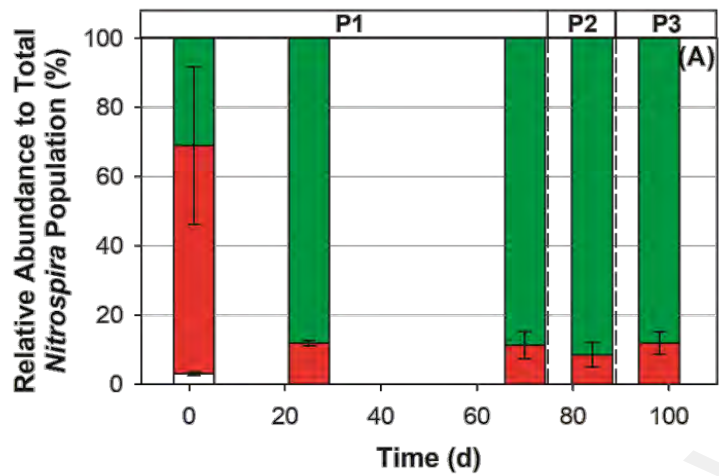


Figure 6.29: Relative abundance of comammox and *Ca. Nitrospira nitrosa* to the total *Nitrospira* population in (A) OA-1 from P1 to P3; (B) OA-1 from P4 to P6 and (C) OA-2 from P4 to P6.

The outcomes of the microbial analyses OA-1 and OA-2 showed that *Nitrospira* was the dominant nitrifier in the process, while betaproteobacterial AOB was 2 to 3 orders of magnitude lower in abundance than *Nitrospira*. The two main groups of *Nitrospira* in the low-DO OA process were closely affiliated with *Nitrospira defluvii* and comammox (*Ca. Nitrospira nitrosa*), respectively. Long SRT operation (20 d) was a key operating strategy to encourage the growth of NOB and comammox related to *Nitrospira*, which could contribute to a stable low-DO nitrification performance. Thus, an improved understanding on the functional microbial community in this study revealed important operating strategy (long SRT) to operate a low-DO OA process in treating low COD/N tropical wastewater successfully.

Though comammox was detected by a primer pair targeting the comammox *amoA*, no known comammox species was identified during the OA SBRs' operation from the qPCR analysis (Figure 6.29). The role of comammox in NH_3 oxidation in the low-DO OA process is still uncertain. Furthermore, the lower population size of betaproteobacterial AOB may contribute to NH_3 oxidation in the low-DO OA process. For example, Yao and Peng (2017) found that the population size of *Nitrospira* was 2 – 6 times larger than that for AOB affiliated with *Nitrosomonas* based on sludge samples from 10 full-scale WWTPs operating with A_2O and oxidation ditch configurations in China. The small *Nitrosomonas* population was still conceptually involved in NH_3 oxidation, while the large *Nitrospira* population could be explained by the simultaneous production of NO_2^- for NOB via NH_3 oxidation by AOB and NO_3^- reduction by DOHOs (Yao & Peng, 2017). Similarly, Law et al. (2019) also suggested AOB related to *Nitrosomonas* was responsible for NH_3 oxidation, albeit with 3 to 6 times lower read abundances than *Nitrospira*. Law et al. (2019) reasoned that comammox *Nitrospira* was not detected in the sludge samples from 2 WWTPs in Singapore operating in MLE and step-feed biological nitrogen removal configurations. Future investigations based on

transcriptomics are warranted to clarify the nitrifying role of each bacteria present in the low-DO OA reactor.

6.5 Estimation of Operating Cost Reduction of Low-Dissolved-Oxygen Oxic-Anoxic Process

The low-DO OA process developed from this study used low-DO nitrification to reduce energy usage at the aeration tank and eliminated the high-flow MLR stream to lower piping and pumping costs. Based on these operating strategies, the reduction in the operating cost when compared with the conventional AO process could be estimated using the equipment energy usage breakdown adapted from Ramli and Abdul Hamid (2017) and Sedlak (2018). The estimated reduction in energy cost was 20% when compared with conventional AO process (Table 6.3). The aerator energy usage may be reduced by 23% as estimated for low-DO nitrification in Section 5.4. The MLR pump can be eliminated in the low-DO OA process.

Table 6.3: Estimation of energy cost reduction of low-DO OA process when compared with conventional AO process with equipment energy usage breakdown adapted from Ramli and Abdul Hamid (2017) and Sedlak (2018)

Equipment	Monthly Electricity Usage (kWh)	
	Conventional AO Process	Low-DO OA Process
Aerator	168502.20	129746.69
RAS pump	58473.90	58473.90
Auto feed water supply unit	54958.20	54958.20
MLR pump	37583.40	0.00
Anoxic tank mixers	34477.20	34477.20
Digested sludge mixer	14530.50	14530.50
Secondary clarifier sludge collector	8166.00	8166.00
Sludge feed pump for dewatering	6131.70	6131.70
Sludge cake conveyor	5392.80	5392.80
Total	388215.90	311876.99
Energy Cost (RM)*	130828.76	105102.55

* RM 0.337/kWh based on Tariff E1 for medium-voltage general industry set by Tenaga Nasional Berhad (2014).

By modifying the existing WWTPs mostly operating in AO process to a low-DO OA process, the local wastewater industry could potentially reduce the energy cost significantly. The modification of AO process into low-DO OA process may also require minimal retrofitting. For instance, since most of the existing AO plants have a large oxic tank designed for EA, aeration may be cut off in part of the oxic tank to induce a low-DO condition and post-anoxic zone. Additional capital cost for extra tank is not needed. Besides, the MLR pump will no longer be needed and may be terminated after modifying into a low-DO OA process. The low-DO OA process is an attractive solution for the local wastewater industry to improve the sustainability of the WWTPs' operation.

The development of a low-DO OA process in this study was based on a controlled lab-scale SBR operations. The process retrofitting and application of the recommended conditions (DO, HRT and SRT) into continuous plug flow reactors commonly used by the plants operating in EA with pre-anoxic tank requires more investigations (National Water Services Commission, 2009). Nonetheless, SBR have been considered to be a robust, cost-effective and efficient reactor technology under tropical settings in Malaysia (Al-Shididi, Henze, & Ujang, 2004). SBR was proposed for the upgrading of WWTPs in Malaysia as the SBR allows the biological nitrogen removal and sedimentation to take place in a tank without using a RAS stream (Al-Shididi et al., 2004; C. Liu, Lee, & Zhang, 2019). The low-DO OA process developed in this study may be also applied to the WWTPs with SBR in Malaysia, but the operating conditions should first be validated in pilot-scale study.

6.6 Summary of Chapter

Objective 3 of the project was achieved in Chapter 6 by investigating the long-term process performance of a biological nitrogen removal by applying low-DO nitrification and utilising sbCOD for denitrification. These strategies help to achieve an improved process design in treating low COD/N tropical wastewater. To address objective 4, a low-DO OA process was established, the DO, HRT and SRT were also optimised to ensure maximum treatment efficiency and capacity could be attained. Part of objective 5 was also addressed in this chapter by investigating the nitrifying and denitrifying microbial community in the AO and OA SBRs.

The results showed that low-DO nitrification process (0.9 ± 0.1 mg O₂/L) successfully produced low ammonia concentration in the effluent (less than 1 mg/L). The AO SBR was modified by incorporating a post-anoxic phase, thus changing the SBR to a low-DO AOA configuration. Utilising sbCOD in the post-anoxic phase

successfully produced effluent $\text{NO}_3\text{-N}$ (5.7 ± 1.3 mg/L) lower than the discharge limit in Environmental Quality (Sewage) Regulations 2009 (10 mg/L). Most of the denitrification activity took place in the post-anoxic phase, while denitrification activity in the pre-anoxic phase was negligible.

Due to the negligible denitrification activity in the pre-anoxic phase, the pre-anoxic phase may be eliminated from the low-DO AOA process. A low-DO OA process improved for treating low COD/N tropical wastewater in Malaysia was then developed. A parent SBR, OA-1, was successfully established and the operating conditions (HRT and SRT) were further optimised by running a parallel SBR, OA-2. By operating the low-DO OA process at the recommended HRT (16 h) and SRT (20 d), OA-1 and OA-2 consistently produced good effluent quality with $\text{NH}_4\text{-N}$ and $\text{NO}_3\text{-N}$ below 0.3 mg/L.

From the microbial analysis data of AO SBR, the presence of comammox *Nitrospira* suggested that low-DO condition and tropical temperature may promote their growth and contribute to a stable low-DO nitrification performance. Similarly, microbial community analyses on both OA-1 and OA-2 showed that *Nitrospira* was the dominant nitrifier. A large fraction of the *Nitrospira* OTUs was closely related to a low-DO NOB (*Nitrospira defluvii*). qPCR analysis also confirmed the presence of comammox related to *Ca. Nitrospira nitrosa*, though at a lower abundance than *Nitrospira defluvii*. Long SRT (20 d) operation was found to promote the growth of *Nitrospira*, which was crucial to operate a low-DO nitrification process efficiently.

The estimated energy cost for a low-DO OA process was 20% less than that for conventional AO process. The modification of existing AO plants in Malaysia to low-DO OA process may be also simple with minimal retrofitting. The applications of the recommended operating conditions (DO, HRT and SRT) in the full-scale WWTPs should first be validated in pilot-scale reactor study. The low-DO OA process was

efficient and has simpler design than conventional AO process in existing WWTPs, which are keys to achieve more sustainable wastewater treatment systems in treating low COD/N wastewater in Malaysia.

University of Malaya

CHAPTER 7: CONCLUSIONS AND RECOMMENDATIONS

7.1 Conclusions

An efficient and low-cost biological nitrogen removal in treating low-COD/N tropical wastewater was developed in this research. The following conclusions could be drawn based on the results obtained:-

- i. Detailed wastewater characterisation revealed that the tropical wastewater samples did not have sufficient soluble biodegradable organics for denitrification because of the low soluble COD/N (3 – 6 g COD/ g N) and low rbCOD content (3 – 40% of TCOD). sbCOD from PSS in the wastewater may supplement the source of biodegradable organics for denitrification as sbCOD was the major source of biodegradable organics and the PSS hydrolysis rate was accelerated at tropical temperature ($30 \pm 2^\circ\text{C}$). Batch experiment using PSS as the sole source of bCOD showed that high PSS hydrolysis rate in tropical temperatures could provide sbCOD for active denitrification.
- ii. Based on the wastewater characterisation study, two operating strategies were formulated to reduce the energy consumption and operating cost of biological nitrogen removal in treating low COD/N tropical wastewater. Tropical wastewater low in soluble biodegradable organics may be conducive for low-DO nitrification ($< 1 \text{ mg O}_2/\text{L}$) to achieve NH_4^+ removal from the tropical wastewater with lower aeration energy consumption. The feasibility of applying low-DO nitrification to treat tropical wastewater was studied in a short-term low-DO nitrification SBR ($0.1 - 0.5 \text{ mg O}_2/\text{L}$), which demonstrated high NH_4^+ removal efficiency ($98 \pm 2\%$). Besides, the sbCOD could be utilised for denitrification to reduce the operating cost associated with external carbon dosage typically applied for wastewater low in biodegradable organics.

- iii. A conventional AO SBR was operated to monitor the long-term nitrogen removal performance in treating low COD/N tropical wastewater. The conventional AO SBR with a high-DO oxic phase (1.7 ± 0.2 mg O₂/L) produced effluent with low NH₄-N (0.6 ± 0.5 mg/L) but high NO₃-N (18 ± 4 mg/L). The process was then modified by applying low-DO nitrification and utilised sbCOD to enhance denitrification performance. Low-DO nitrification (0.9 ± 0.1 mg O₂/L) consistently produced effluent with low NH₄-N below 1 mg/L. A post-anoxic stage was incorporated after the oxic stage in the AO SBR, thus changing the conventional AO configuration into a low-DO AOA configuration to enhance the denitrification performance. Utilising sbCOD in the post-anoxic stage successfully reduced NO₃-N in the effluent (5.7 ± 1.3 mg/L) below the discharge limit in Malaysia (10 mg/L).
- iv. The low-DO AOA reactor was further simplified into a low-DO OA configuration. The HRT and SRT of the low-DO OA reactors were also optimised. The low-DO OA SBR produced effluent with low NH₄-N and NO₃-N (< 0.3 mg/L). The recommended HRT and SRT of the low-DO OA process were 16 h and 20 d, respectively. Based on a cost estimation, adopting the low-DO OA process may reduce WWTPs' operation and maintenance cost by 20% when compared with the conventional AO process currently adopted by WWTPs in Malaysia.
- v. qPCR assays confirmed the presence of comammox (10 – 20% of the total *Nitrospira* population) in the low-DO OA process treating tropical wastewater. A known comammox species (*Ca. Nitrospira nitrosa*) was detected, which made up only 3% of the total *Nitrospira* population. Thus, the low-DO OA SBR may harbour novel comammox species. The long SRT (20 d) contributed to a stable low-DO nitrification performance (0.4 ± 0.2 mg O₂/L) in the low-DO OA SBR by enriching NOB and comammox related to *Nitrospira*.

7.2 Novelties and Implications of Study

The emerging economies in Southeast Asia, such as Malaysia and Indonesia have introduced more stringent regulations for the wastewater effluent quality to address the water pollution issue. Following the introduction of the new regulations in Malaysia, many medium-sized (10000 – 30000 PE) EA plants incorporated a pre-anoxic tank to promote biological nitrogen removal (AO configuration). The findings of this research could serve as a valuable guidelines for these EA plants to achieve more efficient and cost-effective operation on the following aspects:-

- i. With an improved knowledge on the functional microbial community in tropical systems, this study identified key strategies to operate a tropical wastewater treatment system efficiently. For instance, the EA plants with pre-anoxic tank may use long SRT to achieve high NH_4^+ removal efficiency at low-DO condition (0.4 ± 0.2 mg O_2/L). Long SRT operation could promote the growth of k-strategist *Nitrospira* in the tropical systems, which contributed to a stable low-DO nitrification performance. This would be more energy-efficient than meeting the recommended DO concentration (2 mg O_2/L) in the MSIG. The guidelines for high DO concentration (2 mg O_2/L) are good practice in the temperate region, but may not be necessary for WWTPs in the tropics.
- ii. By understanding the detailed wastewater characteristics, the sbCOD in the wastewater was utilised in post-anoxic denitrification to significantly lower the effluent NO_3-N when compared with that of using only pre-anoxic denitrification. Thus, the EA plants combined with pre-anoxic tank could reduce the effluent NO_3-N by modifying part of the oxic tank into a post-anoxic tank. Also, the smaller size of the oxic tank could imply additional energy reduction.

- iii. The low-DO OA configuration developed in this research is an improved biological nitrogen removal in treating tropical wastewater with low COD/N. The process is more energy-efficient and cost-effective than the conventional biological nitrogen removal by eliminating the high pumping and piping cost for MLR stream. Provided that the wastewater has similar characteristics, other Southeast Asian countries with similar tropical climate may adopt the low-DO OA reactor design to promote sustainable wastewater management for nitrogen pollution control in line with Sustainable Development Goal 6.3.

7.3 Recommendations for Future Works

The following future research directions are recommended:-

- i. Scaling up the low-DO OA reactor to a pilot-scale study, both in SBR and plus flow reactors, will be useful to conduct a cost-benefit analysis of modifying a conventional biological nitrogen removal reactor into a low-DO OA reactor. Moreover, setting up a pilot-scale low-DO OA reactor will be critical to explore the effects of potential operational issues, such as inhomogeneous mixing and non-uniform aeration, on the treatment performance.
- ii. A metagenomic analysis on the low-DO OA sludge will allow identification of the potentially novel comammox species present. The metagenome of comammox species could be compared with the NCBI database to elucidate their genomic inventories and prevalence in the tropical systems.
- iii. Future molecular analyses on the pilot-scale low-DO OA reactor should also use metatranscriptomics to confirm nitrifying genes expressed in the process. The analysis will identify the active nitrifiers and validate the potential roles of comammox in tropical biological nitrogen removal system.

REFERENCES

- Al-Shididi, S., Henze, M., & Ujang, Z. (2004). Feasibility study of sequencing batch reactor system for upgrading wastewater treatment in Malaysia. *Water Science and Technology*. 48(11-12): 327-335. doi:10.2166/wst.2004.0872
- Amann, R. I., Krumholz, L., & Stahl, D. A. (1990). Fluorescent-oligonucleotide probing of whole cells for determinative, phylogenetic, and environmental studies in microbiology. *J Bacteriol*. 172(2): 762-770.
- Amann, R. I., Ludwig, W., & Schleifer, K. H. (1995). Phylogenetic identification and in situ detection of individual microbial cells without cultivation. *Microbiological Reviews*. 59(1): 143-169.
- Andrews, J. H., & Harris, R. F. (1986). r- and K-Selection and Microbial Ecology. *Advances in Microbial Ecology*. 9: 99-147.
- Anthonisen, A. C., Loehr, R. C., Prakasam, T. B. S., & Srinath, E. G. (1976). Inhibition of Nitrification by Ammonia and Nitrous Acid. *Water Pollution Control Federation*. 48(5): 835-852.
- APHA/AWWA/WEF. (1998). Standard Methods for the Examination of Water and Wastewater. Washington, D.C., U.S.: APHA/AWWA/WEF.
- Arnaldos, M., Amerlinck, Y., Rehman, U., Maere, T., Van Hoey, S., Naessens, W., & Nopens, I. (2015). From the affinity constant to the half-saturation index: understanding conventional modeling concepts in novel wastewater treatment processes. *Water Res*. 70: 458-470. doi:10.1016/j.watres.2014.11.046
- Arnaldos, M., Kunkel, S. A., Stark, B. C., & Pagilla, K. R. (2013). Enhanced heme protein expression by ammonia-oxidizing communities acclimated to low dissolved oxygen conditions. *Appl Microbiol Biotechnol*. 97(23): 10211-10221. doi:10.1007/s00253-013-4755-7
- Balzer, S., Malde, K., Lanzen, A., Sharma, A., & Jonassen, I. (2010). Characteristics of 454 pyrosequencing data--enabling realistic simulation with flowsim. *Bioinformatics*. 26(18): i420-425. doi:10.1093/bioinformatics/btq365
- Baptista, J. D., Lunn, M., Davenport, R. J., Swan, D. L., Read, L. F., Brown, M. R., . . . Curtis, T. P. (2014). Agreement between amoA gene-specific quantitative PCR and fluorescence in situ hybridization in the measurement of ammonia-oxidizing bacteria in activated sludge. *Appl Environ Microbiol*. 80(19): 5901-5910. doi:10.1128/AEM.01383-14
- Barnard, J. (1974). Cut P and N Without Chemicals. *Water and Wastes Engineering*. 11(7): 41-44.
- Beach, N. K., & Noguera, D. R. (2019). Design and Assessment of Species-Level qPCR Primers Targeting Comammox. *Front Microbiol*. 10: 36. doi:10.3389/fmicb.2019.00036

- Bekiari, V., & Avramidis, P. (2013). Data quality in water analysis: validation of combustion-infrared and combustion-chemiluminescence methods for the simultaneous determination of Total Organic Carbon (TOC) and Total Nitrogen (TN). *International Journal of Environmental Analytical Chemistry*. 94(1): 65-76. doi:10.1080/03067319.2013.763940
- Bell, L. C., Richardson, D. J., & Ferguson, S. J. (1990). Periplasmic and membrane-bound respiratory nitrate reductases in *Thiosphaera pantotropha*. The periplasmic enzyme catalyzes the first step in aerobic denitrification. *FEBS Lett*. 265(1-2): 85-87. doi:10.1016/0014-5793(90)80889-Q
- Bellucci, M., Ofiteru, I. D., Graham, D. W., Head, I. M., & Curtis, T. P. (2011). Low-dissolved-oxygen nitrifying systems exploit ammonia-oxidizing bacteria with unusually high yields. *Appl Environ Microbiol*. 77(21): 7787-7796. doi:10.1128/AEM.00330-11
- Benneouala, M., Bareha, Y., Mengelle, E., Bounouba, M., Sperandio, M., Bessiere, Y., & Paul, E. (2017). Hydrolysis of particulate settleable solids (PSS) in activated sludge is determined by the bacteria initially adsorbed in the sewage. *Water Res*. 125: 400-409. doi:10.1016/j.watres.2017.08.058
- Bergmann, D. J., Arciero, D. M., & Hooper, A. B. (1994). Organization of the hao gene cluster of *Nitrosomonas europaea*: genes for two tetraheme c cytochromes. *Journal of Bacteriology*. 176(11): 3148-3153.
- Blackburne, R., Yuan, Z., & Keller, J. (2008). Partial nitrification to nitrite using low dissolved oxygen concentration as the main selection factor. *Biodegradation*. 19(2): 303-312. doi:10.1007/s10532-007-9136-4
- Braker, G., Fesefeldt, A., & Witzel, K. P. (1998). Development of PCR primer systems for amplification of nitrite reductase genes (*nirK* and *nirS*) to detect denitrifying bacteria in environmental samples. *Appl Environ Microbiol*. 64(10): 3769-3775.
- Bru, D., Sarr, A., & Philippot, L. (2007). Relative abundances of proteobacterial membrane-bound and periplasmic nitrate reductases in selected environments. *Appl Environ Microbiol*. 73(18): 5971-5974. doi:10.1128/AEM.00643-07
- Brun, R., Kühni, M., Siegrist, H., Gujer, W., & Reichert, P. (2002). Practical identifiability of ASM2d parameters—systematic selection and tuning of parameter subsets. *Water Research*. 36(16): 4113-4127. doi:10.1016/s0043-1354(02)00104-5
- Bushnell, B., Rood, J., & Singer, E. (2017). BBMerge – Accurate paired shotgun read merging via overlap. *PLoS One*. 12(10): e0185056. doi:10.1371/journal.pone.0185056
- Camargo, J. A., & Alonso, A. (2006). Ecological and toxicological effects of inorganic nitrogen pollution in aquatic ecosystems: A global assessment. *Environ Int*. 32(6): 831-849. doi:10.1016/j.envint.2006.05.002

- Cao, Y., Daigger, G. T., & van Loosdrecht, M. C. M. (2020). The bottlenecks and causes, and potential solutions for municipal sewage treatment in China. *Water Practice and Technology*. 15(1): 160-169. doi:10.2166/wpt.2020.006
- Cao, Y., Hong, K. B., van Loosdrecht, M. C., Daigger, G. T., Yi, P. H., Wah, Y. L., . . . Ghani, Y. A. (2016). Mainstream partial nitrification and anammox in a 200,000 m³/day activated sludge process in Singapore: scale-down by using laboratory fed-batch reactor. *Water Sci Technol*. 74(1): 48-56. doi:10.2166/wst.2016.116
- Cao, Y., Kwok, B. H., van Loosdrecht, M. C. M., Daigger, G., Png, H. Y., Long, W. Y., & Eng, O. K. (2018). The influence of dissolved oxygen on partial nitrification/anammox performance and microbial community of the 200,000 m³/d activated sludge process at the Changi water reclamation plant (2011 to 2016). *Water Sci Technol*. 78(3): 634-643. doi:10.2166/wst.2018.333
- Cao, Y., van Loosdrecht, M. C., & Daigger, G. T. (2017). Mainstream partial nitrification-anammox in municipal wastewater treatment: status, bottlenecks, and further studies. *Appl Microbiol Biotechnol*. 101(4): 1365-1383. doi:10.1007/s00253-016-8058-7
- Cao, Y., Wah, Y. L., Ang, C. M., & Raajeevan, K. S. (2008). *Biological Nitrogen Removal Activated Sludge Process in Warm Climates*. London, UK: IWA Publishing.
- Caporaso, J. G., Kuczynski, J., Stombaugh, J., Bittinger, K., Bushman, F. D., Costello, E. K., . . . Knight, R. (2010). QIIME allows analysis of high-throughput community sequencing data. *Nat Methods*. 7(5): 335-336. doi:10.1038/nmeth.f.303
- Chao, Y., Mao, Y., Yu, K., & Zhang, T. (2016). Novel nitrifiers and comammox in a full-scale hybrid biofilm and activated sludge reactor revealed by metagenomic approach. *Appl Microbiol Biotechnol*. 100(18): 8225-8237. doi:10.1007/s00253-016-7655-9
- Choi, Y.-Y., Baek, S.-R., Kim, J.-I., Choi, J.-W., Hur, J., Lee, T.-U., . . . Lee, B. (2017). Characteristics and Biodegradability of Wastewater Organic Matter in Municipal Wastewater Treatment Plants Collecting Domestic Wastewater and Industrial Discharge. *Water*. 9(6): 409. doi:10.3390/w9060409
- Costa, E., Pérez, J., & Kreft, J.-U. (2006). Why is metabolic labour divided in nitrification? *Trends in Microbiology*. 14(5): 213-219. doi:10.1016/j.tim.2006.03.006
- Cotto, I., Dai, Z., Huo, L., Anderson, C. L., Vilardi, K. J., Ijaz, U., . . . Pinto, A. J. (2020). Long solids retention times and attached growth phase favor prevalence of comammox bacteria in nitrogen removal systems. *Water Res*. 169: 115268. doi:10.1016/j.watres.2019.115268
- Cui, C., Shu, W., & Li, P. (2016). Fluorescence In situ Hybridization: Cell-Based Genetic Diagnostic and Research Applications. *Front Cell Dev Biol*. 4: 89. doi:10.3389/fcell.2016.00089

- Daebel, H., Manser, R., & Gujer, W. (2007). Exploring temporal variations of oxygen saturation constants of nitrifying bacteria. *Water Res.* 41(5): 1094-1102. doi:10.1016/j.watres.2006.11.011
- Daigger, G. T., & Littleton, H. X. (2014). Simultaneous Biological Nutrient Removal: A State-of-the-Art Review. *Water Environment Research.* 86(3): 245-257. doi:10.2175/106143013x13736496908555
- Daims, H., Brühl, A., Amann, R., Schleifer, K.-H., & Wagner, M. (1999). The Domain-specific Probe EUB338 is Insufficient for the Detection of all Bacteria: Development and Evaluation of a more Comprehensive Probe Set. *Systematic and Applied Microbiology.* 22(3): 434-444. doi:10.1016/s0723-2020(99)80053-8
- Daims, H., Lebedeva, E. V., Pjevac, P., Han, P., Herbold, C., Albertsen, M., . . . Wagner, M. (2015). Complete nitrification by Nitrospira bacteria. *Nature.* 528(7583): 504-509. doi:10.1038/nature16461
- Daims, H., Lucker, S., & Wagner, M. (2016). A New Perspective on Microbes Formerly Known as Nitrite-Oxidizing Bacteria. *Trends Microbiol.* 24(9): 699-712. doi:10.1016/j.tim.2016.05.004
- Daims, H., Nielsen, J. L., Nielsen, P. H., Schleifer, K. H., & Wagner, M. (2001). In situ characterization of Nitrospira-like nitrite-oxidizing bacteria active in wastewater treatment plants. *Appl Environ Microbiol.* 67(11): 5273-5284. doi:10.1128/AEM.67.11.5273-5284.2001
- Daims, H., Ramsing, N. B., Schleifer, K. H., & Wagner, M. (2001). Cultivation-independent, semiautomatic determination of absolute bacterial cell numbers in environmental samples by fluorescence in situ hybridization. *Appl Environ Microbiol.* 67(12): 5810-5818. doi:10.1128/AEM.67.12.5810-5818.2001
- Department of Environment. (2009). Environmental Quality (Sewage) Regulations 2009. Retrieved from http://www.doe.gov.my/portalv1/wp-content/uploads/2015/01/Environmental_Quality_Sewage_Regulations_2009_-_P.U.A_432-2009.pdf
- Department of Environment. (2017). *Environmental Quality Report 2017*. Retrieved from Putrajaya, Malaysia: <https://enviro.doe.gov.my/ekmc/wp-content/uploads/2018/10/EQR-2017.pdf>
- Dionisi, H. M., Layton, A. C., Harms, G., Gregory, I. R., Robinson, K. G., & Sayler, G. S. (2002). Quantification of Nitrosomonas oligotropha-like ammonia-oxidizing bacteria and Nitrospira spp. from full-scale wastewater treatment plants by competitive PCR. *Applied and Environmental Microbiology.* 68(1): 245-253. doi:Doi 10.1128/Aem.68.1.245-253.2002
- Drewnowski, J., & Makinia, J. (2013). Modeling hydrolysis of slowly biodegradable organic compounds in biological nutrient removal activated sludge systems. *Water Sci Technol.* 67(9): 2067-2074. doi:10.2166/wst.2013.092
- Dubber, D., & Gray, N. F. (2010). Replacement of chemical oxygen demand (COD) with total organic carbon (TOC) for monitoring wastewater treatment

performance to minimize disposal of toxic analytical waste. *J Environ Sci Health A Tox Hazard Subst Environ Eng.* 45(12): 1595-1600. doi:10.1080/10934529.2010.506116

- Edgar, R. C. (2013). UPARSE: highly accurate OTU sequences from microbial amplicon reads. *Nature Methods.* 10: 996. doi:10.1038/nmeth.2604
- Ehrich, S., Behrens, D., Lebedeva, E., Ludwig, W., & Bock, E. (1995). A new obligately chemolithoautotrophic, nitrite-oxidizing bacterium, *Nitrospira moscoviensis* sp. nov. and its phylogenetic relationship. *Archives of Microbiology.* 164(1): 16-23.
- Ekama, G. A., & Wentzel, M. C. (2008). Nitrogen Removal. In M. Henze, M. C. M. van Loosdrecht, G. A. Ekama, & D. Brdjanovic (Eds.), *Biological wastewater treatment: Principles, modelling and design.* London, UK: IWA Publishing.
- Fan, H., Qi, L., Liu, G., Zhang, Y., Fan, Q., & Wang, H. (2017). Aeration optimization through operation at low dissolved oxygen concentrations: Evaluation of oxygen mass transfer dynamics in different activated sludge systems. *J Environ Sci (China).* 55: 224-235. doi:10.1016/j.jes.2016.08.008
- Fitzgerald, C. M., Camejo, P., Oshlag, J. Z., & Noguera, D. R. (2015). Ammonia-oxidizing microbial communities in reactors with efficient nitrification at low-dissolved oxygen. *Water Res.* 70: 38-51. doi:10.1016/j.watres.2014.11.041
- Fowler, S. J., Palomo, A., Dechesne, A., Mines, P. D., & Smets, B. F. (2018). Comammox *Nitrospira* are abundant ammonia oxidizers in diverse groundwater-fed rapid sand filter communities. *Environ Microbiol.* 20(3): 1002-1015. doi:10.1111/1462-2920.14033
- Fujitani, H., Nomachi, M., Takahashi, Y., Hasebe, Y., Eguchi, M., & Tsuneda, S. (2020). Successful enrichment of low-abundant comammox *Nitrospira* from nitrifying granules under ammonia-limited conditions. *FEMS Microbiol Lett.* 367(1). doi:10.1093/femsle/fnaa025
- Gabarro, J., Hernandez-Del Amo, E., Gich, F., Rusalleda, M., Balaguer, M. D., & Colprim, J. (2013). Nitrous oxide reduction genetic potential from the microbial community of an intermittently aerated partial nitritation SBR treating mature landfill leachate. *Water Res.* 47(19): 7066-7077. doi:10.1016/j.watres.2013.07.057
- Gao, X., Zhang, T., Wang, B., Xu, Z., Zhang, L., & Peng, Y. (2020). Advanced nitrogen removal of low C/N ratio sewage in an anaerobic/aerobic/anoxic process through enhanced post-endogenous denitrification. *Chemosphere.* 252: 126624. doi:10.1016/j.chemosphere.2020.126624
- Gonzalez-Martinez, A., Rodriguez-Sanchez, A., van Loosdrecht, M. C. M., Gonzalez-Lopez, J., & Vahala, R. (2016). Detection of comammox bacteria in full-scale wastewater treatment bioreactors using tag-454-pyrosequencing. *Environ Sci Pollut Res Int.* 23(24): 25501-25511. doi:10.1007/s11356-016-7914-4

- Guellil, A., Thomas, F., Block, J. C., Bersillon, J. L., & Ginestet, P. (2001). Transfer of organic matter between wastewater and activated sludge flocs. *Water Research*. 35(1): 143-150. doi:10.1016/s0043-1354(00)00240-2
- Guerrero, J., Taya, C., Guisasola, A., & Baeza, J. A. (2012). Glycerol as a sole carbon source for enhanced biological phosphorus removal. *Water Res.* 46(9): 2983-2991. doi:10.1016/j.watres.2012.02.043
- Gujer, W., Henze, M., Mino, T., & van Loosdrecht, M. C. M. (1999). Activated Sludge Model No. 3. *Water Science and Technology*. 39(1). doi:10.1016/s0273-1223(98)00785-9
- Guo, Y., Wu, C., Wang, Q., Yang, M., Huang, Q., Magep, M., & Zheng, T. (2016). Wastewater-nitrogen removal using polylactic acid/starch as carbon source: Optimization of operating parameters using response surface methodology. *Frontiers of Environmental Science & Engineering*. 10(4). doi:10.1007/s11783-016-0845-y
- Hall, B. G. (2013). Building phylogenetic trees from molecular data with MEGA. *Mol Biol Evol.* 30(5): 1229-1235. doi:10.1093/molbev/mst012
- Hanaki, K., Wantawin, C., & Ohgaki, S. (1990). Nitrification at low levels of dissolved oxygen with and without organic loading in a suspended-growth reactor. *Water Research*. 24(3): 297-302. doi:10.1016/0043-1354(90)90004-p
- He, S., Gall, D. L., & McMahon, K. D. (2007). "Candidatus Accumulibacter" population structure in enhanced biological phosphorus removal sludges as revealed by polyphosphate kinase genes. *Appl Environ Microbiol.* 73(18): 5865-5874. doi:10.1128/AEM.01207-07
- Hellinga, C., Schellen, A. A. J. C., Mulder, J. W., van Loosdrecht, M. C. M., & Heijnen, J. J. (1998). The sharon process: An innovative method for nitrogen removal from ammonium-rich waste water. *Water Science and Technology*. 37(9). doi:10.1016/s0273-1223(98)00281-9
- Henry, S., Bru, D., Stres, B., Hallet, S., & Philippot, L. (2006). Quantitative detection of the nosZ gene, encoding nitrous oxide reductase, and comparison of the abundances of 16S rRNA, narG, nirK, and nosZ genes in soils. *Appl Environ Microbiol.* 72(8): 5181-5189. doi:10.1128/AEM.00231-06
- Henze, M., Grady Jr, L., Gujer, W., V. R Marais, G., & Matsuo, T. (1987). *Activated Sludge Model No 1* (Vol. 29).
- Henze, M., Harremoës, P., la Cour Jansen, J., & Arvin, E. (1997). *Wastewater Treatment - Biological and Chemical Process*. Berlin, Germany: Springer-Verlag GmbH.
- Henze, M., Holm Kristensen, G., & Strube, R. (1994). Rate-Capacity Characterization of Wastewater for Nutrient Removal Processes. *Water Science and Technology*. 29(7): 101-107. doi:10.2166/wst.1994.0318

- Henze, M., van Loosdrecht, M. C., Ekama, G. A., & Brdjanovic, D. (2008). *Biological Wastewater Treatment - Principles, Modeling and Design*. London, UK: IWA Publishing.
- Herlemann, D. P., Labrenz, M., Jürgens, K., Bertilsson, S., Waniek, J. J., & Andersson, A. F. (2011). Transitions in bacterial communities along the 2000 km salinity gradient of the Baltic Sea. *The ISME journal*. 5(10): 1571-1579. doi:10.1038/ismej.2011.41
- Heylen, K., Gevers, D., Vanparys, B., Wittebolle, L., Geets, J., Boon, N., & De Vos, P. (2006). The incidence of nirS and nirK and their genetic heterogeneity in cultivated denitrifiers. *Environ Microbiol.* 8(11): 2012-2021. doi:10.1111/j.1462-2920.2006.01081.x
- Hooper, A. B., Vannelli, T., Bergmann, D. J., & Arciero, D. M. (1997). Enzymology of the oxidation of ammonia to nitrite by bacteria. *Antonie van Leeuwenhoek*. 71(1-2): 59-67.
- Insel, G., Orhon, D., & Vanrolleghem, P. A. (2003). Identification and modelling of aerobic hydrolysis - application of optimal experimental design. *Journal of Chemical Technology & Biotechnology*. 78(4): 437-445. doi:10.1002/jctb.807
- Kampschreur, M. J., Temmink, H., Kleerebezem, R., Jetten, M. S., & van Loosdrecht, M. C. (2009). Nitrous oxide emission during wastewater treatment. *Water Res.* 43(17): 4093-4103. doi:10.1016/j.watres.2009.03.001
- Kandeler, E., Deiglmayr, K., Tschirko, D., Bru, D., & Philippot, L. (2006). Abundance of narG, nirS, nirK, and nosZ genes of denitrifying bacteria during primary successions of a glacier foreland. *Appl Environ Microbiol.* 72(9): 5957-5962. doi:10.1128/AEM.00439-06
- Keene, N. A., Reusser, S. R., Scarborough, M. J., Grooms, A. L., Seib, M., Santo Domingo, J., & Noguera, D. R. (2017). Pilot plant demonstration of stable and efficient high rate biological nutrient removal with low dissolved oxygen conditions. *Water Res.* 121: 72-85. doi:10.1016/j.watres.2017.05.029
- Kim, D. J., Lee, D. I., & Keller, J. (2006). Effect of temperature and free ammonia on nitrification and nitrite accumulation in landfill leachate and analysis of its nitrifying bacterial community by FISH. *Bioresour Technol.* 97(3): 459-468. doi:10.1016/j.biortech.2005.03.032
- Kits, K. D., Sedlacek, C. J., Lebedeva, E. V., Han, P., Bulaev, A., Pjevac, P., . . . Wagner, M. (2017). Kinetic analysis of a complete nitrifier reveals an oligotrophic lifestyle. *Nature*. 549(7671): 269-272. doi:10.1038/nature23679
- Koch, H., van Kessel, M., & Lucker, S. (2019). Complete nitrification: insights into the ecophysiology of comammox Nitrospira. *Appl Microbiol Biotechnol.* 103(1): 177-189. doi:10.1007/s00253-018-9486-3
- Kuenen, J. G. (2008). Anammox bacteria: from discovery to application. *Nature Reviews Microbiology*. 6: 320. doi:10.1038/nrmicro1857

- Kumar, S., Stecher, G., & Tamura, K. (2016). MEGA7: Molecular Evolutionary Genetics Analysis Version 7.0 for Bigger Datasets. *Molecular Biology and Evolution*. 33(7): 1870-1874. doi:10.1093/molbev/msw054
- Lackner, S., Gilbert, E. M., Vlaeminck, S. E., Joss, A., Horn, H., & van Loosdrecht, M. C. M. (2014). Full-scale partial nitrification/anammox experiences - An application survey. *Water Research*. 55: 292-303. doi:10.1016/j.watres.2014.02.032
- Law, Y., Matysik, A., Chen, X., Swa Thi, S., Ngoc Nguyen, T. Q., Qiu, G., . . . Wuertz, S. (2019). High Dissolved Oxygen Selection against Nitrospira Sublineage I in Full-Scale Activated Sludge. *Environ Sci Technol*. 53(14): 8157-8166. doi:10.1021/acs.est.9b00955
- Lee, B. P., Chua, A. S. M., Ong, Y. H., & Ngoh, G. C. (2010). *Characterization of municipal wastewater in Kuala Lumpur, Malaysia: carbon, nitrogen and phosphorus*. Paper presented at the 8th International Symposium on Southeast Asian Water Environment, Phuket Graceland Resort & Spa, Phuket, Thailand. <https://pdfs.semanticscholar.org/60a1/538895dc0bb1f91abe562872260f353ec2dd.pdf>
- Li, B., & Wu, G. (2014). Effects of sludge retention times on nutrient removal and nitrous oxide emission in biological nutrient removal processes. *Int J Environ Res Public Health*. 11(4): 3553-3569. doi:10.3390/ijerph110403553
- Li, H., Zhang, Y., Yang, M., & Kamagata, Y. (2013). Effects of hydraulic retention time on nitrification activities and population dynamics of a conventional activated sludge system. *Frontiers of Environmental Science & Engineering*. 7(1): 43-48. doi:10.1007/s11783-012-0397-8
- Li, S., Wu, Z., & Liu, G. (2019). Degradation kinetics of toilet paper fiber during wastewater treatment: Effects of solid retention time and microbial community. *Chemosphere*. 225: 915-926. doi:10.1016/j.chemosphere.2019.03.097
- Li, W., Zheng, T., Ma, Y., & Liu, J. (2019). Current status and future prospects of sewer biofilms: Their structure, influencing factors, and substance transformations. *Sci Total Environ*. 695: 133815. doi:10.1016/j.scitotenv.2019.133815
- Liu, C., Lee, C. T., & Zhang, H. (2019). Design of Sewage Treatment Plants for High-Density Urban Reclamation Land. *Chemical Engineering Transactions*. 72: 187-192. doi:10.3303/CET1972032
- Liu, G., & Wang, J. (2013). Long-term low DO enriches and shifts nitrifier community in activated sludge. *Environ Sci Technol*. 47(10): 5109-5117. doi:10.1021/es304647y
- Liu, X., Kim, M., & Nakhla, G. (2018). Performance and Kinetics of Nitrification of Low Ammonia Wastewater at Low Temperature. *Water Environ Res*. 90(6): 498-509. doi:10.2175/106143017X14902968254818
- Lucker, S., Wagner, M., Maixner, F., Pelletier, E., Koch, H., Vacherie, B., . . . Daims, H. (2010). A Nitrospira metagenome illuminates the physiology and evolution

of globally important nitrite-oxidizing bacteria. *Proc Natl Acad Sci U S A*. 107(30): 13479-13484. doi:10.1073/pnas.1003860107

Ludzack, F. J., & Ettinger, M. B. (1962). Controlling Operation to Minimize Activated Sludge Effluent Nitrogen. *Journal (Water Pollution Control Federation)*. 34(9): 920-931.

Ma, B., Wang, S., Cao, S., Miao, Y., Jia, F., Du, R., & Peng, Y. (2016). Biological nitrogen removal from sewage via anammox: Recent advances. *Bioresour Technol*. 200: 981-990. doi:10.1016/j.biortech.2015.10.074

Maixner, F., Noguera, D. R., Anneser, B., Stoecker, K., Wegl, G., Wagner, M., & Daims, H. (2006). Nitrite concentration influences the population structure of Nitrospira-like bacteria. *Environ Microbiol*. 8(8): 1487-1495. doi:10.1111/j.1462-2920.2006.01033.x

Malaysian Water Association. (2017). *Malaysia Water Industry Guide 2017*. Retrieved from Kuala Lumpur, Malaysia:

Mannina, G., Capodici, M., Cosenza, A., Di Trapani, D., & van Loosdrecht, M. C. M. (2017). Nitrous oxide emission in a University of Cape Town membrane bioreactor: The effect of carbon to nitrogen ratio. *Journal of Cleaner Production*. 149: 180-190. doi:10.1016/j.jclepro.2017.02.089

Manser, R., Gujer, W., & Siegrist, H. (2005). Consequences of mass transfer effects on the kinetics of nitrifiers. *Water Res*. 39(19): 4633-4642. doi:10.1016/j.watres.2005.09.020

Maryland Department of the Environment. (2016). *Design Guidelines for Wastewater Facilities Recommended BNR/ENR Design Criteria*. Maryland, U.S.: Maryland Department of the Environment.

Massara, T. M., Malamis, S., Guisasola, A., Baeza, J. A., Noutsopoulos, C., & Katsou, E. (2017). A review on nitrous oxide (N₂O) emissions during biological nutrient removal from municipal wastewater and sludge reject water. *Sci Total Environ*. 596-597: 106-123. doi:10.1016/j.scitotenv.2017.03.191

Matějů, V., Čížinská, S., Krejčí, J., & Janoch, T. (1992). Biological water denitrification—A review. *Enzyme and Microbial Technology*. 14(3): 170-183. doi:10.1016/0141-0229(92)90062-S

Matsuda, K., Tsuji, H., Asahara, T., Kado, Y., & Nomoto, K. (2007). Sensitive Quantitative Detection of Commensal Bacteria by rRNA-Targeted Reverse Transcription-PCR. *Applied and Environmental Microbiology*. 73(20): 6695-6695. doi:10.1128/aem.01917-07

McIlroy, S. J., & Nielsen, P. H. (2014). The Family Saprospiraceae. In E. Rosenberg, E. F. DeLong, S. Lory, E. Stackebrandt, & F. Thompson (Eds.), *The Prokaryotes* (4th ed., pp. 863-889). Berlin, Germany: Springer-Verlag.

- McTavish, H., Fuchs, J. A., & Hooper, A. B. (1993). Sequence of the gene coding for ammonia monooxygenase in *Nitrosomonas europaea*. *J Bacteriol.* 175(8): 2436-2444. doi:10.1128/jb.175.8.2436-2444.1993
- Mehrani, M. J., Sobotka, D., Kowal, P., Ciesielski, S., & Makinia, J. (2020). The occurrence and role of *Nitrospira* in nitrogen removal systems. *Bioresour Technol.* 303: 122936. doi:10.1016/j.biortech.2020.122936
- Mikola, A., Heinonen, M., Kosonen, H., Leppanen, M., Rantanen, P., & Vahala, R. (2014). N₂O emissions from secondary clarifiers and their contribution to the total emissions of the WWTP. *Water Sci Technol.* 70(4): 720-728. doi:10.2166/wst.2014.281
- Mobarry, B. K., Wagner, M., Urbain, V., Rittmann, B. E., & Stahl, D. A. (1996). Phylogenetic probes for analyzing abundance and spatial organization of nitrifying bacteria. *Appl Environ Microbiol.* 62(6): 2156-2162.
- Moreno-Vivián, C., Cabello, P., Martínez-Luque, M., Blasco, R., & Castillo, F. (1999). Prokaryotic Nitrate Reduction: Molecular Properties and Functional Distinction among Bacterial Nitrate Reductases. *Journal of Bacteriology.* 181(21): 6573.
- Morgenroth, E., Kommedal, R., & Harremoes, P. (2002). Processes and modeling of hydrolysis of particulate organic matter in aerobic wastewater treatment--a review. *Water Sci Technol.* 45(6): 25-40.
- Mulder, J. W., Duin, J. O. J., Goverde, J., Poiesz, W. G., vanVeldhuizen, H. M., vanKempen, R., & Roeleveld, P. (2006). *Full-Scale Experience with the Sharon Process through the Eyes of the Operators*. Paper presented at the WEFTEC 2006, Dallas, U.S.
- Muller, A., Wentzel, M. C., Loewenthal, R. E., & Ekama, G. A. (2003). Heterotroph anoxic yield in anoxic aerobic activated sludge systems treating municipal wastewater. *Water Research.* 37(10): 2435-2441. doi:10.1016/s0043-1354(03)00015-0
- Murakami, C., & Babcock, R. J. (1998). *Effect of Anoxic Selector Detention Time and Mixing Rate on Denitrification Rate and Control of Sphaerotilus Natans Bulking*. Paper presented at the Water Environment Federation 71st Annual Conference & Exposition.
- Naidoo, V., Urbain, V., & Buckley, C. A. (1998). Characterization of wastewater and activated sludge from European municipal wastewater treatment plants using the NUR test. *Water Science and Technology.* 38(1): 303-310. doi:10.1016/S0273-1223(98)00415-6
- Najafpour, G. D. (2015). *Biochemical Engineering and Biotechnology*. Amsterdam, Netherlands: Elsevier B. V.
- National Centers for Environmental Information. (2019). Climate Data Online. Retrieved 28 August 2019, from National Oceanic and Atmospheric Administration

- National Water Services Commission. (2009). *Malaysian Sewerage Industry Guideline* (3rd ed. Vol. IV). Cyberjaya, Malaysia: National Water Services Commission.
- Nowka, B., Off, S., Daims, H., & Spieck, E. (2015). Improved isolation strategies allowed the phenotypic differentiation of two *Nitrospira* strains from widespread phylogenetic lineages. *FEMS Microbiol Ecol.* 91(3). doi:10.1093/femsec/fiu031
- Ofițeru, I. D., & Curtis, T. P. (2009). Modeling Risk of Failure in Nitrification: Simple Model Incorporating Abundance and Diversity. *Journal of Environmental Engineering.* 135(8): 660-665. doi:10.1061/(asce)0733-9372(2009)135:8(660)
- Ong, Y. H., Chua, A. S. M., Lee, B. P., Ngoh, G. C., & Hashim, M. A. (2012). An Observation on Sludge Granulation in an Enhanced Biological Phosphorus Removal Process. *Water Environment Research.* 84(1): 3-8. doi:10.2175/106143011x13184219229335
- Palomo, A., Pedersen, A. G., Fowler, S. J., Dechesne, A., Sicheritz-Ponten, T., & Smets, B. F. (2018). Comparative genomics sheds light on niche differentiation and the evolutionary history of comammox *Nitrospira*. *ISME J.* 12(7): 1779-1793. doi:10.1038/s41396-018-0083-3
- Park, H. D., & Noguera, D. R. (2007). Characterization of two ammonia-oxidizing bacteria isolated from reactors operated with low dissolved oxygen concentrations. *J Appl Microbiol.* 102(5): 1401-1417. doi:10.1111/j.1365-2672.2006.03176.x
- Park, H. D., & Noguera, D. R. (2008). *Nitrospira* Community Composition in Nitrifying Reactors Operated with Two Different Dissolved Oxygen Levels. *J. Microbiol. Biotechnol.* 18(8): 1470-1474.
- Perster, M., Maixner, F., Berry, D., Rattei, T., Koch, H., Lucker, S., . . . Daims, H. (2014). NxrB encoding the beta subunit of nitrite oxidoreductase as functional and phylogenetic marker for nitrite-oxidizing *Nitrospira*. *Environmental Microbiology.* 16(10): 3055-3071. doi:10.1111/1462-2920.12300
- Pester, M., Maixner, F., Berry, D., Rattei, T., Koch, H., Lucker, S., . . . Daims, H. (2014). NxrB encoding the beta subunit of nitrite oxidoreductase as functional and phylogenetic marker for nitrite-oxidizing *Nitrospira*. *Environ Microbiol.* 16(10): 3055-3071. doi:10.1111/1462-2920.12300
- Philippot, L. (2002). Denitrifying genes in bacterial and Archaeal genomes. *Biochim Biophys Acta.* 1577(3): 355-376. doi:10.1016/S0167-4781(02)00420-7
- Pjevac, P., Schauburger, C., Poghosyan, L., Herbold, C. W., van Kessel, M., Daebeler, A., . . . Daims, H. (2017). AmoA-Targeted Polymerase Chain Reaction Primers for the Specific Detection and Quantification of Comammox *Nitrospira* in the Environment. *Front Microbiol.* 8: 1508. doi:10.3389/fmicb.2017.01508
- Quail, M. A., Smith, M., Coupland, P., Otto, T. D., Harris, S. R., Connor, T. R., . . . Gu, Y. (2012). A tale of three next generation sequencing platforms: comparison of Ion Torrent, Pacific Biosciences and Illumina MiSeq sequencers. *BMC Genomics.* 13: 341. doi:10.1186/1471-2164-13-341

- Quince, C., Lanzen, A., Davenport, R. J., & Turnbaugh, P. J. (2011). Removing noise from pyrosequenced amplicons. *BMC Bioinformatics*. 12: 38. doi:10.1186/1471-2105-12-38
- Ramli, N. A., & Abdul Hamid, M. F. (2017). Analysis of energy efficiency and energy consumption costs: a case study for regional wastewater treatment plant in Malaysia. *Journal of Water Reuse and Desalination*. 7(1): 103-110. doi:10.2166/wrd.2016.196
- Reichert, P. (1994). Aquasim – a Tool for Simulation and Data Analysis of Aquatic Systems. *Water Science and Technology*. 30(2): 21-30. doi:10.2166/wst.1994.0025
- Ristow, N. E., & Hansford, G. S. (2001). Modelling of a falling sludge bed reactor using AQUASIM. *Water SA*. 27(4). doi:10.4314/wsa.v27i4.4956
- Roots, P., Wang, Y., Rosenthal, A. F., Griffin, J. S., Sabba, F., Petrovich, M., . . . Wells, G. F. (2019). Comammox Nitrospira are the dominant ammonia oxidizers in a mainstream low dissolved oxygen nitrification reactor. *Water Res*. 157: 396-405. doi:10.1016/j.watres.2019.03.060
- Rosenberg, E. (2014). The Family Chitinophagaceae. In E. Rosenberg, E. F. DeLong, S. Lory, E. Stackebrandt, & F. Thompson (Eds.), *The Prokaryotes* (4th ed., pp. 493-495). Berlin, Germany: Springer-Verlag.
- Rotthauwe, J.-H., Witzel, K.-P., & Liesack, W. (1997). The Ammonia Monooxygenase Structural Gene amoA as a Functional Marker: Molecular Fine-Scale Analysis of Natural Ammonia-Oxidizing Populations. *Applied and Environmental Microbiology*. 63(12): 4704-4712.
- Sakoula, D., Nowka, B., Spieck, E., Daims, H., & Lucker, S. (2018). The draft genome sequence of "Nitrospira lenta" strain BS10, a nitrite oxidizing bacterium isolated from activated sludge. *Stand Genomic Sci*. 13: 32. doi:10.1186/s40793-018-0338-7
- Sanz, J. L., & Köchling, T. (2019). Next-generation sequencing and waste/wastewater treatment: a comprehensive overview. *Reviews in Environmental Science and Bio/Technology*. 18(4): 635-680. doi:10.1007/s11157-019-09513-0
- Satoh, H., Okabe, S., Norimatsu, N., & Watanabe, Y. (2000). Significance of substrate C/N ratio on structure and activity of nitrifying biofilms determined by in situ hybridization and the use of microelectrodes. *Water Science and Technology*. 41(4-5): 317-321.
- Sattayatewa, C., Pagilla, K., Sharp, R., & Pitt, P. (2010). Fate of Organic Nitrogen in Four Biological Nutrient Removal Wastewater Treatment Plants. *Water Environment Research*. 82(12): 2306-2315. doi:10.2175/106143010x12609736966324
- Saunders, A. M., Albertsen, M., Vollertsen, J., & Nielsen, P. H. (2016). The activated sludge ecosystem contains a core community of abundant organisms. *ISME J*. 10(1): 11-20. doi:10.1038/ismej.2015.117

- Schloss, P. D., & Handelsman, J. (2005). Introducing DOTUR, a computer program for defining operational taxonomic units and estimating species richness. *Appl Environ Microbiol.* 71(3): 1501-1506. doi:10.1128/AEM.71.3.1501-1506.2005
- Schmid, M., Twachtmann, U., Klein, M., Strous, M., Juretschko, S., Jetten, M., . . . Wagner, M. (2000). Molecular Evidence for Genus Level Diversity of Bacteria Capable of Catalyzing Anaerobic Ammonium Oxidation. *Systematic and Applied Microbiology.* 23(1): 93-106. doi:10.1016/s0723-2020(00)80050-8
- Sedlak, R. I. (2018). *Phosphorus and Nitrogen Removal from Municipal Wastewater: Principles and Practice* (2nd ed.). Boca Raton, Florida, US: Taylor & Francis Group.
- Seviour, R., & Nielsen, P. H. (2010). *Microbial Ecology of Activated Sludge*. London, UK: IWA Publishing.
- Shen, Y., Yang, D., Wu, Y., Zhang, H., & Zhang, X. (2019). Operation mode of a step-feed anoxic/oxic process with distribution of carbon source from anaerobic zone on nutrient removal and microbial properties. *Scientific Reports.* 9(1): 1153. doi:10.1038/s41598-018-37841-8
- Shen, Z., & Wang, J. (2011). Biological denitrification using cross-linked starch/PCL blends as solid carbon source and biofilm carrier. *Bioresour Technol.* 102(19): 8835-8838. doi:10.1016/j.biortech.2011.06.090
- Shi, L., Ma, B., Li, X., Zhang, Q., & Peng, Y. (2019). Advanced nitrogen removal without addition of external carbon source in an anaerobic/aerobic/anoxic sequencing batch reactor. *Bioprocess Biosyst Eng.* 42(9): 1507-1515. doi:10.1007/s00449-019-02148-z
- Siegrist, H., Krebs, P., Bühler, R., Purtschert, I., Rock, C., & Rufer, P. (1995). Denitrification in secondary clarifiers. *Water Science and Technology.* 31(2). doi:10.1016/0273-1223(95)00193-q
- Sophonsiri, C., & Morgenroth, E. (2004). Chemical composition associated with different particle size fractions in municipal, industrial, and agricultural wastewaters. *Chemosphere.* 55(5): 691-703. doi:10.1016/j.chemosphere.2003.11.032
- Stackebrandt, E., Murray, R. G. E., & Trüper, H. G. (1988). Proteobacteria classis nov., a Name for the Phylogenetic Taxon That Includes the "Purple Bacteria and Their Relatives". *International Journal of Systematic and Evolutionary Microbiology.* 38(3): 321-325.
- Stein, L. Y., & Klotz, M. G. (2016). The nitrogen cycle. *Curr Biol.* 26(3): R94-98. doi:10.1016/j.cub.2015.12.021
- Stoddard, S. F., Smith, B. J., Hein, R., Roller, B. R., & Schmidt, T. M. (2015). rrnDB: improved tools for interpreting rRNA gene abundance in bacteria and archaea and a new foundation for future development. *Nucleic Acids Res.* 43(Database issue): D593-598. doi:10.1093/nar/gku1201

- Strous, M., Heijnen, J. J., Kuenen, J. G., & Jetten, M. S. M. (1998). The sequencing batch reactor as a powerful tool for the study of slowly growing anaerobic ammonium-oxidizing microorganisms. *Applied Microbiology and Biotechnology*. 50(5): 589-596. doi:10.1007/s002530051340
- Tas, D. O., Karahan, O., Insel, G., Ovez, S., Orhon, D., & Spanjers, H. (2009). Biodegradability and denitrification potential of settleable chemical oxygen demand in domestic wastewater. *Water Environ Res*. 81(7): 715-727.
- Tchobanoglous, G., Stensel, H. D., Tsuchihashi, R., Burton, F., Abu-Orf, M., Bowden, G., & Pfrang, W. (2014). *Wastewater Engineering: Treatment and Resource Recovery*. New York, NY: McGraw-Hill Education.
- Tenaga Nasional Berhad. (2014). Pricing & Tariffs. Retrieved from <https://www.tnb.com.my/commercial-industrial/pricing-tariffs1>
- Throbäck, I. N., Enwall, K., Jarvis, A., & Hallin, S. (2004). Reassessing PCR primers targeting nirS, nirK and nosZ genes for community surveys of denitrifying bacteria with DGGE. *FEMS Microbiol Ecol*. 49(3): 401-417. doi:10.1016/j.femsec.2004.04.011
- United Nations World Water Assessment Programme. (2017). *The United Nations World Water Development Report 2017. Wastewater: The Untapped Resource*. Retrieved from Paris, France:
- United States Environmental Protection Agency. (1993). *Nitrogen Control Manual*. Retrieved from Cincinnati, OH:
- van den Berg, E. M., van Dongen, U., Abbas, B., & van Loosdrecht, M. C. (2015). Enrichment of DNRA bacteria in a continuous culture. *ISME J*. 9(10): 2153-2161. doi:10.1038/ismej.2015.26
- van Kessel, M. A., Speth, D. R., Albertsen, M., Nielsen, P. H., Op den Camp, H. J., Kartal, B., . . . Lucker, S. (2015). Complete nitrification by a single microorganism. *Nature*. 528(7583): 555-559. doi:10.1038/nature16459
- van Loosdrecht, M. C. M., Nielsen, P. H., Lopez-Vazquez, C. M., & Brdjanovic, D. (2016). *Experimental Methods in Wastewater Treatment*. London, UK: IWA Publishing.
- Vanparrys, B., Spieck, E., Heylen, K., Wittebolle, L., Geets, J., Boon, N., & DeVos, P. (2007). The phylogeny of the genus *Nitrobacter* based on comparative rep-PCR, 16S rRNA and nitrite oxidoreductase gene sequence analysis. *Systematic and Applied Microbiology*. 30(4): 297-308. doi:10.1016/j.syapm.2006.11.006
- Vetrovsky, T., & Baldrian, P. (2013). The variability of the 16S rRNA gene in bacterial genomes and its consequences for bacterial community analyses. *PLoS One*. 8(2): e57923. doi:10.1371/journal.pone.0057923
- Vuono, D. C., Benecke, J., Henkel, J., Navidi, W. C., Cath, T. Y., Munakata-Marr, J., . . . Drewes, J. E. (2015). Disturbance and temporal partitioning of the activated sludge metacommunity. *ISME J*. 9(2): 425-435. doi:10.1038/ismej.2014.139

- Wagner, M., Rath, G., Koops, H. P., Flood, J., & Amann, R. (1996). In situ analysis of nitrifying bacteria in sewage treatment plants. *Water Science and Technology*. 34(1-2). doi:10.1016/0273-1223(96)00514-8
- Wang, G., Xu, X., Zhou, L., Wang, C., & Yang, F. (2017). A pilot-scale study on the start-up of partial nitrification-anammox process for anaerobic sludge digester liquor treatment. *Bioresour Technol.* 241: 181-189. doi:10.1016/j.biortech.2017.02.125
- Wang, Q., Chen, Q., & Chen, J. (2017). Optimizing external carbon source addition in domestic wastewater treatment based on online sensing data and a numerical model. *Water Sci Technol.* 75(11-12): 2716-2725. doi:10.2166/wst.2017.128
- Wang, X., Wang, S., Xue, T., Li, B., Dai, X., & Peng, Y. (2015). Treating low carbon/nitrogen (C/N) wastewater in simultaneous nitrification-endogenous denitrification and phosphorous removal (SNDPR) systems by strengthening anaerobic intracellular carbon storage. *Water Res.* 77: 191-200. doi:10.1016/j.watres.2015.03.019
- Wang, X., Wang, S., Zhao, J., Dai, X., & Peng, Y. (2016). Combining simultaneous nitrification-endogenous denitrification and phosphorus removal with post-denitrification for low carbon/nitrogen wastewater treatment. *Bioresour Technol.* 220: 17-25. doi:10.1016/j.biortech.2016.06.132
- Water Environment Federation. (2005). *Biological Nutrient Removal (BNR) Operation in Wastewater Treatment Plants*. Alexandria, Virginia: Water Environment Federation.
- Whelan, J. A., Russell, N. B., & Whelan, M. A. (2003). A method for the absolute quantification of cDNA using real-time PCR. *Journal of Immunological Methods.* 278(1-2): 261-269. doi:10.1016/s0022-1759(03)00223-0
- Winkler, M., Coats, E. R., & Brinkman, C. K. (2011). Advancing post-anoxic denitrification for biological nutrient removal. *Water Res.* 45(18): 6119-6130. doi:10.1016/j.watres.2011.09.006
- Winkler, M. K., Bassin, J. P., Kleerebezem, R., Sorokin, D. Y., & van Loosdrecht, M. C. (2012). Unravelling the reasons for disproportion in the ratio of AOB and NOB in aerobic granular sludge. *Appl Microbiol Biotechnol.* 94(6): 1657-1666. doi:10.1007/s00253-012-4126-9
- Winkler, M. K., & Straka, L. (2019). New directions in biological nitrogen removal and recovery from wastewater. *Curr Opin Biotechnol.* 57: 50-55. doi:10.1016/j.copbio.2018.12.007
- Wu, J., Yan, G., Zhou, G., & Xu, T. (2014). Wastewater COD biodegradability fractionated by simple physical-chemical analysis. *Chemical Engineering Journal.* 258: 450-459. doi:10.1016/j.cej.2014.07.106
- Wu, L., Ning, D., Zhang, B., Li, Y., Zhang, P., Shan, X., . . . Zhou, J. (2019). Global diversity and biogeography of bacterial communities in wastewater treatment plants. *Nat Microbiol.* 4(7): 1183-1195. doi:10.1038/s41564-019-0426-5

- Wuhrmann, K. (1964). Nitrogen removal in sewage treatment processes. *SIL Proceedings, 1922-2010*. 15(2): 580-596. doi:10.1080/03680770.1962.11895576
- Xia, Y., Kong, Y., Thomsen, T. R., & Halkjaer Nielsen, P. (2008). Identification and ecophysiological characterization of epiphytic protein-hydrolyzing saprospiraceae ("Candidatus Epiflobacter" spp.) in activated sludge. *Appl Environ Microbiol.* 74(7): 2229-2238. doi:10.1128/AEM.02502-07
- Yang, Q., Shen, N., Lee, Z. M., Xu, G., Cao, Y., Kwok, B., . . . Zhou, Y. (2016). Simultaneous nitrification, denitrification and phosphorus removal (SNDPR) in a full-scale water reclamation plant located in warm climate. *Water Sci Technol.* 74(2): 448-456. doi:10.2166/wst.2016.214
- Yang, Y., Daims, H., Liu, Y., Herbold, C. W., Pjevac, P., Lin, J. G., . . . Gu, J. D. (2020). Activity and Metabolic Versatility of Complete Ammonia Oxidizers in Full-Scale Wastewater Treatment Systems. *mBio.* 11(2). doi:10.1128/mBio.03175-19
- Yao, Q., & Peng, D. C. (2017). Nitrite oxidizing bacteria (NOB) dominating in nitrifying community in full-scale biological nutrient removal wastewater treatment plants. *AMB Express.* 7(1): 25. doi:10.1186/s13568-017-0328-y
- Yun, Z., Yun, G. H., Lee, H. S., & Yoo, T. U. (2013). The variation of volatile fatty acid compositions in sewer length, and its effect on the process design of biological nutrient removal. *Water Sci Technol.* 67(12): 2753-2760. doi:10.2166/wst.2013.192
- Zhao, W., Huang, Y., Wang, M., Pan, C., Li, X., Peng, Y., & Li, B. (2018). Post-endogenous denitrification and phosphorus removal in an alternating anaerobic/oxic/anoxic (AOA) system treating low carbon/nitrogen (C/N) domestic wastewater. *Chemical Engineering Journal.* 339: 450-458. doi:10.1016/j.cej.2018.01.096
- Zhou, H., Li, X., Xu, G., & Yu, H. (2018). Overview of strategies for enhanced treatment of municipal/domestic wastewater at low temperature. *Sci Total Environ.* 643: 225-237. doi:10.1016/j.scitotenv.2018.06.100
- Zipper, H., Brunner, H., Bernhagen, J., & Vitzthum, F. (2004). Investigations on DNA intercalation and surface binding by SYBR Green I, its structure determination and methodological implications. *Nucleic Acids Res.* 32(12): e103. doi:10.1093/nar/gnh101

LIST OF PUBLICATIONS AND PAPERS PRESENTED

Journal articles

How, S. W., Lim, S. Y., Lim, P. B., Aris, A. M., Ngoh, G. C., Curtis, T. P., & Chua, A. S. M. (2018). Low-dissolved-oxygen nitrification in tropical sewage: an investigation on potential, performance and functional microbial community. *Water Sci Technol*, 77(9), 2274-2283. doi:10.2166/wst.2018.143

How, S. W., Chua, A. S. M., Ngoh, G. C., Nittami, T., & Curtis, T. P. (2019). Enhanced nitrogen removal in an anoxic-oxic-anoxic process treating low COD/N tropical wastewater: Low-dissolved oxygen nitrification and utilization of slowly-biodegradable COD for denitrification. *Sci Total Environ*, 693, 133526. doi:10.1016/j.scitotenv.2019.07.332

How, S. W., Sin, J. H., Wong, S. Y. Y., Lim, P. B., Aris, A. M., Ngoh, G. C., Shoji, T., Curtis, T. P. & Chua, A. S. M. (2020). Characterization of slowly-biodegradable organic compounds and hydrolysis kinetics in tropical wastewater for biological nitrogen removal. *Water Sci Technol*, 81(1), 71-80. doi:10.2166/wst.2020.077

How, S. W., Nittami, T., Ngoh, G. C., Curtis, T. P., & Chua, A. S. M. (2020). An efficient oxic-anoxic process for treating low COD/N tropical wastewater: Startup, optimization and nitrifying community structure. *Chemosphere*, 259, 127444. doi:10.1016/j.chemosphere.2020.127444

Conference proceedings

How, S.W., Lim, S.Y., Lim, P.B., Aris, A.M., Ngoh, G.C., Curtis, T.P., & Chua, A.S.M. (2017). Complete Ammonia Oxidation to Nitrate in a Low-Dissolved Oxygen Nitrification Reactor. In Proceedings of the 7th IWA-ASPIRE Conference & Exhibition, Kuala Lumpur Convention Centre, Malaysia, 11-14 Sept.

- How, S.W., Ngoh, G.C., Curtis, T.P., & Chua, A.S.M. (2018). Effect of dissolved oxygen reduction on tropical anoxic-oxic process: nitrification performance and nitrifying community. In Proceedings of the 17th International Symposium on Microbial Ecology (ISME17), Congress Center Leipzig, Germany, 12-17 Aug.
- How, S.W., Ngoh, G.C., Curtis, T.P., & Chua, A.S.M. (2019). Enhanced nitrogen removal from low C/N tropical wastewater: low-DO nitrification and sbCOD for denitrification. In Proceedings of the 16th IWA World Conference on Anaerobic Digestion (AD16), Delft University of Technology, The Netherlands, 23-27 June.
- How, S.W., Ngoh, G.C., Nittami, T., Curtis, T.P., & Chua, A.S.M. (2019). *Nitrospira* Dominated the Nitrifying Community in a low-DO-Anoxic-Oxic Process in the Tropics. In Proceedings of the 8th IWA Microbial Ecology and Water Engineering Specialist Conference (MEWE2019), ANA Crowne Plaza Hiroshima, Japan, 17-20 Nov.
- How, S.W., Ngoh, G.C., Nittami, T., Curtis, T.P., & Chua, A.S.M. (2019). Quantification of Comammox *Nitrospira* in a Low-DO-Oxic-Anoxic Reactor Treating Tropical Wastewater. In Proceedings of the 8th IWA Microbial Ecology and Water Engineering Specialist Conference (MEWE2019), ANA Crowne Plaza Hiroshima, Japan, 17-20 Nov.